Università di Foggia

Department of Science of Agriculture, Food and Environment

Doctorate on **Management of Innovation in the agricultural and food system of the Mediterranean Region**

3D FOOD PRINTING: STUDY AND APPLICATIONS TO PRODUCE INNOVATIVE FOOD PRODUCTS.

Coordinator:
Prof. Dr. Giancarlo Colelli

Supervisor:
Prof. Dr. Carla Severini

PhD student:
Maddalena Paolillo

TABLES OF CONTENTS

CHAPTER 1. Introduction

3D printing (3DP) represents an innovative and emerging technology aiming to build three-dimensional objects starting from the computer-aided model. For the first time, the early concept of 3DP appeared in 1980 by Kodama from Japan (3D Printing Industry, 2014) as rapid prototyping (RP), which defined a fast process of modeling, assembling and fabricating prototypes. Afterwards, RP technology evolved into Additive Manufacturing (AM) consisting of a large group of technologies capable of constructing intricate 3D objects by a layer-by-layer material deposition. Applications of 3DP regarded the mechanical engineering and aeronautics (Chen et al., 2017), biomedical engineering (Singh & Ramakrishna, 2017), pharmaceutical industry (Goole & Amighi, 2016; Icten et al., 2017) jewelry, building houses and production of biopolymers. More recent is the idea of using 3D printing technology in the food sector aiming to obtain a high level of innovation at different angles.

1.1 The ambitions of 3D Food Printing

Before analyzing the technical aspects of 3DFP, it is useful to focus on the ambitions and the potential advantages that this technology could add to the food system. Due to its unique functionalities, 3DFP is an excellent candidate to completely renew how foods are produced. 3DFP is the only technique capable of translating a digital model into a tangible food structure. A large number of degrees of freedom characterizing the 3DFP made possible the production of personalized foods capable of satisfying consumers desires and requirements. Sensory perception can be modulated by printing food with the desired shape, dimensions, color, taste and texture. Furthermore, nutritional customized products may be obtained by printing a nutritionally designed food paste or, alternatively, by printing food ingredients with specific nutritional content that could be individually deposited under a precise design. Ultimately this technology has shown the ability to create foods with innovative shapes, dimensions and internal structure, which has extended to obtain characteristics matching the taste, color and texture, ease of use and nutritional value.
Moreover, 3DFP has ambitions to sustain on-demand food manufacturing, waste reduction, and digitalization of food production. Three-dimensional printing technology has the capacity to reduce food waste by utilizing low-value food products such as meat off-cuts, distorted fruits and vegetables and fish and seafood by-products that would otherwise be discarded (Prakarsh et al., 2019). It has ambition and potential for expressing potential common ambitions such as the customization of products, the possibility of promoting on-demand production, waste reduction, the high degree of freedom of the production process. All these aspects are also declining

in the field of food production with numerous benefits on social, economic and environmental aspects. Many reports reveal that 3DP technology is part of the 4.0 industry revolution (Boutouchent, 2016, Subic and Gallagher, 2017). Therefore, 3DP printing fits perfectly to the future ways of production in a variety of fields, including food manufacturing (Kocovic, 2017).

1.2 3D food printing techniques

Many different 3D printing techniques could be potentially utilized for the deposition of food materials. Such methodologies are classified according to the materials used (paste, powder, solutions, etc.) or based on the mechanisms used to confer structural stability to the final products. This section reviews the basic principles of the methods used for 3D food printing. (Godoi et al., 2019).

Inkjet Printing

Inkjet printing (IJP) uses pneumatic membrane nozzle-jets which lay little drops of liquid-food-ink to form 2D and 3D patterns onto a moving object by computer-aided design. The drops form together with a digital image in a format of graphical decoration, surface fill or cavity deposition (Food Jet, 2019). Inkjet printing (IJP) can be carried out continuously (C-IJP) or through drop-on-demand (DoD-IJP). Both the methods force a fluid through a nozzle, which subsequently breaks up into a stream of droplets with the same volume but less surface area instability (Godoi et al., 2019). This technology, as it works on the deposition of small drops, is applicable only to low viscosity materials - for example water solutions (Ebrahimi et al., 2020; Bilbao et al., 2021) or by using small molecules or nanoparticles dispersed into a liquid (Chou et al., 2021). The fluidity, viscosity, and surface tension of these inks are the most important properties to get a high printing fidelity (Izdebska, 2016, Pekarovicova and Husovska, 2016). Although such a technique shows the best results in pharmaceutical application focusing on the printing of drugs (Elefthrtiadis et al., 2020; He et al., 2020) it has also shown some interesting results in the food sector. Some of these examples are summarized here:

-*Graphical decoration, fillings* (Grood and Grood, 2011) are classified as DoD and commercialized under the name of FoodJet printing. It uses an array of pneumatic membrane nozzle jets which deposit layers of tiny drops onto a moving object. Many approved patents have been based on the application of this technology to deposit inks on edible substrates (US20160021907A1, 2013; US7597752B2, 2012).

-*Microencapsulation* (TNO, 2017) may assist IJP in providing a print head that produces highly monodisperse droplets. For example, mint syrup core with wax shell and linseed oil with carrageenan shell have been converted into powders after drying.

-*3D constructs* (Diaz et al., 2014). A different application of IJP provides the deposition of drops on thin layers of powders one on top to create a 3-dimensional object. The technique is generally named *Binder jetting* and will be detailed in the next paragraph.

Binder jetting

Binder Jetting is a process of binding overlaying layers of powdered material through a drop-on-demand liquid binder (Godoi et al., 2016). The powder is spread typically through a counter-rotating roller. Then, an inkjet print-head deposit the binding agent to the powders to create the desired 2D pattern (Ziaee and Crane, 2019) (Figure 4).

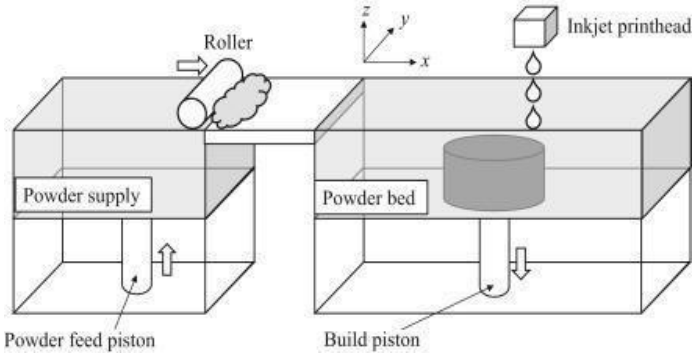

Figure 1. Schematic of binder jetting three-dimensional printing technology (Zhang et al., 2018)

The liquid acts as a binder of the solid parts and it should be selected with high accuracy (Holland et al., 2019). The process of binding can occur physically, chemically or electrostatically, examples of adhesion mechanisms are shown in Fig. 2.

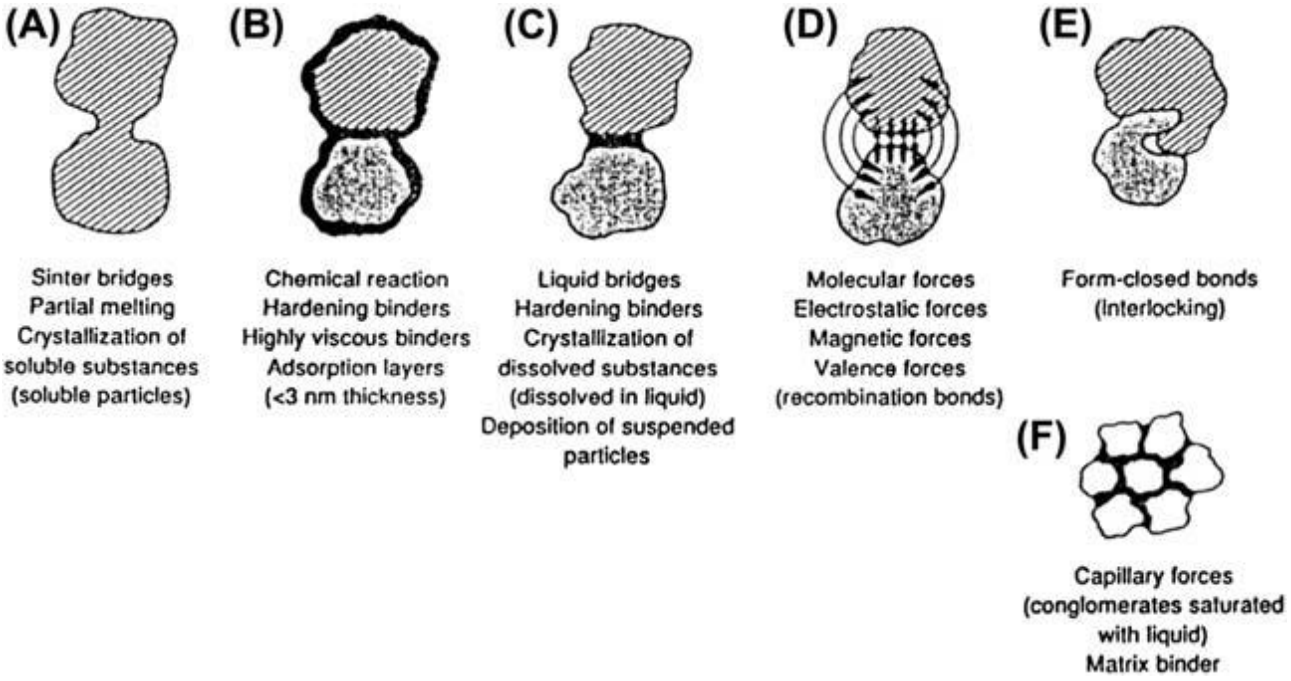

Figure 2. Some agglomeration mechanisms between food particles (Pietsch, 1997)

This technique has shown several advantages including low cost and fast fabrication but, on the other hand, some drawbacks limit the use in the food sector: 1. few printable food materials are easily ready to be used; 2. equipment is expensive in comparison to other techniques; 3. the printed objects result with rough surface finish (Sun et al., 2015). Moreover, it is necessary that the powdered food products have to lend themselves well to agglomeration due to their stickiness and hygroscopicity. While long-life powdered products natural caking over time is considered a negative effect on product quality (Bhandari et al., 2013, Cuq et al., 2013), for Binder jetting controlled agglomeration is one of the principles behind printing. Regarding the possible industrial applications, the confectionery industry looks the most promising one so far. Flavor liquids and colors can be used to bind powdered material such as sugar (Sher and Tutó, 2015). Fabricating unique, complex and flavorful confectionery products is feasible through this method. Previously, creating a complex design would take a longer time (iReviews, 2014).

Selective laser/hot air sintering

This technique could be classified depending on the type of sintering such as selective laser sintering (SLS) or selective hot air sintering and melting (SHASAM). Both such methods use a sintering source to fuse the powder particles and to realize solid layers (Sun et al., 2015). A roller distributes a layer of powder onto the bed of the printer (or the previous layer) while the process of sintering controlled by the CAD model is repeated allowing to get the structural stability of the 3D structure.

The first application of this method have been performed by an homemade printer based on a technology SHASAM that use a moving heat source to melt sugar particles and to create 'caramelized' sculptures (CandyFab, 2019). The advantages of these methods are their capability to sinter any powdered material (Kruth et al., 2003). Furthermore, both SLS and SHASAM are faster than other printing methods because the heating source is directly applied to the powder material without any previous printer bed movement. These methods require no post curing and the use of limited support structure but post processing is needed to remove the excessive powder from the end products such as by scraping the excess powder (Liu et al., 2017). Due to its nature this technology is limited to powder materials and any application on fruit, vegetable, meat or fish has been never tested (Oskay and Edman, 2006).

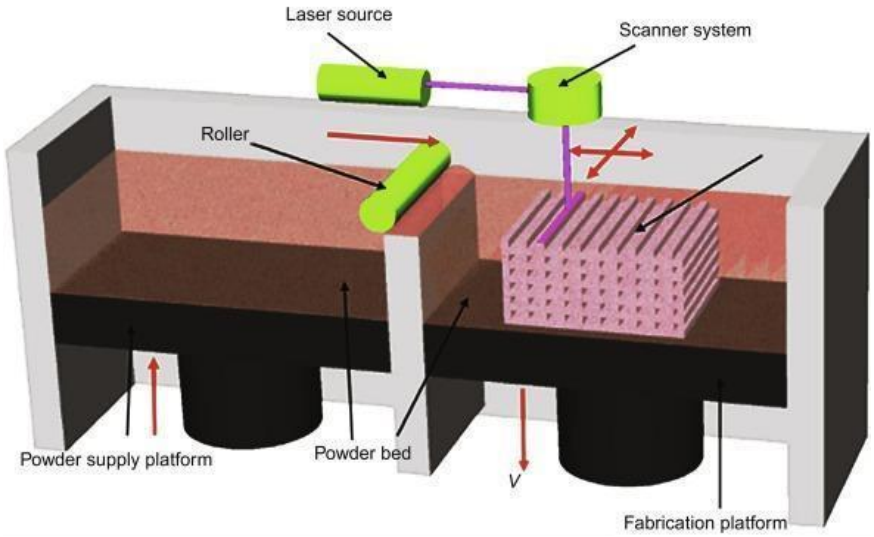

Figure 3. Schematic diagram of SLS 3D printing process (Wang et al., 2017).

Fused deposition modeling

The Fused Deposition Modeling, FDM, involves a layer-by-layer deposition of melted materials. This technique for the first time introduced the fabrication of a 3D object consisting of thermoplastic materials (Ahn et al., 2002). During the printing process, the material is melted and deposited continuously through a moving nozzle. In the field of food manufacturing, apart for the chocolate, the melting is not necessary and the printer typically extrudes different printable food pastes at medium-high viscosity (Yang et al., 2019) such as dough, mashed potatoes, cheese, and meat paste (Lipton et al., 2010, Yang et al., 2015; Tan et al., 2018). The 3D food printers consist of four major body parts: *the printhead* [feed hopper, feed barrel/syringe/cartridge, extruding head(s)], *digital control interface*, *print stage*, and *moveable case*. The printing process could be governed by *screw-based* or *syringe-*

based system (Fig. 4) equipped by a pneumatic pump or a stepper motor that control the amount of material deposited per unit of time.

Three extrusion mechanisms have been applied in 3D food printing: syringe-based extrusion (Fig. 4, A) *screw-based extrusion* (Fig. 4, B), air *pressure-based extrusion* in which food materials are pushed through the nozzle by air pressure (Fig. 4, C). The air pressure-based extrusion is highly suitable liquids or other food materials at low viscosity (Sun, Zhou, Yan, Huang, & Lin, 2017). Diversely, when using a screw-based extrusion process, the food materials are put into the sample feeder and deposited out to the nozzle tip by a screw rotating at different speeds depending on the materials properties and the virtual model to replicate. During the extrusion process, food materials can be fed into the hopper continuously thus realizing the continuous printing. However, the screw-based extrusion is not suitable for the food slurry with high viscosity and high mechanical strength. The syringe-based extrusion unit is suitable to print food materials with high viscosity and high mechanical strength. However, it should be noted that the air pressure-based extrusion and syringe-based extrusion do not allow the continuous feeding of food materials during printing.

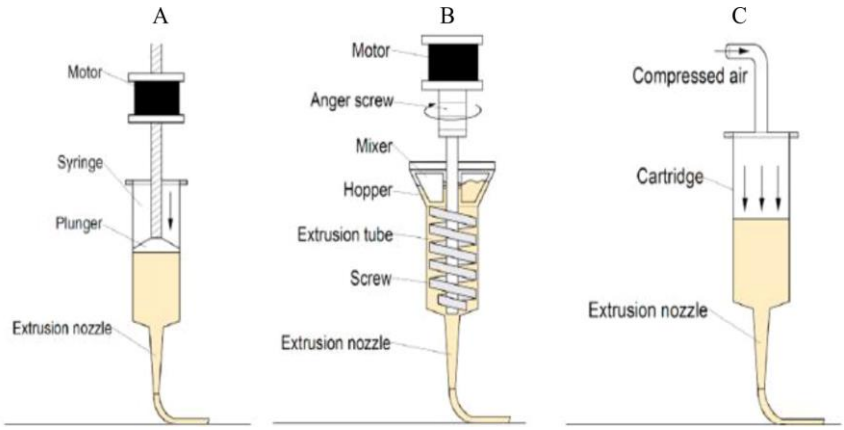

Figure 4. Types of 3D food extrusion mechanisms: syringe-type extrusion (A), screw-type extrusion, air pressure-driven extrusion (C) (Guo et al., 2019)

1.3 Overview of 3D Food Printing process

Unlike other food technologies, the digital nature of 3DFP requires the creation of a virtual 3D model by using computer-aided design (CAD) software (Kewuyemi et al., 2021). The process involves the conceptualization of a three-dimensional object, the design of such an idea by using a CAD that can be saved as a .stl file format. Next,

such a file is studied and optimized by a slicing software that literally slices the virtual model and allows to define the printing conditions by modulating all the relevant variables such as extruding temperature, nozzle size, printing speed, layer height, percentage substrate flow, etc. After the setting of the printing variables the commands controlling the movements of the printer in the 3D space are saved in G-code format, the readable standard printing language for 3D food printers. The 3D printing process is then initiated after loading the G-code that controls the printers during food material deposition (Kewuyemi et al., 2021). Then the 3D printed-food is ready for the market or for the consumers.

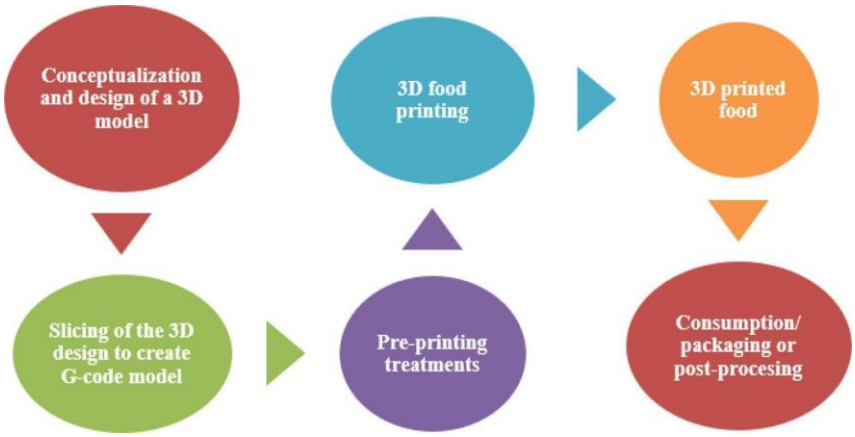

Figure 5. Summary of the main steps to obtain a 3D printed food (Kewuyemi et al., 2021)

The most common 3D food printers consist of different configurations such as the Cartesian, Delta, Polar, or Scara (Derossi et al. 2019) which describe how the print head moves in the X, Y, and Z axes (Figure 6). Although such configurations show advantages and drawbacks, the Cartesian and Delta designs currently are the most used for food applications.

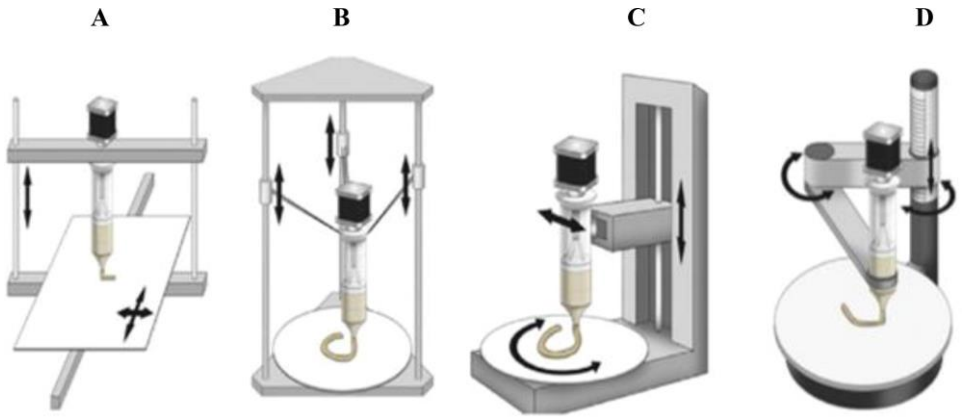

Figure 6. Structural configurations of different 3D printers. (A) Cartesian (B) Delta (C) Polar (D) Scara (Derossi, 2019)

1.3.1 Computer-Aided Design Systems to Create 3D Virtual Models

The creation of a 3D virtual model is the first step for 3D food printing (Derossi et al., 2019). Several professional CAD software is commercially available, some of which are Autodesk (Autodesk Inc.), SketchUp (Trimble Inc.), Blender (Blender Foundation), Design Spark Mechanical (Design Spark, Inc.) and SolidWorks (Dassault Systèmes SolidWorks Corp). Such software exhibits a large diversity of characteristics and they are adapted for a wide range of users, from beginner to expert researchers. Below the most important features of three CAD software for professional use are briefly reported:

-*Autodesk* is a software divided in three main fields of applications having tailored properties and tools: (1) architecture, engineering and construction; (2) product design and manufacturing collection; and (3) media and entertainment collection.

-*SketchUp* was originally developed especially for users who are familiar with building and architectural modeling. The designing of houses, landscapes and entire buildings is the main field of application of this software but it has been used also to develop virtual objects for 3DP applications.

-*Blender* (Blender Foundation, the Netherlands) is a free and open-source 3D software that originally was developed for improving 3D animation. It is a very powerful software containing many functionalities for artistic creation and animators' developers.

Apart from these, other interesting friendly software for beginners widely extends the list of tools to design the 3D models for food applications. These include Tinkercad (Autodesk, Inc., San Rafael, CA), Thingiverse (MakerBot Industries, Brooklyn, CA), AutoCAD (Autodesk, Inc.), Meshmixer (Autodesk, Inc.), etc.

-*Tinkercad* (Tinkercad.com) is a very easy-to-use platform to create several kinds of 3D objects directly on the browser. Tinkercad uses several prebuilt shapes (square, circle, pyramids, tubes, etc.) that are possible to combine, obtaining structures with unlimited numbers of shapes, dimensions and structures.
- *Onshape* (Onshape Inc.) is a cloud-based 3D modelling software. It is parametric 3D modelling by which we may sketch a 2D design and extrude it in a 3D virtual model.
- *3D Builder* (i.materilize.com) is free software to create 3D objects before printing. Among the functionalities, this software allows creating innovative shapes by combining basic simple shapes (cubes, circles, cylinders, etc.) or by downloading and modifying many 3D structures from a wide library at disposal.

A particular mention has to be made for the CAD programming software for which the users write a script describing the movement of the printer that creates the desired structural and dimensional information. Instead of the common CAD software, these are 3D compilers with the highest degree of freedom since no default geometries are used/assembled to get the 3D virtual model. On the other hand, these types of software require important skills in programming. *OpenSCAD* is among the most popular 3D modelling software based on programming languages.

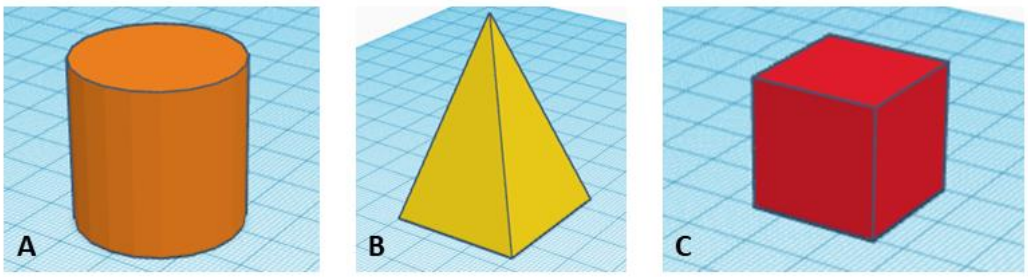

Figure 7. Some examples of 3D virtual models projected by *Tinkercad.com* (A, B, C).

1.3.2 Planning, design and slicing the 3D object

As reported by Jin et al. (2017) the planning process of 3D printing involves four steps: build orientation, support generation, slicing and extruder path planning.
Build orientation means to define the orientation of the virtual model in 3D space before printing. This variable is of great importance because it affects the movements of the printer during extrusion and the number of layers to be deposited, thus

influencing not only the time for printing but also the mechanical properties of the printed object.
The next step is the slicing, a process in which the 3D virtual model is sliced in a set of parallel planes to the object orientation. Each plan contains the extrusion path that defines the 2D trajectory followed by the extruder to deposit the material drawing object's contours and to fill a certain internal area. The slicing definitely affects the quality of the 3D printed structure because it defines not only the printing movements (i.e., the deposition of material contour and its filling) but also the non-printing movements.
More specifically, the slicer is the tool that prepares the 3D model to be printed in an appropriate way to obtain the best results. Moreover, after slicing a G-code containing the information for the printer's movements is created. By correctly using the slicing software, the users are able to fill the gap between the virtual model (the idea) and the real object. The choice about what type of slicing software could be better to use depends on many factors, but the first information to take into account is that they don't slice in the same way depending on some default conditions such as the infill paths – literally the geometry that the printed follow to fill the internal part of the object – may be significantly different among the slicers. Common slicers are Repetier-Host (Hot-World GmbH & Co. KG, Willich, Germany), Slic3r (Microsoft), Cura (Ultimaker B.V., The Netherlands), and Rhinoceros/Rhino 3D (Robert McNeel & Associates).The slicing definitely affects the quality of 3D printed structure because it defines not only the printing movements also the non-printing movements, which mean the movements of the extruder between two points without any material deposition. The study and optimization of path planning is a very important field of research, but for food applications, never it was taken into account to perform detailed experiments.

1.3 3D Printing variables

Apart from the slicing software that is possible to use, the setting of the printing variables is a crucial step to generate a 3D printed food capable of replicating a virtual model with high accuracy. The most important printing variables are reported in Table 1.

Table 1. The main 3D Printing variables in 3DFP

Print speed	The rate of printing movements	mm/s
Layer height	The height of each deposited layer	mm
Nozzle size	Nozzle diameter	mm

Extrusion rate	The speed at which the material is extruded	mm^3/s
Flow or extruder multiplier	The amount of extruder material is a multiplier by this value	%
Infill density	The level of filling of the 3D object	%
Infill speed	The speed at which the infill is printed	mm/s
Retraction distance	The length of the material retraction during retraction movements	mm
Travel speed	The speed of travel movements (non-printing movements)	mm/s

The *print speed (mm/s)* literally defines the rate of printing (Derossi et al.,2019) but it is defined in different ways in many published papers, such as extruder moving speed (Kim et al., 2017), nozzle moving speed (Yang et al., 2018), infill velocity (Vancauwenberghe et al.,2017a, b) or simply speed (Kouzani et al., 2017). Despite these terminologies, with the term *print speed* we define the speed of the printer in X, Y, Z axis but that also influences the speed of E-axis, that is the rate of step motor that controls the amount of material extruded for unit time (mm/s). So, the print speed allows the control of the rate of all four axes and consequently aims to keep the balance between the speed of printer movements and the amount of material deposited per unit of time. Contrarily, an imbalance over- of under material deposition creates many discrepancies between the virtual model and the obtained structure. However, to avoid the condition of imbalance the default values of the rate on the E-axis is under the control of the firmware; so, by increasing (or decreasing) the printing speed to reduce the printing time, also the E-axis accelerate depositing an increased amount of material for unit of time. Nevertheless, foods are characterized by extraordinary differences in terms of rheological properties and often, the behavior of the printer is not appropriate for them with the need of important adjustment.

The *layer height* is the distance between consecutive layers during the printing. In addition, it may be defined as the distance between the tip of the nozzle and the bed of the printer. This is one of the most important variables affecting the visual aspect of the 3D printed objects because it determines the resolution in the Z-axis. In fact, the layer height influences the surface details and printing accuracy: the thinner is the layer height, the greater the number of layers printed per millimeter and the smoother is the surface of the printed object. However, when reducing the layer height, the printing time may significantly increase with negative impact on the practical application of this technique. The layer height must be defined according to the nozzle size being the quality of the final product strictly related to these two

parameters. Moreover, the layer height affects the entire stability of the object as described subsequently.

The *nozzle size* defines the diameter of the nozzle. In theory, nozzle size and layer height need to be set equal; however, for practical use, the rule is the following: the layer height needs to be lower than the nozzle size.

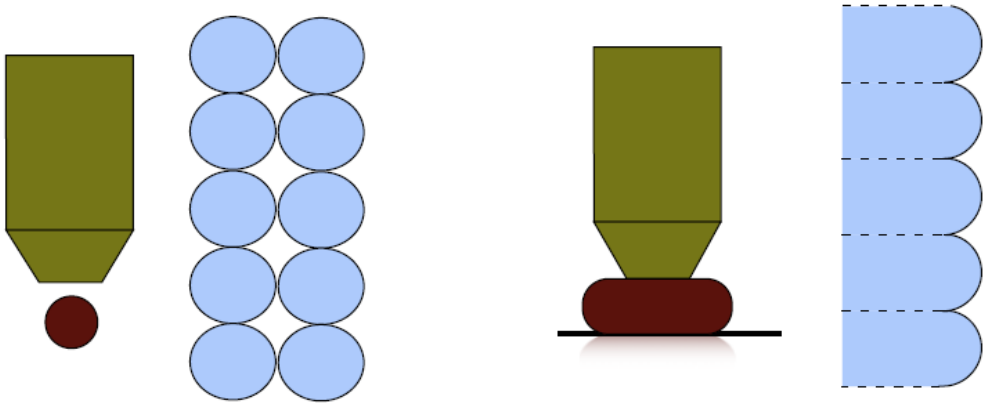

Figure 8. Material deposition by using different layer heights: Layer height equal to nozzle diameter (left side); layer height lower than nozzle diameter (right side).

Figure 8 is a schematic representation of these different conditions. While on the left side the utilized layer height is equal to nozzle size with a circular cross-section that does not allow a good adhesion between the layers, on the right is shown a condition in which the layer height is lower than nozzle size. This situation presents a greater surface contact having the deposited filament a rectangular section that significantly improves the stability of the 3D printed object. For what concerns this common dimension for the printing of thermoplastic materials is 0.3-0.4 mm (Daminabo et al., 2020) that, unfortunately, is not feasible for foods because of their inhomogeneity and the presence of solid particles that could clog the tip. Therefore, for food applications, nozzle sizes ranging between 0.4 mm to 1.5 mm are currently used while the literature (Yang et al., 2018; Derossi et al., 2020; Kim et al., 2021; Nijdam et al., 2021) reports a layer height of about 80% of the nozzle diameter. Also, the Eq. 1 (Wang and Shaw, 2005; Hao et al., 2010) may be used to individuate the critical layer height, h_c, resulting from the ratio between the extruding speed (V_d, mm3/s) and the product of the print speed (v_n, mm/s) and diameter of nozzle (D_n, mm). If layer height is lower than h_c the material deposited is too much and it is squeezed for over deposition. On the other hand, if the layer height is greater than the h_c, too much space between the last layer and the nozzle creates several discrepancies and a very low printing quality. In this case, the layer does not adhere adequately to the previous layer involving an object.

$$h_c = \frac{V_d}{v_n D_n} \qquad (1)$$

The *extrusion rate*, also called flow rate, defines the amount (the volume) of material deposited for unit time (mm^3/s). Unfortunately, it is not possible for the user to directly control this parameter as the slicing software does not contain this variable. Of course, this is because the extrusion rate tightly depends on the materials properties that, in the case of food materials, often are not homogeneous within the same food (highly variables) and completely different any time we change a single ingredient in a complex food formula. Wang and Shaw (2005), studying the 3DP of porcelain slurry for dental applications, proposed different version of Eq. 1:

$$\nu = \frac{Q}{A} = \frac{Q}{\frac{1}{4}\pi d^2} \qquad (2)$$

$$V_d = \frac{\pi}{4} v_n D_n^2 = \frac{\pi}{4} v_n h_c^2 \qquad (3)$$

where h_c (mm) is the critical layer height, V_d (mm^3/s) is the volume extruded per unit of time (i.e., extrusion rate), v_n (mm/s) is the print speed and D_n (mm) is the nozzle diameter. So, the extrusion rate is strictly linked to print speed and the area of the cross-section. The extrusion rate may be also defined as the amount that the piston needs to move to extrude 1 mm of track and it is independent by the nozzle diameter (Fig. 9)

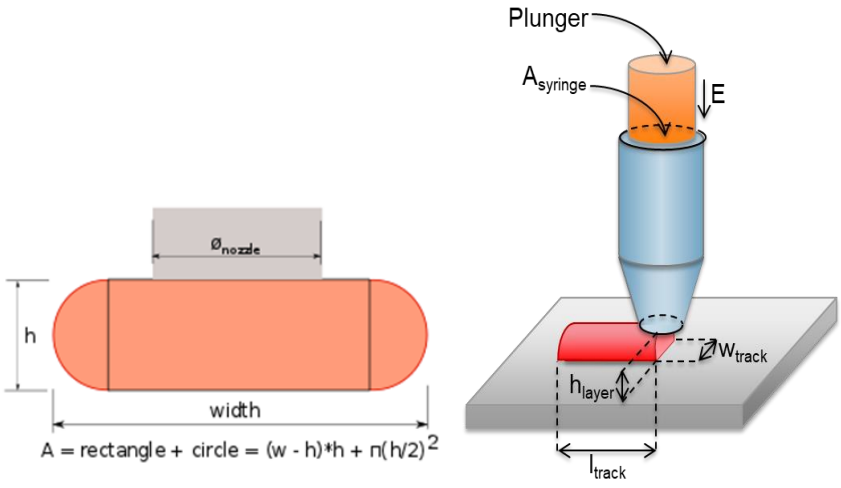

Figure 9. Graphic representation of extrusion formula

Furthermore, there is a ‘compensation parameter’ the *flow (%),* that can be used to reduce or to increase the amount of deposited material during printing. More clearly, the flow allows us to correct the amount of extruded material if, during the printing, it exceeds or fails the right amount.
Another very important parameter is the so-called *infill level of* fill density, which defines the internal filling of the object. For example, an infill of 50%, will allow to fill the inner part of the object of 50% of its volume. Of great importance is the infill path that defines the geometry of the filling (Figure 10). Keeping constant the infill level, the different paths could affect the mechanical properties of the printed object and, for what regard the food materials, the capability to sustain the weight of overlying layers preventing collapses. In addition, the use of different infill levels and infill paths could be used to obtain specific (desired, customized) texture properties (crunchiness, hardness, etc.).

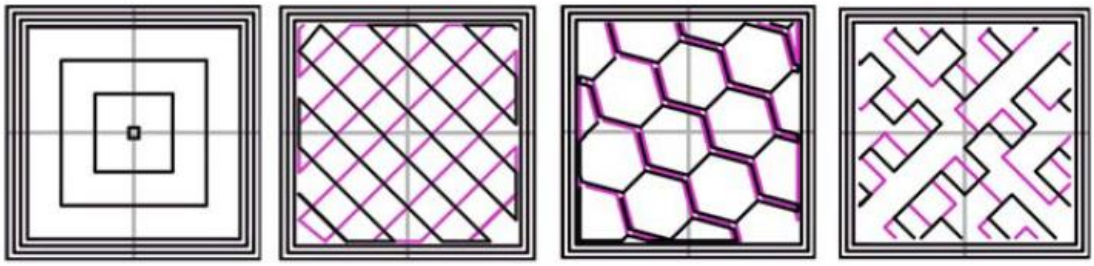

Figure 10 . Schematic representation of some infill patterns used for 3D printing. From right to left: concentric, linear, honeycomb, Hilbert curve (manual.slic3r.org/expert-mode/infill)

Retraction is an important variable for a good quality of printing. It allows us to avoid the oozing of the materials through the nozzle during the non-printing movements. The retraction is controlled by the retraction speed (mm/s) and retraction distance (mm) which are respectively the speed at which the screw rotates in the opposite direction of the deposition and of how much the material must retreat upwards to prevent it from escaping.

Travel speed (mm/s) or the speed of the printer axis during non-printing movements is an important variable especially when the g-code shows long travel movements. It should be faster than print speed with the aim to reduce the overall printing time. However, for food formulas, the syringe produces a small amount of material when it moves before depositing new material above all when the food ink is soft.

1.4 Main printable food materials

During the last 10 years of the application of the 3D printing in the food sector, the published experiments revealed the complexity of printing food materials. All these are completely different from thermoplastic materials such as polylactic acid (PLA) and butadiene styrene acrulonitrile (ABS). Some foods are more suitable for printing by one technology than by another, others show better rheological features extrusion. For example, chocolate was the first food used to print innovative edible structures. This is probably because, as PLA, chocolate easily melts at 50°C and solidifies very fast during its deposition. Also, cereal dough may be easily printed due to its homogeneous viscosity. On the contrary, fruit and vegetables are difficult to print due to their low viscosity as well as the high biological variance affected by environmental conditions (Ricci et al., 2019). Food is a complex system of ingredients that certainly influences its rheological properties and consequently the printability of food formula. To print food inks, it is necessary to fully understand the materials properties and the technologies relevant for it, to be able to construct 3DP structures (Manthial et al., 2020).

1.4.1 Cereal Dough

Cereal dough is a viscoelastic wheat structure characterized by a gluten network, starch granules and trapped air bubbles (Quaglia, 1984). To obtain this matrix, the ingredients are mixed homogeneously, in order to trigger the swelling process of gluten proteins. Due to its viscoelastic properties, wheat flour dough has the ability to set during post processing such as baking and frying. Also, such features allow the dough to be a good candidate for 3DP (Lipton et al. 2015). However, some precautions must be taken in order to obtain a good dough to be printed. As suggested by Lipton et al. (2010), mainly it would be necessary to study the recipe with the object to maintain the stability or the use of additives. For example, an alteration in the amount of butter, eggs and sugar may affect the stability of 3D printed food. Also, the success of printing cereal doughs depends on the resting times of the dough and its stress resistance. There are many published papers focused on the 3D printing of the doughs. Severini et al. (2016) (Fig. 11, B) studied the variables affecting the printability and the printing fidelity of cereal snacks while the same authors (Severini et al., 2018) analyzed the printability of cereal dough enriched with edible insects. Figure 11 shows some recent experiments of 3D printing of cereal-based products that, as clearly shown, improved significantly in terms of complex shape, resolution and printing fidelity.

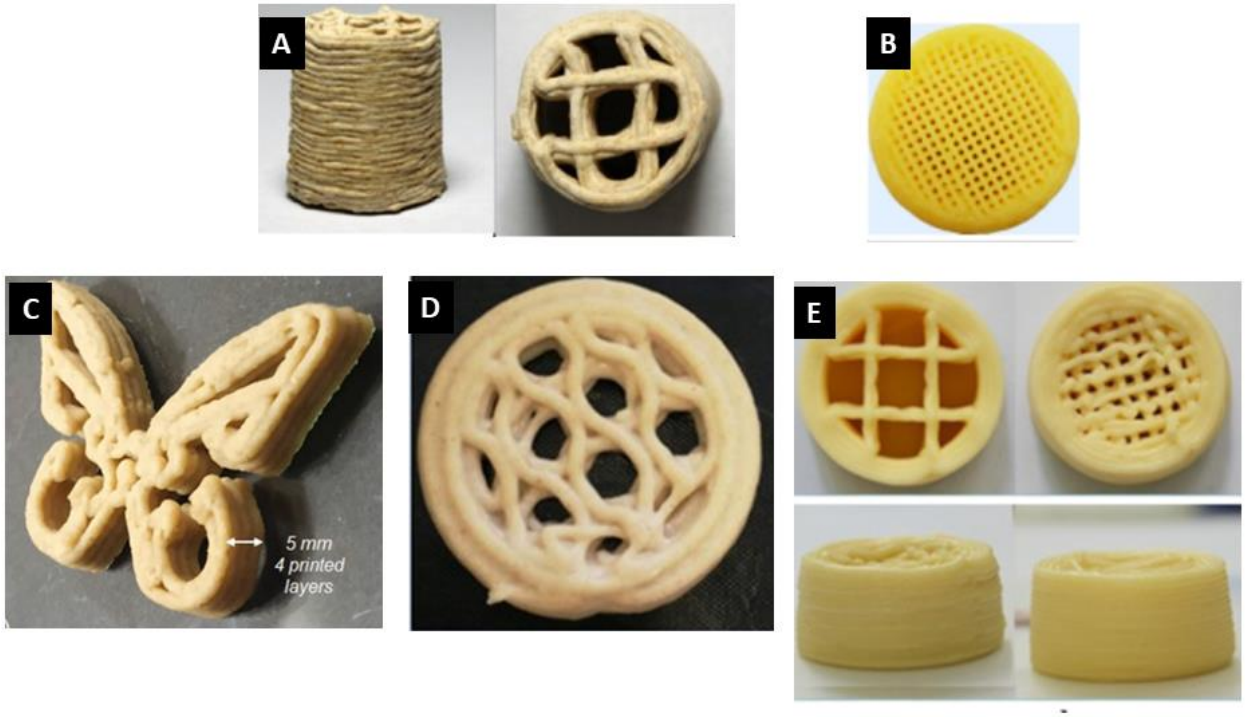

Figure 11. Examples of 3D printed cereal dough: Liu et al., 2021 (A); Severini et al., 2016 (B); Keerthana et al., 2020 (C); Zhang et al., 2018 (D); Liu et al., 2019 (E).

1.4.2 Vegetable blends

Considering their high content in water, fresh fruit and vegetables are highly perishable commodities that, if improperly handled, could deteriorate quickly**.** The majority of fruit and vegetables are consumed fresh; processed to obtain fresh-cut, canned, dried and frozen products or in the form of juice, puree, sauce and soup (Endrizzi et al., 2006; Orsat et al., 2006; Cagno et al., 2011). With the aim of printing plant-based foods, after choosing the fruit and vegetables, the essential step is to prepare a printable paste avoiding accelerating any type of degradation reactions such as browning, microbial growth, oxidations, etc. Moreover, it is important that the obtained paste is homogeneous and has rheological properties suitable for printing. In many cases, it is useful to homogenize or sift the paste; in other cases, the possibility to concentrate the vegetable blend is a good method to improve its printability. Another possibility is the use of hydrocolloids as a thickening agent and for gelling (Burey et al., 2008, Morell et al., 2014). Some examples that can be used for the food industry are agar, alginates, carrageenan, cellulose derivatives, gellan gums however

the most common gelling agent for fruit and vegetable is pectin widely used for many papers (Vancauwenberghe et al., 2015, Vancauwenberghe et al., 2017a, Derossi et al., 2018). Figure 12 represents an example of 3D design and printing of vegetable blend.

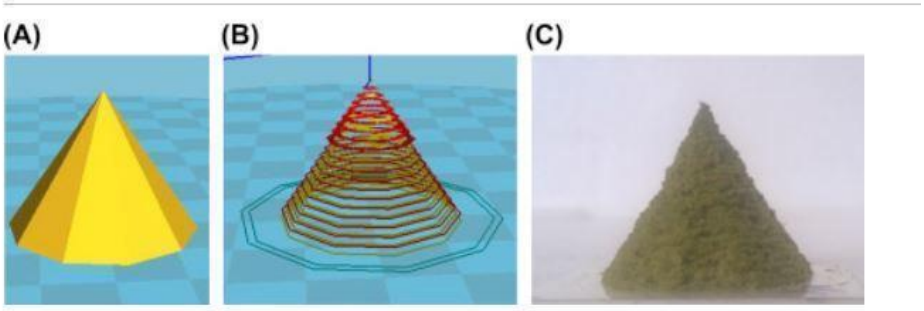

Figure 12. Representative images of the 3D virtual model of printed vegetable blend: overall view (A); sliced model (B) and 3D obtained object (C). (Derossi et al., 2018)

1.4.4 Sugar

With the aim to print granulated or powdered sugar, the only technologies are SLA, SHASAM and binder jetting (Godoi et al., 2016). Sugar can be melted or solubilized by heat or moisture at the surface to fuse adjacent particles (Knecht, 1990). Furthermore, depending on water content, crystalline sucrose melts or decomposes at temperatures from 160 °C to 186 °C (Mantihal et al., 2020). After extrusion processes, powder binding deposition is the second most popular system in 3D food printing. This category can be divided into three sub-types: Selective Laser Sintering (SLS), Selective hot air sintering and melting (SHASAM) and Liquid binding (LB). SHASAM technology uses a narrow and low-velocity hot air beam to selectively fuse together sugar powder, building a two-dimensional (2D) picture out of fused powder. By performing this step many times along the Z direction, a 3D object is gradually built. Selective Laser Sintering (SLS) was used to melt powder by employing a laser. Although SLS has been extensively used to sinter metals, this technology was also adapted for some food applications. In fact, TNO has applied this technology to build objects as a result of the melting sugar of sugar-based powder (Figure 13) (Diaz et al., 2014a, 2014b). Less common is the use of Liquid binding (LB) technology to build 3D sugar structure, most used instead for chocolate and sour candy (Von Hasseln et al., 2014). Some examples of 3d printed sugar are shown in figure 13.

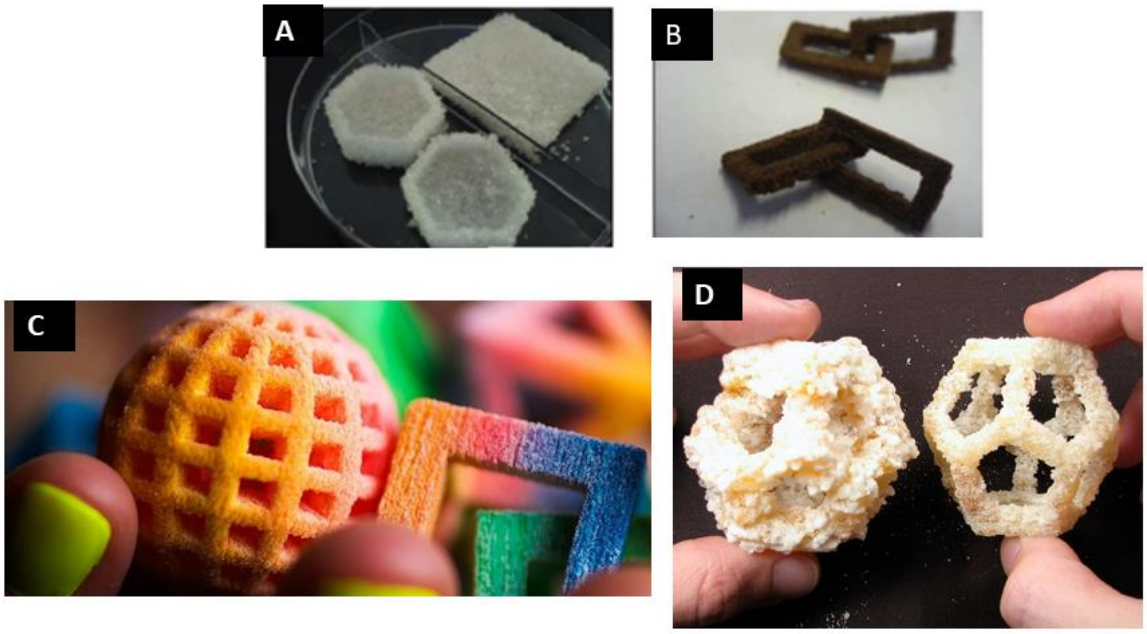

Figure 13. Representative examples of 3D printed sugar sugar (A) and Nesquik (B) (van Bommel, 2014); colourful sugar candies (C) (http://www.3dsystems.com/culinary/gallery); sculpture made of granulated sugar (D) (http://candyfab.org/)

1.4.5 Chocolate

Chocolate is a science-based processing of cocoa products (cocoa liquor, cocoa powder, cocoa butter), sugar, dairy products, spices and surfactants as the basic raw materials after mixing, grinding, refining, tempering, pouring, molding and other scientific processing (Hao et al., 2019). As already mentioned, chocolate was one of the first printed food materials due to its plastic behavior. The first chocolate 3D printer was developed in 2011, and chocolate 3D printers have been available since 2012. Despite the fact that the chocolate melted and solidified at room temperature as happens during the printing of plastic materials, obtaining 3D chocolate objects represented a difficult challenge. As known in fact, during heating the chocolate underwent changes mainly attributable to the forms of cocoa butter crystals. Considering the dark chocolate for example, initially the cocoa butter appearance is as *r* crystals, which have poor stability and a melting point in the range of 16–18°C; followed by α crystalline unstable form with a melting point in the range of 21–24°C. Continuing to maintain at 20°C, the crystalline form of α will gradually become β'' crystalline form with a melting point in the range of 27–29°C, which is a relatively stable crystal form. Under certain conditions, β'' will be changed into β' crystal form and eventually become β crystal form, with a melting point in the range of 34–35°C.

β crystal is the most stable cocoa butter crystal and identifies a good chocolate. Tempering is the process of heating the chocolate to control the pre-crystallization of the beta (β) crystal. The main purpose of chocolate tempering is to stimulate the characterization of triacylglycerols (TAGs) contained in cocoa butter, which provides proper setting characteristics, demolding properties, foam constancy, the snap effect, a glossy appearance, shear and longer shelf-life (Afoakwa et al., 2008; Hao et al., 2019).

During printing chocolate, it is in a fluid state which will solidify at room temperature once deposed. Chocolate is also a non-Newtonian fluid, and there are problems with understanding the flow properties of the material (the relationship between the shear stress and the strain rate is nonlinear) (Hao et al., 2019). Throughout the process of chocolate printing, liquid chocolate is stored in a heated system and passes through a print nozzle with thermal insulation and cooling system to ensure that the ink overlaps layer by layer forming a solid structure. In the 3D extrusion process, controlling the extrusion temperature is fundamental to ensure the pre-crystallization of the beta (β) crystal and also form a stable beta (β) crystal. Given the difficulty of printing a material such as chocolate, some papers investigated the printability of chocolate in terms of nozzle dimension, layer height and print speed (Hao et al., 2010; Lanaro et al, 2017) but sometimes these variables are strictly related to the printer model. For this it is necessary to optimize the printing according to the supplied printer. Figure 14 contains representative images of 3D printed chocolate.

Figure 14. Representative images of 3d printed chocolate: Lanaro et al., 2017 (A, B), ChefJet, 2014(C), Hao et al., 2019 (D), Karavasili et al., 2020 (E), Hao et al., 2010 (F)

1.4.6 Gels

A wide variety of gel materials have been used in 3DP during last year such as semi-solid gel materials like soft single network hydrogels, tough double network gels (Maitra & Sukra, 2014), shape memory gels, ion conductive gels (Wang et al., 2012). Recently, the interest in the use of food-grade gels in 3DFP extensively increased due to their capability to increase the printability of many food materials – including fruit and vegetables - and to mitigate the natural variability of the basic parameters such as viscosity, adhesiveness, fluidity and homogeneity of the food formula. Moreover, these gels are characterized by extended shelf life, customized food design, personalized nutrition, developing edible robots for high impact areas ranging from veterinary care to designing children's toys (Dille et al., 2015; Holland et al., 2018).

The most common gels used in the recently published experiments are of different natures such as vegetable starch made from potato (Chen et al., 2018; Wen et al., 2021); corn (Chen et al., 2019); cassava (Maniglia et al., 2019); buckwheat (Guo et al., 2021); wheat (Maniglia et al., 2020; Zeng et al., 2021). In others works they used some hydrocolloids mixture as agar, gum Arabic, carrageenan, gellan gum, gelatin,

guar gum, xanthan gum, etc (Kim et al., 2018; Gholamipour-Shirazi et al., 2019; Dianez et al., 2019) or they produced gels through the gelation of LM pectin with calcium (Vancauwenberghe et al., 2017; Vancauwenberghe et al., 2018). Figure 15 shows 3d printed food made by gel-inks.

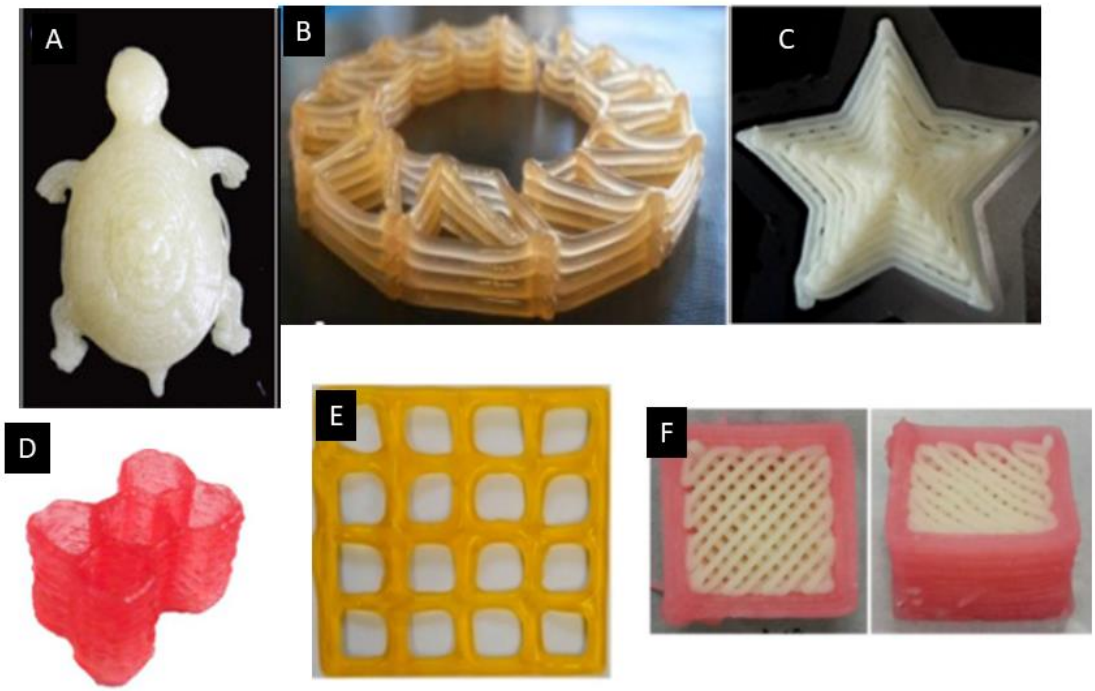

Figure 15. Examples of 3D printed gels: milk protein composite, A (Liu et al., 2019); sodium caseinate dispersion, B (Schutyser et al., 2018); potato starch, C (Shi et al, 2021); pectin based food, D (Vancauwenberghe et al., 2018); gel system of carrageenan-xanthan-starch, E (Liu et al., 2019); mashed potatoes/strawberry juice gel, F (Liu et al., 2018).

1.5 Personalized food products through 3D food printing

The growing interest of researchers and for the creation of unique food properties capable of meeting the consumer's sensory desires and nutritional requirements is translated into the possibility to manufacture personalized foods for people's uniqueness. Among the applications of 3D printing in the food fields, the designing and the production of customized foods is undoubtedly the most relevant application and it represents the greatest possibility in technological and commercial development. 3D printing has the potential to create food with specific properties related to nutritional needs, calorie intake, specific shape, texture, color, or flavor

(Le-Bail et al., 2020). The following section is focused on how food customization has been interpreted through the use of 3D printing.

1.5.1 Nutritional content

Enhancing the nutritional value of food and satisfying the consumer needs through diversification and personalization of food is a new trend in the food market. This trend encourages industrial and scientific organizations to develop new strategies to enhance bioactive constituents in processed foods (Pinheiro et al., 2016). In fact, while the mass customization offers benefits for the economies of scale and economies of scopes, it shows multi-fold problems consisting not only in the obtaining of unique nutritional content and unique sensorial properties but also the guarantee of safety for an appropriate shelf life for a convenient length of time (Derossi et al., 2019). The 3DFP may be considered as the first option to make feasible the concept of food mass-customization. It allows us to create personalized food based on specific properties related to nutritional needs, calorie intake, specific shape, texture, color, or flavor, for example. First of all, the use of different food formulations employed as food inks opens for creating many nutritionally personalized food products. This could be achieved through two different project steps: by developing different ink-foods with a nutritional composition designed for specific groups of consumers or individuals (Derossi et al., 2016), or in the process by using printing techniques called multi-materials that allow depositing different food formulations (each with specific nutritional compositions) on different layers or in different points of the virtual model. In the first case, we have the possibility to modulate the intake of a particular nutrient by changing the size and shape of the printed food, starting from an already balanced formulation for a specific group of consumers. In the second case, the degrees of freedom increase, being able to combine different food formulas obtaining more complex foods. Moreover, 3DFP could improve the consumer's acceptance of some food with high nutritional values but, often, not appreciated for their sensorial properties (i.e. some kind of vegetables or fish). On this point, 3DFP could be used to modulate color, shape, flavor or taste affecting the final sensory experience of the consumers. Taking into account the published data, several studies investigated the possibility to print nutritional balanced food ink obtaining captivating shapes. Kouzani et al. (2017) proposed the use of 3D printing techniques to produce a custom design and production of visually appealing foods, which will be consumed by people with special needs. The authors produced objects based on a mixture of tuna puree (high with protein) to be served for people suffering from dysphagia. Derossi et al. (2018) printed vegetable snacks characterized by the main nutritional requirement for children. The authors were able

to satisfy the 5–10% of the recommended daily intakes (RDA) in energy, vitamin D, calcium and iron. Lille et al. (2018) printed some food pastes made of protein, starch and fiber-rich materials as a first step of the development of healthy and customized snack products as Keerthana et al. 2020 studied the development of fiber-enrich 3D printed snacks based on button mushroom. Several authors investigated the adding of probiotics in 3D printed food as cereal dough (Zhang et al., 2018; Yoha et al., 2021) or potatoes (Liu et al., 2019). With the aim to create food for customized diet Riantinigtyas et al. (2021) focused their efforts on the potential application of 3D printing technology to create protein-rich desserts with multisensory design obtaining an improved acceptance through the printing of multisensory layered design. Shahbazi et al., 2021, instead, printed a reduced-fat cheese with highly poured 3D structure increasing the sensory profile.

1.5.2 Sensorial properties

A second aspect of personalization concerns the control and modification of sensorial properties of foods such as textural properties, aspect, color, odor, etc. Sensory perception is a vital element to determine food quality and its study was introduced by Cohen et al. (2009) who investigated the mouthfeel of different flavouring additives of raspberry, strawberry, banana and chocolate with the addition of xanthan gum and gelatine on 3D printed jelly. The authors reported that the gelatine and xanthan gum only fitted within the weak to firm range within the mouthfeel matrix and shifted more to granularity when these hydrocolloids were combined. Three-dimensional printing technology can potentially improve the visual appeal, can create novel soft texture and, most importantly, can maintain the consistency that is critical for particular consumer groups. The mechanical properties of foods such as texture, crunchiness, chewability, fracturing, adhesiveness, etc. have effects not only on sensory acceptability of consumers, but moreover modulating texture can meet some specific needs of specific people (elderly people, teen-ager, etc.). For instance, Lipton et al. (2015) reported that texturized food from vegetable puree was constructed using 3DP technology to overcome dysphagia among the elderly. This modification of the texture allows the patients to eat the food without any problem thus increasing the quality of the daily diet. In 3DP, the texture can be modified by manipulating the internal structure of the target design. The customization of the mechanical properties is possible through 3D printing technology much more than other traditional techniques because. Several studies have investigated the effects of the internal structure on textural and mechanical properties of 3D constructs. Pant et al., (2020) printed fresh vegetables adding hydrocolloids for dysphagic patients. Derossi et al. (2021) explored the effect of 3D printing on microstructure and the texture of cereal-

based snacks obtained by using different kinds of fats and a blend of wheat/rice flours. The authors proved that 3DFP significantly affects the microstructure of food in comparison to traditional technique and this also affects the mechanical properties of the end-products. Liu et al., (2021) studied the effect of different ingredients and infill structures on microwave post-processed 3D printed potatoes. Xing et al., 2022 used 3D printing was used to develop black fungi-based dysphagia-oriented diet adding xanthan gum.

A different approach to create 3D printed food with modulated/desired texture properties is the designing of digital models and the prediction of the texture before the printing process. The first methodology is the creation of mathematical correlations between some structural properties of the digital model and the texture characteristics of the food, such as the correlation between stress at break point and porosity distribution of printed foods (Derossi, 2020). A second methodology is based on the application of the finite element method (FEM) to 3D printed foods with the aim of obtaining a prediction of mechanical behavior of food structures without a prior correlation between experimental and predicted data (Vancauwenberghe et al., 2018; Piovesan et al., 2020). FEM is a common approach for the prediction of mechanical stress in several non-food materials (Essongue et al., 2021) and consists of four steps-namely: modeling of the geometry, meshing (discretization), specification of material property, specification of boundary, and initial and loading conditions (Liu et al., 2003). It was originally developed for solving problems in solid-state mechanics (plate-bending problems to be more precise), but it is currently applied in all areas of computational physics and engineering (Rapp, 2017) food field included. In the finite element method, the domain (or virtual 3D structure) is discretized into small elements to simplify the physical study.

1.6 References

3D Printing Industry (2014) History of 3D printing: the free beginner's guide Retrieved from http://3dprintingindustry.com/3d-printing-basics-free-beginners-guide/history/

Afoakwa, E., O., Paterson, A., Fowler, M., Ryan, A. (2008). Flavor Formation and Character in Cocoa and Chocolate: A Critical Review. Critical Reviews in Food Science and Nutrition, 48, 2008 - Issue 9. https://doi.org/10.1080/10408390701719272.

Ahn, S., And, A. R., Wright, P., Montero, M., Odell, D., Roundy, S., Wright, P. Anisotropic material properties of fused deposition modeling ABS. Rapid Prototyping Journal doi:10.1108/13552540210441166

Bhandari, B., Bansal, N., Zhang, P. Schuck, M. (2013). Handbook of Food Powders. Processes and Properties. Woodhead Publishing Ltd., UK (2013)

Bilbao, E., Kapadia, S., Riechert, V., Amalvy, J., Molinari, F. N., Escobar, M. M., Baumann, R. R., Monsalve; L. N. (2021). Functional aqueous-based polyaniline inkjet inks for fully printed high-performance pH-sensitive electrodes. Sensors and Actuators B: Chemical, 346, 130558. https://doi.org/10.1016/j.snb.2021.130558

Boutouchent, A., Industry 4.0 : The 4 Technologies Behind (2016). https://www.manufacturing-trends-industry-4-technologies/

Burey, P., Bhandari, B., Howes, T., Gidley, M. (2008). Hydrocolloid gel particles: formation, characterization, and application. Critical Reviews in Food Science and Nutrition, pp. 361-377. https://doi.org/10.1080/10408390701347801.

CandyFab (2019). www.candyfab.org

ChefJet. https://makezine.com/2014/01/07/3d-systems-breaks-the-mold-sugar-chocolate-ceramic-and-full-color-powder-3d-printing-on-your-desktop/

Chen, H., Xie, F., Chen, L., Zheng, B. (2019). Effect of rheological properties of potato, rice and corn starches on their hot-extrusion 3D printing behaviors. Journal of Food Engineering, 244, 150-158. https://doi.org/10.1016/j.jfoodeng.2018.09.011

Chen, Q., Mangadlao, J. D., Wallat, J., De Leon, A., Pokorski, J. K., Advincula, R. C. (2017). 3D Printing Biocompatible Polyurethane/Poly(lactic acid)/Graphene Oxide Nanocomposites: Anisotropic Properties. ACS Appl. Mater. Interfaces 2017, 9, 4, 4015–4023. https://doi.org/10.1021/acsami.6b11793

Chou, W., Gamboa, A., Morales, J. O. (2021). Inkjet printing of small molecules, biologics, and nanoparticles. Inkjet printing of small molecules, biologics, and nanoparticles, 600, 120462. https://doi.org/10.1016/j.ijpharm.2021.120462

Cohen, D.L., Lipton, J.I., Cutler, M., Coulter, D., Vesco, A., Lipson, H. (2009). Hydrocolloid Printing: A Novel Platform for Customized Food Production Lipton, J.I., Cutler, M., Nigl, F., Cohen, D., Lipson, H. (2015). Additive manufacturing for the food industry. Trends in Food Science & Technology, 43, Issue 1, Pages 114-123. https://doi.org/10.1016/j.tifs.2015.02.004

Cuq, B., Mandato, S., Supagro, M., Jeantet, R., Ouest, A., Saleh, K., De, U. Y., Ruiz, T., Montpellier, U. 2013. Agglomeration/Granulation in Food Powder Production in Handbook of Food Powders: Processes and Properties Woodhead Publishing Limited, doi: 10.1533/9780857098672.1.150

Daminabo, S. C., Goel, S., Grammatikos., S. A., Nezhad, H. Y., Thakur, V. K. (2020). Fused deposition modeling-based additive manufacturing (3D printing): techniques for polymer material systems. Materials Today Chemistry, 16, 100248. https://doi.org/10.1016/j.mtchem.2020.100248

Derossi, A., A. Husain, R. Caporizzi, and C. Severini. 2020. Manufacturing personalized food for people uniqueness. An overview from traditional to emerging technologies. Critical Reviews in Food Science and Nutrition 60 (7):1141–59. doi: 10.1080/10408398.2018.1559796.

Derossi, A., A. Husain, R. Caporizzi, and C. Severini. 2020. Manufacturing personalized food for people uniqueness. An overview from traditional to emerging technologies. Critical Reviews in Food Science and Nutrition 60 (7):1141–59. doi: 10.1080/10408398.2018.1559796.

Derossi, A., Caporizzi, R., Ricci, I., Severini, C. 2019. Critical Variables in 3D Food Printing.

Fundamentals of 3D Food Printing and Application, 41-91. https://doi.org/10.1016/B978-0-12-814564-7.00003-1

Derossi, A., Husain, A., Caporizzi, R., Severini, C. (2020). Manufacturing personalized food for people uniqueness. An overview from traditional to emerging technologies. Critical Reviews in Food Science and Nutrition, 60, 2020 - Issue 7. https://doi.org/10.1080/10408398.2018.1559796

Derossi, A., R. Caporizzi, D. Azzollini, and C. Severini. 2018. Application of 3D printing for customized food. A case on the development of a fruit-based snack for children. Journal of Food Engineering 220:65–75. doi: 10.1016/j.jfoodeng.2017.05.015.

Derossi, A., R. Caporizzi, D. Azzollini, and C. Severini. 2018. Application of 3D printing for customized food. A case on the Development of a fruit-based snack for children. Journal of Food Engineering 220:65–75. doi: 10.1016/j.jfoodeng.2017.05.015.

Derossi, A., R. Caporizzi, L. Ricci, and C. Severini. 2019. Critical variables in 3D food printing. In Fundamentals of 3D food printing and applications, F. C. Godoi, B. R. Bhandari, S. Prakash, and M. Zhang, 41–91. London, UK: Academic Press. doi: 10.1016/B978-0-12-814564-7.00003-1

Derossi, A., R. Caporizzi, L. Ricci, and C. Severini. 2019. Critical variables in 3D food printing. In Fundamentals of 3D food printing and applications, F. C. Godoi, B. R. Bhandari, S. Prakash, and M. Zhang, 41–91. London, UK: Academic Press. doi: 10.1016/B978-0-12-814564-7.00003-1.

Derossi, A., R. Caporizzi, M. Paolillo, and C. Severini. 2021. Programmable texture properties of cereal-based snack mediated by 3D printing technology. Journal of Food Engineering 289:110160. doi: 10.1016/j.jfoodeng.2020.110160.

Derossi, A., R. Paolillo, C. Caporizzi, and C. Severini. 2020. Extending the 3D food printing tests at high speed. Material deposition and effect of non-printing movements on the final quality of printed structures. Journal of Food Engineering 275:109865. doi: 10.1016/j. jfoodeng.2019.109865.

Dianez, I., Gallegos, C., la Fuente, E. B., Martinez, I., Valencia, C., Sanchez, M.C., Diaz, M.J., Franco, J.M. (2019). 3D printing in situ gelification of κ-carrageenan solutions: Effect of printing variables on the rheological response. Food Hydrocolloids, 87, Pages 321-330. https://doi.org/10.1016/j.foodhyd.2018.08.010

Diaz, J.V. , Van Bommel, K.J.C., Noort, M.W., Henket, J., Brier, P. (2014). Preparing Edible Product, Preferably Food Product Including Bakery Product, and Confectionary Product, Involves Providing Edible Powder Composition, and Subjecting Composition to Selective Laser Sintering. The Netherlands.

Diaz, J.V., Van Bommel, K.J.C, Noort, M.W, Henket, J., Briër, P. (2014). Method for the Production of Edible Objects Using Sls and Food Products. Google Patents (2014)

Dille, M. J., Draget, K. I., Hattrem, M. N. (2015). The effect of filler particles on the texture of food gels. In Modifying Food Texture. Volume 1: Novel Ingredients and Processing Techniques Woodhead Publishing Series in Food Science, Technology and Nutrition, Pages 183-200. https://doi.org/10.1016/B978-1-78242-333-1.00009-7

Ebrahimi, A., Tovar-Lopez, F. J., Scott, J., Ghorbani, K. (2020). Differential microwave sensor for characterization of glycerol–water solutions. Sensors and Actuators B: Chemical, 321, 128561. https://doi.org/10.1016/j.snb.2020.128561

Eleftheriadis, G. K., Katsiotis, C. S., Andreadis, D. A., Tzetzis, D., Ritzoulis, C., Bouropoulos, N., Katsiotis, C. S. (2020). Inkjet printing of a thermolabile model drug onto FDM-printed substrates: formulation and evaluation. Drug Development and Industrial Pharmacy, 46, 8, 1253-1264. https://doi.org/10.1080/03639045.2020.1788062

Essongue, S., Couégnat, G., Martin, E. (2021). Finite element modelling of traction-free cracks: Benchmarking the augmented finite element method (AFEM). Engineering Fracture Mechanics, 253, 107873. https://doi.org/10.1016/j.engfracmech.2021.107873

FoodJet. 2019. https://www.foodjet.com/

Gholamipour-ShiraziIan, A. Nortno, I. T., Mills, T. (2019). Designing hydrocolloid based food-ink formulations for extrusion 3D printing. Food Hydrocolloids, 95, Pages 161-167. https://doi.org/10.1016/j.foodhyd.2019.04.011.

Godoi, F. C., Bhandari, B. R., Prakash, S., Zhang, M. (2019). An Introduction to the principles of 3D Food Printing. In Fundamentals of 3D food printing and applications, F. C. Godoi, B. R. Bhandari, S. Prakash, and M. Zhang, 41–91. London, UK: Academic Press. doi: 10.1016/B978-0-12-814564-7.00001-8

Godoi, F. C., Prakash, S., & Bhandari, B. R. (2016). 3D Printing technologies applied for food design: Status and prospects. Journal of Food Engineering, 179, 44–54. https://doi.org/10.1016/j.jfoodeng.2016.01.025

Goole, J., Amighi, K. (2016). 3D printing in pharmaceutics: A new tool for designing customized drug delivery systems. International Journal of Pharmaceutics, 499, 376-394.

Grood, J.P.W. , Grood, P.J. (2011). Method and device for dispensing a liquid. Google Patents (2011)

Grood, J.P.W., Grood, P.J., 2011. Method and device for dispensing a liquid. Google Patents.

Guo, C, Zhang, M., Bhandari, B. (2019). Model Building and Slicing in Food 3D Printing Processes: A Review. Comprehensive Reviews in Food Science and Food Safety. https://doi.org/10.1111/1541-4337.12443

Hao , L., Mellor, S., Seaman, O., Henderson, J., Sewell, N., Sloan, M. (2010). Material characterisation and process development for chocolate additive layer

manufacturing. Virtual and Physical Prototyping, 5, 2010 - Issue 2. https://doi.org/10.1080/17452751003753212

Hao, L., Li, Y., Gong, P., Xiong, W. (2019). Material, Process and Business Development for 3D Chocolate Printing. In Fundamentals of 3D food printing and applications, F. C. Godoi, B. R. Bhandari, S. Prakash, and M. Zhang, 207-255. London, UK: Academic Press. https://doi.org/10.1016/B978-0-12-814564-7.00008-0.

Hao, L., Mellor, S., Seaman, O., Henderson, J., Sewell, N. Sloan, M. (2010).Material characterization and process development for chocolate additive layer manufacturing. Virtual and Physical Prototyping, 5 (2), pp. 57-64. Doi: 10.1080/17452751003753212.

He, Y., Foralosso, R., Trindade, G.F., Ilchev, A., Ruiz-Cantu, L., Clark, E.A., Khaled, S., Hague, R.J.M., Tuck, C.J., Rose, F.R.A.J., Mantovani, G., Irvine, D.J., Roberts, C.J., Wildman, R.D., 2020. A reactive prodrug ink formulation strategy for inkjet 3D printing of controlled release dosage forms and implants. Adv. Therap. 3, 1900187.https://doi.org/10.1002/adtp.201900187.

Holland, S., Foster, T., Tuck, C. (2019). Creation of Food Structures Through Binder Jetting. In Fundamentals of 3D food printing and applications, F. C. Godoi, B. R. Bhandari, S. Prakash, and M. Zhang, 257-288. London, UK: Academic Press. doi:10.1016/B978-0-12-814564-7.00009-2

Holland, S., Tuck, C., Foster, T. (2018). Fluid Gels: a New Feedstock for High Viscosity Jetting. Food Biophysics, 13, 175–185.

Icten, E., Purohit, H.S., Wallace, C., Giridhar, A, Taylor, L.S., Nagy, Z. K. et al. (2017). Dropwise additive manufacturing of pharmaceutical products for amorphous and self-emulsifying drug delivery systems. International Journal of Pharmaceutics, 524, 424-432.

Izdebska, J.(2016). Printing on Polymers: theory and practice. In Printing on Polymers. Fundamentals and Applications. https://doi.org/10.1016/B978-0-323-37468-2.00001-4

Jiang, Q., Zhang, M., Mujumdar, A. S. (2021). Novel evaluation technology for the demand characteristics of 3D food printing materials: a review. Critical Reviews in Food Science and Nutrition. https://doi.org/10.1080/10408398.2021.1878099.

Jin, Y., He, Y., Fu, G., Zhang,, A., Du, J. (2017). A non-retraction path planning approach for extrusion-based additive manufacturing. Robotics and Computer-Integrated Manufacturing, 48 (2017), pp. 132-144 . doi: 10.1016/j.rcim.2017.03.008.

Karavasili, K., Gkaragkounis, A., Moschakis, T., Ritzoulis, C., Fatouros, D. G. (2020). Pediatric-friendly chocolate-based dosage forms for the oral administration of both hydrophilic and lipophilic drugs fabricated with extrusion-based 3D printing. European Journal of Pharmaceutical Sciences, 147, 105291. https://doi.org/10.1016/j.ejps.2020.105291

Keerthana, K., Anukiruthika, T., Moses, J.A., Anandharamakrishnan, C. (2020). Development of fiber-enriched 3D printed snacks from alternative foods: A study on button mushroom. Journal of Food Engineering, 287, December 2020, 110116. Doi: 10.1016/j.jfoodeng.2020.110116Get

Kewuyemi, Y. O., Kesa, H., O. A. Adebo. 2021. Trends in functional food development with three-dimensional (3D) food printing technology: prospects for value-added traditionally processed food products. Critical Reviews in Food Science and Nutrition. https://doi.org/10.1080/10408398.2021.1920569

Khong, D., Maniruzzaman, M., Nokhodchi, A. (2018). Advanced Pharmaceutical Applications of Hot-Melt Extrusion Coupled with Fused Deposition Modelling (FDM) 3D Printing for Personalised Drug Delivery, 0(4), 203; https://doi.org/10.3390/pharmaceutics10040203.

Kim, H. W., Bae, H., Park, H. J. (2021). Preparation and characterization of surimi-based imitation crab meat using coaxial extrusion three-dimensional food printing. Innovative Food Science & Emerging Technologies, 71, 102711. https://doi.org/10.1016/j.ifset.2021.102711

Kim, H.W., Bae, H., Park, H.J. (2017). Classification of the printability of selected food for 3D printing: development of an assessment method using hydrocolloids as reference material. Journal of Food Engineering, 215,pp. 23-32. doi: 10.1016/j.jfoodeng.2017.07.017.

Kim, H.W., Lee, J. H., Park, S. M., Lee, M. H., Lee, I. W., Doh, H. S., Park, H. J. (2018). Effect of Hydrocolloids on Rheological Properties and Printability of Vegetable Inks for 3D Food Printing. JOURNAL OF Food Science. https://doi.org/10.1111/1750-3841.14391

Knecht, R. L. (1990). Properties of sugar. In Chemistry of sucrose, Chapter 4.

Kouzani, A. Z., Adams, Scott, Whyte, Daniel J, Oliver, Russell, Hemsley, Bronywn, Palmer, Stuart and Balandin, Susan 2017, 3D printing of food for people with swallowing difficulties, in DesTech 2016: Proceedings of the International Conference on Design and Technology, Knowledge E, Dubai, United Arab Emirates, pp. 23-29, doi: 10.18502/keg.v2i2.591.

Kouzani, A.Z., Adams, S., Whyte, D.J., Oliver, R., Hemsley, B., Palmer, S., Balandin, S. 3D printing of food for people with swallowing difficulties. DesTech Conference Processdings, The International Conference on Design and Technology, vol. 2017, KnE Engineering (2017), pp. 23-29

Kruth, J. P., Wang, X., Laoui, T., Froyen, L. (2003). Lasers and Materials in Selective Laser Sintering. Assembly Automation, 23, doi: 10.1108/01445150310698652.

Lanaro, M., Forrestal, D. P., Scheurer, S., Slinger, D. J., Liao, S., Powell, S. K., Woodruff, M. A.(2017). 3D printing complex chocolate objects: Platform design, optimization and evaluation. Journal of Food Engineering, 215, Pages 13-22. https://doi.org/10.1016/j.jfoodeng.2017.06.029

Le-Bail, A., Manigli, B.C., Le-Bail, P.(2020). Recent advances and future perspective in additive manufacturing of foods based on 3D printing. Current Opinion in Food Science, 35, Pages 54-64. https://doi.org/10.1016/j.cofs.2020.01.009

Lille, M., Nurmela, A., Nordlund, E.,Metsä-Kortelainen, S., Soz, N. (2018). Applicability of protein and fiber-rich food materials in extrusion-based 3D printing Journal of Food Engineering, 220, March 2018, Pages 20-27. https://doi.org/10.1016/j.jfoodeng.2017.04.034

Lipton, J., D. Arnold, F. Nigl, N. Lopez, D. Cohen, N. Noren, and H. Lipson. 2010. Mutli-material food printing with complex internal structure suitable for conventional post-processing. Paper presented at the 21st Annual International Solid Freeform Fabrication (SFF) symposium, Texas, August 9–11, 2010, 809–15. http://sffsymposium. engr.utexas.edu/Manuscripts/2010/2010-68-Lipton.pdf.

Liu, Y., Liang, X., Saeed, A., Lan, W., Qin, W. (2019). Properties of 3D printed dough and optimization of printing parameters. Innovative Food Science & Emerging Technologies, 54, June 2019, Pages 9-18. Doi: doi.org/10.1016/j.ifset.2019.03.008.

Liu, Y., Yi, S., Ye, T., Leng, Y., Hossen, M. A., Sameen, D. E., Dai, J., Li, S., Qin, W. (2021). Effects of ultrasonic treatment and homogenization on physicochemical

properties of okara dietary fibers for 3D printing cookies. Ultrasonics Sonochemistry, 77, September 2021, 105693

Liu, Y., Yu, Y., Liu, C., Regenstein, J. M., Liu, X., Zhou, P. (2019). Rheological and mechanical behavior of milk protein composite gel for extrusion-based 3D food printing. LWT,102, Pages 338-346. https://doi.org/10.1016/j.lwt.2018.12.053.

Liu, Z., Bhandari, B., Prakash, S., Mantihal, S., Zhang, M. (2019). Linking rheology and printability of a multicomponent gel system of carrageenan-xanthan-starch in extrusion based additive manufacturing. Food Hydrocolloids, 87, Pages 413-424. https://doi.org/10.1016/j.foodhyd.2018.08.026

Liu, Z., Bhandari, B., Zhang, M. (2020). Incorporation of probiotics (Bifidobacterium animalis subsp. Lactis) into 3D printed mashed potatoes: Effects of variables on the viability. Food Research International, 128, 108795. https://doi.org/10.1016/j.foodres.2019.108795.

Liu, Z., Zhang, M. (2021). Texture properties of microwave post-processed 3D printed potato snack with different ingredients and infill structure. Future Foods, 3, 100017. https://doi.org/10.1016/j.fufo.2021.100017

Liu, Z., Zhang, M., Bhandari, B., Wang, Y. (2017). 3D printing: printing precision and application in food sector. Trends in Food Science and Technology, doi: 10.1016/j.tifs.2017.08.018.

Liu, Z., Zhang, M., Yang, C. (2018). Dual extrusion 3D printing of mashed potatoes/strawberry juice gel LWT, 96, Pages 589-596. https://doi.org/10.1016/j.lwt.2018.06.014

Maniglia, B. C., Lima, D. C., da Matta Junior, M. Oge, A., Le-Bail, P., Augusto, P.E.D., Le-Bail, A. (2020). Dry heating treatment: A potential tool to improve the wheat starch properties for 3D food printing application. Food Research International, 137, 109731. https://doi.org/10.1016/j.foodres.2020.109731

Mantihal, S., Kobun, R., Lee, B. (2020). 3D food printing of as the new way of preparing food: A review. International Journal of Gastronomy and Food Science, 100260. https://doi.org/10.1016/j.ijgfs.2020.100260

Mantihal, S., Prakash, S., Condi Godoi, F., Bhandari, B. (2018). Optimization of chocolate 3D printing by correlating thermal and flow properties with 3D structure modeling. Innovative Food Science and Emerging Technologies (2018), 10.1016/j.ifset.2017.09.012.

Morell, P., Fiszman, S., Varela, P., Hernando, I. (2014). Hydrocolloids for enhancing satiety: relating oral digestion to rheology, structure and sensory perception. Food Hydrocolloids, 41, pp. 343-353. https://doi.org/10.1016/j.foodhyd.2014.04.038.

Nijdam, J. J., Agarwal, D., Schon, B. S. (2021). An experimental assessment of filament-extrusion models used in slicer software for 3D food-printing applications. Journal of Food Engineering., 110711. https://doi.org/10.1016/j.jfoodeng.2021.110711

Oskay, W., Edman, L. (2019). The CandyFab Project

Pekarovicova, A., Husovska, V. 2016. Printing Ink Formulations. in Printing on Polymers. https://doi.org/10.1016/B978-0-323-37468-2.00003-8

Pietsch, W. (1997). Size enlargement by agglomeration. Fayed, M. E., Otten, L., Handbook of Powder Science & Technology, Springer, Boston, MA, 202-377.

Pinheiro, A. C., Coimbra, M. A., Vicente, A. A. (2016). In vitro behaviour of curcumin nanoemulsions stabilized by biopolymer emulsifiers – Effect of interfacial composition. Food Hydrocolloids, 52, Pages 460-467. https://doi.org/10.1016/j.foodhyd.2015.07.025

Prakash, S., Bhandari, B. R., Godoi, F. C., Zhang, M. (2019). Future Outlook of 3D Food Printing. Fundamentals of 3D Food Printing and Applications, Chapter 13, Pages 373-381

Rapp, B.E. (2017). Microfluidics: Modeling, Mechanics and Mathematics. Elsevier.

Riantiningtyas, R.R., Sager, V.F., Chow, C.Y., Thybo, C.D., Bredie, W.L.P., Ahrné, L.(2021). 3D printing of a high protein yoghurt-based gel: Effect of protein enrichment and gelatine on physical and sensory properties. Food Research International147, 110517. https://doi.org/10.1016/j.foodres.2021.110517

Ricci, I., Derossi, A., Severini, C. (2019). 3D Printed Food From Fruits and Vegetables. In Fundamentals of 3D food printing and applications, F. C. Godoi, B. R. Bhandari, S. Prakash, and M. Zhang, 117-149. London, UK: Academic Press. doi: 10.1016/B978-0-12-814564-7.00005-5

Severini, C., Derossi, A., Azzollini, D. (2016). Variables affecting the printability of foods: preliminary test on cereal-based products. Innovative Food Science and Emerging Technologies, 38, pp. 281-291. Doi: https://doi.org/10.1016/j.ifset.2016.10.001.

Shahbazi, M., Jäger, H., Ettelaie, R. (2021). Application of Pickering emulsions in 3D printing of personalized nutrition. Part II: Functional properties of reduced-fat 3D printed cheese analogues. Colloids and Surfaces A: Physicochemical and Engineering Aspects, 624, 5 September 2021, 126760. https://doi.org/10.1016/j.colsurfa.2021.126760

Shi, Y.,Zhang, M., Bhandari, B. (2021). Effect of addition of beeswax based oleogel on 3D printing of potato starch-protein system. Food Structure, 27, 100176. https://doi.org/10.1016/j.foostr.2021.100176.

Singh, S., Ramakrishna, S. (2017). Biomedical applications of additive manufacturing: Present and future. Current Opinion in Biomedical Engineering , 2, 105-115.

Subic, A., Gallagher, S. (2017) Industry 4.0 testlabs in Australia. Business, 169662842

Sun, J., Zhou, W., Huang, D., Fuh, J.Y.H., Hong, G., 2015. An overview of 3D printing technologies for food fabrication. Food Bioprocess Technol. 8 (8), 1605e1615

Sun, J., Zhou, W., Yan, L., Huang, D., Lin, L. (2017). Extrusion-based food printing for digitalized food design and nutrition control. Journal of Food Engineering, 1-11, doi:10.1016/j.jfoodeng.2017.02.028.

TNO (2017). The Future of Food. Retrieved from:https://www.tno.nl/media/2216/future_of_food.pdf

TNO, 2017. The Future of Food. https://www.tno.nl/media/2216/future_of_food.pdf.

Vancauwenberghe, V., Katalagarianakis, L., Wang, Z., Meerts, M., Hertog, M., Verboven, P., Moldenaers, P., Hendrickx, M.E., Lammertyn, J., Nicolai, B. (2017, a). Pectin based food-ink formulations for 3-D printing of customizable porous food stimulants. Innovative Food Science and Emerging Technologies, 42 (2017), pp. 138-150. Doi: 10.1016/j.ifset.2017.06.011.

Vancauwenberghe, V., Katalagarianakis, L., Wang, Z., Meerts, M., Hertog, M., Verboven, P., Moldenaers, P., Hendrickx, M. E., Lammertyn, J., Nicolai, B. (2017). Pectin based food-ink formulations for 3-D printing of customizable porous food simulants. Innovative Food Science and Emerging Technologies, 42 (2017), pp. 138-150. https://doi.org/10.1016/j.ifset.2017.06.011

Vancauwenberghe, V., Mbong, V.B.M., Vanstreels, E., Verboven, P., Lammertyn, J., Nicolai, B. (2017). 3D printing of plant tissue for innovative food manufacturing: encapsulation of alive cells into pectin based bio-ink. Journal of Food Engineering (2017), pp. 1-11, doi:10.1016/j.foodeng.2017.12.003.

Vancauwenberghe, V., Mbong-Mfortaw, V. B., Kokalj, T., Wang, Z., Verboven, P., Lammertyn, J., Nicolai, B. (2015). Pectin based bio-ink formulations for 3-D printing of porous foods. Proceedings of 29th EFFoST Conference, 10-12 November, Athens, Greece (2015), pp. 409-414

Von Hasseln, K.W., Von Hasseln, E. M., Williams, D. X., Gale, R.R. (2014). Making an Edible Component, Comprises Depositing Successive Layers of Food Material According to Digital Data that Describes the Edible Component, and Applying Edible Binders to Regions of the Successive Layers of the Food Material. 3d Systems Inc (Thde-C) 3d Systems Inc (Thde-C).

Wang, J., Shaw, L.L. (2005). Rheological and extrusion behavior of dental porcelain slurries for rapid prototyping applications. Materials Science and Engineering A, 397 pp. 314-321. Doi:10.1016/j.msea.2005.02.045.

Wen, Y., Che, Q. T., Kim, H. W., Park, H. J. (2021). Potato starch altered the rheological, printing, and melting properties of 3D-printable fat analogs based on inulin emulsion-filled gels. Carbohydrate Polymers, 269, 118285. https://doi.org/10.1016/j.carbpol.2021.118285.

Xing, X., Chitrakar, B., Hati, S., Xie, S., Li, H., Li, C., Liu, Z., Moa, H. (2022). Development of black fungus-based 3D printed foods as dysphagia diet: Effect of gums incorporation. Food Hydrocolloids, 123, 107173. https://doi.org/10.1016/j.foodhyd.2021.107173

Yang, F., C. Guo, M. Zhang, B. Bhandari, and Y. Liu. 2019. Improving 3D printing process of lemon juice gel based on fluid flow numerical simulation. LWT - Foo

Yang, F., M. Zhang, and Y. Liu. 2019. Effect of post-treatment microwave vacuum drying on the quality of 3D-printed mango juice gel. Drying Technology 37 (14):1757–65. doi: 10.1080/07373937.2018.1536884.

Yang, F., M. Zhang, B. Bhandari, and Y. Liu. 2018. Investigation on lemon juice gel as food material for 3D printing and optimization of printing parameters. LWT - Food Science and Technology 87:67–76. doi: 10.1016/j.lwt.2017.08.054.

Yang, F., M. Zhang, S. Prakash, and Y. Liu. 2018. Physical properties of 3D printed baking dough as affected by different compositions. Innovative Food Science & Emerging Technologies 49:202–10. doi: 10.1016/j.ifset.2018.01.001.

Yang, F., M. Zhang, Z. Fang, and Y. Liu. 2019. Impact of processing parameters and post-treatment on the shape accuracy of 3D-printed baking dough. International Journal of Food Science & Technology 54 (1):68–74. doi: 10.1111/ijfs.13904.

Yang, F., Zhang, M., Bhandari, B., 2015. Recent development in 3D food printing. Crit. Rev. Food Sci. Nutr. 1094732. http://dx.doi.org/10.1080/10408398.2015.

Yang, F., Zhang, M., Bhandari, B., Liu, Y. (2018).Investigating on lemon juice gel as food material for 3D printing and optimization of printing parameters. LWT-Food Science and Technology, 87, pp. 67-76. Doi: 10.1016/j.lwt.2017.08.054.

Yoha, K. S., Anukiruthika, T. Anila, W., Moses, J. A., Anandharamakrishnan, C. (2021). 3D printing of encapsulated probiotics: Effect of different post-processing methods on the stability of Lactiplantibacillus plantarum (NCIM 2083) under static in vitro digestion conditions and during storage. LWT, 146, July 2021, 111461. https://doi.org/10.1016/j.lwt.2021.111461

Zeng, L., Ren, A., Liu, R., Xing, Y., Yu, X., Jiang, H. (2022). Effect of sodium chloride solution on quality of 3D-printed samples molded using wheat starch gel. Food Hydrocolloids,123, 107197. https://doi.org/10.1016/j.foodhyd.2021.107197.

Zhang, L., Lou, Y., Schutyser, M. A. I. (2018). 3D printing of cereal-based food structures containing probiotics. Food Structure, 18, October 2018, Pages 14-22. Doi: doi.org/10.1016/j.foostr.2018.10.002.

Zhang, L., Lou, Y., Schutyser, M.A.I.(2018). 3D printing of cereal-based food structures containing probiotics. Food Structure, 18, Pages 14-22. https://doi.org/10.1016/j.foostr.2018.10.002

Ziaee, M., Crane, N. B. (2019). Binder Jetting: A Review of Process, Materials, and Methods. Additive Manufacturing, 28, 781-801. https://doi.org/10.1016/j.addma.2019.05.031

CHAPTER 2 Objects and outlines of research

The main aim of this research was the better understanding and the implementation of 3D Printing in the food sector aiming to contribute to the creation of innovative food with unprecedented properties. A variety of relevant aspects have been studied, primarily, the printing at high speed that could open for a more practical application at industrial level and the capability of modifying the texture properties of the end products by means of accurate design of the digital models. To do this, the thesis is structured in 8 chapters. After a brief introduction of the main ambitions and basic technical background of the 3D food printing (**chapter 1**), the other sections consists of six published papers in international peer reviewed journals.

The **chapter 3** analyze the temporal evolution of 3DFP by drawing the global scientific landscape in these first 13 years of experiments by using bibliometric and data visualization approaches. Precisely the paper analyzed the distribution of scientific documents as a function of time, space, subject area and co-authorship. The paper was titled '*Drawing the scientific landscape of 3D Food Printing. Maps and interpretation of the global information in the first 13 years of detailed experiments, from 2007 to 2020'*

Chapter 4 is dedicated to the study on printing starch-ink-gel materials to deepen the effect of some undervalued variables on the final quality of 3D printed samples. In particular the effect of tapioca starch concentration, the temperature at which it was printed and the resting time of the gels after preparation and before printing were studied by measuring the rheological properties of gels, the force needed to extrude the food ink and dimensions of printed objects that showed the printing fidelity. The paper was titled '*Rheological properties, dispensing force and printing fidelity of starchy-gels modulated by concentration, temperature and resting time'*.

The chapters 5 and 6 has been dedicated to the creation of 3D-printed food with desired and programmable mechanical properties.

C**hapter 5** analyzes the hardness of the printed snacks against the relative density on the basis of the principles of cellular solids through the printing of 3D designs different in the number and the position of the internal voids. The paper was titled '*Programmable texture properties of cereal-based snack mediated by 3D printing technology*.'

Chapter 6 introduces the study of texture based on the Finite Element Method of innovative multi-layers snacks in terms of design. In addition, for the first time in order to extend the common applications of 3D food printing, the 2D X-ray images of plant tissues microstructure were used as CAD model to create unprecedented food

products. The paper was titled '*Extending 3D food printing application. Apple tissues microstructure as CAD model to create innovative cereal-based snacks.*

Chapter 7 addresses on the most important reasons limiting for the large-scale application of 3D. For its practical use, in fact, the increase of the speed of material deposition is a challenge to tackle. For the first time, increasing the print speed of a commercial 3D printer more than the common limits used up to now, we demonstrated it is possible to replicate, with high fidelity, a designed 3D virtual model. In addition, the study of undervalued variables such as retraction distance, the travel speed and retraction speed has shown how these are crucial to high quality printing at high speed. The paper was titled '*Extending the 3D food printing tests at high speed. Material deposition and effect of non-printing movements on the final quality of printed structures*'

Finally, **chapter 8** contains the conclusions and some general discussion of the thesis

Below is reported a list of publications included in the thesis and the participation of international and national congresses

Publications included in this thesis

Derossi, A., Caporizzi, R., Paolillo, M., Oral, M. O., Severini, C. (2021). **Drawing the scientific landscape of 3D Food Printing. Maps and interpretation of the global information in the first 13 years of detailed experiments, from 2007 to 2020**. *Innovative Food Science & Emerging Technologies, 2021; 70: 102689.* This publication is in Chapter 3

Contributors	Statement of contribution
Derossi, Antonio	Conceptualization, Investigation, Formal analysis, Methodology, Data curation, Visualization, writing - original draft
Caporizzi, Rossella	Formal analysis, Methodology, Visualization, Writing – review and editing
Paolillo, Maddalena (Candidate)	Visualization, Writing – review and editing
Memet, Onur Oral	Visualization, Writing – review and editing
Severini, Carla	Supervision, Methodology, Visualization, Writing – review and editing

Paolillo, M., Derossi, A., van Bommel, K., Noort, M., Severini, C. (2021)

Rheological properties, dispensing force and printing fidelity of starchy-gels modulated by concentration, temperature and resting time. (2021). *Food Hydrocolloids; 117: 106703.* This publication is in Chapter 3. *Food Hydrocolloids, 2021, 106703.* This publication is in Chapter 4.

Contributors	Statement of contribution
Paolillo, Maddalena (Candidate)	Investigation, Methodology, Data curation, Formal analysis, Writing – original draft
Derossi, Antonio	Conceptualization, Methodology, Writing – review & editing
Van Bommel, Kjeld	Supervision, Resources, Writing – review & editing
Noort, Martijn	Resources, Writing – review & editing
Severini, Carla	Supervision, Project administration, Writing – review & editing.

Derossi, A., Caporizzi, R., Paolillo, M., Severini, C. (2021)

Programmable texture properties of cereal-based snack mediated by 3D printing technology. *Journal of Food Engineering, 2021, 110160.* This publication is in Chapter 5.

Contributors	Statement of contribution
Derossi, Antonio	Conceptualization, Methodology, Software, Formal analysis, Writing - original draft
Caporizzi, Rossella	Formal analysis, Investigation, Writing - original draft
Paolillo, Maddalena (Candidate)	Investigation, Writing - original draft
Severini, Carla	Writing - original draft, Supervision

Derossi, A., Paolillo, M., Verboven, P., Nicolai, B., Severini, C. (2021)

Extending 3D food printing application: apple tissue microstructure as a digital model to create innovative cereal-based snacks. Journal of Food Engineering, *Journal of Food Engineering*, 2022, 110845. This publication is in Chapter 6.

Contributors	Statement of contribution
Derossi, Antonio	Conceived the original idea, analyzed the data and performed statistical analysis, Writing the original draft
Paolillo, Maddalena (Candidate)	Conceived the original idea, analyzed the data and performed statistical analysis, wrote the original draft;
Pieter Verboven	Performed X-ray images, revised the paper, critical feedback, contributed to the final version of manuscript
Bart Nicolai	Revised the paper, critical feedback, contributed to the final version of manuscript
Severini, Carla	Revised the paper, critical feedback, contributed to the final version of manuscript

Derossi, A., Paolillo, M., Caporizzi, R., Severini, C. (2020)

Extending the 3D food printing tests at high speed. Material deposition and effect of non-printing movements on the final quality of printed structures. *Journal of Food Engineering, 2020, 109865.* This publication is in Chapter 7.

Contributors	Statement of contribution
Derossi, Antonio	Conceptualization, Methodology, Formal analysis, Writing - original draft
Paolillo, Maddalena (Candidate)	Formal analysis, Investigation, Data curation, Writing - original draft
Caporizzi, Rossella	Investigation, Writing - original draft
Severini, Carla	Writing - original draft, Supervision

Conference abstracts and presentations

International conference

Derossi, A., Severini, C., Caporizzi, R., Fiore, G. A., Paolillo, M. (2018)
New advances in 3D food printing. Fast Printing and combined cooking-printing. 32nd Effost International Conference, 6-8 November 2018, Nantes, France.

Derossi, A., Caporizzi, R., Paolillo, M., Severini, C. (2018).
3D printing for producted with personalized textural properties: a case study on the food structure of multilayered wheat based snack. 3° Food structure design conference. Debrecen University Congress, 20-22 September 2018.

Derossi, A., Severini, C., Caporizzi, R., Paolillo, M., Verboven, P., Nicolai, B.(2019)
From Plant Tissue microstructure to new foods with novel sensory perception. An example of biomimetics of food mediated by 3D printing. 8th International Symposium on 'Delivery of Functionality in Complex Food Systems DOF2019.

Derossi, A., Caporizzi, R., Palillo, M., Gerks, K., Severini, C.
Design and production of 3D printed food with desired textural properties. ICEF 13 – 13-26 September 2019. Melbourne, Australia.

Derossi, A., Caporizzi, R., Palillo, M., Gerks, K., Severini, C.
Design and production of 3D printed food with desired textural properties. ICEF 13 – 13-26 September 2019. Melbourne, Australia.

Italian conference

Paolillo, M.

Application of 3D printing for manufacturingof customizable food products

XXIII Workshop on the Developments in the Italian PhD Research on Food Science, Technology and Biotechnology. Oristano, Sardinia, 19-21 September 2018.

Paolillo, M.

3D Food Printing: new advances on printing speed and predict texture.

XXIV Workshop on the Developments in the Italian PhD Research on Food Science, Technology and Biotechnology. Florence, Tuscany, 11-13 September 2019.

Paolillo, M.

Printing cereal dough: novel sensory perception of food from plant tissue microstructure

1° Joint Meeting of Agriculture-oriented PhD Programs. Catania- Salina 17-21 June 2019

Paolillo, M.

3D Printing in Food Manufacturing: a case of Starch Gels

2° Joint Meeting of Agriculture-oriented PhD Programs. (Online) 14-16 September 2020

CHAPTER 3 Drawing the scientific landscape of 3D Food Printing. Maps and interpretation of the global information in the first 13 years of detailed experiments, from 2007 to 2020

Antonio Derossi, Rossella Caporizzi, Maddalena Paolillo, Mehmet Onur Oral, Carla Severini

Innovative Food Science & Emerging Technologies

Volume 70, June 2021, 102689

Abstract

3D Food Printing is a hot field of research in which many efforts are concentrating to unleash its potential for renewal. To facilitate this process, we have drawn the global scientific landscape in these first 13 years of experiments by using bibliometric and data visualization approaches. We find a total of 170 documents between 2007 and 2020. China and Australia are the most productive countries followed by Italy. On a total of 582 co-authors, not more than 10 researchers are collaborating out of their research group/institution. This is a weakness that urges sharing information and experiences. Also, the networks of the keywords have shown some hidden opportunities. The interrelationship between digital design, microstructure and personalized food need to be reinforced to create unprecedented sensory perceptions and alleviate the mastication and swallowing problems of vulnerable consumers. Also, there is a shortage of papers on the printing of protein-rich inks.

Industrial relevance

The paper critically analyzes the global production of scientific experiments in 3D food printing. The results discovered that the level of collaborative researches is weak while the involvement of the industrial sector, being a crucial process to unleash the great ambitions of personalized food manufacturing, is urgent. What emerged is the need to study parallel deposition methodologies such as selective laser sintering (SLS) or hot-air sintering (HAS) that would open for fast printing and the use of highly stable food powders. Other opportunities to make feasible the application of 3DFP could be the use of protein-rich food inks and to make closer the topics of digital design and personalized consumers requirements.

1. Introduction

Additive Manufacturing (AM) is a broad range of technologies having the capability to transform 3D digital images in real objects through a layer-by-layer deposition process. In the last 20 years, AM technologies – popularly known as 3D printing

(3DP) – have triggered a process of renewal of the manufacturing of items, as we traditionally know. The potentials of designing complex structures with customized end-user properties such as desired shape, dimension and physical properties are the main reasons of its notable success in several industrial sectors and the interest of many scientific fields. While the use of 3DP for rapid prototyping (Rayna & Striukova, 2016) has been the first application, its usage currently occurs in pharmaceutical (Beg et al., 2020; Manoj, Bhuyan, Raj Banik, & Ravi Sankar, 2020), regenerative medicine (Agostinacchio, Mu, Dirè, Motta, & Kaplan, 2020; Bueno et al., 2019), biomedical implants (Murr, 2020) bioengineering (Nesic et al., 2020), architecture (Chan, Pennings, Edwards, & Franks, 2020), jewellery (Stamati, Antonopoulos, Azariadis, & Fudos, 2011), aerospace (NASA, 2017; Jiang, Zhang, Bhandari, & Cao, 2020), construction (Buchanan & Gardner, 2019), etc. Moreover, after the deposition of thermoplastic materials, the printing of metal (Gibson et al., 2018), clothing (Want, 2020), glass (Li, Zhang, Xing, Ouyang, & Liu, 2018), concretes (Comminal, Leal da Silva, Andersen, Stang, & Spangenberg, 2020), etc., have become popular. The awesome interest in 3DP is proved by over than 28k of scientific publications listed on the Scopus database since 1987 (data from Scopus database). While 3D printing of thermoplastic materials is advanced and realizes highly complex structures, the 3D printing of food is taking its first steps even though it is also becoming of great interest with an unparalleled level of innovation capable of transforming the way in which foods will be manufactured, stored and consumed. Cohen et al. (2009) stated that 'after solving the main issues of slow printing and price, the remaining question is what the ways in which 3DFP will completely modify the food sector, while no doubts on whether 3DFP may affect food manufacturing and consumption'. As reported by several authors the main ambitions of 3D food printing (3DFP) are personalized food manufacturing (Cohen et al., 2009; Lipton, Cutler, Nigl, Cohen, & Lipson, 2015; Severini & Derossi, 2016; Derossi, Caporizzi, Oral, & Severini, 2020; Pulatsu & Lin, 2021), on-demand production, food waste reduction and consumers-food co-creation (Godoi, Prakash, & Bhandari, 2016; Jiang, Zheng, Zou, Han, & Wang, 2019; Pulatsu, Su, Lin, & Lin, 2020). Personalized food manufacturing by using 3D Printing has the potential of creating food not only with desired shapes and dimensions but also to get nutritional and functional properties right for people uniqueness (Godoi et al., 2016; Le-Bail, Maniglia, & Le-Bail, 2020). So, the level of innovation may also be augmented by interrelating personal medical data, telemedicine, planned diet, lifestyle, gender, sex, etc. (Tagami et al., 2021). In addition, 3DFP has the potentials of creating customized sensory properties by using multi-food materials (Park, Kim, & Park, 2020), by modeling mechanical properties (Derossi, Caporizzi, et al., 2020; Derossi, Paolillo, Caporizzi,

& Severini, 2020) or creating food with the desired shape (Severini, Azzollini, Albenzio, & Derossi, 2018; Schutyser, Houlder, de Wit, Buijsse, & Alting, 2018; Pulatsu & Lin, 2021), color (He, Xhang, & Guo, 2020) and flavor (Guo, Zhang, & Devahastin, 2021). To date, researchers focused their work on the effects of printing variables (Derossi, Caporizzi, Ricci, & Severini, 2018; Perez, Nykvist, Brogger, Larsen, & Falkeborg, 2019), the printability of food formulas (Liu, Zhang, Bhandari, & Yang, 2018; Tian et al., 2021) through the use of hydrocolloids and analyzing the corresponding rheological properties (Kuo, Qin, Cheng, Jiang, & Shi, 2021; Pant et al., 2021; Gholamipour-Shirazi, Norton, & Mills, 2019; Zhu, Stieger, van der Goota, & Schutyser, 2019), on programmable 3D structures aiming to get desired texture properties (Derossi, Caporizzi, Paolillo, & Severini, 2021) and, more recently, on the time evolution of color, aroma and shape as affected by some external factors, as first examples of 4D food printing (Guo et al., 2021; Phuhongsung, Zhang, & Bhandari, 2020; He, Zhang, & Fang, 2020). The bibliography of 3D food printing is getting large with an exponential trend of the papers published in the last years as well as large is the number of the reviews aiming to delineate the most important features of 3DFP.

Scientometrics is a wide field of research aiming to analyze the quantitative aspects of science and technology and its dynamic nature seen on the angle of the process of communication (El Mohadab, Bouikhalene, & Safi, 2020). While the advent of digital information products has generated a massive amount of scientific documents published online, the researchers are slow in searching, collecting, studying and interpreting this large mass of data. This is called a typical information overload problem (Shao, Li, & Bian, 2021). Bibliometrics is a specific field of scientometrics defined as ‘the application of mathematics and statistical methods to books and other media of communication’ (Otlet, 1934). In practice, bibliometric is a tool for clustering and mapping the information from scientific documents such as keywords, abstract, authors, countries, references, journals, citation, etc., delineating the salient traits of a scientific domain and discovering novel features, network, potentials and weakness/strengthens of that field. As reported by Waltman, van Eck, and Noyons (2010), bibliometrics drives people in understanding how research topics are, or could be, how they are related to each other, or to delineate how to scientific topics are evolving over time, to define the impact of some journals, institutions, authors, countries, etc. on the research topic under evaluation. For instance, Mingers and Leydesdorff (2015) stated that the act of citing papers creates a link between ideas, points of view, methods, people, journals and institutions generating a scientific network that may be analyzed. Furthermore, bibliometric methods allow creating

invisible links between highly cited papers to research frontiers (Mingers & Leydesdorff, 2015; Price, 1976) paving the way for innovative ideas.

In the field of 3D food printing, several reviews have been published (Mantihal, Kobun, & Lee, 2020; Baiano, 2020; Dankar, Haddarah, Omar, Sepulcre, & Pujolà, 2018; Jiang et al., 2020; He, Zhang, & Fang, 2020; Zhao, Zhang, Chitrakar, & Adhikari, 2020; Handral, Hua Tay, Wan Chan, & Choudhury, 2020; Feng, Chang, & Bhandari, 2019) but a complete quantitative analysis of the global scientific production – original papers, review, letter to Editor, books, proceeding of international conferences – has not been performed. Although the usefulness of the reviews is globally recognized, the obtained benefits remain limited if we are not able to manage this large mass of publications that increases monthly. The reading of reviews, often focused on specific hot-points, limits to a high extent the exploration of the research status of 3D food printing with missed opportunities in individuating strengthens and weakness points and innovative bridges between hidden sub-topics. Our belief is that 3D Food Printing technology will definitely transform the future of food production and consumption but its level of maturity is too low to collect the high level of investments needed for direct employment in the food chain. For this, the interpretations of all global scientific information aiming to highlight novel networks and interrelations could act as driver to activate a scientific discussion on the weakness and strengthens on 3DFP and fuel new cross-contamination between different topics.

This is an original paper that uses as input-data the main information and indicators of the global production of scientific documents on the topic of 3D Food Printing with the aim to draw the scientific landscape of 3DFP highlighting weakness and opportunities. With this aim we have combined bibliometric and statistical methods, mapping and clustering analysis, and visualization approaches to manage the large body of scientific documents in the field of 3D Food Printing.

2. Material and methods

2.1. Collecting bibliographic information

We used SciVerse Scopus as the main database because it contains the largest number – 20,000 items - of indexed journals, books and conference proceedings (Mingers & Leydesdorff, 2015); also, although Scopus retrieves back till 1996, 3D Food Printing is a relatively young field of research and there are no reasons to search scientific documents before 1996. A schematic representation of the strategy used to

collect the most relevant scientific documents belonging to the field of 3DFP, is reported in Figure 1. The search was conducted on 25 November 2020.

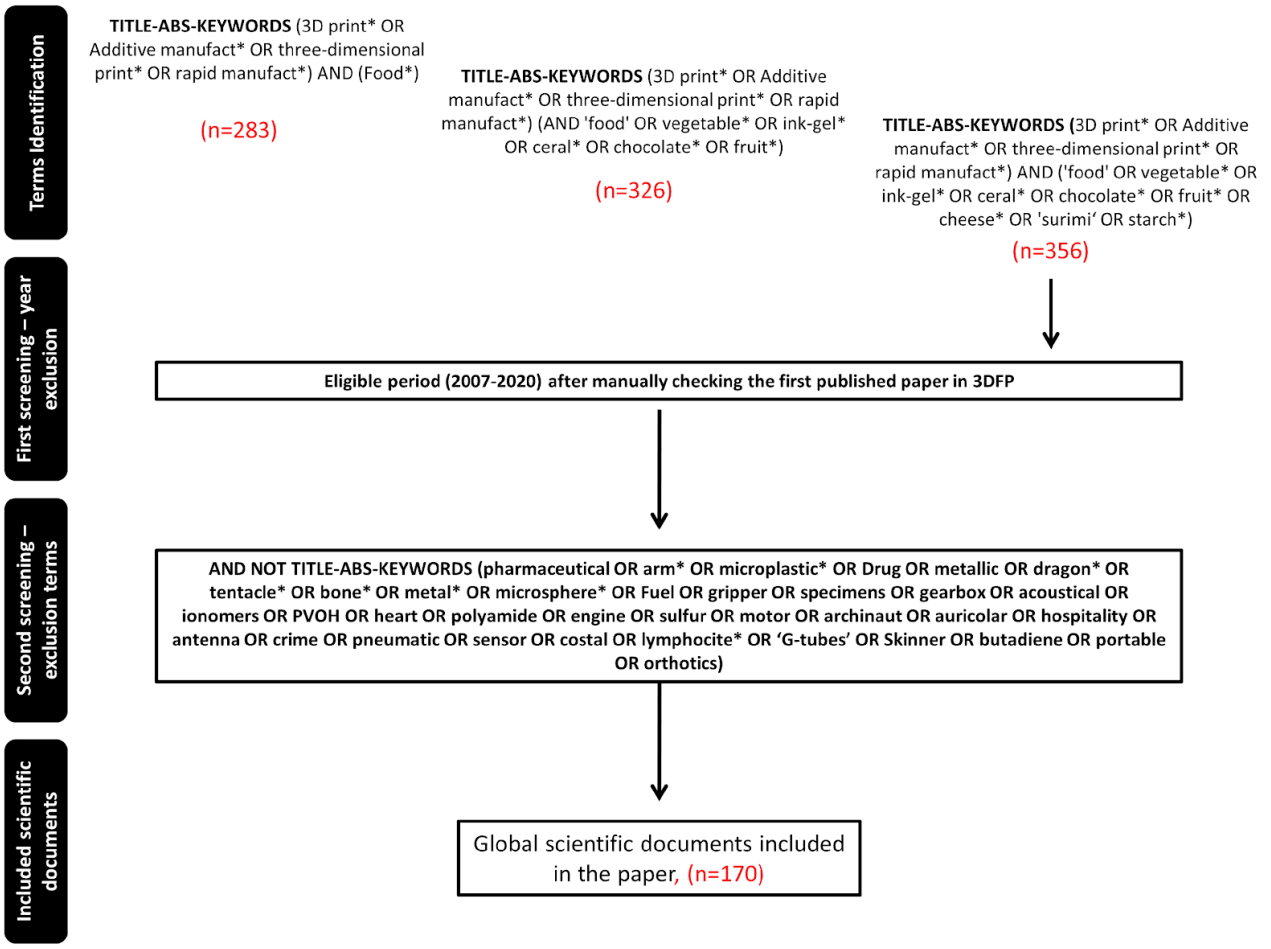

Fig. 1. Strategy employed to collect scientific documents in the field of 3D Food Printing.

First, different techniques and operators have been used to improve the accuracy of our search. For instance, asterisks have been used to collect related words as in the case of using 3D print* which enlarge the searching for combined words such as 3D printing, 3D printed. Also, the operators [AND], [OR] and [AND NOT] were used for including or excluding specific terms from the search. The type and number of terms used in the search query of Scopus was decided by preliminary tests aiming to collect the maximum number of papers belonging to the field of 3DFP.

First, using specific terms in a step-by-step approach of searching we retrieved a maximum of N=356 documents. Then, the obtained documents were limited first for the 2007–2021 and, second, a manual screening to avoid some 'false-positives' was performed. For instance, the recent paper publication by Jerman et al. (2021) contains in the abstract and as keywords the terms 'food', 'additive manufacturing' and 'food

processing' are focused on the field of abrasive waterjet technology with only negligible interrelation with the food sector.

Finally, a total of 170 documents have been retrieved and the following information were downloaded in format files .CSV: citation information; bibliographical information, abstract & keywords. Further properties of the documents such as the time distribution, subject area, countries and the types of document, have been obtained directly from the Scopus website. All the bibliometric information have been used in the following analyses: 1. Analysis of overall publication indicators; 2. Analysis of the co-authorship; 3. Analysis of the co-occurrence for the author's keywords.

While the analysis and visualization of some general indicators were performed by using the software Power BI (Microsoft), the other techniques were performed by using the software VosWiever, ver. 1.6.16 initially realized and released by van Eck and Waltman (2009) and widely used in many fields of research (Mascarenhas, Ferreira, & Marques, 2018; Park & Nagy, 2018; Perianes-Rodrguez, Waltman, & van Eck, 2016; Shao et al., 2021; Sweileh, Al-Jabi, Zyoud, Sawalha, & Abu-Taha, 2018).

2.2. Co-authorship analysis

The analysis of co-authorship was performed by using as input data the authors and countries information of the retrieved papers with the aim to create the networks of active collaborations in the field of 3D Printing. For the analysis, an entry-level of one documents per country has been used while no entry-levels have been assigned for the number of citations received for each country. The fractional counting method was used by assigning to each author/country weight of 1/N, with N the number of total authors or countries involved in the paper (Perianes-Rodrguez et al., 2016).

2.3. Co-occurrence analysis of the author's key-words

The generation of the map for the author's keywords involved three different steps. A first analysis was carried out without any entry-level value for the number of occurrences. This approach allowed extracting a global list of 526 keywords and the corresponding list of the number of occurrences. These data have been used to define a relative weight for each keyword. We assumed a maximum weight of 1 for the keyword showing the highest occurrence which, in our case, was the term 'additive manufacturing' with 66 occurrences. Then, the weight of the other keywords was defined by computing the fraction of the occurrences on the total of 66; relative weight = highest number of occurrence/number of occurrences of each keyword. Next, we decided to include in the network visualization only the keywords showing

a weight > 0.05 corresponding to a minimum number of occurrences of 3. Finally a thesaurus file was used for data cleaning consisting of the capability of merging similar words - i.e. ‘food printing’, ‘3D food printing’ and ‘3D food manufacturing’ - or to delete potential unrelated words. Fig. 2 schematically describes the approach used for the analysis of the author’s keywords.

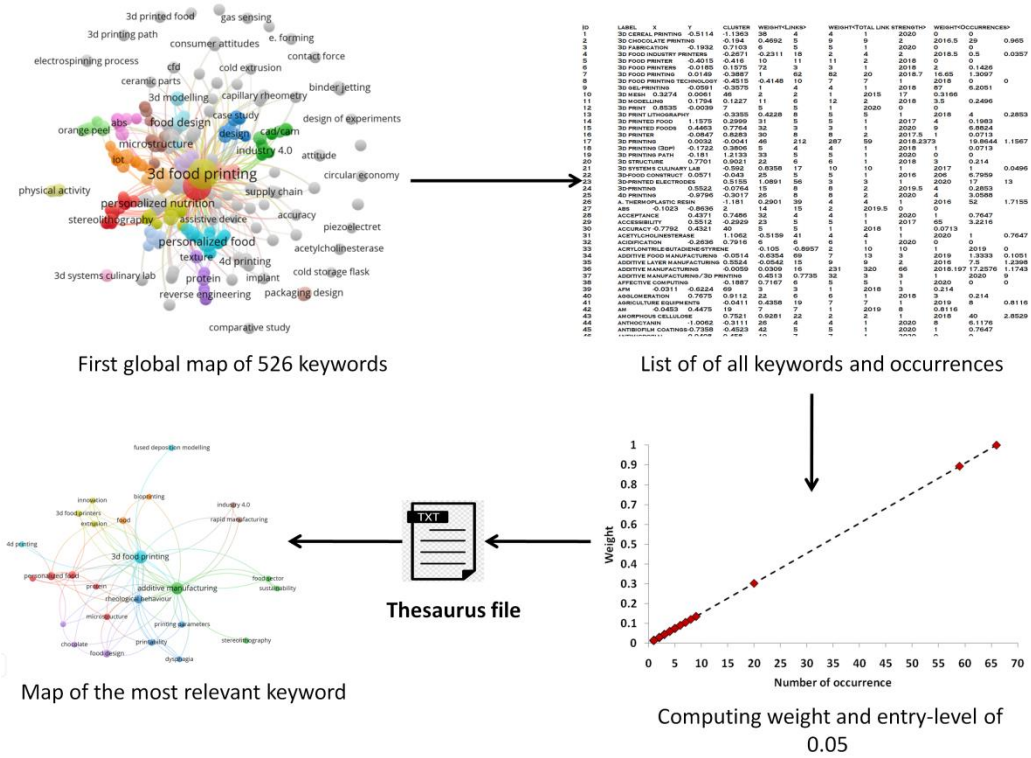

Fig. 2. Schematic representation of the method used for the analysis of the author’s key-words

3. Result and discussion

3.1. Distribution of publications over time, space and subject area

The evolution over time of the scientific documents clearly shows a rapid increase in the interest of the scientific community in 3D Food Printing. While less than 9 papers were published in the period of 2007–2015, an average of 29 papers/per year was obtained from 2016 to 2020 with a peak of 48 documents in 2018 (Fig. 3a). At the moment of writing this paper only 6 papers result in 2021 that is lower than what is possible to observe in the general field of 3D printing. This suggests a shortage of new data on 3D food printing but during 2020, COVID-19 has been a calamity for scientific society with the closure of universities, research centers, laboratories and the cancellation of many scientific congresses and workshop (Subramayna, Lama, & Acharya, 2020). Also, COVID-19 has collected extraordinary efforts from all

scientific sectors limiting the development of other themes of research. For instance, Kambhampati, Vaishya, and Vaish (2020) retrieved 1638 publications on COVID-19 in the first 17 weeks of 2020.

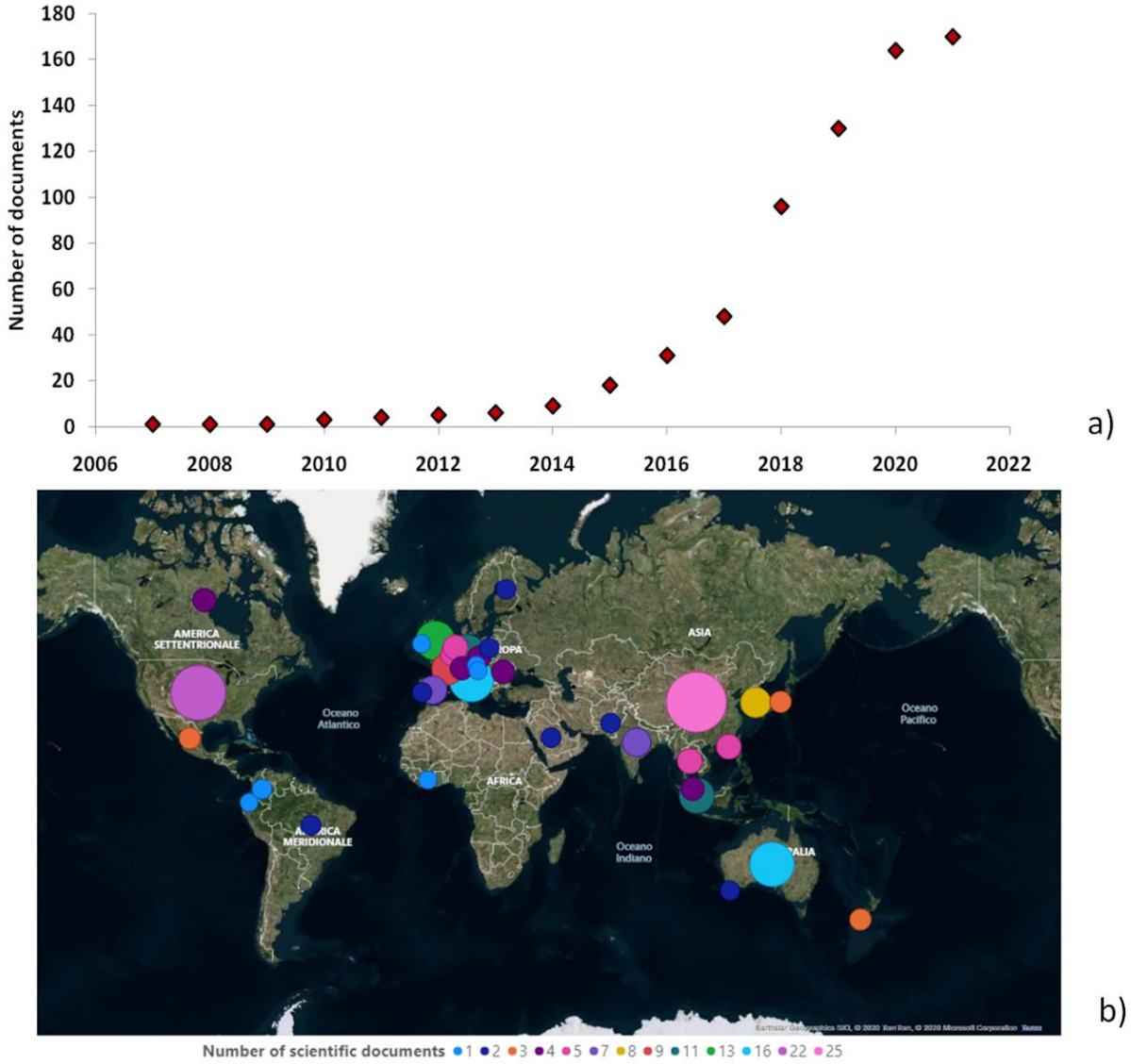

Fig. 3. Evolution over time (a) and geographical distribution (b) of the global publications on the emerging topic of 3D Food Printing

Additional information may be obtained from the geographical distribution of the published documents (Fig. 3b). China, the USA, Australia and Italy are listed as the first productive countries in the field of 3D food printing with 25, 22, 16 and 16 scientific documents, respectively. However, when analyzing in detail the type of journals, significant differences have emerged with the USA that has disseminated data mainly in the scientific areas of intelligent systems, computer application, medicine and 3D digital design and fabrication while only 2 papers on a total of 25 were published in food science and technology (Jiang et al., 2019; Lipton et al., 2015). On the other hand, more than 80% of the papers coming from China, Australia

and Italy have been published in the food science and technology area (data not shown). Table 1 delineates the main features of the global scientific production on 3DFP. As expected for a young research topic, the majority of the documents are classified as original articles (N = 90; 53%) and conference papers (N = 38; 22.3%) but it is worth noting an interesting number of reviews (N = 20; 11.7%). Of these reviews, some are generally focused on the main potentials and ambitions of 3DFP (Le-Bail, Maniglia, & Le-Bail, 2020; Mantihal et al., 2020; Nachal, Moses, Karthik, & Chinnaswamy, 2019) while others have analyzed specific topics such as the development of food-inks (Feng et al., 2019; Gholamipour-Shirazi, Kamlow, Norton, & Mills, 2020; Jiang et al., 2019; Voon, An, Wong, Zhang, & Chua, 2019), 3D printing of meat (Dick, Bhandari, & Prakash, 2019), regulatory and economic issues (Baiano, 2020) and materials and machines used for food printing (Tan, Toh, Wong, & Lin, 2018). The analysis of the subject category shows as the majority of the papers have been published under 'engineering' and 'agricultural and biological science' areas but another important category is 'computer science'. This is in accordance with the nature of 3DFP that allows creating foods from digitalized images obtained by computer-aided design (CAD). The multi-disciplinary features of 3DFP allow it to grow in closer fields of research such as Human-Computer-Interaction (HCI) which recently begun to pay interest in the food sector with the birth of the Human-Food-Computer-Interaction (HFCI) area that promises to reshape the way in which food is produced, transported, prepared and consumed. Relevant examples have been published by Chaundry, Connelly, Siek, and Welch (2012); Hashimoto, Funatomi, Ueda, and Yamakata (2012); Comber, Choi, Hoonhout, and O'Hara (2014); Betran, Jhaveri, Lutz, Isbister, and Wilde (2019). Tools to support the nutritional assessment such as the size portions for diet intake have been published by Hashimoto et al. (2012) who studied smart kitchen capable to help people of preparing unfamiliar food recipe – or nutritionally personalized food formula – by using a complex system providing recipe information by using visual and sound data to recognize ingredients.

Table 1 – Distribution of 3D Food Printing papers for type of document and subject category.

Type of documents		**Subject category**		**References for Subject Category**
Article	91	Engineering	87	Fahmy et al. (2020)
Conference Paper	38	Agricultural and biological science	71	Portanguen et al., (2019)
Review	20	Computer science	40	Ramundo et al., (2016

Book Chapter	16	Materials science	27	D'angelo et al., (2016
Conferece Review	2	Chemistry	26	Gholamipour-Shirazi et al., (2019)
Book	1	Chemical engineering	19	Dianez et al., (2019)
Short Survey	1	Business, management and accounting	13	Charlebois and Juhasz (2018)
Note	1	Decision sciences	11	Steenhuis et al., (2018)
Editorial	0	Biochemistry, genetics and molecular biology	9	Sun et al., (2015)
Erratum	0	Mathematics	9	Kim et al., (2018)
Letter	0	-		

The scientific productivity of the top 10 institutions is shown in Fig. 4. A total of 56 documents, 33% of the global production, were published. Of these, the most productive institutions have been the University of Queensland, Jiangnam University and the University of Foggia, respectively with 9, 8 and 8 publications. The top ten institutions produced their papers from 2016 to 2020 suggesting they strongly believe in the high potential of 3D Food Printing deciding to invest significant research efforts in a limited period of time. In addition, they published on a total of 32 different journals while the total number of journals publishing 3DFP experiments has been 116 with high diversity in their main scopes. This proves that editors now consider 3DFP an important topic in food engineering, food polymers application, computer in agriculture, computers in industry, etc.

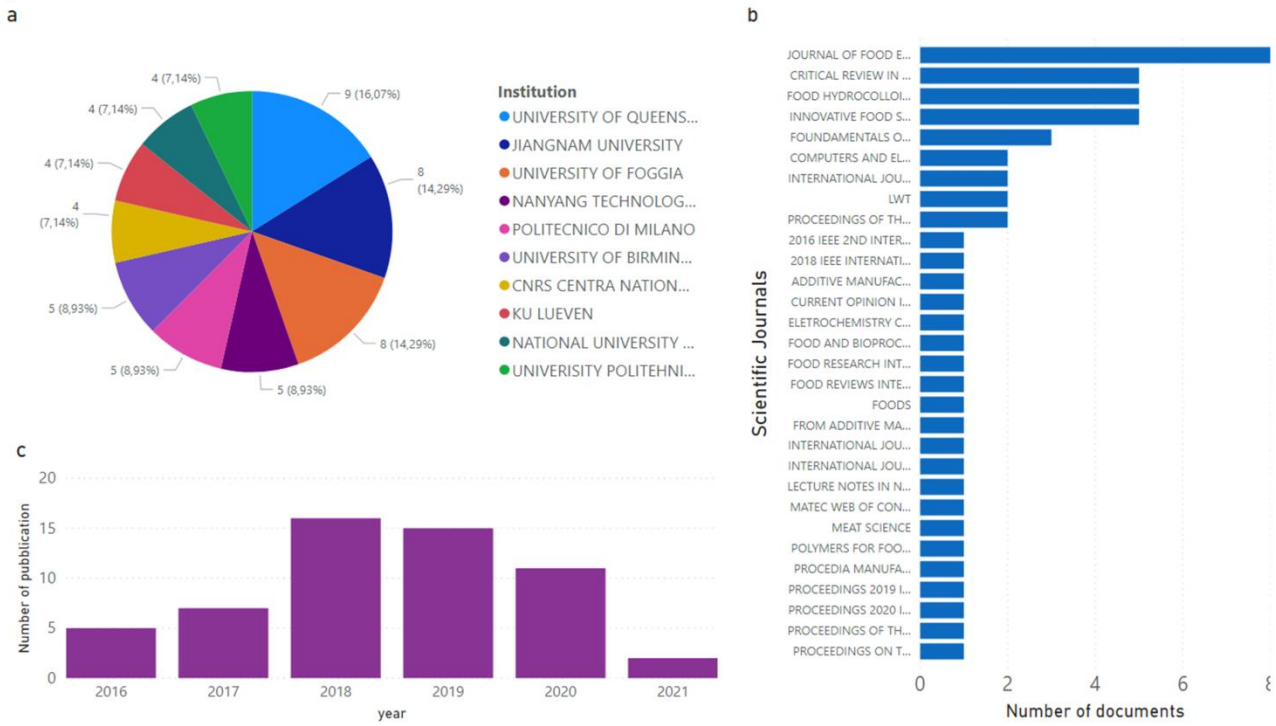

Fig. 4. Results of the first 10 institutions publishing on 3D Food Printing. A) fraction of the number of publications. B) distribution over times; c) publications by source.

3.2. Analysis of co-authorship

With the aim to examine the active collaborations among countries, the network visualization of the active countries in 3DFP gives great opportunities for immediate responses and novel discussion. In the map, the size and color of data respectively represent the number of occurrences and the cluster type. Two countries co-occur if they co-authored a publication on 3DFP. Moreover, a link between two countries is created when they co-occur in the same documents and the greater the strength link is, the higher the number of the papers co-authored by the countries is or, in other words, they show a strong collaboration. The global network of the co-occurrence is featured by 38 countries indicating that 3D food printing is broadly considered an interesting and promising field of research all around the world; however, 15 countries look like ‘isolated island’ without active international collaborations (Fig. 5A). The other 27 countries create the largest cluster with a total of 41 links (Fig. 5B) of which China and Australia count the higher number of links toward other countries and respectively of 9 and 4. Also, China and Australia formed the highest links strength - respectively, 18 and 10 on a total of 55 - proving they have very productive international collaborations with many published papers in the field of 3D food printing. More specifically, with link strength of 7, China and Australia are the countries with the most prolific collaborative endeavors (Feng et al., 2019; Guo, Zhang, & Bhandari, 2019; Wang, Zhang, Bhandaru, & Yang, 2018; Yang, Zhang,

Bhandari, & Liu, 2018). In addition, the map shows that China and Australia might be considered the bridge between USA, Europe and Asia enlarging the global network of collaboration and making visible to the researchers the potential countries to invite for novel collaborations. Italy, for instance, that is one of the most productive countries (Fig. 5b), shows only 2 links with Switzerland and Brazil while its involvement in other international collaborations could help to improve the quality of the 3D food printing technologies. It is important to note that the label of some countries is not clearly visualized in the map due to the default scale used by the software VosViewer but they actively participate in the network of active countries in the field of 3D Food Printing. Some of these are for instance Germany (Kern, Weiss, & Hinrichs, 2018), Portugal (Sartal, Carou, Dorado-Vicente, & Mandayo, 2019) and India (Piyush & Kumar, 2019).

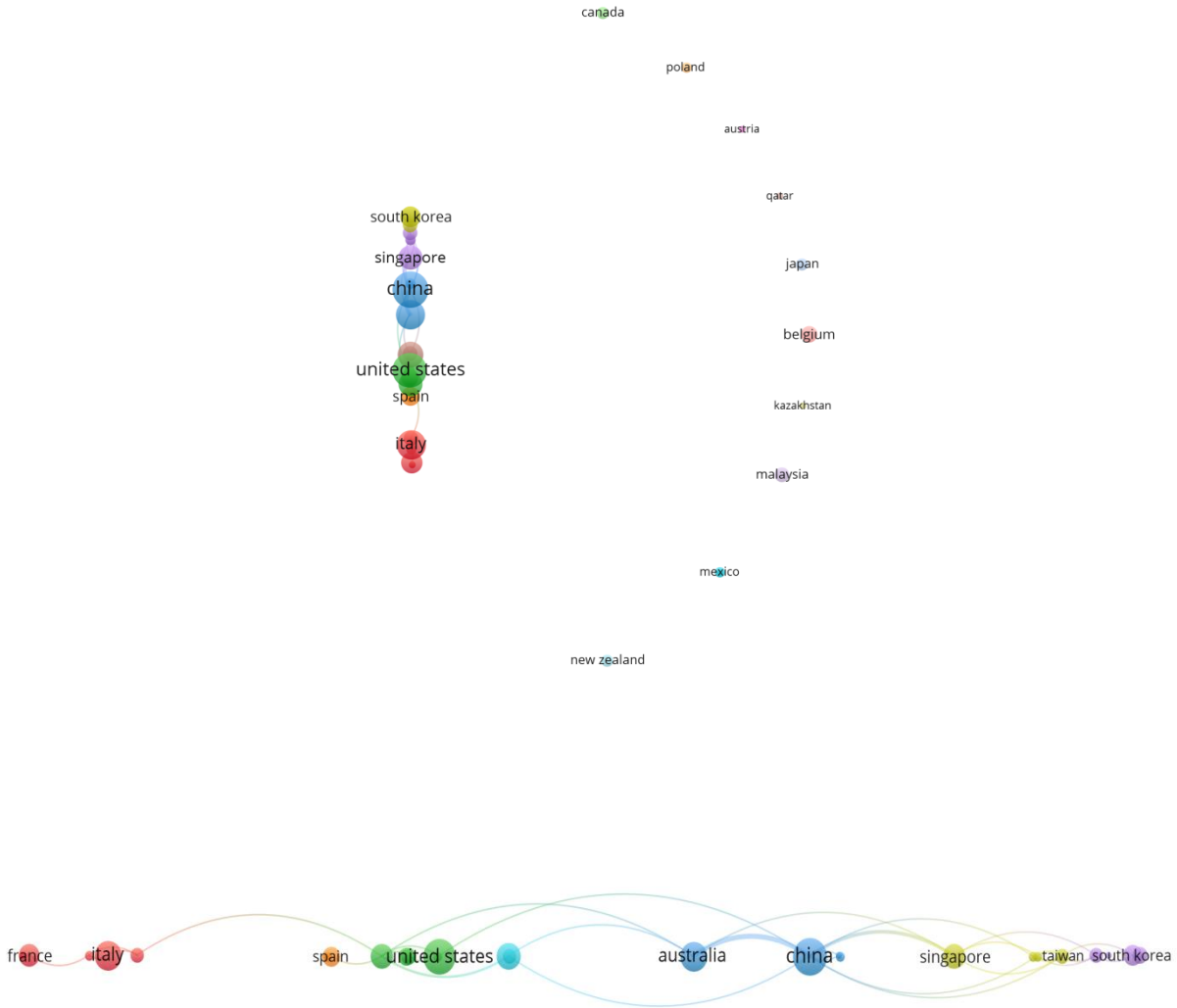

Fig. 5. Map of the active countries in the field of 3D food printing. A) Global map of countries contributing in the field of 3D food printing; b) Largest cluster of interconnected countries.

When analyzing the network of the authors a total of 582 names have been visualized. The map of the co-authored papers indicated a large number of colored clusters suggesting that all researchers are working in small groups (data not shown). More specifically, the most productive clusters appeared under the main label of the following authors: 'Bhandari, B.', 'Lipson, H.', 'Lammertyn, J.', 'Hao, L.', 'Lanaro, M.', and 'Liu, Y'. Also, only the clusters of 'Bhandari', 'Hao' and 'Liu' are linked stating that they are sharing results, data and efforts in 3D food printing activities. Furthermore, the visualization of many islands of authors proves that the majority of the researchers are collaborating mainly in their own research groups or institutions.

The largest set of connected authors, as shown in Fig. 6a and b, is characterized by 51 authors, 6 clusters, 194 links and a total strength link of 208. The maps also report color scales indicating the average year of publication (Fig. 6a) and the average number of citations received by each author (Fig. 6b). With the aim to avoid multiple and repetitive figures we have used colored dot circles to highlight the clusters including authors who have strictly collaborated in co-authoring papers. On the left hand is located the largest cluster with 15 linked authors (red) who singularly show at least 14 links and publishing papers in the last years 2019–2020. Of these authors, the larger fraction showed a limited average citation value of 2 while only Liu, Y., who clearly has collaborated outside his 'birth cluster', received an excellent number of average citations value of 52.5 with only two papers (a total of 105 citations). Also, this cluster is connected with the grey cluster by three links between Liu, Y. and Zhang, M., Yang, F., and Bhandari B. On the opposite side is located the green cluster including 9 authors who published between 2014 and 2018 obtaining average citations values between 1 and 23. Another important cluster is highlighted in grey color, located in the middle of the map, and containing the most collaborative researchers being they linked out with others 4 clusters. Also, to this cluster belong the most productive and cited authors such as Zhang, M., who published 8 documents and showed an average citation of 40.12 while Bhandari, B., signed a total of 9 papers and received an average citations of 66.78. In addition, these two authors have created the strongest collaboration with a strength link of 7 between the years 2018 and 2019. So, they are tightly collaborating resulting very productive with 7 co-

authored documents in two years. Similarly to the grey cluster, the light blue cluster is located in the middle of the map representing conjunction with other clusters of authors. The light blue is featured by the highest diversities with authors who are collaborating in a wide period of time – from 2016 to 2020 – and receiving very different average citations with values between 0 (Kobun R. and Lee, B.B.) and 132.50 of Godoi, F.C. that has been the first editor of the only book on 3D Food Printing titled 'Fundamentals of 3D Food Printing and Applications' (Godoi, Bhandari, Prakash, & Zhang, 2018). So, Godoi, F.C. shows the highest average citations resulting from a total of 265 citations and 2 published papers. Finally, when analyzing the total number of citations the highest cited authors follow the next order: Bhandari, B. (601), Prakash, S. (326), Zhang, M., (321), Godoi, F.C. (265), Yang, F. (163) and Manthial, S. (97).

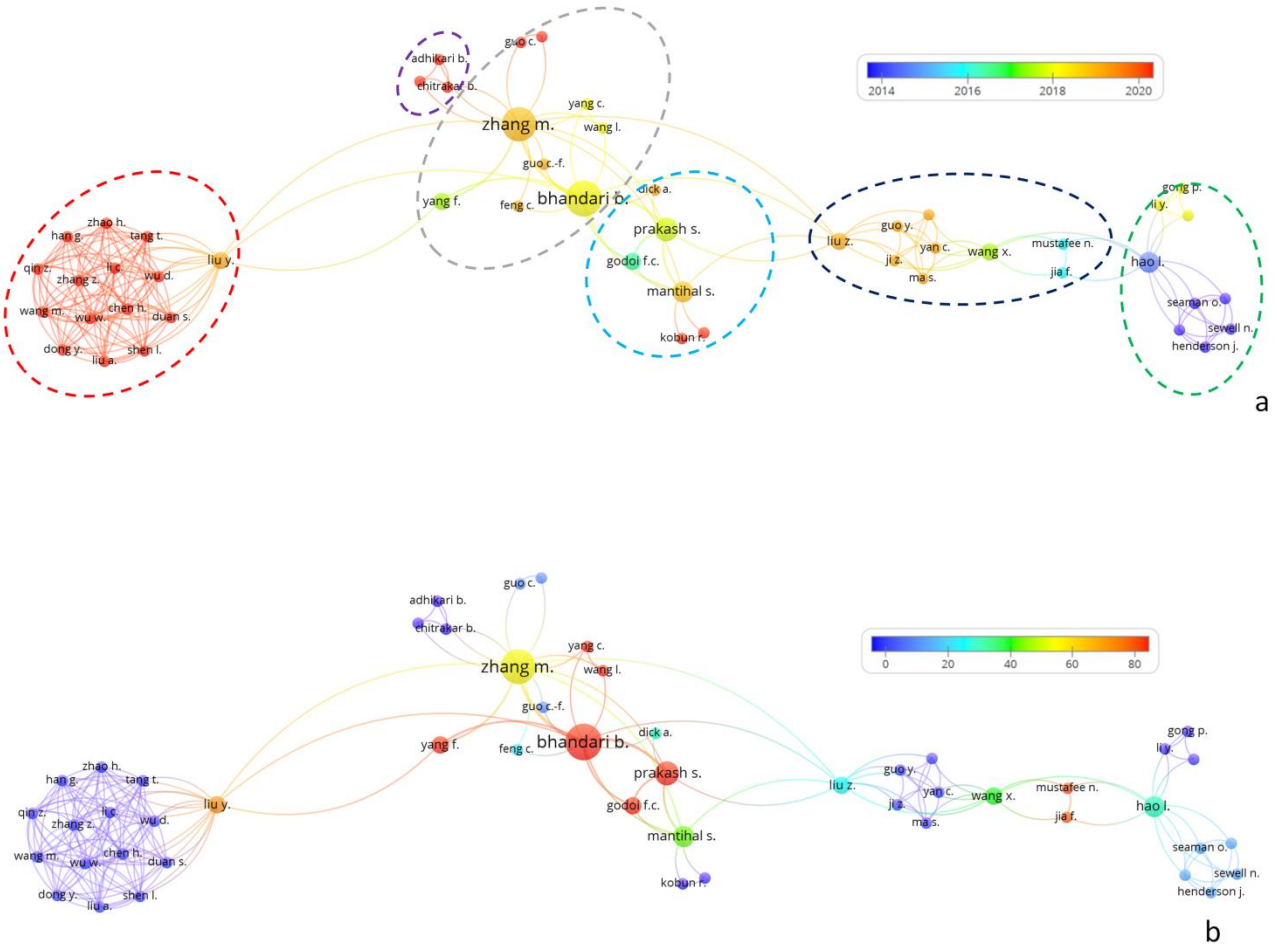

Fig. 6. Map of the largest set of interconnected authors. Color map indicates the year distribution (a) and the average number of received citations (b).

3.3. Analysis of co-occurrence

Being the keywords the backbone of a scientific paper, used to resume the main issues and ambitions of the research, we have performed the analysis of the co-occurrence by using as input data the author's keywords. After the preliminary analysis – without entry-level for the number of occurrences – a total of 491 keywords have been retrieved and mapped (data not shown). Then, according to the method described in the previous section of the paper, we have limited the number of keywords building the map of the most representative terms by using an entry-level of n.3 occurrences corresponding to the relative weight of 0.05. The most characterizing keywords for the field of 3D food printing – a total of 28 terms - are graphically illustrated in Fig. 7 with the corresponding number of occurrences. Some keywords appear to be interchangeable such as 'food printing', '3D food printing', '3D printing' and all of them were replaced with the term '3D Food printing' by the cleaning approach of Fig. 2. However, before discussing the main results, we want to note the repeated usage of keywords such as 'personalized nutrition', 'customized food', 'customized food fabrication' which prove as the 3DFP is considered one of the most promising technologies to make real the fabrication of nutritionally and sensorial personalized food products.

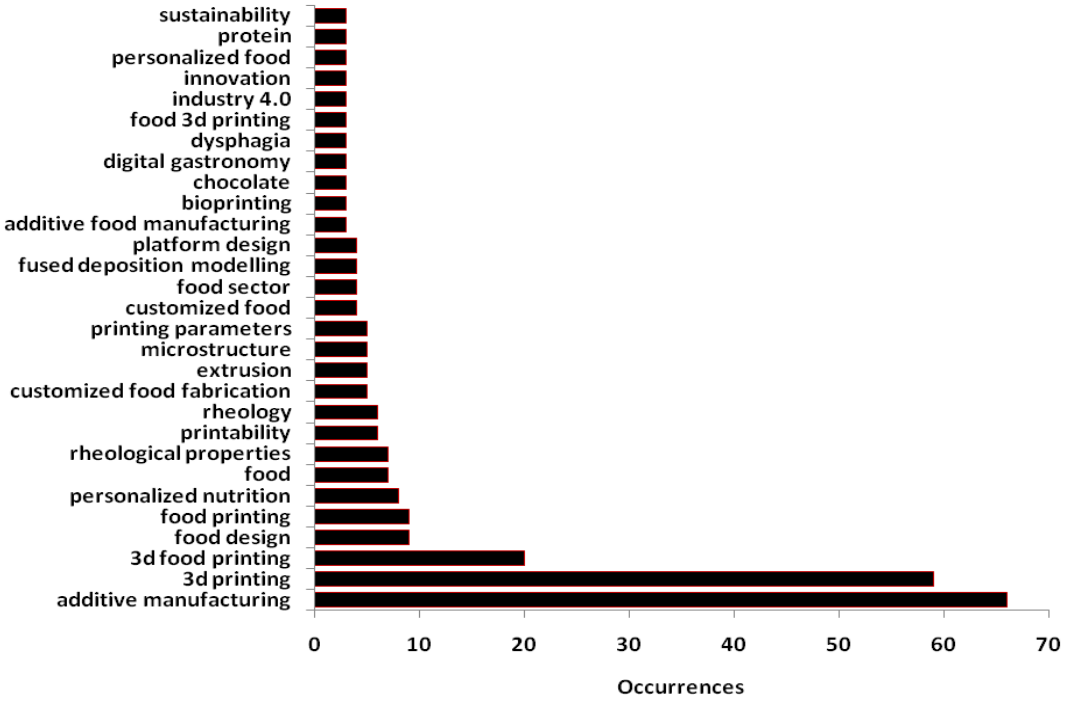

Fig. 7. The first 28 keywords with co-occurrences greater than 3.

The maps of the most representative keywords in the field of 3DFP are reported in Fig. 8 where the number of occurrences is represented by the size of the data point and the color scale indicates the average year of publication (Fig. 8a) and the normalized average number of citations (Fig. 8b). Only a period of time between 2016 and 2020 is reported because the representative keywords fall later than 2016 with the only except of 'platform design' with the average year of 2015. Again, the thickness and the length of the links between two keywords indicate the coupling strength. So, the thicker and shorter is the link, the closer the linkage between two keywords. The specific keywords 'rheological properties', 'protein', 'extrusion' and 'fused deposition modelling' indicate recent hot-points in the 3D food printing area with an average years between 2019 and 2020. This is consistent with the increasing efforts of many research group for the creation of food pastes exhibiting shear thinning behaviour that makes easy the extrusion through a narrow nozzle, and other additional properties such as adhesiveness, viscosity and consistency which provide the capability to not collapse under the weight of the overlying layers enabling a good fidelity of printing (Gholamipour-Shirazi et al., 2019; Zhu et al., 2019). Also, the development of methods to estimate rheological properties with the aim to get a high printability is one of the most challenging points for the practical applications of 3D food printing at the industrial level or for home use (Liu, Bhandari, Prakash, Mantihal, & Zhanga, 2019; Zhu et al., 2019). The importance of this hot-point is also proved by the high number of occurrences of the keywords 'rheological properties', N=13, placed as third in the list of the keyword's occurrence after general terms of 'additive manufacturing', N = 91, and '3D food printing', N = 32 (Table 2). This amplifies the importance of defining the essential rheological information and their ranges by which it is possible to expect a good printability; moreover, not less important will be to discover methods to design and create ink-foods that match the proper rheology.

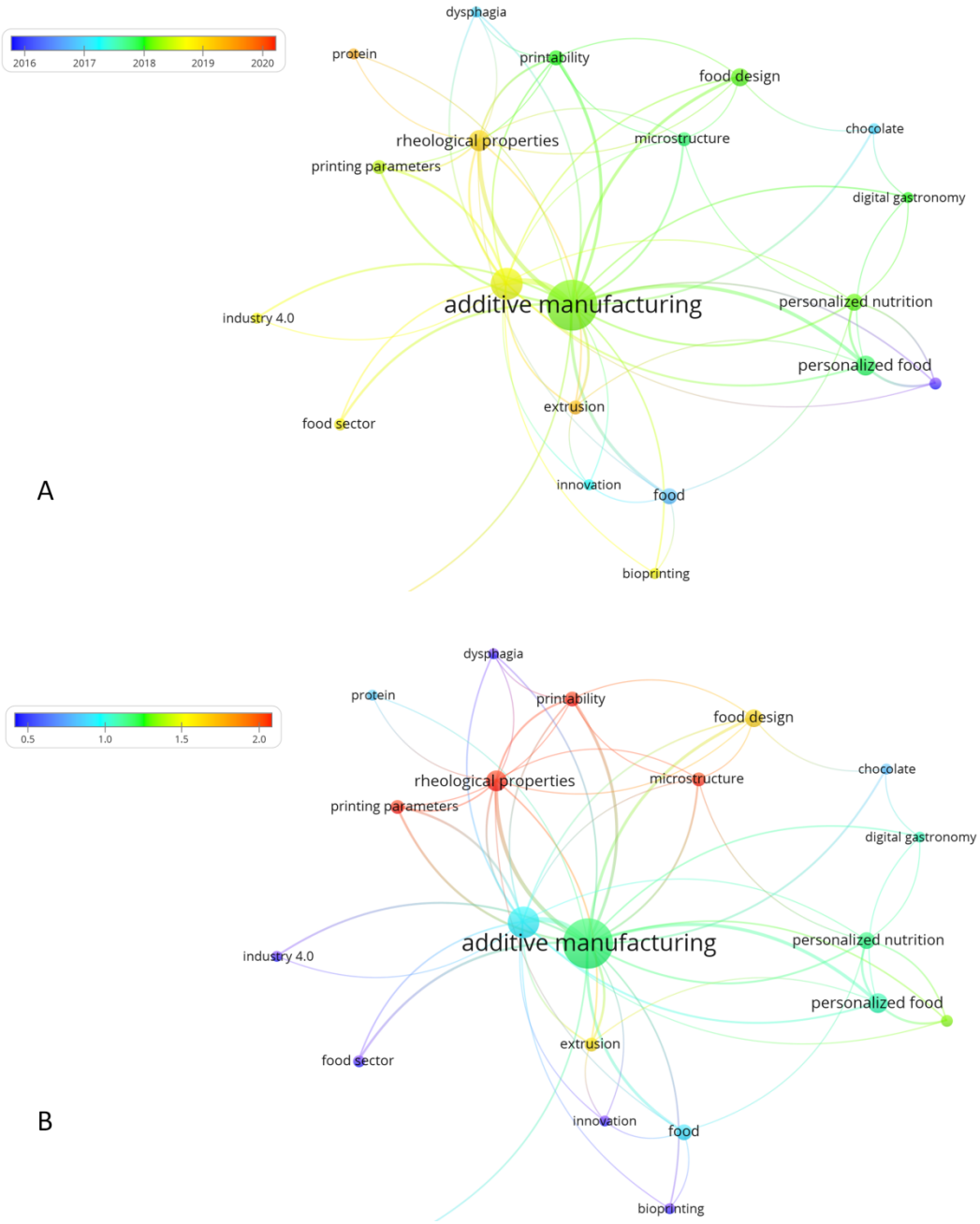

Fig. 8. Network visualization of the author's keywords used in the field of 3D food printing. A) color scale indicates the average year of publication; B) color scale indicate the average normalized citations

Table 2 – Main results of the co-occurrences analysis performed using author's keyword as input data.

Author's keywords	Links	Total Link Strength	Occurrences	Avg. Pub. Year	Avg. Citations	Avg. Norm. Citations
3d food printing	15	44	32	2018.59	12.31	0.95
additive manufacturing	20	91	91	2018.18	18.60	1.16
bioprinting	3	4	3	2018.66	3.00	0.40
chocolate	3	5	3	2017.00	16.33	0.81
digital gastronomy	4	5	3	2018.00	18.00	1.08
dysphagia	4	6	3	2017.00	7.00	0.48
extrusion	5	10	5	2019.20	13.20	1.57
food	5	10	7	2016.85	12.85	0.89
food design	6	12	9	2018.11	31.66	1.62
food sector	2	6	4	2018.75	5.50	0.19
fused deposition modelling	1	2	3	2019.00	9.66	0.88
industry 4.0	2	4	3	2018.66	5.33	0.41

innovation	4	4	3	2017.33	4.00	0.15
microstructure	6	8	5	2017.80	33.20	1.96
personalized food	6	21	12	2017.83	32.50	1.09
personalized nutrition	7	13	8	2018.12	29.50	1.14
platform design	4	9	4	2015.75	78.00	1.32
printability	7	15	6	2018.00	45.00	2.07
printing parameters	4	11	5	2018.40	46.40	3.46
protein	2	2	3	2019.33	10.00	0.84
rheological properties	10	26	13	2019.00	28.92	2.50

The time evolution of 3D food printing reveals as the keywords ‘dysphagia’, ‘platform design’, ‘chocolate’ show an average year of publication of 2017. Mainly, the first experiments on 3D food printing have been performed by testing the chocolate due to its similarities with the thermoplastic materials used in fused deposition modelling (Jia, Wang, Mustafee, & Hao, 2016; Mantihal, Prakash, Godoi, & Bhandari, 2017). Also, the keyword ‘dysphagia’ that seems no longer used in the recent year it is rather included in the most general theme of the creation of personalized food structure capable of mitigating mastication or swallowing problem of elderly people (Derossi, Caporizzi, et al., 2020; Derossi, Paolillo, et al., 2020). Finally, we can observe the keywords ‘printability’, ‘microstructure’, ‘food design’, ‘personalized food’ and ‘personalized nutrition’ that fall approximately in 2018.

With the aim to dig out the most important points of 3D food printing, it is useful to analyze the normalized average citations of the author’s keywords as reported in Fig.

8B. Also, other indexes of the co-occurrences analysis are listed in Table 2. The keyword ‘printing parameters’, ‘rheological properties’, ‘printability’ and ‘microstructure’ exhibited the highest average normalized citations with values of 3.46, 2.51, 2.07 and 1.97 respectively. So, the most read and cited papers in the field of 3D food printing share information about the optimization of printing parameters and the printability of food paste which are the biggest obstacles to overcome for the practical application of 3DFP at a large scale. In addition, the study of the ‘microstructure’ of 3D printed samples is gaining great importance because it gives deep information on the structural weakness of the printed samples (Severini, Azzollini, et al., 2018; Derossi, Caporizzi, et al., 2020) allowing the improvement of 3D printed food stability. Next, the keywords ‘food design’ and ‘extrusion’ reached an average normalized citation respectively of 1.62 and 1.57. This allows making two main considerations: 1. The use of extrusion units to deposit food filaments through syringe-based or screw-based systems is the most used method in 3D food printing; 2. The food design is and must be considered in a broad sense not only indicating the potential of forming complex food shapes but the workflow of making tangible a unique project thought on the specific nutritional and sensorial needs of the consumers.

Contrarily, these data highlight a weak point of the current research in 3D food printing: the lack of experiments and information on different deposition methods such as selective laser sintering (SLS) or hot-air sintering (HAS), binder jetting, inkjet printing (Sun, Peng, Yan, Fuh, & Hong, 2015). For instance, SLS or HAS, that use powder material and laser or hot air to fuse particles in a layer-by-layer building process, have the great advantages of being very fast allowing to create a massive amount of products. But these techniques are currently undervalued and only tested on sugars or sugar-rich formula (Gray, 2010; Mantihal et al., 2020). Furthermore, being the powders highly-stable and because the un-sintered powder may be easily re-used, SLS or HAS would be very efficient techniques to study in detail.

Finally, we want to analyze the keywords ‘chocolate’ that by three occurrences and an average normalized citation of 0.81 apparently is a field in which the interest of researcher is decreasing although some papers have been recently published mainly by Mantihal and co-authors (Mantihal, Prakash, & Bhandari, 2019; Mantihal et al., 2017; Karyappa & Hashimoto, 2019; Mantihal et al., 2020; Rando & Ramaioli, 2021). The reasons why the keywords appear with weak importance in the map of Fig. 9 is that the authors decided to not include the terms ‘chocolate’ in the choice of the keywords but they classified the papers in a more general manner by using

keywords such as ‘3D food printing’, ‘printable material’, ‘texture modification’, ‘infill percentage’, ‘sensory’ etc. (Mantihal, Prakash, & Bhandari, 2019; Mantihal, Prakash, Godoi, & Bhandari, 2019; Mantihal et al., 2020). This would suggest to all authors a surgical choice and use of the keywords avoiding general terms – often already included in the title - that limits the capability to make visible and to share their results and, in turn, to improve the level of understanding of 3D food printing technology.

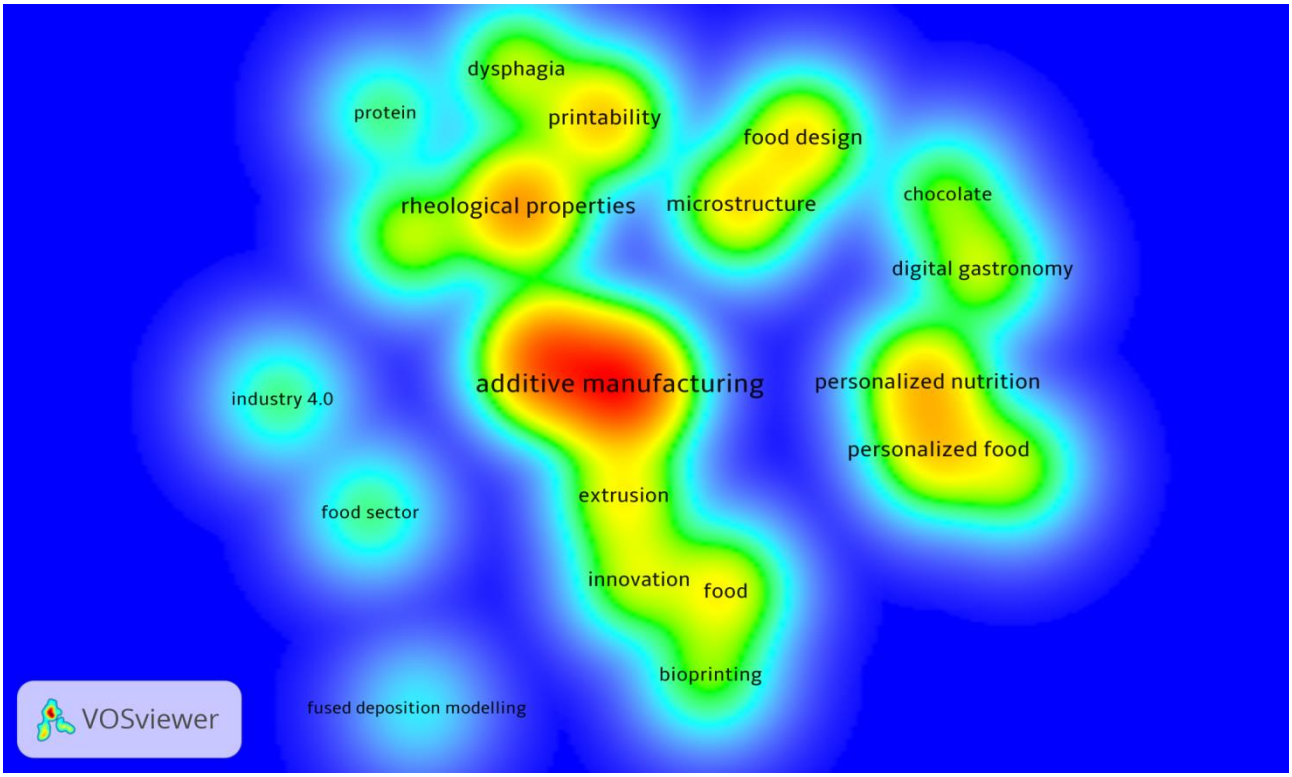

Fig. 9. Visualization of the density of link of the map of the author’s keywords used in 3FDP literature

To conclude, we want to analyze the interrelations of 3D food printing topics. The density visualization of Fig. 9 displays for any point of the map the density of the links at that point. In other words, we can assume the figure as a geographical map with islands in the sea of 3D food printing. While the contours of the island are shaped by the interrelation of the keywords that co-occurs in the same papers, the altitude of the island represents the number of links of each keyword. The density visualization has been obtained by setting the parameter Kernel width of the software VosViewer at 1.22. Four main islands can be observed.

The largest is shaped by the keywords ‘additive manufacturing’, ‘3D food printing’, ‘extrusion’, ‘innovation’, ‘food’ and ‘bioprinting’ and we want to label it with the name of Innovative 3D Food Printing by Extrusion. The second island of research may be labeled as Rheology Control and Printing Fidelity Optimization being featured by topics such as ‘printability’, ‘rheological properties’, ‘printing parameters’ and ‘dysphagia’. These two first islands are physically interconnected but mainly through the topic of rheological properties of food ink which of course is central for the innovation in 3D food printing. Another interesting result is given from the single island Protein that is located very close to the previous island but it shows only two links (Table 1) with the keywords ‘rheological properties’ and ‘additive manufacturing’. Here we can figure out a weak point of current research or – contrarily – a good opportunity to study in detail the use of food formula rich in proteins for 3D food printing experiments aiming to get novel personalized food and improving the knowledge about the effects of printing parameters, microstructure, dysphagia. The use of novel sources of proteins also coming from the recovery of other food manufacturing processes would be of great relevance for many current challenges of food security and nutrition (FAO, 2020). However, apart from some previous studies on the use of cereal-based food formula (Zhang, Lou, & Schutyser, 2018; Derossi, Caporizzi, et al., 2020; Derossi, Paolillo, et al., 2020; Derossi, Caporizzi, Paolillo, & Severini, 2021) and insect powder (Severini, Azzollini, et al., 2018), the body of the knowledge of 3D printed food rich in protein is fragile (Uribe-Wandurraga et al., 2020). Others islands in the left part of the map that worth mentioning can be labeled as Design at Macro- and Microstructure and Personalized Food. These are themes of crucial importance for the future development of 3DFP but they appear only weakly linked with the others research topics allowing to highlight additional opportunities such as to study the creation of food with personalized mechanical properties that based on the deep information on digital design, microstructure properties and rheological feature of food-ink may unleash novel potentials of 3DFP by creating unprecedented texture perceptions and helping to mitigate the mastication and swallowing problems of elderly or patients.

4. Conclusions

3D Food Printing, 3DFP, is an emerging field of research with unprecedented ambitions of creating foods with sensorial and nutritional personalized properties from digital images. This paper creates a physical map of the global production of scientific documents aiming to contribute to the future development of 3DFP highlighting weaknesses and discovering hidden latent opportunities.

We find a total of 170 documents from 38 Countries of which China and Australia are the most productive and collaborative. In addition, only 51 authors on a total of 582 researchers shape the largest map of the active collaboration although more limited – not more than 10 - is the number of authors directly connected out of their own group/institution. This is a weakness in the actual field of 3DFP and novel international collaborations should be activated to speed up the real implementation of 3D printing in the food sector. When mapping the most representative author's keywords fall in the period between 2016 and 2020. Current hot-points, in which the majority of the efforts are concentrated, are the 'rheological properties', 'printability', 'printing parameters' and 'microstructure' which show the highest average normalized citations. In fact, the hottest and urgent topic regards the capability to design and develop ink-food with excellent rheological properties and the ability to customize the printing parameters on the features of the ink-food. Also, the analysis of the co-occurrences revealed the shortage of experiments on alternative printing methods such as SLS and HAS which could introduce two main novelties: fast printing and the use of dehydrated food-ink with a prolonged shelf life. Finally, four main islands of research have been individuated in the field of 3D food printing such as Innovative 3D Food Printing by Extrusion, Rheology Control and Printing Fidelity Optimization, Design and Macro- and Microstructure and Personalized Food. While the first two are connected by the study of rheological properties of food-ink, the others appear weakly connected. This result highlights the opportunity to reinforce the relationship between digital design, microstructure and novel personalized food products with unprecedented sensory perception or capability of mitigating the mastication and swallowing problems of vulnerable consumers. Finally, the study of food-inks rich in protein – which appears few and isolated - should be enlarged and linked to other aspects such as the digital design, the effects on microstructure and the creation of personalized food products.

References

Agostinacchio, F., Mu, X., Dirè, S., Motta, A., & Kaplan, D.L. (2020). In situ 3D printing: Opportunities with Silk Inks. *Trends in Biotechnology*, in press, https://doi.org/10.1016/j.tibtech.2020.11.003 .

Baiano, A. (2020). 3D printed Foods: A comprehensive Review on Technologies, Nutritional value, safety, consumer, attitude, nutritional value, safety, consumer attitude, regulatory framework, and economic and sustainability issues. *Food Reviews International*, in press, https://doi.org/10.1080/87559129.2020.1762091.

Beg, S., Almalki, W.H., Malikm A., Farhan, M., Aatif, M., Rahman, Z., Alruwaili, N.K., Alrobaian, M., Tarique, M., & Rahman, M. (2020). 3D printing for drug delivery and biomedical applications. *Drug Discovery Today*, 25, 9, 1668-1681. https://doi.org/10.1016/j.drudis.2020.07.007

Betran, F.A., Jhaveri, S., Lutz, R., Isbister, K., & Wilde, D. (2019). Making Sense of Human-Food Interaction. CHI 2019, may 4-9, Slasgiw, Scotland, UK. https://doi.org/10.1145/3290605.3300908

Bueno, G., Altes, P., Carnovale, L., Hernandez, N., Sancho, J., Zamora, G., Esteban, C., & Llagostera, S. (2019). Present or Future: Rapid 3d Printing Prototyping Technology for Aortic Aneurysm Surgery Planning and Its Utility in Open and Endovascular Treatment. *European Journal of Vascular and Endovascular Surgery*, 58, 6, e271-e272, https://doi.org/10.1016/j.ejvs.2019.06.869 .

Buchanan, C., & Gardner, L., (2019). Metal 3D printing in construction: A review of methods, research, applications, opportunities and challenges. *Engineering Structures*, 180, 332-348. https://doi.org/10.1016/j.engstruct.2018.11.045

Chan, S.S.L., Pennings, R.M., Edwards, L., Franks, G. (2020). 3D printing of clay for decorative architectural applications: effect of solids volume fraction on rheology and printability. Additive manufacturing, 35, 101335, https://doi.org/10.1016/j.addma.2020.101335

Charlebois, S., & Juhasz, M. (2018). Food futures and 3D printing: Strategic market foresight and the case of structure 3D. *International Journal on Food System Dynamics*, 9 (2), 138-148.

Chaundry, B.M., Connelly, K., Siek, K.A., & Welch, J.L. (2012). Formative evaluation of a mobile liquid portion size estimation interface for people with varying literacy skills. *Journal of Ambient Intelligence and Humanized Computing*, https://doi:10.1007/s12652-012-0152-9 .

Cohen, D., Lipton, J., Cutler, M., Coulter, D., Vesco, A., & Lipson, H. (2009). Hydrocolloid printing: a novel platform for customized food production. Proceedings of the 20th Annual International Solid Freeform Fabrication Symposium, pp. 807–818. Austin, TX.

Comber, R., Choi, J.H.j. Hoonhout, J., & O'Hara, K. (2014). Designing for human-food-interaction: an introduction to the special issue on 'food and interaction design'. Int. J. Human-Computer Studies, 72, 181-184. https://doi.org/10.1016/j.ijhcs.2013.09.001

Comminal, R., Leal da Silva, W.R., Andersen, T.J., Stang, H., & Spangenberg, J. (2020). Modelling of 3D concrete printing based on computational fluid dynamics. *Cement and Concrete Research*, 138, 106256. https://doi.org/10.1016/j.cemconres.2020.106256

D'Angelo, G., Hansen, H.N., & Hart, A.J. (2016). Molecular Gastronomy Meets 3D Printing: layered Construction via reverse Spherification. *3D Printing and Additive Manufacturing*, 3, 153-159.

Dankar, I., Haddarah, A., Omar, F.E.L., Sepulcre, F., & Pujolà, M. (2018). 3D printing technology: The new era for food customization and elaboration, *Trends in Food Science & Technology*, 75, 231-242, ISSN 0924-2244, https://doi.org/10.1016/j.tifs.2018.03.018 .

Derossi, A., Caporizzi, R., Ricci, I., & Severini, C. (2018). Critical variables in 3D food printing. In: Godoi, F.C., Bhandari, B., Prakash, S., Zhang, M. *Fundamentals of 3D Food Printing and Applications*, 2018, 41-91. https://doi.org/10.1016/B978-0-12-814564-7.00003-1

Derossi, A., Caporizzi, R., Oral, M.O., & Severini, C. (2020a). Analyzing the effects of 3D printing process per se on the microstructure and mechanical properties of cereal food products, *Innovative Food Science & Emerging Technologies*, 66, 102531, https://doi.org/10.1016/j.ifset.2020.102531 .

Derossi, A., Paolillo, M., Caporizzi, R., & Severini, C. (2020b). Extending the 3D food printing test at high speed. Material deposition and effect of non-printing movements on the final quality of printed structures. *Journal of Food Engineering*, 275, 109865. https://10.1016/j.jfoodeng.2019.109865

Derossi, R. Caporizzi, M. Paolillo, & C. Severini (2021). Programmable texture properties of cereal-based snack mediated by 3D printing technology. *Journal of Food Engineering*, 289, 110160, https://doi.org/10.1016/j.jfoodeng.2020.110160.

Dianez, L., Gallegos, C., Brito-de la Fuente, E., Martinez, I., Valencia, C., Sanchez, M.C., Diaz, M.J., & Franco, J.M. (2019). 3D printing in situ gelification of k-carrageenan solutions: effect of printing variables on the rheological response. *Food Hydrocolloids*, 87, 321-330.

Dick, A., Bhandari, B., & Prakash, S. (2019). 3D printing of meat. *Meat Science*, 153, 35-44. https://doi.org.10.1016/j.meatsci.2019.03.005

El Mohadab, M., Bouikhalene, B., & Safi, S. (2020). Bibliometric method for mapping the state of the art of scientific production in Covid-19. *Chaos, Solitons and Fractals*, 139, 110052. https://doi.org/10.1016/j.chaos.2020.110052

FAO (2020). The state of Food Security and Nutrition in the World. http://www.fao.org/3/ca9692en/CA9692EN.pdf

Fahmy, A.R., & Becker, T., (2020). 3D printing and additive manufacturing of cereal-based materials: Quality analysis of starch-based systems using a camera-based morphological approach. *Innovative Food Science and Emerging Technologies*, 63, 102384

Feng, C., Chang, M., & Bhandari, B. (2019). Materials properties of printable edible inks and printing parameters optimization during 3D printing: a review. *Critical review in food science and nutrition*, 59 (19), 3074-3081, https://doi.org/10.1080/10408398.2018.1481823

Gholamipour-Shirazi, A., Norton, I.T., & Mills, T. (2019). Designing hydrocolloids based food-ink formulations for extrusion 3D printing. *Food Hydrocolloids*, 95, 161-167. https://doi.org/10.1016/j.foodhyd.2019.04.011 .

Gholamipour-Shirazi, A., Kamlow, M.A., Norton, I.T., & Mills, T. (2020). How to formulate for structure and texture via medium of additive manufacturing-A review. *Foods*, 9 (4), 497, https://doi.org/10.3390/foods9040497.

Gibson, M.A., Mykulowycz, N.M., Shim, J., Fontana, R., Schmitt, P., Roberts, A., Ketkaew, J., Shao, L., Chen, W., Bordeenithikasem, P., Myerberg, J.S., Fulop, R., Verminski, M.D., Sachs, E.M., Chiang, Y.M., Schuh, C.A., Hart, J., & Schroers, J. (2018). 3D printing metals like thermoplastics: Fused filament fabrication of metallic glasses. *Materials Today*, 21, 7, 697-702, https://doi.org/10.1016/j.mattod.2018.07.001.

Godoi, F.C., Prakash, S., & Bhandari, B. (2016). 3d printing technologies applied for food design: status and prospects. *Journal of Food Engineering*, 179, 44-54. https://doi.org/10.1016/j.jfoodeng.2016.01.025

Godoi, F., Bhandari, B., Prakash, S., & Zhang, M. (2018). Fundamentals of 3D Food Printing and Applications. Academic press. ISBN 9780128145647. https://doi.org/10.1016/B978-0-12-814564-7.00003-1

Gray, N. (2010). Looking to the future: creating novel food using 3D printing. http://www.foodnavigator.com/Science/Looking-to-the-future-Creating-novel-foods-using-3D-printing.

Guo, C.F., Zhang, M., & Bhandari, B. (2019). A comparative study between syringe-based and screw-based food printers by computational simulation. *Computers and Electronics in Agriculture*, 162, 397-404. 10.1016/j.compag.2019.04.032

Guo, C., Zhang, M., & Devahastin, S. (2021). Color/aroma changes of 3D-Printed buckwheat dough with yellow flesh peach as triggered by microwave heating of gelatin gum Arabic complex coacervates. *Food Hydrocolloids*, 112, 106358. https://doi.org/10.1016/j.foodhyd.2020.106358

Handral, H., Hua Tay, S., Wan Chan, W., & Choudhury, D. (2020). 3D printing of cultered meat products. *Critical reviews in food science and nutrition*, 21, 1-10. 10.1080/10408398.2020.1815172

Hashimoto, A., Funatomi, T., Ueda, M., & Yamakata, Y. (2012). Recognizing ingredients at cutting process by integrating multimodal features. CEA'12. November, 2, doi:10.1145/2390776.2390780.

He, C., Xhang, M., & Guo, C. (2020a) 4D printing of mashed potato/purple sweet potato puree with spontaneous color change.. *Innovative Food Science and Emerging Technologies*, 59, 102250. https://doi.org/10.1016/j.ifset.2019.102250

He, C., Zhang, M., & Fang, Z. (2020b). 3D printing of food: pretreatment and post-treatment of materials. *Critical reviews in food science and nutrition*, 60 (14), 2379-2392. https://doi.org/10.1080/10408398.2019.1641065

Jerman, M., Zelenak, M., Lebar, A., Foldyna, V., Foldyna, J., & Valentincic, J. (2021). Observation of cryogenically cooled ice particles inside the high-speed water jet. *Journal of Materials Processing Technology*, 289, 116947. https://doi.org/10.1016/j.jmatprotec.2020.116947

Jia, F., Wang, X., Mustafee, N., Hao, L. (2016). Investigating the feasibility of supply chain-centric business models in 3D chocolate printing: A simulation study. Technological Forecasting and Social Change, 102, 202-213. DOI: 10.1016/j.techfore.2015.07.026

Jiang, H., Zheng, L., Zou, Y., Han, S., & Wang, S. (2019). 3D food printing: main components selection by considering rheological properties. *Critical Reviews in Food*

Science and Nutrition, 59 (14), 2335-2347. https://doi.org/10.1080/10408398.2018.1514363

Jiang, J., Zhang, M., Bhandari, B., & Cao, P. (2020). Current processing and packing technology for space foods: a review. *Critical reviews in Food Science and Nutrition*, 60 (21), 3573-3588. https://doi.org/10.1080/10408398.2019.1700348

Julkarnyne M. Habibur Rahman, MD Nahin Islam Shiblee, Kumkum Ahmed, Ajit Khosla, Masaru Kawakami, & Hidemitsu Furukawa (2020). Rheological and mechanical properties of edible gel materials for 3D food printing technology. *Heliyon*, 6, 12, e05859, https://doi.org/10.1016/j.heliyon.2020.e05859.

Kambhampati, S.B.S., Vaishya, R., & Vaish, A. (2020). Unprecedented surge in publications related to COVID-19 in the first three months of pandemic: A bibliometric analytic report. *Journal of Clinical Orthopaedics and Trauma*, 11, 3, S304-S306, https://doi.org/10.1016/j.jcot.2020.04.030 .

Karyappa, R., & Hashimoto, M. (2019). Chocolate-based ink three-dimensional printing (Ci3DP). *Scientific Report*, 9 (1), 14178. https://doi.org/10.1038/s41598-019-50583-5

Kim, N.P., Cepeda, B., Kim, J., Yue, G., Kim, S., & Kim, H. (2018). IoT controlled screw-type 3D food printer using single line design technique. International Conference on Computational Science and Computational Intelligence, CSCI 2018, December 2018, Las Vegas.

Kern, C., Weiss, J., & Hinrichs, J. (2018). Additive layer manufacturing of semi-hard model cheese: effect of calcium levels on thermo-rheological properties and shear behavior. *Journal of Food Engineering*, 235, 89-97.

Kuo, C.C., Qin, H., Cheng, Y., Jiang, X., & Shi, X. (2021). An integrated manufacturing strategy to fabricate delivery system using gelatin/alginate hybrid hydrogels: 3D printing and freeze-drying. *Food Hydrocolloids*, 111, 106262, https://doi.org/10.1016/j.foodhyd.2020.106262 .

Le-Bail, Maniglia, B.C., & Le-Bail, P. (2020). Recent advances and future perspective in additive manufacturing of foods based on 3D printing. *Current Opinion in Food Science*, 35, 54-64, https://doi.org/10.1016/j.cofs.2020.01.009 .

Li, N., Zhang, J., Xing, W., Ouyang, D., & Liu, L. (2018). 3D printing of Fe-based bulk metallic glass composites with combined high strength and fracture toughness. *Materials & Design*, 143, 285-296, https://doi.org/10.1016/j.matdes.2018.01.061 .

Lipton, J.I., Cutler, M., Nigl, F., Cohen, D., & Lipson, H. (2015). Additive manufacturing for the food industry. *Trends in Food Science & Technology*, 43, 114-123. https://doi.org/10.1016/j.tifs.2015.02.004

Liu, Z., Zhang, M., Bhandari, B., & Yang, C. (2018). Impact of rheological properties of mashed potatoes on 3D printing. *Journal of Food Engineering*, 220, 76-82. https://doi:10.1016/j.foodeng.2017.04.017 .

Liu, Z., Bhandari, B., Prakash, S., Mantihal, S. & Zhanga, M. (2019). Linking rheology and printability of a multicomponent gel system of carrageenan-xanthan-starch in extrusion based additive manufacturing. *Food Hydrocolloids*, 87, 413-424. https://doi.org/10.1016/j.foodhyd.2018.08.026 .

Manoj, A., Bhuyan, M., Raj Banik, S., & Ravi Sankar, M. (2020). 3D Printing of Nasopharyngeal Swabs for COVID-19 Diagnose: Past and Current Trends. *Materials Today*: Proceedings. doi: 10.1016/j.matpr.2020.11.505

Mantihal, S., Prakash, S., Godoi, F.C., Bhandari, B. (2017). Optimization of chocolate 3D printing by correlating thermal and flow properties with 3D structure modeling. Innovative Food Science and Emerging Technologies, 44, 21-29. DOI: 10.1016/j.ifset.2017.09.012

Mantihal, S., Prakash, S., & Bhandari, B. (2019a). Texture-modified 3D printed dark chocolate: sensory evaluation and consumer perception study. *Journal of Texture Studies*, 50 (5), 386-399. DOI: 10.1111/jtxs.12472

Mantihal, S., Prakash, S., Godoi, F.C., Bhandari, B. (2019b). Effect of additives on thermal, rheological and tribological properties of 3D printed dark chocolate. *Food Research International*, 119, 161-169. DOI: 10.1016/j.foodres.2019.01.056

Mantihal, S., Kobun, R., & Lee, B.-B (2020). 3D food printing of as the new way of preparing food: A review. *International Journal of Gastronomy and Food Science*, 22, 100260. https://doi.org/10.1016/j.ijgfs.2020.100260

Mascarenhas, C., Ferreira, J.J., & Marques, C. (2018). University-industry cooperation: a systematic literature review and research agenda. *Science and Public Policy*, 45, 708-718. https://doi.org/10.1093/scipol/scy003

Mingers, J., & Leydesdorff L. (2015). A review of theory and practice in scientometrics. European *Journal of Operational Research*, 246, 1-19. https://doi.org/10.1016/j.ejor.2015.04.002

Murr, L.E. (2020). Metallurgy principles applied to powder bed fusion 3D printing/additive manufacturing of personalized and optimized metal and alloy biomedical implants: an overview. *Journal of Materials Research and Technology*, 9, 1087-1103. https://doi.org/10.1016/j.jmrt.2019.12.015

Nachal, N., Moses, J.A., Karthik, P., & Chinnaswamy, A. (2019). Application of 3D printing in Food processing. *Food Engineering Reviews*, 11, 3, https://doi:10.1007/s12393-019-09199-8

NASA. Funds system for 3D printing in space (2017). *Metal Powder Report*, 72, 6, Pages 434-435, https://doi.org/10.1016/j.mprp.2017.10.024.

Nesic, D., Durual, S., Marger, L., Mekki, M. Sailer, I., & Scherrer, S.S. (2020). Could 3D printing be the future for oral soft tissue regeneration?. *Bioprinting*, 20, e00100, https://doi.org/10.1016/j.bprint.2020.e00100 .

Otlet, P. (1934). Traité de documentation: le livre sur le livre, théorie et pratique. Brussels: Editions Mundaneum.

Pant, A., Lee, A.Y., Karyappa, R., Lee, C.P., An, J., Hashimoto, M., Tan, U.X., Wong, G., Chua, C.K., & Zhang, Y. (2021). 3D food printing of fresh vegetables using food hydrocolloids for dysphagic patients. *Food Hydrocolloids*, 114, 106546, ISSN 0268-005X, https://doi.org/10.1016/j.foodhyd.2020.106546 .

Park, J.Y., & Nagy, Z. (2018). Comprehensive analysis of the relationship between thermal comfort and building control research – A data-driven literature review. *Renewable and sustainable energy reviews*, 82, 2664-2679. https://doi.org/10.1016/j.rser.2017.09.102

Park, S.M., Kim, H.W., & Park, H.J. (2020). Callus-based 3D printing for food exemplified with carrot tissues and its potential for innovative food production. *Journal of Food Engineering*, 271, 109781, https://doi.org/10.1016/j.jfoodeng.2019.109781 .

Perianes-Rodrguez, A., Waltman, L., & van Eck, N.J. (2016). Constructing bibliometric networks: A comparison between full and fractional counting. *Journal of Informetrics*, 10, 4, 1178-1195, https://doi.org/10.1016/j.joi.2016.10.006 .

Perez, B., Nykvist, H., Brogger, A.F., Larsen, M.B., & Falkeborg, M.F. (2019). Impact of macronutrients printability and 3D-printer parameters on 3D-food printing: A review. *Food Chemistry*, 287, 249-257. https://doi.org/10.1016/j.foodchem.2019.02.090

Phuhongsung, P., Zhang, M., & Bhandari, B. (2020). 4D printing of products based on soy protein isolate via microwave heating for flavor development. *Food Research International*, 137, 109605. https://doi.org/10.1016/j.foodres.2020.109605

Piyush, Kumar, R., & Kumar, R., (2019). 3D printing of food materials: A state of art review and future applications. Materials Today: Proceedings of the 1st International Symposium on Synthesis, Characterization and Processing of Inorganic, Bio and Nano Materials, 33, 1463-1467. https://doi.org/10.1016/j.matpr.2020.02.005

Portanguen, A., Tournayre, P., Sicard, J., Astruc, T., Mirade, P.S. (2019). Toward the design of functional foods and biobased products by 3D printing: A review. *Trends in Food Science and Technology*, 86, 188-198.

Price, D.J.d.S. (1976). A general theory of bibliometric and other cumulative advantage processes. *Journal of the American Society for Information Science*, 27, 292-306. https://doi.org/10.1002/asi.4630270505

Pulatsu, E., Su, J.W., Lin, J., & Lin, M. (2020). Factors affecting 3D printing and post-processing capacity of cookie dough. *Innovative Food Science & Emerging Technologies*, 102316. https://doi.org/10.1016/j.ifset.2020.102316

Pulatsu, E., & Lin, M. (2021a). A review on customizing edible food materials into 3D printable inks: Approaches and strategies. *Trends in Food Science & Technology*, 107, 68-77, https://doi.org/10.1016/j.tifs.2020.11.023 .

Pulatsu, E., Su, J.W., Kenderes, S.M., Lin, J., Vardhanabhuti, B., & Lin, M. (2021). Effects of ingredients and pre-heating on the printing quality and dimensional stability in 3D printing of cookie dough. *Journal of Food Engineering*, 294, 1104, https://doi.org/10.1016/j.jfoodeng.2020.110412 .

Ramundo, L., Taisch, M., Terzi, S. (2016). State of the art of technology in the food sector value chain towards the IoT. *IEEE 2nd International Forum on Research and Technologies for Society and Industry Leveraging a Better Tomorrow*, Bologna; Italy; 7 September.

Rando, P, & Ramaioli, M. (2021). Food 3D printing: effect of heat transfer on print stability of chocolate. *Journal of Food Engineering*, 294, 110415. https://doi.org/10.1016/j.jfoodeng.2020.110415

Rayna, T., & Striukova, L., (2016). From rapid prototyping to home fabrication: How 3D printing is changing business model innovation. *Technological Forecasting and Social Change*, 102, 214 224, https://doi.org/10.1016/j.techfore.2015.07.023.

Sartal, A., Carou, D., Dorado-Vicente, R., & Mandayo, L. (2019). Facing the challenges of the food industry: Might additive manufacturing be the answer?. Proceedings of the Institution of Mechanical Engineers, Part B: *Journal of Engineering, Manufacture*, 233, (8), 1902-1906.

Schutyser, M.A.I., Houlder, M., de Wit, M., Buijsse, C.A.P., & Alting, A.C. (2018). Fused deposition modeling of sodium caseinate dispersions. *Journal of Food Engineering*, 220, 49-55. https://doi.org/10.1016/j.jfoodeng.2017.02.004

Severini, C., & Derossi, A. (2016). Could the 3D printing technology be a useful strategy to obtain customized nutrition?. *Journal of clinical Gastroenterology*, 50, S175-S178. DOI: 10.1097/MCG.0000000000000705

Severini, C., Azzollini, D., Albenzio, M., & Derossi, A. (2018a). On printability, quality and nutritional properties of 3D printed cereal based snacks enriched with edible insects. *Food Research International*, 106, 666-676. https://doi.org/10.1016/j.foodres.2018.01.034

Severini, C., Derossi, A., Ricci, I., Caporizzi, R., & Fiore, A. (2018b). Printing a blend of fruit and vegetables. New advances on critical variables and shelf life of 3D edible objects. *Journal of Food Engineering*, 220, 89-10, https://doi.org/10.1016/j.jfoodeng.2017.08.025 .

Shao, B., Li, X., & Bian, G. (2021). A survey of research hotspots and frontier trends of recommendation system from the perspective of knowledge graph. *Expert Systems with applications*, 165, 113764. https://doi.org/10.1016/j.eswa.2020.113764

Stamati, V., Antonopoulos, G., Azariadis, Ph., Fudos, I. (2011). A parametric feature-based approach to reconstructing traditional filigree jewelry (2011). Computer-Aided Design, 12, 1814-1828, https://doi.org/10.1016/j.cad.2011.07.002

Steenhuis, H.J., Fang, X., & Ulusemre, T. (2018). Strategy in 3D printing of Food. PICMET - Portland International Conference on Management of Engineering and Technology: Managing Technological Entrepreneurship: The Engine for Economic Growth, Proceedings4 October 2018, Honolulu; United

Subramayna, S.H., Lama, B., & Acharya, K.P. (2020). Impact of COVID-19 pandemic on the scientific community. *Qatar Med J.*, 1, 21. doi: 10.5339/qmj.2020.21

Sun, J., Zhou, W., Huang, D., Fuh, J.Y., & Hong, G.S. (2015). An overview of 3D printing technologies for food fabrication. *Food Bioprocess Technology*, 8 (8), 1605e1615. http://dx.doi.org/10.1007/s11947-015-1528-6 .

Sun, J., Peng, Z., Yan, L., Fuh, J.Y.H., & Hong, G.S. (2015). 3D food printing-An innovative way of mass customization in food fabrication. *International Journal of Bioprinting*, 1 (1), 27-38.

Sweileh, W.M., Al-Jabi, S.W., Zyoud, A.H., Sawalha, A., & Abu-Taha, A. (2018). Global research output in antimicrobial resistance among uropathogens: A bibliometric analysis (2002-2016). *Journal of Global Antimicrobial Resistance*, 13, 104-114. DOI: 10.1016/j.jgar.2017.11.017

Mantihal, S., Prakash, S., Godoi, F.C., Bhandari, B. (2017). Optimization of chocolate 3D printing by correlating thermal and flow properties with 3D structure modeling. *Innovative Food Science & Emerging Technologies*, 44, 21-29, https://doi.org/10.1016/j.ifset.2017.09.012 .

Mantihal, S, Kobun, R, Lee, B.B. (2020). 3D food printing of as the new way of preparing food: a review. International journal of Food Gastronomy and Food Science, 22, 100260, https://doi.org/10.1016/j.ijgfs.2020.100260.

Tagami, T., Ito, E., Kida, R., Hirose, K., Noda, T., & Ozeki, T. (2021). 3D printing of gummy drug formulations composed of gelatin and an HPMC-based hydrogel for pediatric use. *International Journal of Pharmaceutics*, 594, 120118, https://doi.org/10.1016/j.ijpharm.2020

Tan, C., Toh, W.Y., Wong, G., & Lin, L. (2018). Extrusion-based 3D food printing – Material and machines, International Journal of Bioprinting, 4 (2). doi: 10.18063/IJB.v4i.143.

Tian, H., Wang, K., Lan, H., Wang, Y., Hu, Z., & Zhao, L. (2021). Effect of hybrid gelator systems of beeswax-carrageenan-xanthan on rheological properties and printability of litchi inks for 3D food printing. *Food Hydrocolloids*, 113, 106482. https://doi.org/10.1016/j.foodhyd.2020.106482 .

Uribe-Wandurraga, Z.N., Zhang, L., Noort, M.W.J., Schutyser, M.A.I., Garcia-Segovia, P., & Martinez-Monzo, J. (2020). Printability and physicochemical properties of microalgae-enriched 3D printed snacks. *Food and Bioprocess technology*, 13, 2029-2042. https://doi.org/10.1007/s11947-020-02544-4

van Eck, N.J., & Waltman, L. (2009). How to normalize co-occurrence data ? An analysis of some well-know similarity measures. *Journal of the American Society for Information Science and technology*, 60, (8), 1635-1615. https://doi.org/10.1002/asi.21075

Voon, S.L., An, J, Wong, G., Zhang, Y., & Chua, C.K., (2019). 3D food printing a categorized review of inks and their development. *Virtual and Physical Prototyping*. 10.1080/17452759.2019.1603508

Waltman, L., van Eck, N.J., & Noyons, E.C.M. (2010). A unified approach to mapping and clustering of bibliometric networks. *Journal of Infometrics*, 4, 629-635. https://doi.org/10.1016/j.joi.2010.07.002

Wang, L., Zhang, M., Bhandaru, B., & Yang, C. (2018). Investigation of surimi gel as primising food material for 3D printing. *Journal of Food Engineering*, 220, 101-108. https://doi.org/10.1016/j.jfoodeng.2017.02.029

Want, S. (2020). 3D Printing clothing design based on wireless sensors and FPGA. *Microprocessors and Microsystems*, 103407, https://doi.org/10.1016/j.micpro.2020.103407 .

Yang, F., Zhang, M., Bhandari, B., & Liu, Y. (2018). Investigation on lemon juice gel as food material for 3D printing and optimization of printing parameters. *LWT, Food Science and technology*, 87, 67-76. https://doi.org/10.1016/j.lwt.2017.08.054

Zhang, L., Lou, Y., & Schutyser, M.A.I. (2018). 3D printing of cereal-based food structures containing probiotics. *Food Structure*, 18, 14-22. https://doi.org/10.1016/j.foostr.2018.10.002

Zhao, L., Zhang, M., Chitrakar, B., & Adhikari, B. (2020). Recent advances in functional 3D printing of foods: a review of functions of ingredients and internal structures. *Critical Reviews in Food Science and Nutrition*, in press. https://doi.org/10.1080/10408398.2020.1799327

Zhu, S., Stieger, M. A., van der Goota, A. J., & Schutyser, M. A. I. (2019). Extrusion-based 3D printing of food pastes: Correlating rheological properties with printing behaviour. *Innovative Food Science & Emerging Technologies*, 58, 102214. https://doi.org/10.1016/j.ifset.2019.102214.

CHAPTER 4 Rheological properties, dispensing force and printing fidelity of starchy-gels modulated by concentration, temperature and resting time

Maddalena Paolillo, Antonio Derossi, Kjeld van Bommel, Martijn Noort, Carla Severini

Food Hydrocolloids

Volume 117, August 2021, 106703

Abstract

3D Food Printing (3DFP) is capable of creating a specific 3D food structure starting from a digital image. This capability can renew the way in which food manufacturing is thought. To this end, we modulated the properties of a starchy-gel system by systematically varying starch composition (the weight fraction of tapioca dextrin and cold water swelling waxy maize starch), the storage time before printing (ST), and printing temperature (PT). For each starchy-gel we have analyzed its rheological properties, printing behavior and the quality of the 3D printed replica and its microstructure. Analysis of the viscosity profile allowed determining the minimum stress (6.5 × 102 mPa s) at which the gels start to flow and are extruded from the syringe. We also determined the dispensing force needed to extrude the gels from the syringe, which at the extrusion rate of 26.4 mm3/s, showed a maximum value of 645.7 N at which the printing completely failed. Between these limits, a wide range of printing fidelities of gels was identified, where the printability was affected not only by the weight fraction of starch and printing temperature but also, and with high extent, by the time before printing. For instance, viscosity increased from 5 × 105 mPa s and 1 × 106 mPa s in the first 24 h of resting. Discrepancy from the 3D digital model regards not only the visual (external) aspect but also the microstructure features. The results of our research allow us to control the printability of starchy-gels and to create innovative food structures in which the local porosity/structure can be controlled based on the digital design.

Graphical abstract

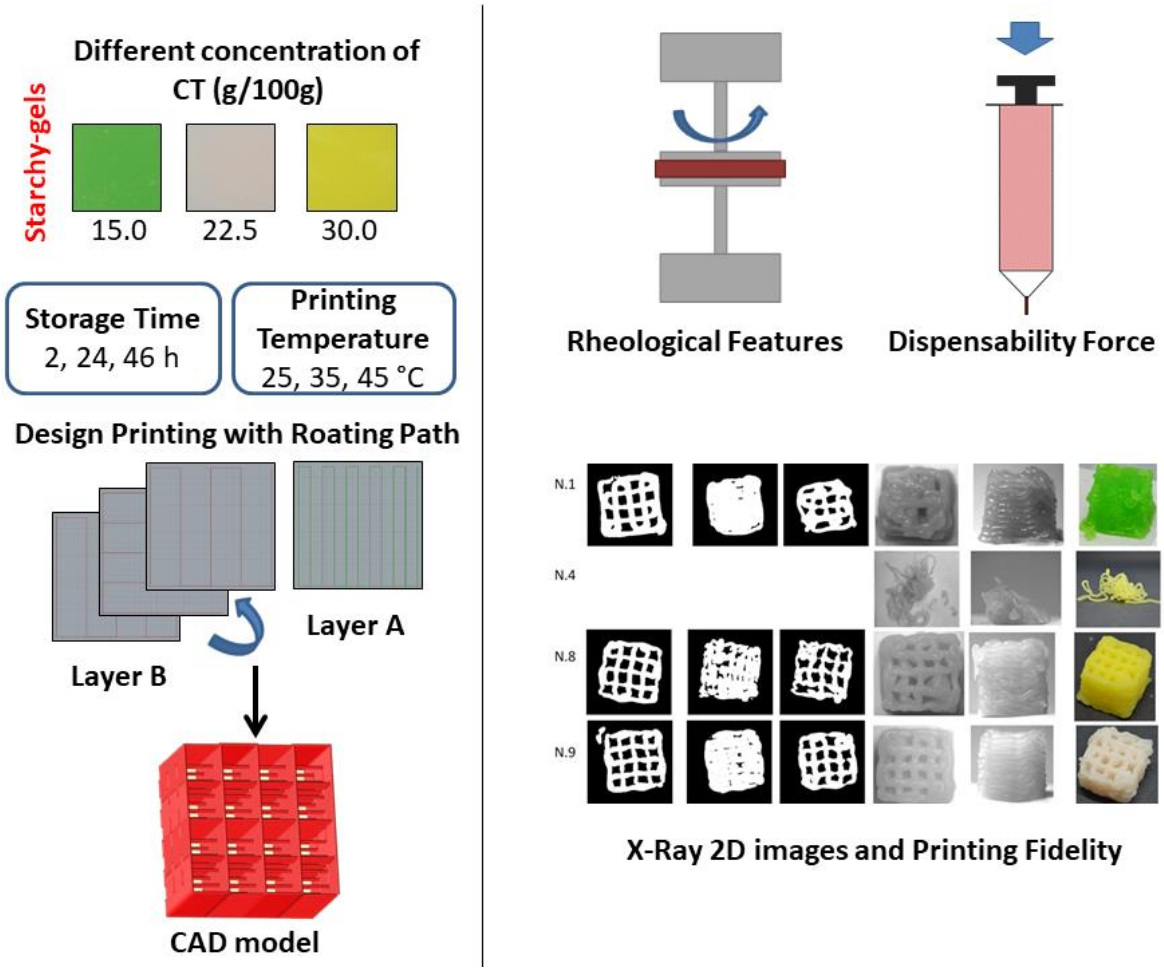

1. Introduction

Recently, the interest for layer-by-layer deposition of food materials, popularly called 3D Food Printing (3DFP), is increasing a dizzying rate (Godoi, Prakash, & Bhandari, 2016; Lipton, Culter, Nigl, Cohen, & Lipson, 2015). 3D Printing (3DP) consists of a wide series of technologies based on a digitally-controlled process capable of producing customized products and rapid prototypes (Berman, 2012). These include selective sintering (SLS), fused deposition modeling (FDM), inkjet printing (IJP), binder jet printing (BJP) and extrusion deposition modeling (Godoi et al., 2016; Sun, Peng, Yan, Fuh, & Hong, 2015). The general principles of 3DP involve the deposition of materials in 3D space by controlled movements that follow a computer-assisted design model (CAD). In the food sector the great interest on 3DP is mainly interrelated with the benefits generated by creative food design with respect to novel structure, shapes and textures and consequently even new eating experience (van

Bommel, 2012). In addition, personalized food manufacturing, decentralization of food production and novel start-ups, may be indicated as potential key-advantages for the practical application of 3DFP (Le-Bail, Maniglia, & Le-Bail, 2020; Piyush, Kumar, & Kumar, 2020).

Definitely, the extrusion deposition modeling is the most used 3D printing method in food sector because it allows to employ a wide range of non-Newtonian edible materials such as potato (Feng, Zhang, Bhandari, & Ye, 2020; Liu et al., 2018, Liu et al., 2018b), chocolate (Lanaro et al., 2020; Mantihal, Prakash, Godoi, & Bhandari, 2019), fruit and vegetables (Severini, Derossi, Ricci, Caporizzi, & Fiore, 2018), cereal doughs (Derossi, Caporizzi, Paolillo, & Severini, 2020; Derossi, Paolillo, Caporizzi, & Severini, 2020; Pulatsu, Su, Lin, & Lin, 2020), meat (Dick, Bhandari, Dong, & Prakash, 2020), eggs (Xu et al., 2020), surimi (Liu et al., 2018, Liu et al., 2018b), etc. However, essential features for the usage of food in 3D printing are firstly the capability to be easily deposited – extruded from the nozzle - that requires shear thinning behavior (Gholamipour, Shirazi, Norton, & Mills, 2019) and, secondly, the capacity to keep shape and dimension of the 3D printed structure. The latter aspect includes properties such as adhesiveness, viscosity and consistency providing stability and avoiding the collapse of the 3D printed food.

With this aim several papers have been focused on the rheological properties of raw ingredients and their printability (Liu, Liu, et al., 2018; Liu et al., 2018, Liu et al., 2018b; Wang et al., 2018; Zhu, Stieger, van der Goot, & Schutyser, 2019) as well as on the addiction of gelling/structuring agents to improve aforementioned properties (Anukiruthika, Moses, Anandharamakrishnan., 2020; Cohen, Laviv, Berman, Nashef, & Abu-Tair., 2009; Dick et al., 2020; Liu, Liu, et al., 2018; Wegrzyn, Golding, & Archer, 2012). Liu et al., 2018, Liu et al., 2018b used a model system made of carrageenan-xanthan-starch to define the relationship between rheological attributes and the printability of food formula. Liu, Bhandari, Prakash, Mantihal, and Zhanga (2019) studied the rheological, textural and mechanical behavior of milk protein composite gel proposing criteria to get information on the printability of soft food materials.

More recently, some authors have created a map of the relationship between rheological properties and printability of food materials with the aim to furnish a useful guideline for a more effective realization of high-printable formulations (Zhu, Stieger, van der Goota, & Schutyser, 2019).

However, several papers agree with the usefulness of using starchy materials because very effective in increasing viscosity, adhesiveness, texture, and other features that

help the feasibility of 3D food printing process (Wang & Shi., 2020; Chen, Xie, Chen, & Zhenga, 2019; Maniglia et al., 2019). Starchy-gels are pseudoplastic fluids with shear-thinning behavior, easily extruded under high-shear printing conditions (Zhang, Li, Zhang, Wei, & Fang, 2019) and capable of maintaining the weight of overlying layers. However, when using starch in 3DFP, the paste properties, i.e. retrogradation effects, different botanical origins (wheat, maize, rice cassava, potato starch) (Breuninger, Piyachimkwan, & Srioroth, 2009), the change of proportions between amylose and amylopectin (Liu et al., 2018, Liu et al., 2018b) have a great importance on the aforementioned properties. On this specific topic – the use of starchy-gels in 3D printing – the published experiments have performed mainly testing different types of starch from maize (Lille, Nurmel, Nordlund, Metsä-Kortelainen, & Sozer, 2018), potato (Liu et al., 2018, Liu et al., 2018b; Liu, Chen, Zheng, Xie, & Chen, 2020; Yang, Guo, Zhang, Bhandari, & Liu, 2019), corn (Chen, Xie, Chen, & Zheng, 2019), native cassava (Maniglia et al., 2020), or curcuma (Leonel, Sarmento, & Cereda, 2003) while few information are available on the effect of 3D printing temperature on the fidelity of printing. Furthermore, the pre-printing conditions, such as storage temperature and storage time before material deposition, have been completely underrated although is this widely known that during storage the molecular chains of starch rearrange rapidly, forming gel networks with rheological and mechanical diversities which alter the properties of the 3D printed objects (Zheng et al., 2019). So, a better understanding of the behaviors of starchy-gels in 3D printing is necessary to strengthen our ability to create a good replica of a 3D digital model. Two different starches have been employed during this study: a modified waxy maize starch that exhibits excellent dispersibility and imparts superior sheen, clarity, and smoothness and a speciality dextrin refined from tapioca starch. This is the first time that these two starches are combined to study their effect on 3D printing experiments.

In this paper we have dedicated a series of experiments to the mapping of rheological properties, dispensing force and printing fidelity of 3D printed starchy-gels in different pre-processing and printing conditions.

To do this, we have systematically varied (i) the concentration of two different starches – a tapioca dextrin and a modified, cold water-swollen waxy maize starch – in starchy-gel formulations; (ii) the printing temperature and (iii) we explored, for the first time, the storage time of the gels before printing that is considered of great importance for the structure and mechanical properties of starchy-foods (Rezler & Poliszko, 2010) but never analyzed in 3D printing experiments. Rheological analyses have been performed on the starchy-gels before printing while the force required to

extrude the material (dispensing force) has been measured during printing. Finally, 3D printed structures have been qualitatively characterized by visual properties, morphological and microstructure features as well as texture properties.

2. Materials and methods

2.1. Materials

Starchy-gels were obtained by varying the weight fraction of two commercial starch products: Ultra Sperse M 32566109 (US), and Crystal Tex 644 (CT) were provided by Ingredion (USA). These two starch products were selected for their specific properties: US is a modified, cold water swelling waxy maize starch. According to the supplier's application information, US is particularly well suited for instant food preparations subjected to severe processing like microwaving or colloid milling and provides highly smooth gels.

CT is a dextrin from tapioca starch, selected for its low hot viscosity, and fast thermo-reversible gelling upon cooling. As it is low in amylose content and rich in amylopectin it provides a strong gel and low tendency to retrogradation (Sánchez, Dufour, Moreno, & Ceballos, 2010). For CT, the following chemical composition is reported by the producer for 100 g, fat <0.15 g/100 g, carbohydrates >97 g/100 g of which starch >97 g/100 g, protein <0.5 g/100 g, salt <500 mg. For US, the proximate composition is reported as follows for 100 g, fat <0.1 g/100 g, carbohydrates 91 g/100 g of which sugar <0.1 g, protein <0.1 g/100 g, salt 537 mg/100 g. Common sugar (purchased locally) and liquid food colorants (McCormick, Canada) have been employed to prepare the different starchy-gels as reported in the next section of the paper.

2.2. Preparation of starchy-gel printing inks

Three types of starchy-gels have been prepared to serve as printing inks. The weight fractions of the ingredients used for the gels preparation are reported in Table 1. Demineralized water and liquid colorants were heated at 85 °C while stirring the solution by using a lab stirrer (Janke&Kunkel Ika-Rw 15) with 3 straight blades at speed 1. Then, the dry materials – CT, US and sugar - were added to the solution under constant heating till a temperature of 85 °C was reached again. Finally, an additional amount of demineralized water was added to compensate for weight loss due to water evaporation. Next, the hot ink-gel was immediately poured into plastic syringes of 30 mL, closed, cooled to room temperature and maintained for various storage times (ST) as reported in Table 2. Before printing, the syringes containing the starchy-gels were heated for 2 h by placing the syringes in a water bath at the desired

printing temperature (PT, see Table 2). The pre-defined variations of the mass fraction of CT (g/100 g), ST and PT were used to set up the design of experiments (see next section).

Formulation	**CT (g/100g)**	**US (g/100g)**	**Sugar (g/100g)**	**Water (g/100g)**	**Colorant (g/100g)**
1	15.0	10.0	10.0	64.7	0.3 - green
2	22.5	10.0	10.0	57.2	0.3 - red
3	35.0	10.0	10.0	44.7	0.3 - yellow

Table 1 - Mass fraction of the different ingredients used to prepare starchy-gels.

Sample	**Mass fraction of CT (g/100g)**	**ST (h)**	**PT (°C)**
1	15.0	2	35
2	30.0	2	35
3	15.0	46	35
4	30.0	46	35
5	15.0	24	25
6	30.0	24	25
7	15.0	24	45
8	30.0	24	45
9	22.5	2	25

10	22.5	46	25
11	22.5	2	45
12	22.5	46	45
13	22.5	24	35
14	22.5	24	35
15	22.5	24	35
16	22.5	24	35
17	22.5	24	35

Table 2 - Experimental Design describing the conditions used for 3D printing experiments.

2.3. Experimental design

The workflow was designed according to a full fractional Central Composite Design (Box, Hunter, & Hunter, 2005). Three variables such as the mass fraction of Crystal Tex, CT (g/100 g), the storage time, ST (h), indicating the resting time at room temperature before printing, and the printing temperature, PT (°C), indicating the temperature of the ink-gel have been modulated. A Box-Behnken Design (BBD) was used to study the effect of independent variables on the quality of 3D printed samples. The total number of experiment for BBD is defined as $N = 2k*(k-1)+C0$, where k is the number of independent variables, C0 is the number of central points (Ferreira et al., 2007). Three different levels of variation for each variable (CT of 15 g/100 g, 22.5 g/100 g, 30 g/100 g; ST of 2 h, 24 h, 46 h and PT of 25 °C, 35 °C and 45 °C) and N = 5 repeated central points, were used during experiments for a total of 17 experimental conditions. The temperature values were chosen based on preliminary experiments aiming to get rheological properties coherent and proper with the printing process. Table 2 shows the experimental conditions used for each 3D printing experiment.

2.4. Rheological properties of starchy-gels

For the rheological characterization of starchy-gel, oscillatory tests were carried out using rheometer (MCR 52 series, Anton Paar Co. Ltd., Austria) with a fixed frequency of 1 Hz and a variable amplitude ϕ = 0.001–100 mrad with support of a measuring cone CP25-1, D: 25 mm, ANGLE 1° and Vaseline oil. Storage modulus (G′), loss modulus (G″), loss tangent (tanδ = G''/G') and the complex viscosity η* were measured. The analyses were carried out at the temperature reported in Table 2 with the aim to obtain insight in the properties of the material during the 3D printing process. Shear rate values were computed as ratio between shear stress (Pa) viscosity (Pa.s) (Hauswirth et al., 2020; Pipe, Majmudar, & McKinley, 2008).

2.5. 3D printing experiments

A TNO in-house manufactured printer has been used during the experiment. It consists of a syringe-based extruder that comprises the extruder motor, 30 mL plastic syringe, temperature controllable syringe holder, and plunger, piston and force sensor. Also, the stepper motor is capable of producing a maximum driving force of 900 N. The digital model was designed by using Rhinoceros 6 – Grasshopper (McNeel Europe SL, Spain). The digital structure consisted of two infill paths – named Layer A and Layer B – varying in their line distances of 2.2 mm and 5.5 mm, respectively. These two paths were repeatedly stacked in Z direction with the aim to generate the desired 3D digital models. More specifically, we can identify a main block consisting of a Layer A (L-1) and N = 7 Layers B (from L-2 to L-8) which are stacked by a rotation of 90°. The main block was repeated for 3 times in Z direction for a total of N = 24 layers. This digital model was defined based on preliminary experiments aimed to create modular gel structures consisting of layers with different morphology and porosity fraction. This could open for modulating texture by interchanging the position of the layers. More specifically, a schematic representation of the infill paths and the overall 3D digital model is shown in Fig. 1. This workflow generates a 3D cube with dimensions of 2.42 cm, 2.42 cm, 1.92 cm respectively in the X, Y and Z plane. The G-code controlling the 3D printer movements was processed using Pronterface software using the following printing parameters: nozzle size = 1 mm, track width = 2.2 mm (Slicer, 2017), layer height = 0.8 mm, printing and non-printing speed = 900 mm/min with extrusion speed of 300 mm/min. More specifically a layer height corresponding to 80% of nozzle diameter has been employed assuring a slight compression of the material aiming to improve the

adhesion of overlying layers and a better structural stability of the 3D printed sample. These printing conditions result in an overall porosity fraction of the digital model of 34.67% of which the porosity of Layer A and Layer B are of 0.00% and 39.62% respectively.

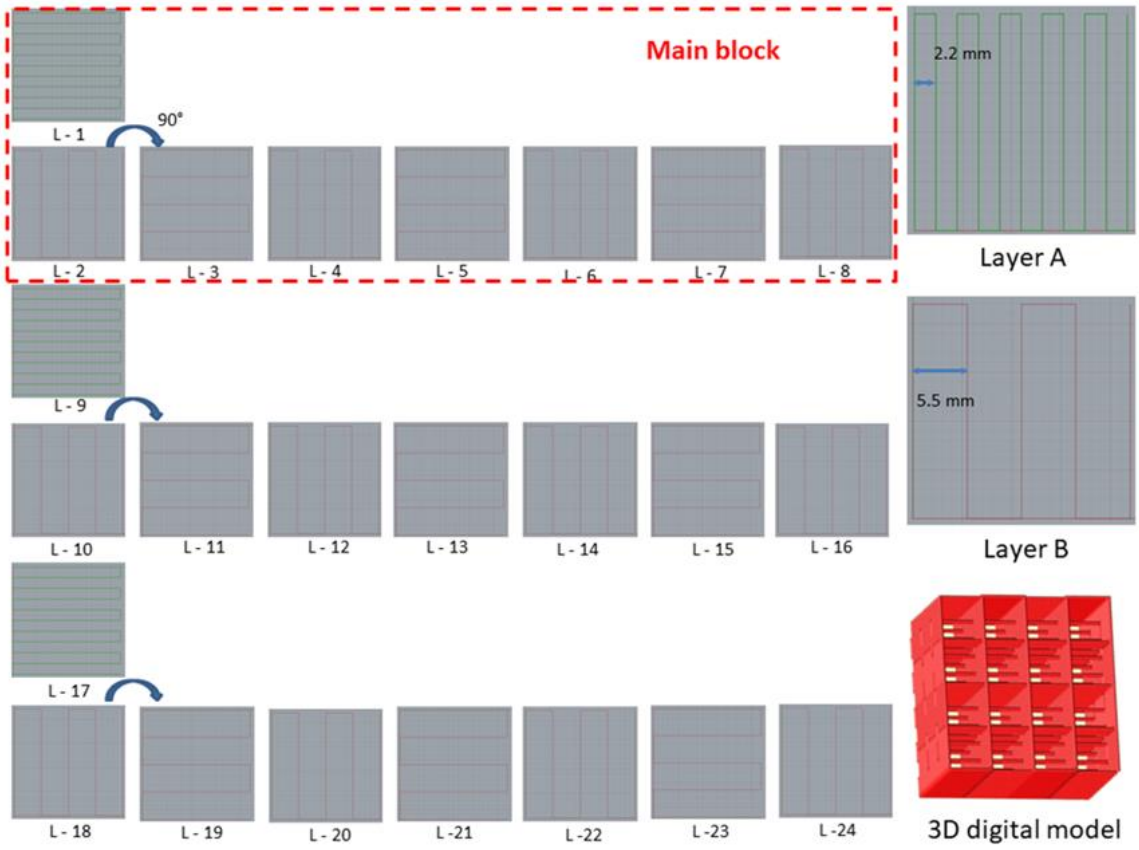

Fig. 1. Schematic representation of the 3D digital model used for 3D printing experiments

2.6. Dispensing force and shear rate during printing

The food material is deposited under the action of a stepper motor with a non-captive leadscrew which applies the force required to get material deposition. This force – dispensing force – is measured at any moment of printing by using a sensor located at the base of the piston syringe. Also, the data are acquired with a 1-s interval and visualized by a display unit. For our experiments, the data of dispensing forces are reported as an average of 7 measurements acquired during printing movements. Also, the shear rate during printing movements was computed as reported by using the

following equation (Le Tohic et al., 2018; Douglas, Gasoriek, Swaffield, & Jack, 2005; Mansfield & O'Sullivan, 2010):

$$\gamma = \frac{8v}{d_n} \quad (1)$$

Where γ is the shear rate (s−1); $\bar{\upsilon} = Q/A$ (2) and dn is the filament width (mm).

In Eq. (2), Q is the extrusion rate (mm3/s) and A represents the cross-sectional area of the nozzle (mm2). Furthermore, Q was computed by the following equation

$$Q = d_n \, x \, h \, v_n \quad (2)$$

Where h is the layer height (mm) and n is the print speed (mm/s) (Khalil and Sun, 2007).

2.7. Dimensional properties of 3D printed samples

The fidelity of printing, in terms of shape and dimension of 3D printed samples, has been evaluated by image analysis. The images of each sample were acquired immediately after printing using two monochrome cameras (iDS-Navitar) placed to give side and top-view images equipped with visual software Dual Vision. Also, color images were acquired by a Canon EOS 1200D camera to obtain perspective photos. The main dimensions of the samples – height (H), the width at the top (L), the width at the bottom (B) and diameter of filament (D) – were measured by using ImageJ software (version 1.52a). The fractional deviations (Δd/d) from the digital model for each dimension (d) were calculated through the following formula:

(3)Δd = [d(measured) – d(designed)] x 100

We analyzed 7 samples for each condition and 3 repetitions for each dimension.

2.8. weight and moisture content determination

The 3D printed samples were weighed immediately after printing using an analytical balance (Mettler AT200). Moisture content Xw (gH20/g) was determined by using the gravimetric method as described in AOAC–925.10.

2.9. Microtomography X-ray images of 3D printed samples

After 3D printing the samples were individually packed in airtight containers and stored at 4 °C overnight with the aim to prevent possible and potential morphological changes. X-ray CT images were acquired 24 h after 3D printing by using a Phoenix v [tome]x m scanner. Micro-CT setting was set to a source voltage of 140 Kv, current

of 140 μA with an image resolution of 21.3 μm. The images were 2014 × 1900 pixels by using a step angle of 0.24° over 360°. The reconstruction of the projection images was performed by using Avizo 7.1 (VSG, an FEI Company). Cross-sectional images were analyzed by CTAn 1.12.0.0 software (Bruker microCT, Belgium). First, the images were cropped to a quadratic region of 700 × 700 pixels, and then binary images were obtained by using Otsu's method and finally analyzed in 2D with the aim to obtain the porosity of samples. Finally, the porosity of layer A (ΦA) and B (ΦB) were measured as an average of the porosity of 100 slices from the ranges 700–750 and 1150–1200 (Layer A); and 550–580, 880–910 and 1190–1220 (Layer B).

2.10. Statistical analysis

Experimental data were analyzed by using a polynomial model (Eq. (1)) in order to define the effects of independent variables on the quality attributes of sample: $y = B0+\sum Bixi+\sum Biixi2+\sum Bijxij$ (Eq. (1)).Where B0 is the initial value of the dependent variables, Bi, Bii, Bij are the regression coefficients, xi and xj indicate the linear effect of the independent variables, xi2 refers to the non-linear (quadratic) effect of each independent variable while xij refers to the linear and interactive effect between two independent variables. The goodness of fitting was evaluated by correlation coefficient (r), significance (p-level) and corresponding standard error (SE) of each regression coefficient estimated. Pareto charts were used to show the significance ($p < 0.05$) of each studied variable on the quality parameters while 3D plots were used to describe the effect of independent variables on each quality index analyzed (Derossi et al., 2019, Derossi et al., 2020; Derossi, Paolillo, Caporizzi, & Severini, 2020). All statistical analyses were carried out through STATISTICA 10 software (Tulsa, USA).

3. Results

3.1. Rheological properties of gels before printing

As the first step we want to analyze the effects of the studied variables on the rheological properties of the starchy-gels because of primary importance for material deposition during printing and, therefore, for the quality of 3D printed samples. Rheological properties as well as the other analyses were performed according to the experimental design conditions. The rheological features of starchy-gels are the responses of heating at different temperatures (Liu et al., 2019a, 2020) responsible of absorbing water and swelling of starch granules while the cooling and resting time drive the intensity of crystallization and recombination phenomena (Debet & Gidley, 2007; Eliasson, 1986; Qiu, Punzalan, Abbaspourrad, & Padilla-Zakour, 2020; Yu et

al., 2020; Zhang, Dhital, Flanagan, & Gidley, 2014). These phenomena, playing essential roles for the effective quality of 3D printed food, were analyzed in detail. The viscosity of ink-gels was determined under the same conditions of resting time and temperature as adopted during the printing experiments. The Pareto chart of Fig. 2 shows the statistical effects of each independent variable and their interactions.

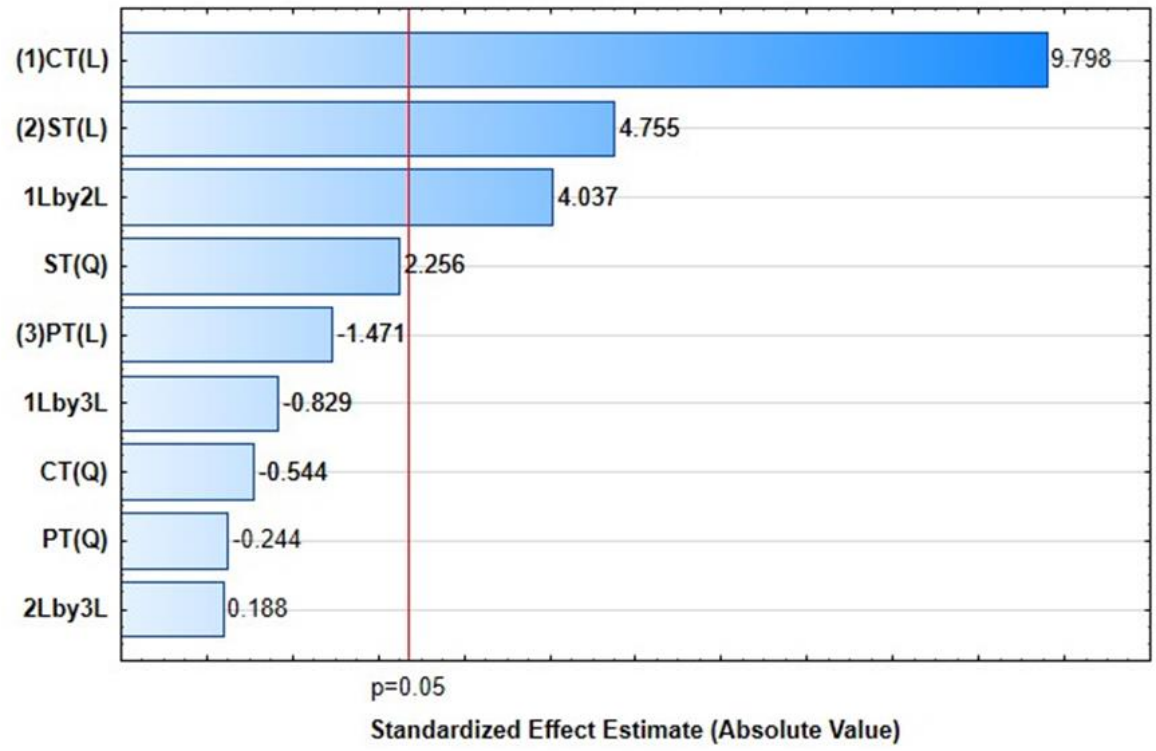

Fig. 2. Pareto chart describing the statistical effect of independent variables on the viscosity of ink-gels.

The measured complex viscosity of the starch gel during printing is primarily dependent on mass fraction of CT and ST with estimated effects of 9.79 and 4.75 respectively. In addition, these variables show a synergistic interaction (1Lby2L) increasing the viscosity with an estimated effect of 4.04. As expected, CT was the variable showing the highest ability to increase gel viscosity with average values of 3.3 × 105 mPa s, 8.1 × 105 mPa s and 14.7 × 105 mPa s for mass fraction of CT of 15 g/100 g w. b., 22.5 g/100 g w. b. And 30 g/100 g w. b., respectively (Fig. 3). Increasing the printing temperature (PT) from 25 to 45 °C the viscosity slightly reduced, but PT had not a significant contribution.

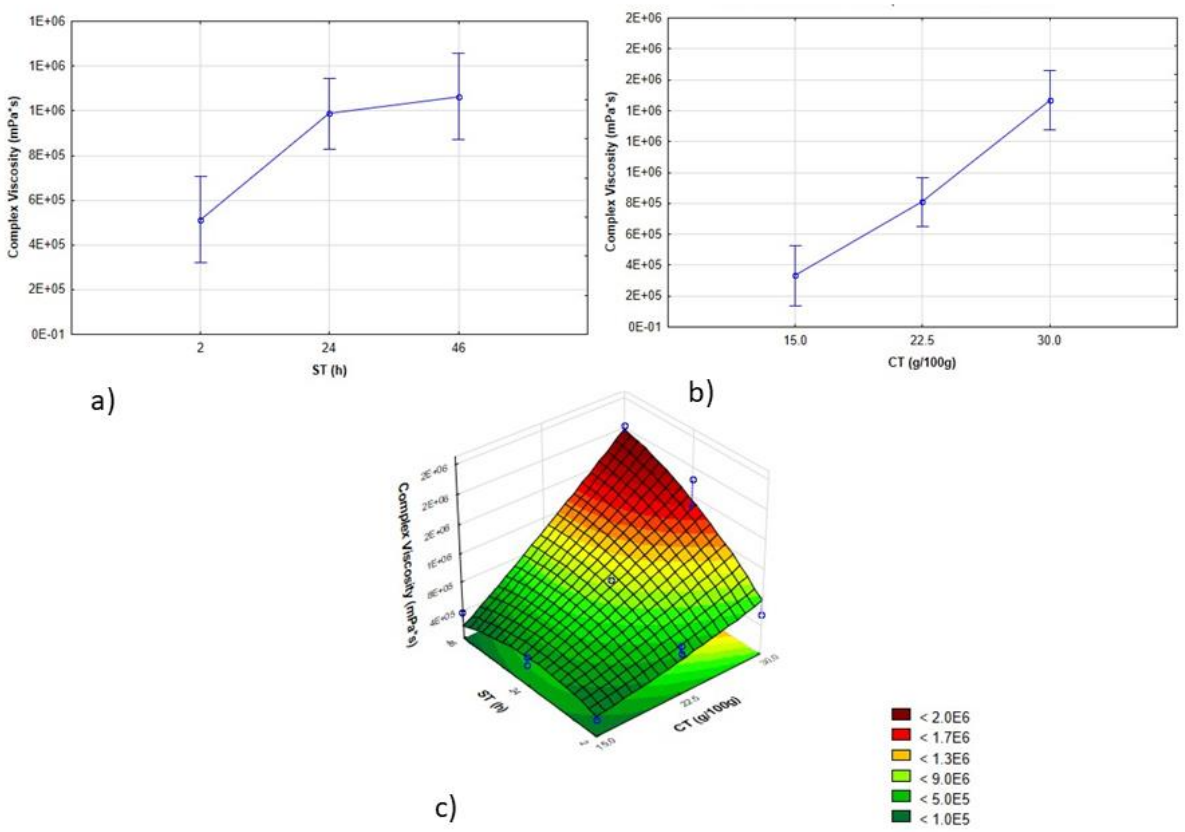

Fig. 3. Effect of the mass fraction of CT (a), ST (b) on complex viscosity of starchy-gel and c) interaction effect between CT and ST.

We want to note that the error bars represent the data variability obtained by all experiments when grouped for different mass fraction of CT; these, therefore, contain the effect of ST and PT employed during 3D printing tests. With the aim to better highlight the single effect of CT, we have separated its contribution for the experiments conducted with ST of 46 h and PT of 35 °C. Under these conditions, viscosity values of 3.8 × 105 mPa s and 20.6 × 105 mPa s respectively for mass fractions of 15 g/100 g and 30 g/100 g. This confirms the primary effect of CT with an increase of viscosity that results 5.4 times higher when using a double mass fraction of CT. Similarly, the data published by Liu, Zhang, Bhandari, and Wang (2017) and Breuninger, Piyachomkwa, & Srioroth (2009) showed that the use of potato starch and tapioca starch, greatly increased the viscosity of food system. When analyzing the effect of the storage time (Fig. 3b) again a significant rise in viscosity is observed, with a maximum increase during the first 24 h. Values of 5 × 105 mPa s and 1 × 106 mPa s were measured after 2 and 24 h respectively, while further 22 h of

storage, for a total of 46 h, induced only a slight increase of viscosity till 1.1 × 106 mPa s. Moreover, the synergistic interaction between CT and ST is clearly reported in Fig. 3c where maximum viscosity value of 2 × 106 mPa s was measured for mass fraction of CT = 30% and ST of 46 h. On the other hand viscosity lower than 2.5 × 105 mPa s was measured for CT of 15% and ST of 2 h.

This effect can be attributed to starch retrogradation, as during ambient storage amylopectin recrystallizes, increasing the rigidity of starch gels (Kettles, Oostergetel, & van Vliet, 1996; Karim, Norziah, & Seow, 2000). This might confer non-desirable properties with difficulty to masticate and to digest (Yu et al., 2020). So, a better understanding and control of starch recrystallization would allow creating starchy-food with high quality (Karim et al., 2000; Oladebeye, Oshodi, Amoo, & Karim, 2013). Starches from different botanical origins are known to exhibit different behavior with respect to gelatinization, retrogradation, pasting and paste properties (Breuninger, Piyachomkwan, & Srioroth, 2009). For tapioca starch – the base material of which CT is made – reported that the retrogradation is very low (25%). In addition, other researchers (Russ, Zielbauer, Ghebrmedhin, & Vilgis, 2015) showed that tapioca pastes exhibit a low setback after gelatinization due to the limited fraction of amylose with high molecular weight. In our case, the reason why we observed a high increase of viscosity could be because of the interaction between CT and US, the latter of which contains waxy maize for which starch retrogradation effect is more noticeable (47%) (Liu et al., 2018, Liu et al., 2018b). The use of CT could have increased the retrogradation of US due to reduced mobility of the complex matrix. As a second step we want to show the changes in viscosity occurring during the 3D printing process (Liu et al., 2019a, 2019b). To do this, the viscosity of the starchy-gels as a function of shear rate is reported in Fig. 4.

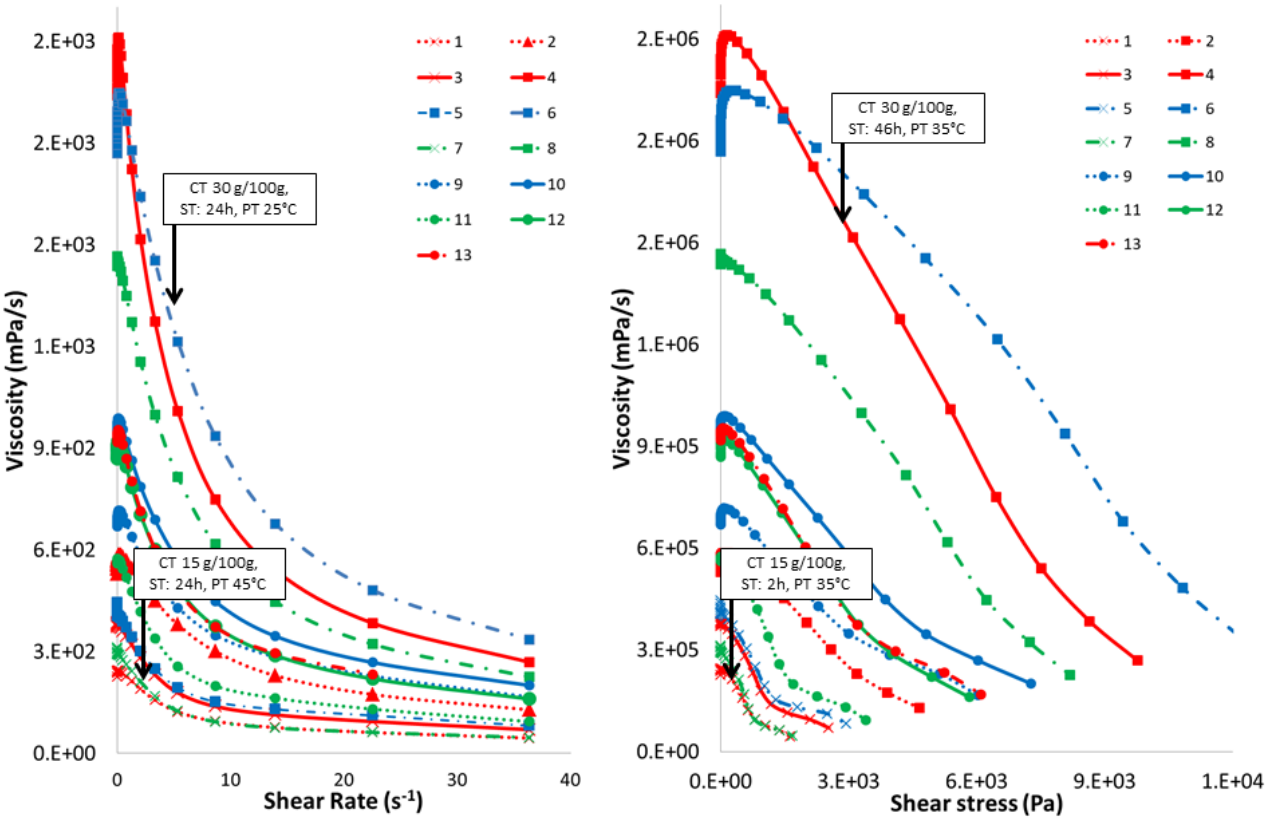

Fig. 4. Flow curve of starch gels at different conditions (left side) and estimated yield stress of starch gels based on the stress ramp method (right side).

This information is relevant for 3D printing being directly related to the flow-ability of the material and the capability to be easily extruded through the nozzle, thereby reducing the risk of blockage of the nozzle (Liu et al., 2019, Liu et al., 2019; Xu et al., 2020). The flow curves show a typical non-Newtonian character, with shear-thinning behavior in accordance with the results of many others 3D printing tests performed on other types of edible-gels (Dick et al., 2020; Liu et al., 2019a, 2019b; Loveday, Rao, Creamer, & Singh, 2010). At low shear stress values, the measured gel viscosity is representative for the properties of the material inside the syringe before deposition (Dick et al., 2020), while the yield stress – the applied stress at which irreversible deformation is first observed - may be considered the minimum stress needed to initiate the material flow (Dick et al., 2020; Liu, Yu, et al., 2019; Sun & Gunasekaran, 2009). The viscosity increased with increasing shear stress and then reached a peak – with significant diversity among the samples – corresponding to the shear stress under which the sample remains completely elastic and can absorb the external stress without changing its inner structure or being deformed (Liu, Yu, et al.,

2019). Samples N.4 and N.6 exhibited the maximum resistance to deformation as a result of the higher mass fraction of CT (30g/100 g), the highest storage time (46 h) (sample N.4) and the lowest printing temperature (25 °C) for sample N.6. Contrarily, the lower viscosities have been measured for the sample at lower weight fraction of CT (15%) and printed at 45 °C (sample N.7), and for the shorter storage time of 2 h (sample N.1). In between of these two limits, all other starchy-gels formulated with a medium amount of CT are placed.

For such samples, the statistical effects of ST and PT as reported before (Fig. 2, Fig. 3) comply with the interpretation given above. Samples stored for 46 h (i.e. sample N.10), showed a higher viscosity than sample N.9 (ST = 2 h) while a sample produced at the higher PT of 45 °C (sample N.11) exhibited a lower viscosity value than sample N.9 which was printed at 25 °C. Liu et al. (2020) explained that a thermo-responsive behavior associated with a strong shear-thinning and a rapid shear recovery is a desirable property for starchy-gels to employ in 3D printing experiments (Paxton et al., 2017). The effect of storage time is definitely related to the reordering of the amylopectin which occurs at a much slower rate than amylose gelation (Rezler et al., 2010; Ring et al., 1987). However, since other variables such as the variation in amylose:amylopectin ratio and the size and shape of granules are known to play an important role too, the storage effect needs to be studied for starches from other botanical origins when these are used to create starch-based 3D printed food (Liu & Thompson, 1998; Rezler, 2007).

To get a complete map of the rheological features of ink-gels we measured the storage (G′) and loss (G″) modulus. For all samples it was observed that G’ ≫ G″ indicating a more solid-like behavior than liquid-like characteristics (data not shown). Also, the loss tangent (tanδ = G’‘/G’) values get useful information of what can occur to the starchy-gels after storage inside the cartridge of syringe. As well known, tan δ > 1 indicates predominance for viscous property with fluid-like behavior while values < 1 means predominance for elastic property with solid-like behavior (Eidam, Kulicke, Kuhn, & Stute, 1995; Liu et al., 2018b, Liu et al., 2018; Fischer & Windh, 2011). Fig. 5 shows that tanδ mainly depends on CT and PT with significant estimated linear effects of −11.28 and 4.41, respectively. Additionally, CT showed a significant quadratic (non-linear) effect of −3.52. The minimum tanδ of 0.359 was obtained for sample N.6 (CT = 30g/100 g; ST = 24 h; PT = 25 °C) which displayed the most pronounced solid-like behavior. On the contrary, the highest tanδ (= 1.062) was measured for sample N.7 (weight fraction of CT = 15g/100 g; ST = 24 h; PT = 45 °C). According to the Pareto chart of Fig. 5, the reduction of the weight fraction of CT had the major effect on the increase of loss tangent of these two samples. These

results are supported by the data of Liu et al. (2020), who showed that the material fluidity during printing get worse as the tanδ value reduces and this, in our case, occurred in line with the increase of CT content while a higher temperature facilitates the destruction of intermolecular hydrogen bonds in the starch granule thereby increasing loss tangent (Liu et al., 2020). More specifically, the obtained results indicate an undesired limit for tanδ of 0.393 (sample N.4) for which was not possible to get material deposition. Liu et al., 2018, Liu et al., 2018b who studied the printability of milk protein by using a stepping motor with a torque of 0.45 Nm. printing speed of 35 mm/s, flow rate of 100% (19.39 mm3/s), showed an average limit of 0.34.

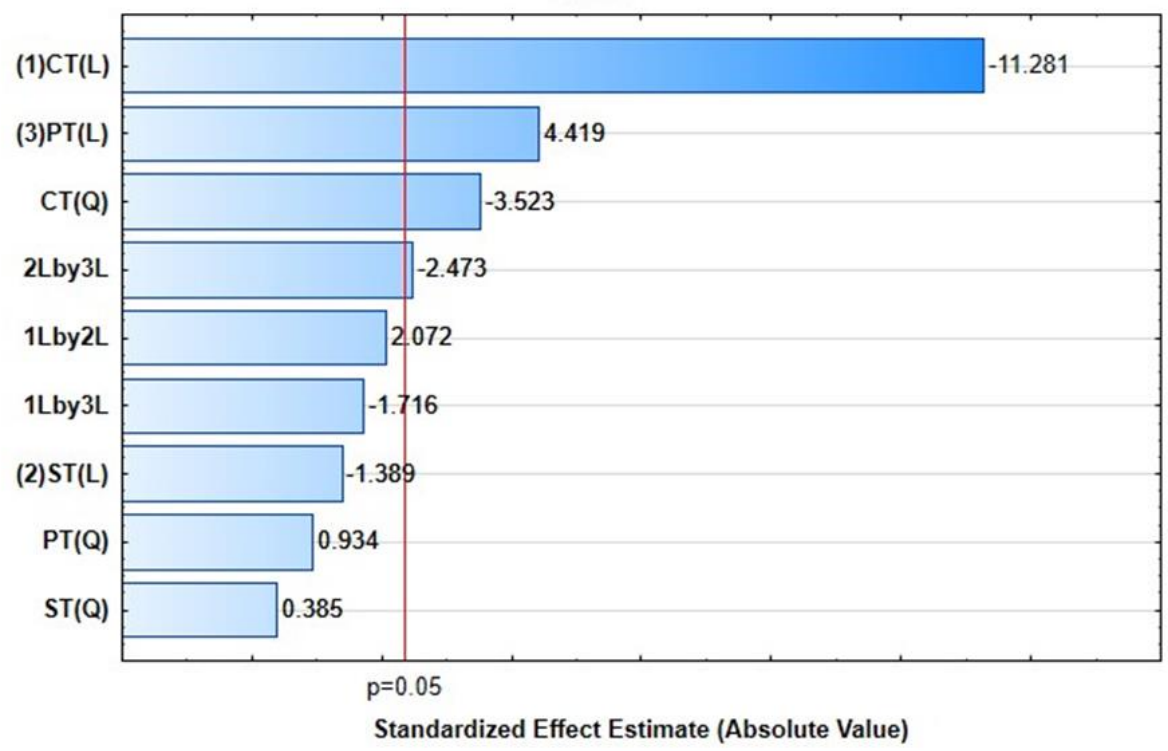

Fig. 5. Pareto Chart describing the statistical effects of independent variables on the loss tangent, tanδ, of starchy-gels.

3.2. Effects on dispensing force

The force required to extrude material through the nozzle can be defined as the dispensing force and is expected to be closely related to the viscosity of the material (Dick et al., 2020). Before analyzing the main results of the starchy-gel sample, we

want to recall that the applied force cannot be completely controlled by the user when employing a commercially available 3D food printer. As reported from Dick et al. (2020) and Derossi. Caporizzi, Ricci,& Severini (2019a) the extrusion rate – the amount of material deposited per unit of time – is governed by several parameters such as nozzle diameter, printing speed, etc. which are easy to define in the slicing software. But it is also strictly linked to the rotation of the stepper motor on the head of the piston's cartridge which is dependent of the equipment and by the firmware of the printer. Only a slight control of the rotation rate is possible by a multiplier variable commonly known as flow multiplier. Fig. 6 shows the estimated effect of the independent variables on the dispensing force of the samples. In addition, Fig. 7 shows the changes of dispensing force as a function mass fraction of CT, PT and ST.

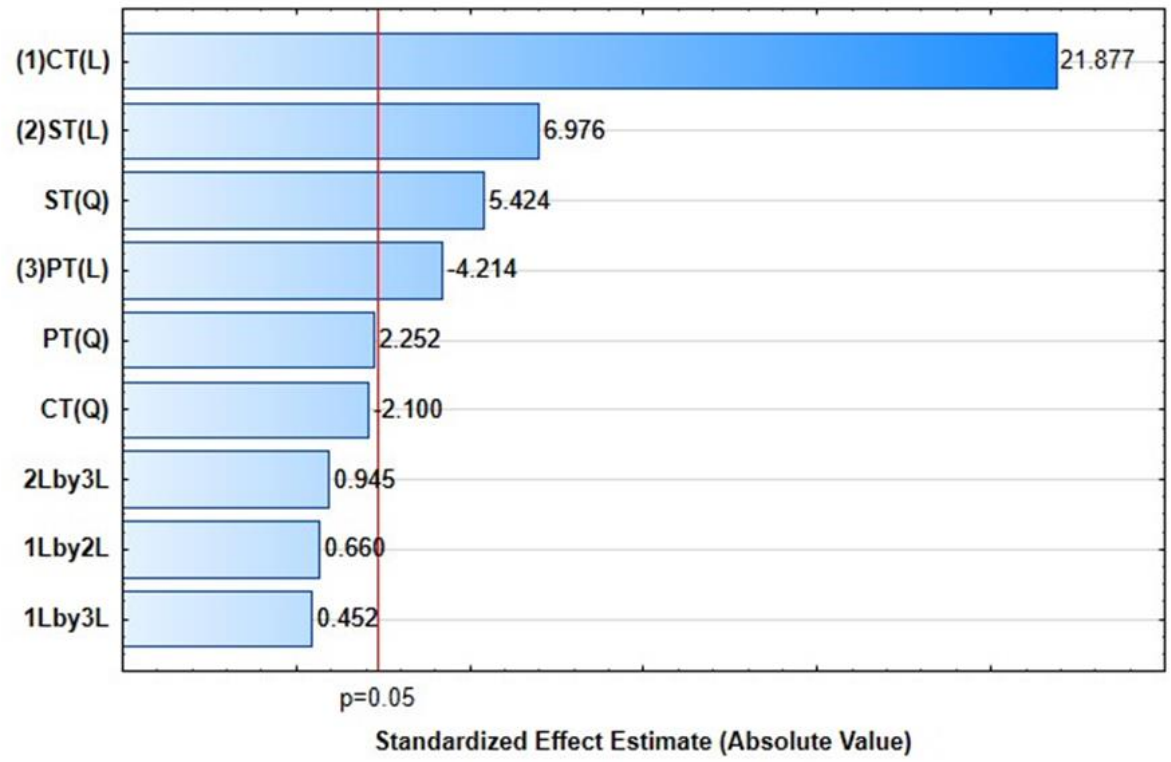

Fig. 6. Standardized effect of the independent variables, CT, ST and PT on the dispensing force measured during 3D printing tests.

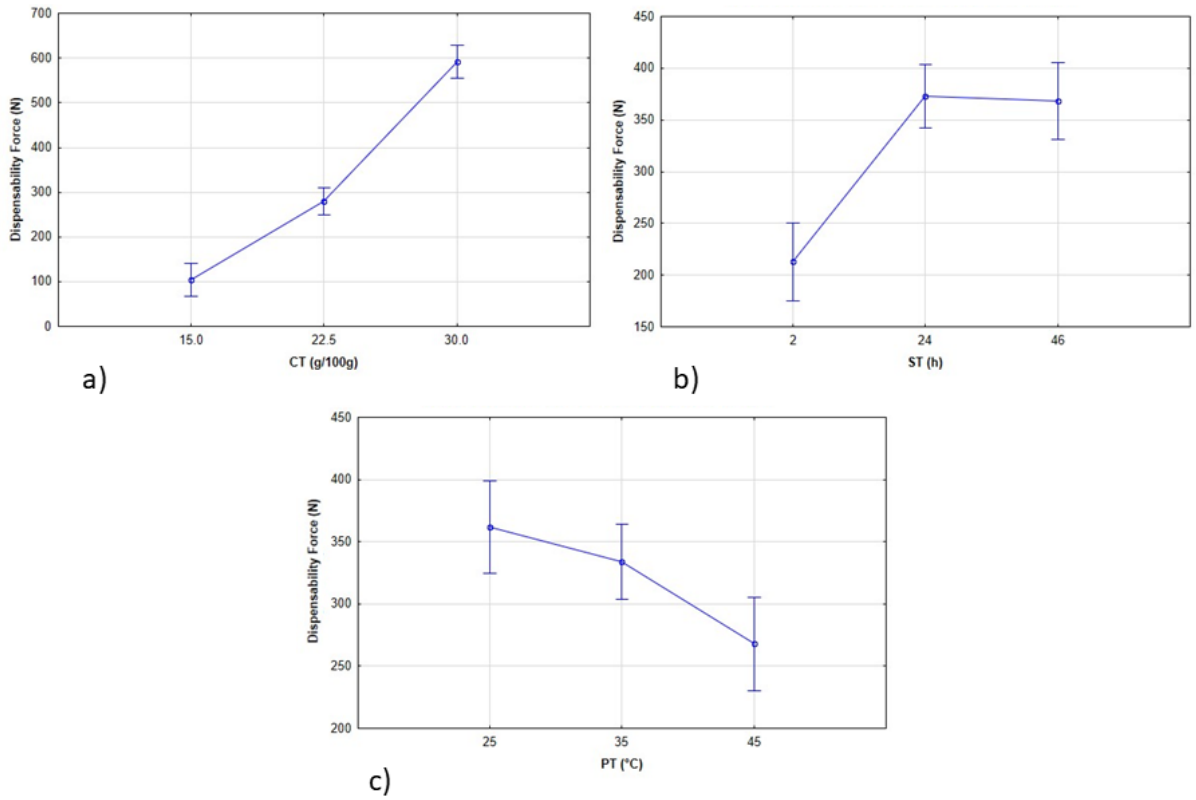

Fig. 7. Dispensing forces required to deposit ink-gel as a function of the concentration of CT (a), ST (b) and PT (c).

The weight fraction of CT strongly increased the force required to extrude starchy-gels with an estimated effect of 21.87. The storage time ST increased the required force for printing with an estimated linear effect of 6.97 and a quadratic effect of 5.43, both effects being significant. This is in line with the increased viscosity previously observed for CT and ST. Also, the printing temperature PT showed a significant and inverse effect on the dispensing force with an estimated effect of –4.21, while it had a non-significant effect on the ink's viscosity. Maybe the temperature has a larger effect in reducing the wall friction of the material than its effect on reducing the viscosity.

Recently, Zhu et al. (2019) observed a linear correlation between extrusion force and flow stress of food pastes and they assumed that the extrusion force depends not only from the material properties but also by nozzle geometry. Indeed, material is subject to shear flow and also to elongation flow along the symmetry axis of the syringe (Zhu et al., 2019). Furthermore Oliveira, Santos, & Miranda (2020) studied the estimation of extrusion force at the plunger validating a model that correlates it even to

slicing/print settings (i.e., nozzle diameter, layer height, line width, and speed), rheology model, flow dynamics and energy conservation principles. From Fig. 7a, a sudden increase of the force required to extrude the starchy-gels is observed by increasing the mass fraction of CT from 15% to 30%, with average required force of 104.7 ± 37.2 N and 591.4 ± 37.2 N, respectively. As expected, the conditions showing the highest dispensing force, N.4 and N.6 (626.2 N and 645.7 N, respectively) produced 3D printed objects of poorest quality because the maximum force applied to the syringe was not enough to overcome the shear force of the gel (as shown below in Fig. 10). The higher mass fraction of CT (30 g/100 g) created unsuitable material for printing, having a high viscosity and tan δ below 0.36 (Yang, Zhang, & Bhandari, 2017) with solid-like behavior and poor fluidity (Liu, Yu, et al., 2019; Tabilo-Munizaga & Barbosa-Cánovas, 2005). When the viscosity of food formulation increased beyond some limits, the stepper motor would require more power to extrude it (Guo, Xang, & Bhandari., 2019); so, the engineering and mechanical properties of the printer should be considered when printing food materials with high viscosity (Derossi, Caporizzi, Ricci, & Severini, 2019). On the other hand, by increasing the printing temperature the dispensing force reduced significantly from 361.5 ± 37.2 N to 267.8 ± 37.2 N as consequence of the reduced viscosity of the gel (Fig. 7b). Furthermore, the storage time increased the required force to extrude the starchy-gels but only in the range 2–24 h, showing values of 212.8 ± 37.2 N and 373.7 ± 30.5 N, while a further increase of ST did not affect the force (Fig. 7c).

Finally, we compared the dispensing force and the viscosity of the starchy-gel (Fig. 8). What is worth to note is that, for the first time here the actual force applied to the piston of the syringe was measured at any time of printing movements by using an in-house modified printer and employed to better explain printing behavior and interrelation with printing quality. Before our experiments, Dick at al. (2020) showed interesting results regarding the extrusion force, but they measured the required force out the syringe by using a texture analyzer under static conditions and, as reported by the author, these data cannot be directly related to the actual extrusion force since the conditions are not comparable. To do this, we have computed the shear rate value exhibited during printing experiments by using the methods of Le Tohic et al. (2018) resulting in a value of 122.3/s. Then, we have estimated the complex viscosity at shear rate of 122.3/s by using the Cross model (Cross, 1965) and, finally, we compared the complex viscosity and the dispensing force (Fig. 8).

Samples	**X_w (g H_2O/g)**	**W (g)**	**ΔH/H (%)**	**ΔL/L (%)**	**ΔB/B (%)**	**ΔD/D (%)**	**Φ_A (%)**	**Φ_B (%)**
1	64.39 ±0.17	9.89 ±0.42	3.09 ±0.00	-8.49 ±0.03	24.61 ±0.04	41.36 ±0.05	0.56 ±0.59	20.79 ±7.66
2	48.97 ±0.21	10.92 ±0.50	6.38 ±0.03	2.90 ±0.00	19.26 ±0.03	21.21 ±0.11	9.50 ±2.75	33.07 ±7.63
3	64.17 ±0.33	9.66 ±0.59	7.93 ±0.01	3.03 ±0.03	18.12 ±0.03	19.09 ±0.09	6.02 ±2.05	34.07 ±3.01
4	39.24 ±1.51	0.80 ±0.12	-15.44 ±0.12	-31.32 ±0.03	-24.36 ±0.02	-45.40 ±0.04	-	-
5	64.76 ±0.24	9.76 ±0.35	11.60 ±0.01	1.15 ±0.01	17.59 ±0.03	6.59 ±0.11	3.89 ±2.38	30.93 ±1.72
6	47.53 ±1.00	0.76 ±0.33	-30.49 ±0.07	-29.39 ±0.13	-23.69 ±0.13	-47.23 ±0.11	-	-
7	63.85	9.61	10.06	0.59	17.13	21.21	3.73	29.70

	±0.35	±0.40	±0.01	±0.02	±0.03	±0.09	±1.93	±6.48
8	49.97 ±0.21	10.75 ±0.19	11.81 ±0.02	0.80 ±0.00	17.77 ±0.02	5.68 ±0.06	7.34 ±3.03	31.88 ±4.00
9	57.86 ±0.37	10.11 ±0.64	10.79 ±0.01	5.31 ±0.00	20.35 ±0.03	20.00 ±0.05	11.02 ±1.05	35.67 ±3.14
10	57.24 ±0.86	10.11 ±0.49	14.58 ±0.02	2.70 ±0.01	18.15 ±0.02	9.70 ±0.08	12.92 ±4.41	36.41 ±4.25
11	56.77 ±0.23	10.44 ±0.23	8.22 ±0.01	1.19 ±0.02	15.36 ±0.02	30.30 ±0.09	2.79 ±1.01	30.97 ±4.14
12	56.60 ±0.56	10.28 ±0.55	10.65 ±0.04	3.49 ±0.00	19.67 ±0.01	31.89 ±0.09	4.53 ±1.83	21.34 ±6.64
13	56.50 ±0.21	10.20 ±0.34	12.49 ±0.02	0.65 ±0.01	17.45 ±0.02	10.15 ±0.04	5.08 ±2.93	34.21 ±4.77
14	56.71 ±0.47	10.14 ±0.18	9.67 ±0.01	-1.10 ±0.00	17.23 ±0.02	11.50 ±0.04	-	-
15	56.87	10.31	10.97	-0.90	17.89	10.20	-	-

	±0.16	±0.41	±0.02	±0.00	±0.03	±0.03		
16	58.32 ±0.34	10.13 ±0.34	13.44 ±0.02	-1.46 ±0.01	17.63 ±0.03	10.36 ±0.02	-	-
17	57.21 ±0.14	10.06 ±0.54	12.09 ±0.00	-0.44 ±0.00	17.29 ±0.03	10.12 ±0.03	-	-

X_w (g H_20/g), *W* (weight, g), *ΔH/H* (fractional deviation of height, %), *ΔL/L* (fractional deviation of the width at the top, %), *ΔB/B* (fractional deviation of the width at the bottom, %), *ΔD/D* (fractional deviation of the diameter of filament, %), Φ_A (porosity fraction of layer A, %), Φ_B (porosity fraction of layer B, %)

3.3. Printing fidelity

As the first step to evaluate printing fidelity, we analyzed the deviation of the main dimensional properties of 3D printed samples against the virtual design (Table 3). The data of samples N.4 and N.6, which clearly failed and can be considered as non-printable materials, were not included in any analyses. This proves the inability to deposit these gels according to the above discussed dispensing force and a solid-like property of gel (Eidam et al., 1995; Liu et al., 2018b, Liu et al., 2018). As expected, the moisture content of the samples is strictly influenced by the weight fraction of CT employed to prepare the starchy-gels. By performing a linear regression (data not shown), we found a robust relation with determination coefficient, $r2 = 0.98$ while no relation was found for the printing temperature ($r2 < 0.4$). Reasonably, by performing the 3D printing between 25 °C and 45 °C did not affect water evaporation among the samples. Similarly, no relationship was found between weight of 3D printed samples and storage time ($r2 < 0.2$) (data not shown).

Analyzing the fractional deviations of H, D and L for 3D printed samples, we can observe an overall satisfying printing fidelity of all samples. The largest deviations were 14.58% and 8.49% for H and L, respectively, while a greater deviation from the virtual design was observed for the length at the bottom of the structure, B, with values between 17.13% and 24.61%. These observations will be analyzed and discussed with more detail later by using the microCT images of Fig. 10. Here, considering that the morphological deviations of the 3D printed samples from the virtual design are strictly related to the diameter of the deposited filament (Breuninger et al., 2009; Derossi, Caporizzi, Ricci, & Severini, 2019; Nijdam, Agarwal, & Schon, 2021) we have analyzed the effects of independent variables on the width of the starchy-gels filament (Fig. 9).

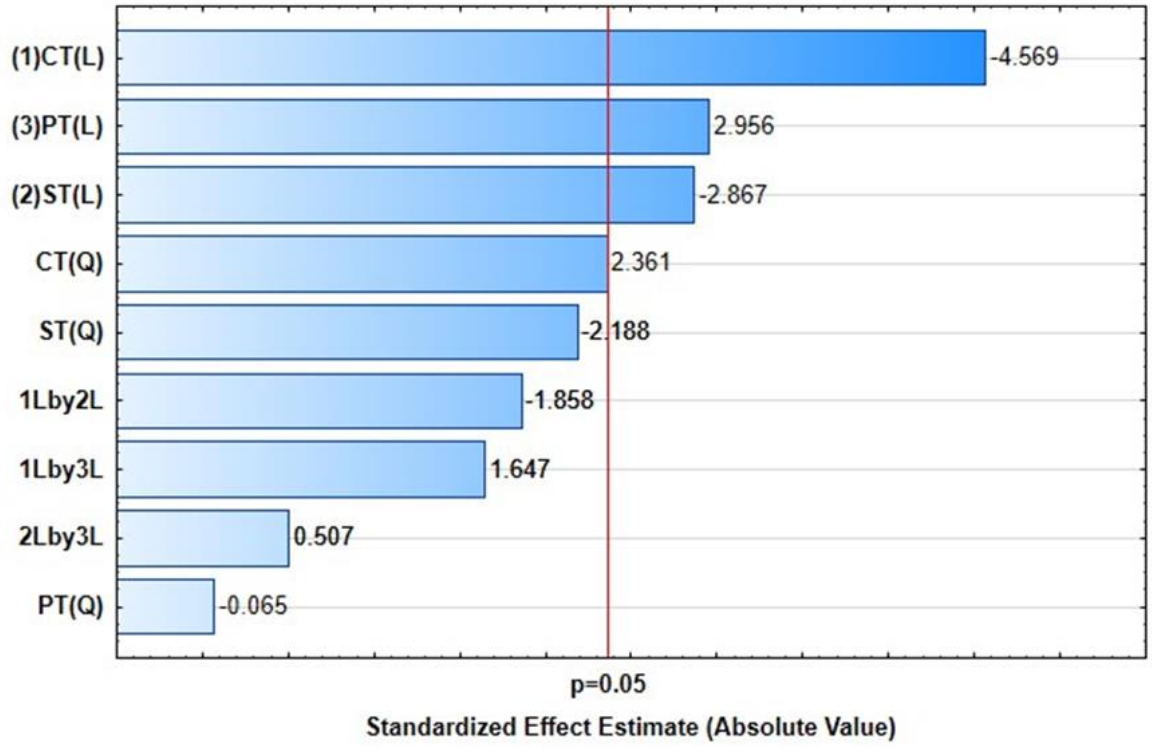

Fig. 9. Pareto chart representing the effect of independent variables on the size of the diameter of filament.

All independent variables significantly affected the diameter of the filament with weight fraction of CT was a predominant factor with a standardized effect (linear effect) of −4.56. Furthermore, PT and ST respectively showed linear effects with values of 2.96 and −2.86, respectively. By employing a low amount of CT the resulting reduced viscosity was responsible for the spreading of gel on the print bed creating a very broad (and flat) filament.

Indeed, by analyzing the fractional deviation of the diameter of filament, for sample N.1 (weight fraction of CT = 15%, ST 2 h and PT = 45 °C) we observed the highest positive fractional deviation of 41.36% (Table 3). Interestingly, when increasing ST at 46 h while keeping weight fraction of CT and PT constant (sample N.3), the fractional deviation was reduced to 19.09%, proving that a higher ST (before printing) positively contributes for a reduction of spreading of the starchy-gel after deposition. The smallest deviation of the width of 3D printed filament from the

designed model was obtained for sample N.5 (6.59%) obtained employing a weight fraction of CT = 15%, ST = 24 h and PT = 25 °C. We want to recall that the fractional deviation, ΔD/D, has been computed by considering the track width (instead of than the nozzle size) obtained by adopting an extrusion rate value of 26.4 mm3/s and layer height of 0.8 mm. This condition enables to get a cross-sectional shape of the filament that is shaped like a rectangle with semicircular ends (Slic3r, 2017) improving the adhesiveness of the layers and, in turn, the overall print stability (Zhu et al., 2019; Nair, Panda, Santhanam, Sant, & Neithalath, 2020).

The filament deposited for the sample N.4 and N.6 showed negative fraction deviation (−45% and −47%, respectively) being thinner than the expected track width. The reason why the filament sizes were smaller is due to the great imbalance between extrusion rate and printing speed resulting in the stretch of the filament during printing (Gibson, David, & Stucker, 2015; Severini, Derossi, & Azzollini, 2016).

For the complete mapping of the printing fidelity it is useful to study the photographic images of printed objects and the related 2D microtomographic cross sectional images (Fig. 10). With the aim to highlight the most important differences, only some representative samples are reported. The images of all samples have been uploaded in Supplementary materials (SM1). Green, red and yellow colors respectively define gels with weight fractions 15%, 22.5% and 30% of CT, respectively.

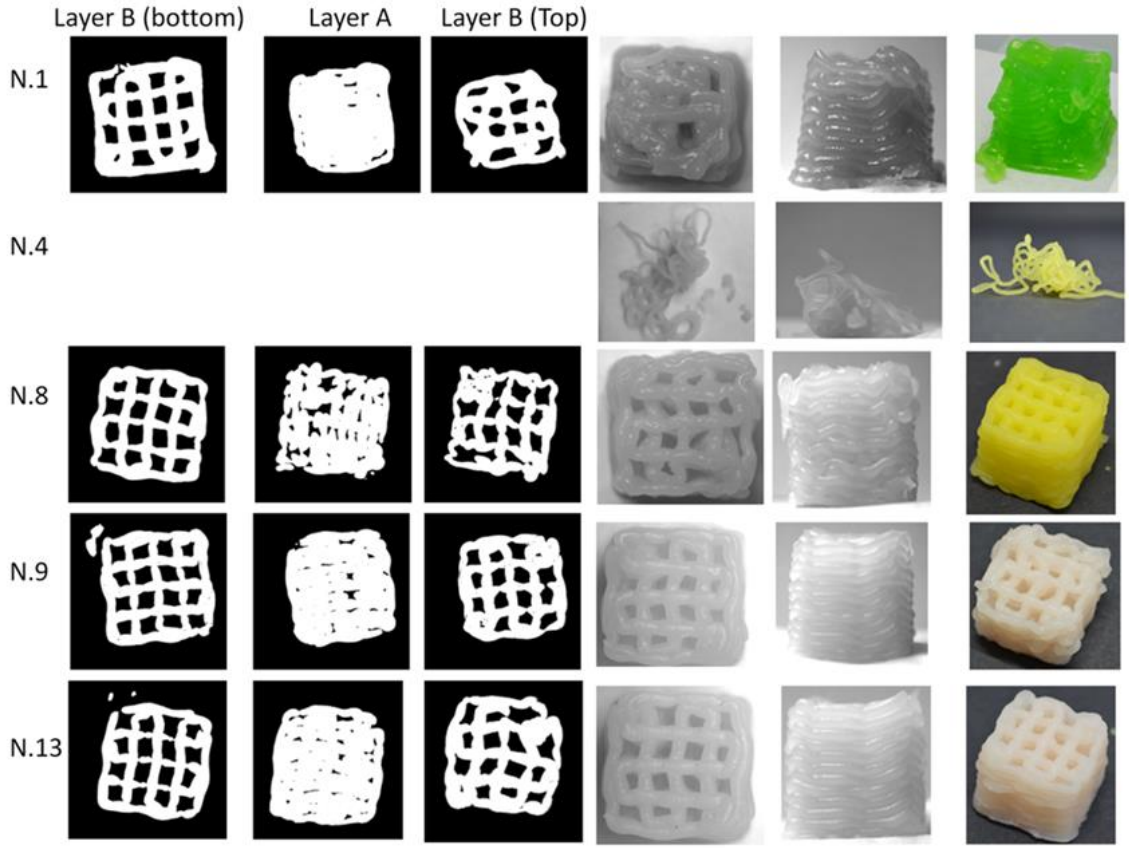

Fig. 10. Photographic images and 2D X-ray cross sectional images of some representative 3D printed samples obtained in different experimental conditions.

The first row of images (sample N.1), representing the lower weight fraction of CT, displays significant defects in the overall structure (sixth column) as well as on the top of the object (fourth column), which appears defectively printed in comparison with the designed structure (Fig. 1). In the case of the Layer B, on the bottom of the printed structure, some squared voids are definitely visible. Such voids are expected and correctly generated by the 90° of rotation of the designed printing paths (Fig. 1). On the other hand, the Layer A as expected is almost completely filled with only minor random voids as a result of general defects in the material deposition such as air bubbles inside the gel, the weight of overlying layers, etc. However, the result for Layer A is consistent with the programmed line distance of 2.2 mm and the track width that design a deposition of two adjacent gel-filaments that overlap with no spacing between them. Moreover, on the bottom of the samples the width of the filament is greater than of other printed samples due to the effect of the low viscosity of sample N.1 which favor the enlargement of the starchy-gel. Finally the third column shows the cross-sectional images of Layer B acquired on the top of the 3D

printed structure. This layer is significantly smaller than at the bottom of the sample. We can better observe this effect from the lateral view (fifth column) of the 3D printed object, in which the width of the structure significantly decreases from the bottom to the top. This is caused by the well-known increase of the weight on the bottom layers due to the printing of overlaying layers leading, therefore, to the crushing of such bottom layers (Mantihal, Prakash, Condi Godoi, & Bhandari, 2017; Lille et al., 2018; Liu, Yu, et al., 2019). Similarly, Liu, Yu, et al. (2019) noticed that samples were considerably deformed and larger approaching the sample bottom, but significantly smaller approaching the sample top. Moreover, the crushing of the layers at the bottom of the sample reduces the height of the samples thereby inducing the imbalance between the actual layer height and the values set at 0.8 mm. Derossi, Caporizzi, Paolillo, Gerkes, and Severini (2019) clearly showed that this imbalance leads to shapeless and smaller top layers. Accordingly, other authors reported the great importance of the layer height on the shape and dimension of 3D printed food structures (Severini et al., 2016; Wang et al., 2018; Yang et al., 2018). More generally, it is extensively proved that the disproportion between some printing variables produces serious structural defects (Khalil and Sun, 2007; Severini et al., 2016; Derossi et al., 2019, Derossi et al., 2019b; Guo, Zhang, & Bhandari, 2019).

As previously reported, the sample N.4 (weight fraction of CT = 30%) completely failed to print according to the high viscosity (Fig. 3) and insufficient dispensing force. But when the same amount of CT was used with a higher printing temperature of 45 °C and a reduced storage time of 24 h (sample N.8) the starchy-gel was easily deposited with significant improvement of the 3D printed structure. Moreover, the diameter of the deposited filaments was thin showing the lowest relative deviation of 6% from the estimated track width. Finally, the samples N.9 and N.13 were prepared with the middle weight fraction of CT = 22.5% but in the case of using of the longer ST = 24 h and a PT = 35 °C (sample N.13) the lower dimensional deviations for L, B and D were measured. Liu et al., 2019, Liu et al., 2019 showed the increase of filament diameter of ink-gels and the reduction of the voids of a lattice scaffold formulated with xanthan gum, kappa-carrageenan and potato starch.

Doubtless the diameter of filament has significant repercussions on the fraction porosity of the samples. For instance, sample N.1 showed the lowest porosity of 15.65% (data not shown). A better analysis of the porosity inside the 3D printed samples was performed by visualizing the data as a function of z direction (Fig. 11). The data well matches the designed structures showing two areas with very low

porosity, approximately at slice numbers 750 and 1100, corresponding to the printing of Layer A. In these sections the samples showed porosity fractions between 0.56 ± 0.50% and 12.92 ± 4.41% as a result of the bubble air inside the gel or the minor defects of deposition previously reported. In addition, the wide variation of the data among the samples is the result of the different experimental conditions adopted during 3D printing. For instance, the lowest porosity with values close to zero was measured for sample N.1 at the bottom of the structure (slice N ≈ 720). Furthermore, we can observe a slight trend to reduce the porosity fraction from the top to the bottom of the structure. This strengthens the aforementioned effect of crushing on the bottom layers due to the weight of the overlying layers that reduced the size and the amount of pores (Fig. 10). Furthermore, the samples showing the lower porosity fraction (N.1 and N.12) were the same who exhibited the higher diameter of the printed filament (Table 3). Finally, the porosity fraction of Layer B ranges from 20.79 ± 7.66 to 36.41 ± 4.25, showing an important variability probably due to the difficulty related to depositing a filament on top of a high porosity layer, as the filament may sag into the pores present in the underlying structure.

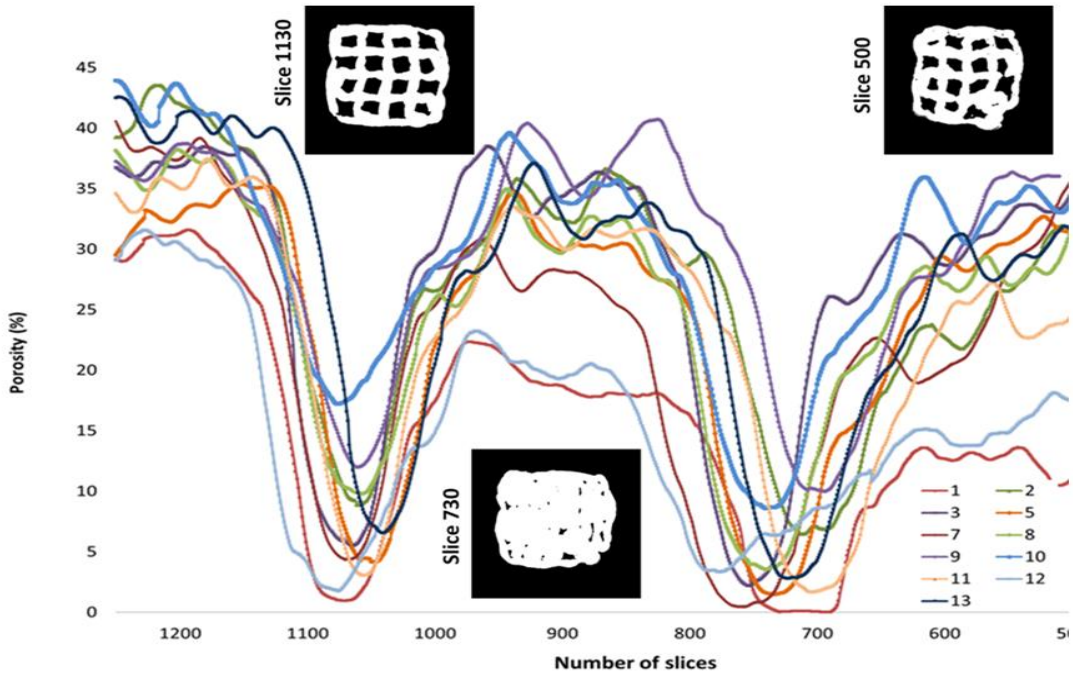

Fig. 11. Porosity fraction of 3D printed samples along z direction, top side, and representative 2D slices for 3D printed sample N.5.

4. Conclusion

In this research we show that 3D printing can be used to create innovative 3D printed food structures in which the local porosity/structure can be controlled based on the digital design. To this end, in this research we studied how this can be achieved. We varied the ingredient composition of a starchy-gel food ink, storage time and printing temperature of the gel to control the properties of the ink. Subsequently, we studied how the ink properties affect the printability and the structural quality of the printed object. All these variables largely contributed to the mechanical properties of gel network and the ability to get a good replica of the CAD model – i.e. the printing fidelity – changes to a large extent. The increase of storage time of the starchy-gel before printing works synergistically with the weight fraction of CT and the reduction of printing temperature. For cases where the viscosity of the starchy-gel was very high and exceeding the maximum dispensing force of the printer (600 N), it was not possible to properly extrude the ink-gel, resulting in a failed print. Medium viscosity gels could be successfully extruded and printed objects that closely resembled the CAD model could be obtained. Recommendations for the best printing conditions have been identified as follows: 30g/100 g of mass fraction of CT, 24 h of resting time and printing temperature of 45 °C (sample 8). When, however, the viscosity was too low, the weight of the structure resulted in the deformation of the bottom layers, in turn resulting in a widening of the bottom of the structure and a decrease in height as compared to the CAD design. The results of this research extend our abilities to control the 3D printing process of food materials and provide avenues to create innovative food products with specifically designed functionalities by means of 3D food printing.

Supplementary Material - 2D X-ray cross sectional images and photographic images of 3D printed samples obtained in different experimental conditions.

Samples	Layer B (bottom)	Layer A	Layer B (top)			
N.1				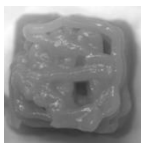	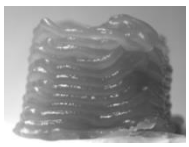	
N.2						
N.3				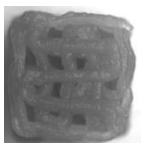	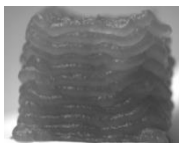	
N.4				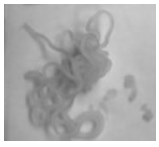		
N.5					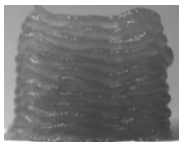	
N.6				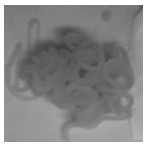	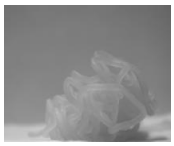	
N.7				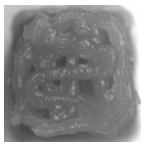	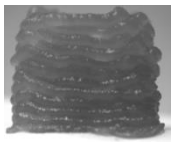	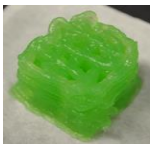
N.8		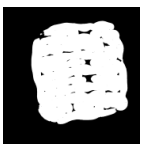				
N.9						
N.10						
N.11						
N.12						

N.13 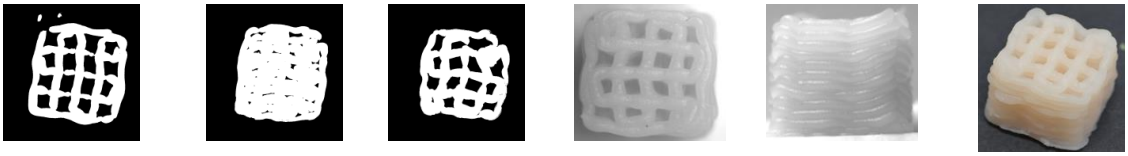

Acknowledgements

This work was possible thanks to the precious contribution of Jolanda Henket from Wageningen University - Food & Biobased Research- and Martijn de Schipper from TNO - Netherlands Organization for Applied Scientific Research (Netherland) which collaborated in the preliminary stages of the work.

5. References

AACC (2012). American association of cereal chemists, approved methods. Method 32-07.01 soluble, insoluble, and total dietary fiber in foods and food products(11th ed.). (St.Paul, MN).

Anukiruthika, T., Moses, J. A., Anandharamakrishnan, C. (2020). 3D printing of egg yolk and white with rice flour blends. Journal of Food Engineering, 265, 109691. https://doi.org/10.1016/j.jfoodeng.2019.109691.

Allen, JE, Hood, LF, Chalbot, JF. (1977). Effect of heating on the freeze-etch ultrastructure of hydroxypropyl distarch phosphate and unmodified tapioca starches. Cereal Chemistry, 54:783-793.

Berman, B. (2012). 3-D printing: The new industrial revolution. Business Horizons, 55, 155-162. https://doi.org/10.1016/j.bushor.2011.11.003.

Box, G. E. P., Hunter, J. S., Hunter, W. J. (2005). Statistics for Experimenters: Design, Innovation, and Discovery, 2nd Edition Wiley (Edt.).

Breuninger, W. F., Piyachomkwan, K., & Srioroth, K. (2009). Tapioca/Cassava starch: production and use. https://doi.org/10.1016/B978-0-12-746275-2.00012-4.

Chen, H., Xie, F., Chen, L., & Zheng, B. (2019). Effect of rheological properties of potato, rice and corn starches on their hot-extrusion 3D printing behaviors. Journal of Food Engineering, 244, 150-158. https://doi.org/10.1016/j.jfoodeng.2018.09.011

Cohen, A., Laviv, A., Berman, P., Nashef, R., & Abu-Tair, J. (2009). Mandibular reconstruction using stereolithographic 3-dimensional printing modeling technology. Oral Surgery, Oral Medicine, Oral Pathology, Oral Radiology, and Endodontology, 108, 661-666. https://doi.org/10.1016/j.tripleo.2009.05.023.

Cross, M.M. (1965). Rheology of Non-Newtonian Fluids—A New Flow Equation for Pseudoplastic Systems. Journal of Colloid Science, 20, 417-437. http://dx.doi.org/10.1016/0095-8522(65)90022-X

Debet, M. R., & Gidley, M. J. (2007). Why Do Gelatinized Starch Granules Not Dissolve Completely? Roles for Amylose, Protein, and Lipid in Granule "Ghost" Integrity. Journal of Agricultural and Food Chemistry, 55, 12, 4752–4760. https://doi.org/10.1021/jf070004o.

Derossi, A., Caporizzi, R., Ricci, I., Severini, C. (2019a). Chapter 3 - critical variables in 3D food printing F.C. Godoi, B.R. Bhandari, M. Zhang (Eds.), Fundamentals of 3D Printing and Applications, vol. 3, 9780128145647, Elsevier Inc. (2019), pp. 41-91, https://doi.org/10.1016/B978-0-12-814564-7.00003-1.

Derossi, A., Caporizzi, R., Paolillo, M., Gerkes, K., & Severini, C. (2019b). Design and production of 3D printed food with desired textural properties. ICEF13, 23-26 September, Melbourne, Australia.

Derossi, A., Paolillo, M., Caporizzi, R., & Severini, C. (2020a). Extending the 3D food printing tests at high speed. Material deposition and effect of non-printing movements on the final quality of printed structures. Journal of Food Engineering, 275, 109865. https://doi.org/10.1016/j.jfoodeng.2019.109865.

Derossi, A., Caporizzi, R., Paolillo, M., Severini, C. (2020b). Programmable texture properties of cereal-based snack mediated by 3D printing technology, Journal of Food Engineering, 289, 11-0160.

Dick, A., Bhandari, B., Dong, X., & Prakash, S. (2020). Feasibility study of hydrocolloid incorporated 3D printed pork as dysphagia food. Food Hydrocolloids, 107, 105940. https://doi.org/10.1016/j.foodhyd.2020.105940.

Douglas, J., Gasoriek, J. Swaffield, J., Jack,L. (2005) Fluid Mechanics, (fifth ed.), Prentice Hall

Eliasson, A. C. (1986). Viscoelastic behaviour during the gelatinization of starch i. comparison of wheat, maize, potato and waxy-barley starches. Journal of Texture Studies, https://doi.org/10.1111/j.1745-4603.1986.tb00551.x.

Eidam, D., Kulicke, W. M., Kuhn, K., & Stute, R. (1995). Formation of maize starch gels selectively regulated by the addition of hydrocolloids. Starch, 47, 378-384.

Feng, C., Zhang, M., Bhandari, B. and Ye, Y. (2020).Use of potato processing by-product: effects on the 3D printing characteristics of the yam and the texture of air-fried yam snacks. LWT, 125, 109265, 1-9 https://doi.org/10.1016/j.lwt.2020.109265.

Ferreira, S.L.C., Bruns, R.E., Ferreira, H.S., Matos, G.D , David, J.M., Brandão, G.C, da Silva, E.G.P., Portugal, L.A., .dos Reisc, P.S, Souza, A.S & dos Santos, W.N.L. Box-Behnken design: An alternative for the optimization of analytical methods, Analytica Chimica Acta, 597, 179-186 https://doi.org/10.1016/j.aca.2007.07.011.

Fischer, P. & Windh, E. J. (2011). Rheology of food materials. Current Opinion in Colloid & Interface Science, 16, 36-40. https://doi.org/10.1016/j.cocis.2010.07.003.

Gholamipour-Shirazi, A., Norton, I.T., Mills, T. (2019). Designing hydrocolloids based food-ink formulations for extrusion 3D printing. Food Hydrocolloids, 95, 161-167. https://doi.org/10.1016/j.foodhyd.2019.04.011.

Gibson, I., Rosen, D., Stucker, B. (2015). 3D Printing, Rapid Prototyping, and Direct Digital Manufacturing. Additive Manufacturing Technologies

Godoi, C. F., Prakash, S., & Bhandari, B. R. (2016). 3d printing technologies applied for food design: Status and prospects. Journal of Food Engineering, 179, 44-54. https://doi.org/10.1016/j.jfoodeng.2016.01.025.

Guo, C., Zhang, M., & Bhandari, B. (2019). Model Building and Slicing in Food 3D Printing Processes: A Review. Comprehensive Reviews in Food Science and Food Safety, 18, 1059-1069. https://doi.org/10.1111/1541-4337.12443

Hauswirth, S. C., Bowers, C. A.; Fowler, C. P., Schultz, P. B., Hauswirth, A. D., Weigand, T., Miller, C. T. (2020). Modeling cross model non-Newtonian fluid flow in porous media. Journal of Contaminant Hydrology, 235, 103708. https://doi.org/10.1016/j.jconhyd.2020.103708

Karim, A. A., Norziah, M. H., & Seow, C. C. (2000). Methods for the study of starch retrogradation. Food Chemistry, 71, 9-36. https://doi.org/10.1016/S0308-8146(00)00130-8.

Kettles, C.J.A.M., Oostergetel, G.T., van Vliet, T. (1996). Recrystallization of amylopectin in concentrated gels. Carbohydrates Polymers, 30, 61-64. https://doi.org/10.1016/S0144-8617(96)00057-4.

Khalil, S., & Sun W. (2009). Bioprinting endothelial cells with alginate for 3D tissue constructs. Engineering, Medicine, Journal of biomechanical engineering, 131(11): 111002. https://doi.org/10.1115/1.3128729.

Le-Bail, A., Maniglia, B. C., & Le-Bail, P. (2020). Recent advances and future perspective in additive manufacturing of foods based on 3D printing. Current Opinion in Food Science, 35, 54-64. https://doi.org/10.1016/j.cofs.2020.01.009.

Le Tohic, C., J.O'Sullivan, J., Drapala, K., Chartrin, V., Chan, T. Morrison, A. P., Kerry, J. P., & Kelly, A. L. (2018). Effect of 3D printing on the structure and textural properties of processed cheese. Journal of Food Engineering, 220, 56-64. https://doi.org/10.1016/j.jfoodeng.2017.02.003.

Lanaro, M., Forrestal, D. P., Scheurer, S., Slinger, D. J., Liao, S., Powell, S. K., Woodruff, M. A. (2020). Journal of Food Engineering,215, 13-22. https://doi.org/10.1016/j.jfoodeng.2017.06.029

Leonel, M., Sarmento, S. B. S., & Cereda, M. S. (2003). New starches for the food industry: Curcuma longa and Curcuma zedoaria. Carbohydrate Polymers 54, 385–38. https://doi.org/10.1016/S0144-8617(03)00179-6.

Lille, M., Nurmel, A., Nordlund, E., Metsä-Kortelainen, S., & Sozer; N. (2018). Applicability of protein and fiber-rich food materials in extrusion-based 3D printing. Journal of Food Engineering, 220, 20-27. https://doi.org/10.1016/j.jfoodeng.2017.04.034.

Lipton, J. I., Cutler, M., Nigl, F., Cohen, D., & Lipson, H. (2015). Additive manufacturing for the food industry. Trends in Food Science & Technology, 43, 114-123. https://doi.org/10.1016/j.tifs.2015.02.004.

Liu, Q. & Thompson, D. B. (1998). Effects of moisture content and different gelatinization heating temperatures on retrogradation of waxy-type maize starches. Carbohydrate Research, 314, 3–4, 221-235. https://doi.org/10.1016/S0008-6215(98)00310-3.

Liu, Z., Zhang, M., Bhandari, B., Wang, Y. (2017). 3D printing: Printing precision and application in food sector. Trends in Food Science & Technology, 69 (2017), 83-94. https://doi.org/10.1016/j.tifs.2017.08.018

Liu, Y., Liu, D., Wei, G., Ma, Y., Bhandari, B., & Zhou, P. (2018a) 3D printed milk protein food simulant: Improving the printing performance of milk protein concentration by incorporating whey protein isolate. Innovative Food Science & Emerging Technologies, 49, 116-126. https://doi.org/10.1016/j.ifset.2018.07.018.

Liu, Z., Zhang, M., Yang, C. (2018b). Dual extrusion 3D printing of mashed potatoes/strawberry juice gel. LWT, 96, 589-596. https://doi.org/10.1016/j.lwt.2018.06.014.

Liu, Z., Bhandari, B., Prakash, S., Mantihal, S. & Zhanga, M. (2019a). Linking rheology and printability of a multicomponent gel system of carrageenan-xanthan-starch in extrusion based additive manufacturing. Food Hydrocolloids, 87, 413-424. https://doi.org/10.1016/j.foodhyd.2018.08.026.

Liu, Y., Yu, Y., Liu, C., Regenstein, J, M, Liu, X., & Zhou, P. (2019b). Rheological and mechanical behavior of milk protein composite gel for extrusion-based 3D food printing. LWT, 102, 338-346. https://doi.org/10.1016/j.lwt.2018.12.053.

Liu, Z., Chen, H., Zheng, B., Xie, F., & Chen, F. (2020). Understanding the structure and rheological properties of potato starch induced by hot-extrusion 3D printing. Food Hydrocolloids, 105, 105812. https://doi.org/10.1016/j.foodhyd.2020.105812.

Loveday, S. M., Rao, M. A., Creamer, L. K., & Singh, H. (2010). Rheological behavior of high-concentration sodium caseinate dispersions. Journal of Food Science, 75, N30-N35.

Maniglia, B. C., Lima, D. C., Matta Junior, M. D., Le-Bail, P., Le-Bail, A., Augusto, P. E. D. (2019). Hydrogels based on ozonated cassava starch: Effect of ozone processing and gelatinization conditions on enhancing 3D-printing applications. International Journal of Biological Macromolecules, 138, 1087-1097, https://doi.org/10.1016/j.ijbiomac.2019.07.124.

Maniglia, B. C.,Lima, D. C., Matta Junior, M. D., Le-Bail, P., Le-Baila, A., Augusto, P. E. D. (2020). Preparation of cassava starch hydrogels for application in 3D printing using dry heating treatment (DHT): A prospective study on the effects of DHT and gelatinization conditions. Food Research International, 128, 108803. https://doi.org/10.1016/j.foodres.2019.108803.

Mantihal, S., Prakash, S., Condi Godoi, F., & Bhandari, B. (2017). Optimization of chocolate 3D printing by correlating thermal and flow properties with 3D structure modeling. Innovative Food Science & Emerging Technologies, 44, 21-29. https://doi.org/10.1016/j.ifset.2017.09.012.

Mantihal, S., Prakash, S. Godoi, F. C., Bhandari, B. (2019). Optimization of chocolate 3D printing by correlating thermal and flow properties with 3D structure modeling. Innovative food science & emerging technologies,44, 21-29. https://doi.org/10.1016/j.ifset.2017.09.012,

Mansfield, M., O'Sullivan, C. (2010) Understanding Physics, Wiley

Nair, S. A. O., Panda, S., Santhanam, M., Sant, G., Neithalath, N. (2020). A critical examination of the influence of material characteristics and extruder geometry on 3D printing of cementitious binders. Cement & Concrete Composites https://10.1016/j.cemconcomp.2020.103671,

Nijdam, J. J., Agarwal, D., Schon, B. S. (2021). Assessment of a novel window of dimensional stability for screening food inks for 3D printing. Journal of Food Engineering, 292, 110349. https://doi.org/10.1016/j.jfoodeng.2020.110349,

Oladebeye, A. O., Oshodi, A. A., Amoo, I. A., & Karim, A. A. (2013). Hydroxypropyl derivatives of legume starches: Functional, rheological and thermal properties. Starch/Stärke, 65, 762-772. https://doi.org/10.1002/star.201300003

Paxton, N., Smolan, W., Böck, T., Melchels, F., Groll, J., & Jungst, T. (2017). Proposal to assess printability of bioinks for extrusion-based bioprinting and evaluation of rheological properties governing bioprintability. Biofabrication, 9, 044107. https://doi.org/10.1088/1758-5090/aa8dd8.

Pipe, C. J., Majmudar, T. S., McKinley, G. H. (2008). High shear rate viscometry. Rheol Acta, 47, 621–642. https://doi.org/10.1007/s00397-008-0268-1

Piyush, Kumar, R., & Kumar, R. (2020). 3D printing of food materials: A state of art review and future applications, Materialstoday Proceedings, In Press, Corrected Proof. https://doi.org/10.1016/j.matpr.2020.02.005.

Pulatsu, E., Su, J., Lin, J., Lin, M. (2020). Factors affecting 3D printing and post-processing capacity of cookie dough. Innovative Food Science & Emerging Technologies, 61, 102316. https://doi.org/10.1016/j.ifset.2020.102316.

Qiu, S., Punzalan, M. E., Abbaspourrad, A., & Padilla-Zakour, O. A. (2020). High water content, maltose and sodium dodecyl sulfate were effective in preventing the long-term retrogradation of glutinous rice grains - A comparative study. Food Hydrocolloids, 98, 105247. https://doi.org/10.1016/j.foodhyd.2019.105247.

Rezler, R. (2007). The effect of the plant fat akoroma om on the mechanical properties of finely comminuted sausage batters. Acta Agrophysica, 9(1), 209-219.

Rezler, R. & Poliszko, S. (2010). Temperature dependence of starch gel rheological properties. Food Hydrocolloids, 24, 570-577. https://doi.org/10.1016/j.foodhyd.2010.02.003.

Ring, S. G., Colonna, P., I'Anson, K. J., Kalichevsky, M. T., Miles, M. J., Morris, V. J., & Orford, P. D. (1987). The gelation and crystallisation of amylopectin. Carbohydrate Research, 162, 2, 277-293. https://doi.org/10.1016/0008-6215(87)80223-9.

Russ, N., Zielbauer, B. I., Ghebremedhin, M., & Vilgis, T. A. (2015). Pre-gelatinized tapioca starch and its mixtures with xanthan gum and ι-carrageenan. Food Hydrocolloids, 56, 180-188. https://doi.org/10.1016/j.foodhyd.2015.12.021.

Sánchez, T., Dufour, D., Moreno, I. X., & Ceballos, H. (2010). Comparison of pasting and gels stabilities of waxy and normal starches from potato, maize, and rice with those of a novel waxy cassava starch under thermal, chemical and mechanical stress. Journal of Agricultural And Food Chemistry, 58, 5093-5099. https://doi.org/10.1021/jf1001606.

Severini, C., Derossi, A., & Azzollini, D. (2016). Variables affecting the printability of foods: Preliminary tests on cereal-based products. Innovative Food Science & Emerging Technologies 38, 281-291. https://doi.org/10.1016/j.ifset.2016.10.001.

Severini, C, Derossi, A., Ricci, I., Caporizzi, R., & Fiore, A. (2018). Printing a blend of fruit and vegetables. New advances on critical variables and shelf life of 3D edible objects. Journal of Food Engineering, 220, 89-100. https://doi.org/10.1016/j.jfoodeng.2017.08.025.

Sun, A., & Gunasekaran, S. (2009). Yield stress in foods: Measurements and applications. International Journal of Food Properties, 12, 70-101. https://doi.org/10.1080/10942910802308502.

Sun, J., Peng, Z., Zhou, W. ,.Fuh, J. Y.H, Hong, G. S., & Chiu, A. (2015). A Review on 3D Printing for Customized Food Fabrication. Procedia Manufacturing, 1, 308-319. https://doi.org/10.1016/j.promfg.2015.09.057.

Tabilo-Munizaga, G., Barbosa-Cánovas, G. V. (2005). Rheology for the food industry. Journal of Food Engineering, 67, 147-156 https://doi.org/10.1016/j.jfoodeng.2004.05.062.

van Bommel, K. J. C., (2012). 3D printing: now printing food too.

Wang, L., Zhang, M., Bhandari, B., & Yang, C. (2018). Investigation on fish surimi gel as promising food material for 3D printing. Journal of Food Engineering, 220, 101-108. https://doi.org/10.1016/j.jfoodeng.2017.02.029.

Wang, W., & Shi, Y. 2020. Gelatinization, pasting and retrogradation properties of hydroxypropylated normal wheat, waxy wheat, and waxy maize starches. Food Hydrocolloids, 106, 105910. https://doi.org/10.1016/j.foodhyd.2020.105910.

Wegrzyn, T. F., Golding, M., & Archer, R. H. (2012). Food Layered Manufacture: A new process for constructing solid foods. Trends in Food Science & Technology, 27, 66-72. https://doi.org/10.1016/j.tifs.2012.04.006.

Xu, L., Gu, L., Su, Y., Chang, C., Wang, J., Dong, S., Liu, Y., Yang, Y., & Li, J. (2020). Impact of thermal treatment on the rheological, microstructural, protein structures and extrusion 3D printing characteristics of egg yolk. Food Hydrocolloids, 100, 105399. https://doi.org/10.1016/j.foodhyd.2019.105399.

Yang, F., Zhang, M., & Bhandari, B. (2017). Recent development in 3D food printing. Critical Reviews in Food Science and Nutrition, 57, 3145-3153. https://doi.org/10.1080/10408398.2015.1094732.

Yang, F., Zhang, M., Bhandari, B., & Liu, Y. (2018). Investigation on lemon juice gel as food material for 3D printing and optimization of printing parameters. LWT, 87, 67-76. https://doi.org/10.1016/j.lwt.2017.08.054.

Yang, F., Guo, C., Zhang, M., Bhandari, B., & Liu. (2019). Improving 3D printing process of lemon juice gel based on fluid flow numerical simulation. LWT, 102, 89-99. https://doi.org/10.1016/j.lwt.2018.12.031.

Yu, M., Xu, Z., Ji, N., Dai, L., Xiong, L., & Sun, Q. (2020). Inhibition of normal and waxy corn starch retrogradation by sodium borohydride. International Journal of Biological Macromolecules

Zhang, B., Dhital, S., Flanagan, B. M., & Gidley, M. J. (2014). Mechanism for Starch Granule Ghost Formation Deduced from Structural and Enzyme Digestion Properties. Journal of Agricultural and Food Chemistry, 62, 3, 760–771. https://doi.org/10.1021/jf404697v.

Zhang, Y., Li, J., Zhang, Z., Wei, Q., & Fang, K. (2019). Rheological law of change and conformation of potato starch paste in an ultrasound field. Journal of Food Measurement and Characterization, 13, 1695–1704. https://doi.org/10.1007/s11694-019-00086-8.

Zheng, L., Yu, Y., Tong, Z., Zou, Q., Han. S., Jiang, H. (2019). The characteristics of starch gels molded by 3D printing. Journal of Food Processing and Preservation, 43,13993. https://doi.org/10.1111/jfpp.13993.

Zhu, S., Stieger, M. A., van der Goota, A. J., & Schutyser, M. A. I. (2019). Extrusion-based 3D printing of food pastes: Correlating rheological properties with printing behaviour. Innovative Food Science & Emerging Technologies, 58, 102214. https://doi.org/10.1016/j.ifset.2019.102214.

CHAPTER 5 Programmable texture properties of cereal-based snack mediated by 3D printing technology

Antonio Derossi, Rossella Caporizzi, Maddalena Paolillo, Carla Severini

Journal of Food Engineering

Volume 289, January 2021, 110160

Abstract

3D food printing (3DFP) creates edible structures by a layer-by-layer deposition with the main aim of creating personalized food structures. We studied the capability to create 3D printed cereal snacks with different texture by a controlled generation of pores. The snacks well captured the overall features of the virtual model with size reduction less than 8%. Contrarily, the 3D printed snacks exhibited a great increase in porosity fraction, from 5 to 25%, while the pore's length reduced due to the crushing of dough's filament. The hardness of the snacks reduced from 289 N to 84 N following the reduction of the relative density, from 0.569 to 0.401. The model of Gibson and Ashby satisfactory fitted the experimental data showing that printed snacks with controlled voids follow the rule of cellular material. The results open interesting perspectives of creating novel foods with desired texture addressing specific requirements, or novel sensory/satiety perception.

1. Introduction

Food texture is one of the most important food properties for consumers' acceptance (Chen and Opara, 2013; Kohyama, 2015; Laureati et al., 2020). Also it affects the bioavailability of nutrients and functional compounds (Dupont et al., 2018; Foegeding et al., 2017; McClements and Xiao, 2017). During eating the perception of food texture is the result of a complex system of interrelated stimuli that involves many senses such as vision, hearing, touch and kinesthetics (Devezeaux de Lavergne et al., 2015; Gao et al., 2017; Hutching & Lillford, 1988; Pascua et al., 2013; Szczesniak, 2002). Under these considerations and with the aim to design and deliver highly accepted foods capable to satisfy dietary requirements, the mechanisms participating in texture perception have been widely studied (Cakir et al., 2012; Endo et al., 2017; Hutching & Lillford, 1988; Laureati et al., 2020; Santagiuliana et al., 2018; Szczesniak, 2002). Current literature recognize that texture perception of food strictly depends by 3D structure (Szczesniak, 2002) which may be characterized only

by several information that span from micro- to macro-scale (Aguilera, 2005; Day & Goldin, 2016; Derossi et al., 2019a; Paula and Conti-Silva., 2014).

3D Food Printing (3DFP) is an emerging technology capable to create innovative food products by a controlled layer-by-layer deposition of food materials that replicates the structure of a 3D virtual model (Lipton et al., 2015; Vancauwenberghe et al., 2018). 3DFP has the main ambition of tailored/personalized food manufacturing both in term of sensory properties and nutritional content (Derossi et al., 2020; Park et al., 2020; Pulatsu et al., 2020). In last 10 years, scientific community has explored 3DFP from different perspectives by studying the printing properties of food formula (Cohen et al., 2009; Grood and Grood, 2011; Yang et al., 2018a), the effects of printing variables (Derossi et al., 2019b; Lille et al., 2018; Mantihal et al., 2017; Severini et al., 2016), the improvement of nutritional properties (Derossi et al., 2018; Lille et al., 2018; Severini et al., 2018), the effect on the texture (Le Tohic et al., 2018; Liu et al., 2018a), colour and flavour on 3D products (Izdebska and Tryznowska, 2016). The creation of 3D printed food products with desired texture properties could be obtained by controlling the internal structure (Lille et al., 2018) or adopting multi-material extruded with dual extrusion printing (Liu et al., 2018a) but this specific topic still has limited results. Lipton et al. (2015) and Feng et al. (2020) modulated the infill level and the infill pattern of 3D structures evaluating the effect on the texture of corn-based food formula or a mixture of yam powder and potato by-products. In particular, Feng et al. (2020) showed a linear and positive relationship between infill level and the hardness of the end products after air-frying process; also, the authors reported as 3D food structure printed with the same infill level but with different infill pattern showed significant differences in hardness. Contrarily, the infill pattern did not show any effect when a softer food formula (mashed potato and brown rice) was used (Huang et al., 2019; Liu et al., 2018a). Another interesting approach has been to print a like-scaffold consisting of edible gels in which plant cells (Valerianella locusta) have been encapsulated (Vancauwenberghe et al., 2019) or carrot callus tissue has been included in a alginate ink-gel, then printed and left to growth till different cell concentration is reached; in the latter case the results showed real capacities to obtain unique texture properties (Park et al., 2020). Also, Derossi et al. (2019c), studied the possibility to mimic the 3D structure of apple tissue by using 3D X-ray microtomographic images as virtual model that drives the 3D printing of multi-layers cereal-based snack with different texture properties (Derossi et al., 2019c). However above papers did not evaluate the possibility of defining others important 3D structure properties such as the number,

the size and the position of internal voids which are essential for materials and food microstructure (Aguilera, 2005; Derossi et al., 2019c; Torquato, 2002). To our knowledge the only relevant experiments on this topic has been performed by Vancauwenberghe et al. (2018) who printed a 3D pectin-based by using honeycomb structure with different number of voids estimating the main mechanical properties of such gels by using analytical model and FEM method. Therefore, additional experiments focused on the 3D food printing of structures with controlled generation of voids are needed.

The main objective of this paper was to study the capability to obtain cereal-snacks with different texture properties by means 3D printing technology. With this aim, we have designed several 3D virtual models modulating the number and the position of the internal voids. Such virtual models have been used to print innovative cereal-snacks for which the fidelity of printing was tested by analyzing the most important morphological and microstructure metrics while the hardness of the printed snacks was analyzed against the relative density on the basis of the principles of cellular solids.

2. Materials and methods

2.1. Dough preparation and characterization

Wheat flour 00 (Granoro, Italy) (62 g/100 g w.b.), olive oil (Desantis, Italy) (6 g/100 g w.b.), sodium chloride (1 g/100 g w.b.) and water (Lilia, Italy) (31 g/100 g w.b.) were purchased locally. All ingredients were mixed for 3 min by using a planetary kneader (model cooking chef, Kenwood Ltd. UK) at speed level of 1 (22 rpm). After mixing, the dough was rest at room temperature for 30 min before to be used for 3D printing process. With the aim to characterize the basic mechanical behavior of the dough, farinograph analysis was performed by a Farinograph-AT (Brabender 230V, 50/60 Hz, Germany) according to the method Brabender/ICC/BIPEA 300. The dough exhibited a maximum consistency of 1004 ± 46 B.U.; a development time (Pasqualone et al., 2018) of 453 ± 39 s; the corresponding curve bandwidth – also considered the dough elasticity (Sudha et al., 2007) - of 363 ± 26 B.U.; WZ (the water absorption rate) of 31.0 ± 0.1%; WAC (the water absorption rate corresponding to the consistency) of 44.0 ± 2.5%.

2.2. Sample design and 3D printing process

A parallelepiped shape of size of 50 x 16 x 25 mm and internal cube-shaped pores of 6 x 6 x 25 mm were utilized to create a total of 6 different structures having significant variations in porosity fraction (from 18% to 54%, for sample Q1_4 and

Q2_6 respectively) and 3D architecture (Fig. 1). All the 3D models have been created by using computer-aided design (CAD) software (TinkerCad, Autodesk Inc.). Then, the CAD models were converted in .stl files and the slicing software CURA ver. 3.3.1 was employed to define the printing variables. 3D printing experiments were performed by using a 3D printer Delta 2040 equipped with a clay extruder kit 2.0 (Wasp Project, Italy). Preliminary tests were conducted in order to define the best setting parameters which are reported in Table 1. With the aim to mitigate the shape deformation usually occurring during the baking of cereal-based 3D printed structure (Kim et al., 2019; Pulatsu et al., 2020), we have performed the dough deposition on a heated plate at 70 °C. Such temperature was defined on the basis of some preliminary experiments (between 50 °C and 100 °C) and allowed to increase the consistency of the first 3–4 layers as a result of a partial starch gelatinization; this allowed to keep the weight of the other 27 layers of dough avoiding shape deformation and macroscopic collapse. After 3D printing, the objects were cooked in ordinary oven at 150 °C for 18 min, pre-heated at 150 °C for 1 h. Temperature inside oven was homogenous with variation less than 1 °C. Each sample was cooked individually positioning the 3D printed snacks at the centre of the oven, and leaving them at room temperature for 3 h before physical analysis.

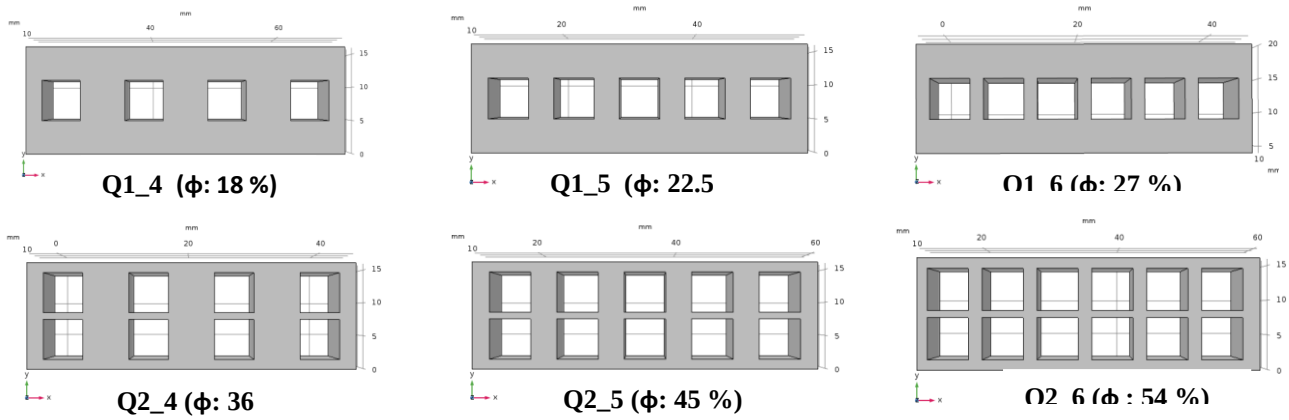

Fig. 1. Schematic representation of designed structure. In parenthesis porosity fraction (φ) of each sample was indicated.

Printing parameters	**Value**
Shell thickness (mm)	0.84
Bottom/Top thickness	0.6
Fill density (%)	100

Print speed (mm/s)	22.8
Bottom layer speed (mm/s)	20
Retraction Speed (mm)	30
Travel speed (mm/s)	30
Infill speed (mm/s)	30
Flow (%)	177
Layer height (mm)	0.8
Nozzle size (mm)	0.84

Table 1. Printing setting parameters

	Number of pores	**Distance between pores (mm)**	**Longitudinal wall Thickness (x) (mm)**	**Vertical wall thickness (y) (mm)**	**Total volume (m^3)**	**Porosity Fraction (%)**
Q1_4	4	7	2.5	5	0.02	18
Q1_5	5	4	2.5	5	0.02	22.5
Q1_6	6	2	2	5	0.02	27
Q2_4	8	7	2.5	1.5	0.02	36
Q2_5	10	4	2.5	1.5	0.02	45
Q2_6	12	2	2	1.5	0.02	54

2.3. Analysis of the main morphological properties

The main dimensional properties, height (H), length (L), thickness (T), were measured on cooked samples by using a universal Crafsman calliper by repeating the

measurements in triplicates for each sample. The length of the pores (Lp) was also evaluated (Fig. 2).

Fig. 2. Schematic representation of main dimensions evaluated on printed samples. H: height; L: length; T: thickness; Lp: dimension of pores.

2.4. Physical analysis

On cooked samples weight loss, water activity and moisture content were assessed in triplicates. Weight loss was computed as fractional decrease between the weight of the samples immediately after printing (raw material) and the weight after cooking and cooling at room temperature.

Moisture content was determined according to the gravimetric method as described in AOAC–925.10. Water activity was measured by using a dew-point system (AquaLab, Decagon Devices, US) previously calibrated with standard solutions.

The colour was recorded by using a colour meter Mod. CR 400 (Minolta, Japan) and the CIE L*a*b* international scale parameters was used to express data. Independent measures were randomly carried out on the surface of both sides of the samples performing at least 5 replicates for each sample.

2.5. Textural properties

Hardness of samples was determined by penetration test of Tyagi et al. (2007) with minor modifications. A TA-XT plus texture analyser (Stable Microsystems, Surrey, UK) equipped with a 50 N load cell was used for analysis. The samples were axially compressed to a distance of 8 mm with an aluminum cylinder of 6 mm diameter (P/6; Stable Micro Systems, Surrey, UK) from the original height by using a 5 g trigger force. Texture analyzer settings were kept as: pre-test speed of 1.5 mm/s, test speed of 5 mm/s and post-test speed of 10 mm/s. The force required to compress the sample was recorded as the Hardness (N) of the product. All results were analyzed adopting the software EXPONENT version 2.0.6.0 (Stable Micro System, Surrey, UK). The results represented the average of five measurements.

2.6. Microstructural analysis

Cross-sectional microtomographic images of 1304(x) x 1024(y) pixels with a resolution of 28.5 μm were obtained with a SkyScan 1174 micro-CT scanner (Brüker, Kontich, Belgium) by using the conditions reported by Severini et al. (2020) with

minor modifications: 50 kV, exposure time of 1200 ms, source current of 800 μm, averaging frame of 3, rotation step of 0.3°, total scanning time of 72 min.
Images reconstruction was performed by using Nrecon 1.6.2.0 software (Bruker, Kontich, Belgium). Image processing consisted in the image segmentation, with the aim to binarized the images in voids and solid phases. 2D and 3D analyses of the samples were performed by using CTAn 1.12.0.0 (Bruker microCT, Belgium). The main microstructure properties were evaluated on a region of interest (ROI) fitting the entire surface of the object and considering a total cross-sectional images of N = 700. Analyses were performed on a representative sample for each structure.

2.7. Relative density model

The analytical model used to study the mechanical properties of the 3D printed objects is based on the principles of the mechanics of cellular materials for three-dimensional cell (foam) as described by Gibson et al. (1982a), and Gibson and Ashby (1982b, 1997). The authors explained the deformation of cellular materials as a function of the quantitative and qualitative properties of the cells. Gibson and Ashby (1982b) proposed a simple expression in which the moduli and collapse strengths are related with the relative density of such materials (Gibson and Ashby, 1982b). However, the shape (i.e. cubic, hexagonal, circular), size, density, position of the wall thickness of such cells and the way in which they are interconnected are responsible of the mechanical properties of food (Scanlon and Zghal, 2001; Van Hecke et al., 1995; Xu et al., 2016; Zghal et al., 2001).
Considering our 3D model as structure with cubic voids (i.e. the cells) repeatedly positioned in a 3D structure the following generalized Gibson and Ashby equation for a 3D materials consisting of open cell may be used:

$$\frac{E}{E^*} = C\left(\frac{\rho}{\rho^*}\right)^n \quad [1]$$

Where E is the Young modulus of the foam and E* is the Young modulus of the cell wall material of which the foam is made (Gibson and Ashby, 1982b), is the density of the foam (i.e. apparent density), is the density of the cell wall material (i.e. real density), n is a constant depending on cellular structure and C is a constant that depends on the type of deformation (Gibson and Ashby, 1982b). This equation has been extensively used in food sector considering Young's modulus or other mechanical properties (Le-Bail et al., 2009; Vancauwenberghe et al., 2018; Zghal et al., 2002). For instance a similar relationship is expected between relative density and critical stress value (σcr) such as the peak of the compression for the stress-strain

curve. So, the following form may be used (Gibson and Ashby, 1997; Scanlon and Zghal, 2001):

$$\frac{\sigma_{cr}}{\sigma_{cr^*}} = c\left(\frac{\rho}{\rho^*}\right)^n \quad [2]$$

In our case, corresponds to the maximum force to break the 3D samples, Fmax. is the hardness of the cellular material and represents the hardness of the solid material (Gibson et al., 1982a; Gibson and Ashby, 1982b). However, due to the difficulty to prepare a printable dough that after cooking exhibits zero porosity – the solid material – we used Eq. (2) in a form in which was included in the parameter C. This is also possible because, as widely reported, C is a dimensionless fitting parameter with values close to 1 (Gibson and Ashby, 1997; Zghal et al., 2002). Also, the relative density (may be expressed in function of the fraction porosity of the material (Φ):

$$\frac{\rho}{\rho^*} = 1 - \varphi \quad [3]$$

2.8. Statistical analysis

Results are presented as mean values and standard deviation. Analysis of variance (one-way ANOVA) was performed on the data. A Tukey's test was used to evaluate the significant difference of the samples. The software package Statistica ver 10.0 (StatSoft, Tulsa, USA) was used.

3. Results and discussion

3.1. Physical characteristics of 3D printed samples

Table 3 shows the results of the main properties of 3D printed snacks. Moisture content and water activity decreased with the increase of the number of designed pores. Specifically, moisture contents of 13.80 ± 0.189% and 11.37 ± 0.049% were measured for sample Q1_4 and Q2_6, respectively, while water activity values decreased from 0.776 ± 0.002 to 0.702 ± 0.001 for the same samples. This reduction is the result of the higher surface exposed to the heating during baking that significantly promoted water evaporation (Zhang et al., 2018). However, the fractional weight increase of 3D printed snacks after baking indicates average values of ≈24%. Considering the colours of samples, slight but significant changes were observed among 3D printed objects. The samples Q2_5 and Q2_6 were less red and yellow – as shown by the decrease of a* and b* indices – although from a visual evaluation, all samples appear homogeneous (Fig. 3).

Table 3 Main physical characteristics of 3D printed snacks

	Moisture content (%)	a_w	Fractional weight increase (%)	L*	a*	b*
Q1_4	13.80±0.189[a]	0.776±0.002[a]	22.54±1.05[a]	69.78±4.17[b]	3.17±3.15[a]	35.97±2.25[b]
Q1_5	13.30±0.027[b]	0.770±0.001[b]	23.04±2.18[a]	72.96±3.55[a]	1.54±2.35[a]	34.93±2.09[b]
Q1_6	12.16±0.123[d]	0.733±0.001[d]	25.46±2.05[a]	71.04±3.55[a]	3.19±4.10[a]	36.75±2.40[a]
Q2_4	12.57±0.085[c]	0.758±0.003[c]	23.55±1.52[a]	73.55±2.48[a]	2.44±3.46[a]	34.16±3.55[b]
Q2_5	11.25±0.108[e]	0.712±0.001[e]	24.80±0.96[a]	71.20±4.27[a]	0.36±3.05[ab]	32.60±2.59[c]
Q2_6	11.37±0.049[e]	0.702±0.001[f]	25.00±1.07[a]	74.44±1.92[a]	-2.50±1.74[b]	28.24±2.74[d]

Means followed by different lowercase letters are significantly different at $P \leq 0.05$ (L*: lightness, a*: red index, b*: yellow index)

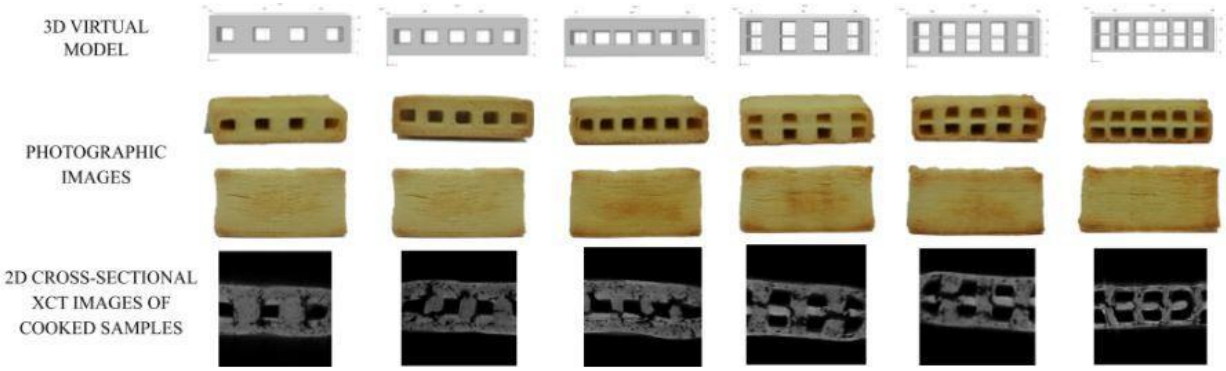

Fig. 3. Cross section design of the virtual model (row 1), photographic images (row 2 and 3) and 2D-cross sectional images (row 4) of cooked samples.

3.2. Fidelity of printing

The fidelity of printing was assessed in terms of precision of material deposition, stability of the printed dough and accuracy of the main morphological properties of the snacks after baking. The comparison of the photographic images of the 3D cooked snacks against the virtual models (Fig. 3) reveals high printing fidelity. The overall shape and size of the snacks, the shape, the number of internal pores as well as their size and the distance between them, closely match the designed structures recognizing the high ability of 3D printing to capture the main characteristics of CAD models (Hertafeld et al., 2018; Lipton et al., 2015; Severini et al., 2016; Yang et al., 2018b). However, some minor defects are observed, e.g. some layers do not adhere precisely creating internal fractures and new pores, while the corners of the samples showed round-shape rather than squared. Moreover, after the layer-by-layer deposition of filaments of dough the water loss during baking tends to lift the filaments increasing the distance between the layers (Severini et al., 2018). With the aim to better analyze the fidelity of printing, the fractional deviations of 3D printed samples from the corresponding virtual models have been measured for several morphological metrics (Table 4).

Table 4. Fractional deviation of the main morphological properties of 3D printed snack against the virtual model.

Structure	$\Delta H/H_0$ (%)	$\Delta L/L_0$ (%)	$\Delta T/T_0$ (%)	$\Delta Lp/Lp_0$ (%)	$\Delta V/V_0$ (%)	$\Delta\varphi/\varphi_0$ (%)
Q1_4	2.00±2.59^{bc}	-7.83±0.29^{a}	-3.81±2.17^{c}	-14.94±9.1^{a}	-9.56±3.79^{b}	140^{a}
Q1_5	4.16±0.29^{a}	-6.33±0.88^{ab}	1.041±1.80	-17.48±10.3^{a}	-1.41±2.73^{a}	100^{b}
Q1_6	-0.50±0.50^{c}	-6.66±0.14^{a}	-1.736±1.59^{b}	-25.70±3.2^{a}	-8.74±1.96^{b}	86^{c}
Q2_4	-0.85±0.30^{cb}	-7.66±0.38^{a}	4.166±0.10^{a}	-13.24±9.8^{a}	-4.63±0.28^{b}	48^{d}
Q2_5	-5.21±4.12^{d}	-7.75±3.25^{ab}	0.694±4.81	-15.64±7.6^{a}	-11.64±11.3^{b}	27^{e}
Q2_6	-7.16±0.58^{d}	-8.08±0.38^{a}	-3.125±1.04^{c}	-26.92±11.6^{a}	-17.33±0.67^{c}	10^{f}

Different letters indicate significant difference between samples at $p \leq 0.05$. (H: height, L: lenght, T: thickness, Lp: size of pores, V:volume, φ: porosity fraction).

The fractional deviations of the height (H), length (L) and thickness (T) showed values below 8.1% proving a high printing accuracy. Moreover, the majority of the results showed negative values indicating the shirking of the considered lengths in comparison to the virtual model. Also, the samples Q2 showed higher deviations than Q1 with values, as examples, of −7.16 ± 0.58% for H, and −8.08 ± 0.38% for L for sample Q2_6. This greater shirking resulted from the greater water evaporation during baking due to the higher surface of evaporation for Q2 samples. In addition, for intricate constructs (such as Q2_6) the slicing step of the virtual model has

created additional very small pores as a consequence of the inability of printing areas smaller than the nozzle size. Zhang et al. (2018), who tested the 3D printing of cereal-based snacks by using two infill patterns such as ‘concentric’ and ‘honeycomb’, showed that the moisture content lost during baking was higher for ‘honeycomb’ structure due to its larger surface area that improved dehydration process. Also, Severini et al. (2016) and Yang et al. (2018b) reported as the water removal during cooking is responsible of the reduction of the main sizes of 3D printed cereal-based samples.

The changes of Lp showed negative values between −13.24% and −26.92%, indicating that after baking the pores were smaller than those designed in the virtual model. In general, the food formulas deposited during 3D printing are soft materials and often they slightly enlarge under the weight of the others printed layers leading to shape deformation and the possibility of structure collapse with significant loss of printing fidelity. These effects on 3D printed structures has been widely observed for many food materials such as fruit and vegetable (Severini et al., 2018), hydrocolloids based edible ink (Kim et al., 2018), lemon juice gel (Yang et al., 2018a), mashed potatoes (Liu et al., 2018b), cereal-based dough (Yang et al., 2018c), fish surimi gel (Wang et al., 2018). In our case, the shell of the designed pores slightly crushed under the weight of the other layers of dough, leading to a reduction of their size. In addition, the crushing of dough was caused by the use of a layer height smaller than nozzle size leading to the enlargement of the dough and the size reduction of designed pores. Finally, in the initial phase of baking the reduction of the consistency of the dough improved the crushing of the deposited filaments increasing the effect on the pores size. However, the shape deformation caused during baking was smaller than the data reported in other papers (Pulatsu et al., 2020). It is important to point out that albeit these phenomena limit the printing accuracy, the fractional variation of pore size, between 13.24% and 26.92%, may be considered more than acceptable for the designed complex structures.

While the overall volume of printed snacks, V, was smaller than the virtual models according to the size reduction previously reported, the fractional deviation of the porosity fraction, Φ, exhibited values between 10% and 140% stating a very high increase of porosity.

This was due to the creation of new pores during the layer-by-layer deposition of the dough. Considering that 3D food printer movements are not optimized as for thermoplastic materials (Godoi et al., 2019), the lack of accurate equilibrium between the speed of printing movements and the extrusion rate is responsible of over- or under-depositions that generates many additional pores inside the printed structure (Fig. 3) (Derossi et al., 2020; Severini et al., 2016; Yang et al., 2018a). In addition,

during kneading the dough includes approximately the 10–20% of voids as a result of entrapping air (Severini et al., 2016), and during cooking the water evaporation makes the pre-existing pores bigger as well as it creates additional pores (Severini et al., 2016, 2018).

To better analyze the changes in porosity fraction during baking, Fig. 4 shows the relationship between the weight and the porosity fraction of samples after grouping them in raw and cooked samples. While for raw samples the linear relationship is very high, r2 = 0.99, proving that the weight of samples linearly decreased with the number of designed pores, after cooking the porosity fraction significantly increased between 35% and 60% and determination coefficient reduced to 0.855. This proves the creation and the further expansion of pores, not previously designed in the 3D virtual model, but generated during material deposition of dough and baking.

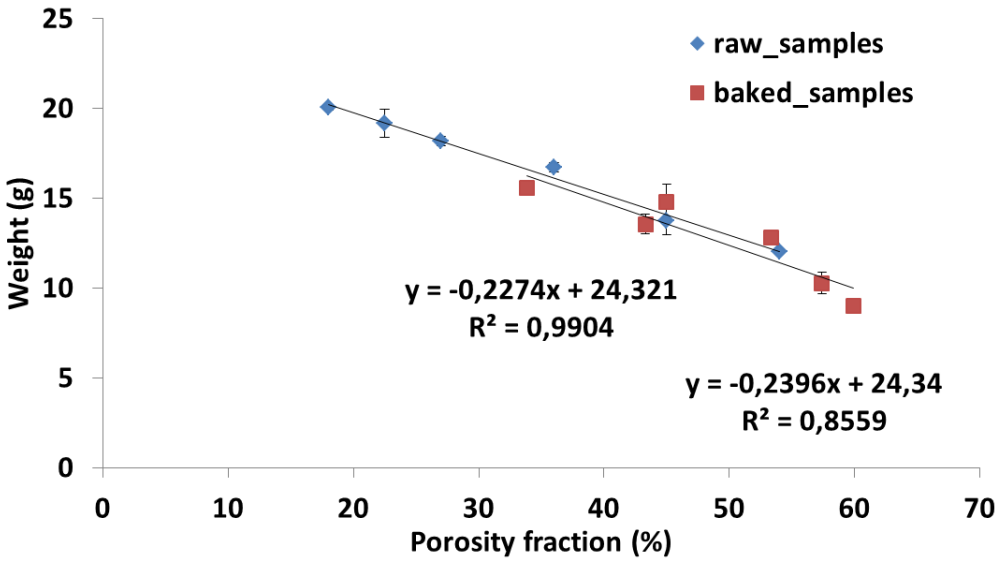

Fig. 4. Relationship between weight and porosity fraction of raw and cooked 3D printed samples.

With the aim to deeply analyze the discrepancies between printed snacks and virtual models, the changes in porosity fraction along the x direction are shown in Fig. 5. For each sample a total number of 700 slices were analyzed representing an overall length of ~2 cm. Along x direction, the red line – representing the virtual model – first crosses the fully dense section of the structure and, secondly, the porous section with porosity fraction of 37%. On the other hand, the 3D printed sample shows significant differences of porosity values although we can observe that the overall profile keep the same evolution of the virtual model along the x direction. Where the sample should exhibit a porosity fraction of zero, an average value of 29.30% was measured; while it increased at about 49% against the 37% of the virtual model where the

desired pores are positioned. These discrepancies are in accordance with the data of Fig. 4 where the creation of new pores during material deposition and baking were observed.

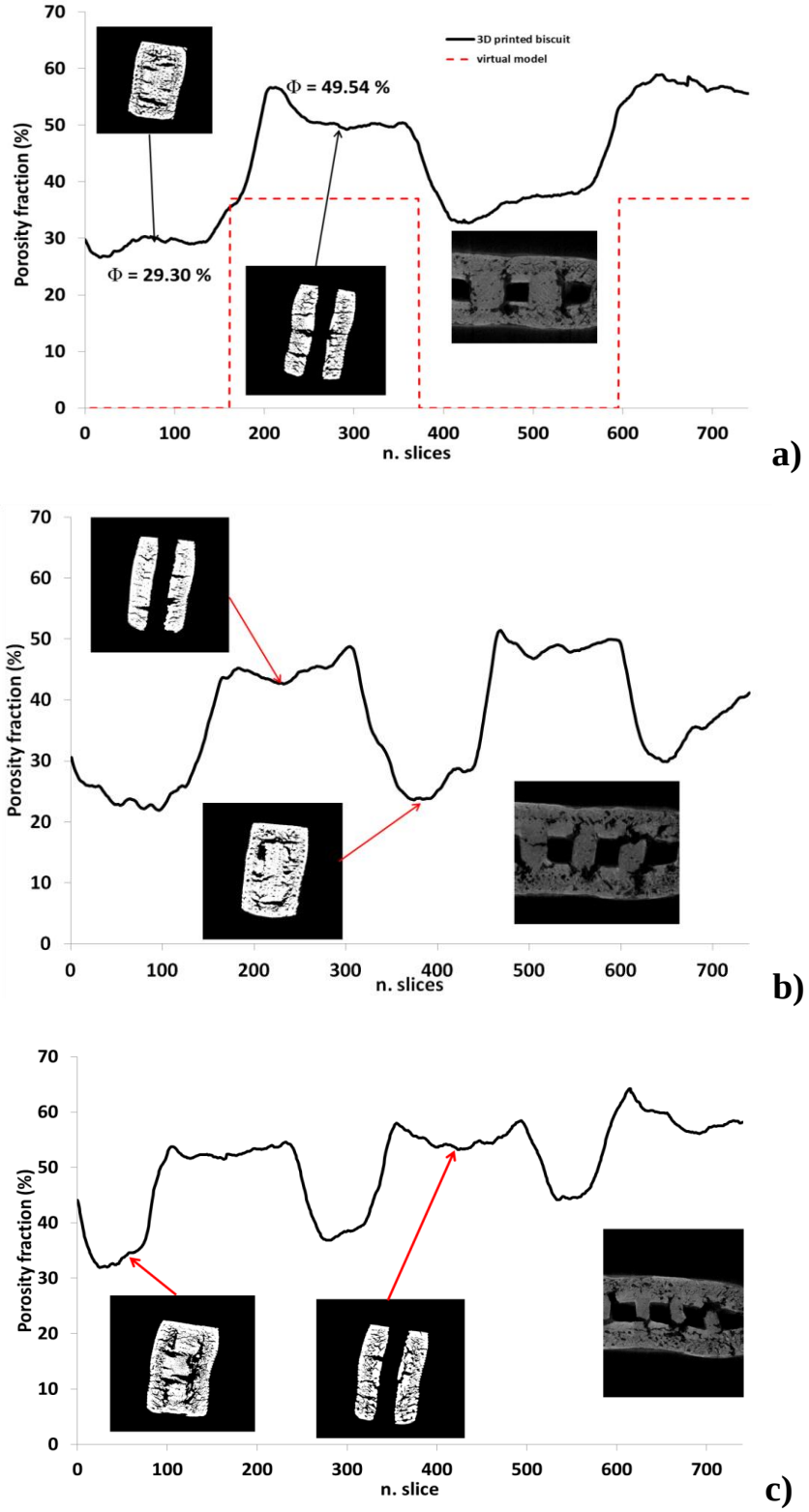

Fig. 5. Porosity profile of 2D cross-sectional images of 3D printed snack as a function of x direction. a) sample Q1_4; b) sample Q1_5; c) sample Q1_6.

Another interesting observation is the existence of some large fractures at the corners of the designed pores, as observed in the gray-scale image of Fig. 5a. One of these fractures – for the pore designed in the middle of the snack – lead to the maximum porosity fraction of ~58.9% at the slice n. 643. Similar deviations and porosity distribution have been observed for the other designed structures, as depicted from Fig. 5b and c for which several new voids and fractures are clearly observed for the baked snacks.

Fig. 6 reports the changes of porosity fraction along samples Q2_4, Q2_5 and Q2_6. For instance, sample Q2_4 was designed with a distance between two pores of 7 mm where the structure is completely dense, with porosity fraction of 0% (Table 2). The printed samples shows, after baking, a separation length between two voids of ~ 5 mm (between the slices n. 429 and n. 605); in addition, in this portion of the sample the measured porosity fraction was of 47.35% that is significantly higher than the designed fully dense material. Considering the sample Q2_6 the distance between two pores (designed of 2 mm) was of 1.3 mm (from slice n. 267 to n. 312). Again, in this case, the porosity fraction was higher than the designed structure with average value of 30.12%.

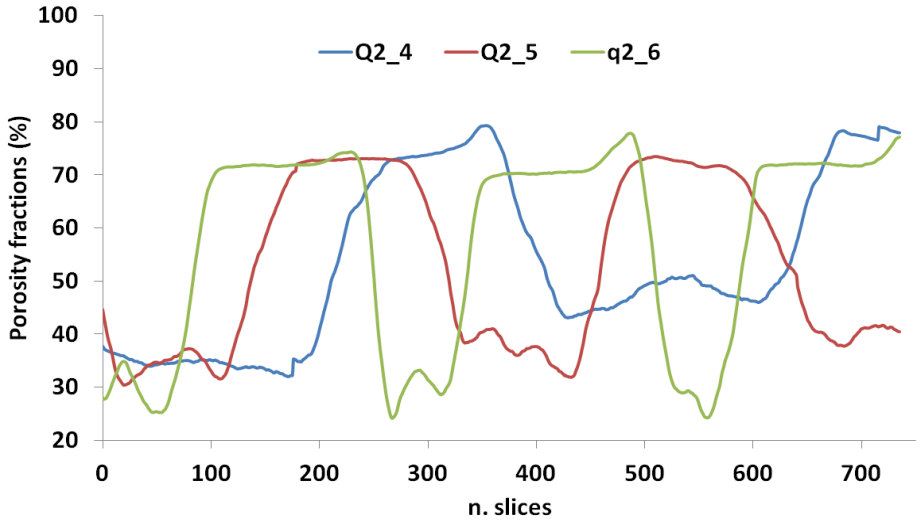

Fig. 6. Comparing porosity profile of 2D cross-sectional images of Q2_4, Q2_5, Q2_6 3D printed snack as a function of x direction.

Finally, Fig. 7 compares the porosity distributions for samples Q1_5 and Q2_5 along x direction. While the virtual models were designed with a maximum porosity fraction of 37% and 75% for Q1_5 and Q2_5, the printed samples displayed values of

45–53% and 70%, respectively. The reason of the increased porosity fraction of Q1_5 is definitely the result of the formation of new pores during printing and after baking, as previously discussed. In contrast, for sample Q2_5 the negligible differences between virtual model and printed structure could be the result of the reduction of pores size, as reported in Table 4, which induced the decrease of the porosity fraction and, on the other hand, the formation of new small pores inside the dense structure around the voids, which lead to an increase. These two opposite actions probably contributed similarly to the porosity fraction, with a counterbalance of their effects.

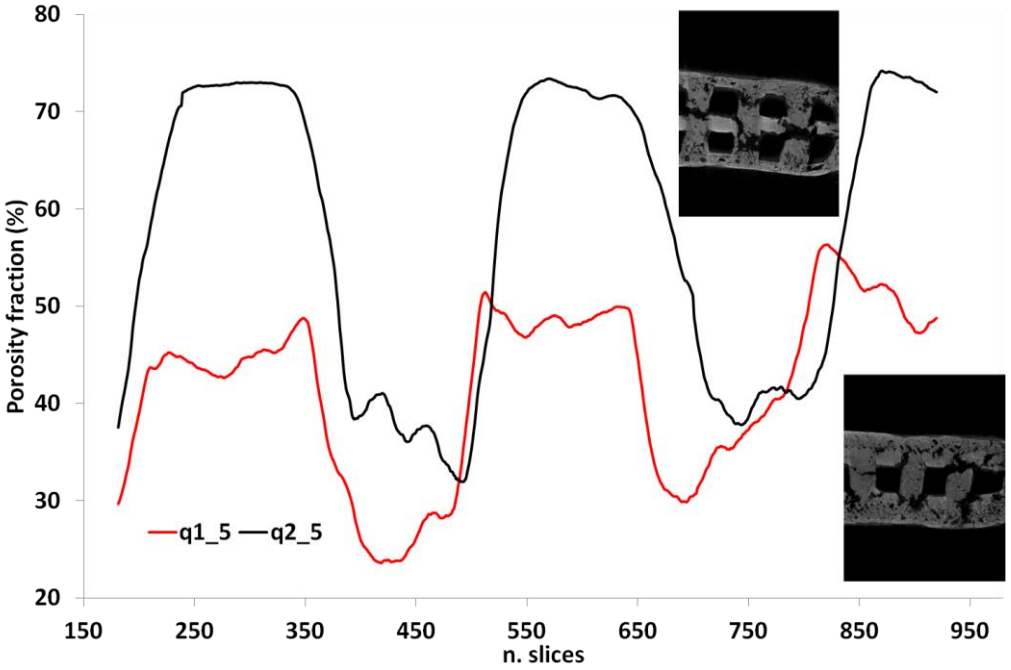

Fig. 7. Comparing porosity profile of 2D cross-sectional images of Q1_5 and Q2_5 3D printed snack.

3.3. Mechanical properties of the 3D printed snacks and their dependence with porosity and relative density

Firstly, Fig. 8 shows representatives stress-strain curves for the 3D printed samples. After a first region of linear elastic behaviour, a second 'plateau-plastic' region may be considered the result of brittle fractures of the cell walls and their broken fragment that pack together keeping the compression stress approximately in the 'plateau' during further deformation (Gibson and Ashby, 1997). A schematic representation of this behavior as explained for honeycomb structure by Gibson and Ashby (1982b) is reported in the inner part of Fig. 8. Furthermore, as expected the peak of the compression stress significantly reduced from Q1_4 to Q1_6. The hardness of all 3D printed samples (Fig. 9) shows a decreasing as function of the number of pores from 289 N for sample Q1_4 to 84 N for sample Q2_6. Also, the statistical analysis proves

that above differences are statistically significant ($p < 0.05$). This is in accordance with the relation between mechanical properties and the relative density of the printed snacks (Gibson et al., 1982a; Gibson and Ashby, 1982b, 1997; Liu and Scanlon, 2003; Robin et al., 2010; Vancauwenberghe et al., 2018). However, despite this overall behavior, the sample Q2_4 shows a greater hardness than the sample Q1_6 even though it was designed with a higher porosity. This can be explained by considering the effect of the position of the pores within the structure of 3D printed snacks on the mechanical properties. For the baked sample Q1_6 the distance between two pores was of ≈1.2 mm that is considerably smaller than that for sample Q2_4 with value of 5.15 mm. By analyzing these differences on the basic principle of cellular structure materials (Gibson and Ashby, 1997) this lead to a ratio t/l, where t is the thickness of the wall of material cell (i.e. half of the distance between two pores in x direction) and l is the length of the cell that is significantly greater for Q2_4 than for Q1_6 with values respectively of 0.087 and 0.159. The higher is the value of t/l the greater is the expected resistance to compression stress (Gibson and Ashby, 1982b). So, although the samples Q2_4 show a lower relative density, the greater thickness of the wall of pores led to the higher resistance to the compression stress.

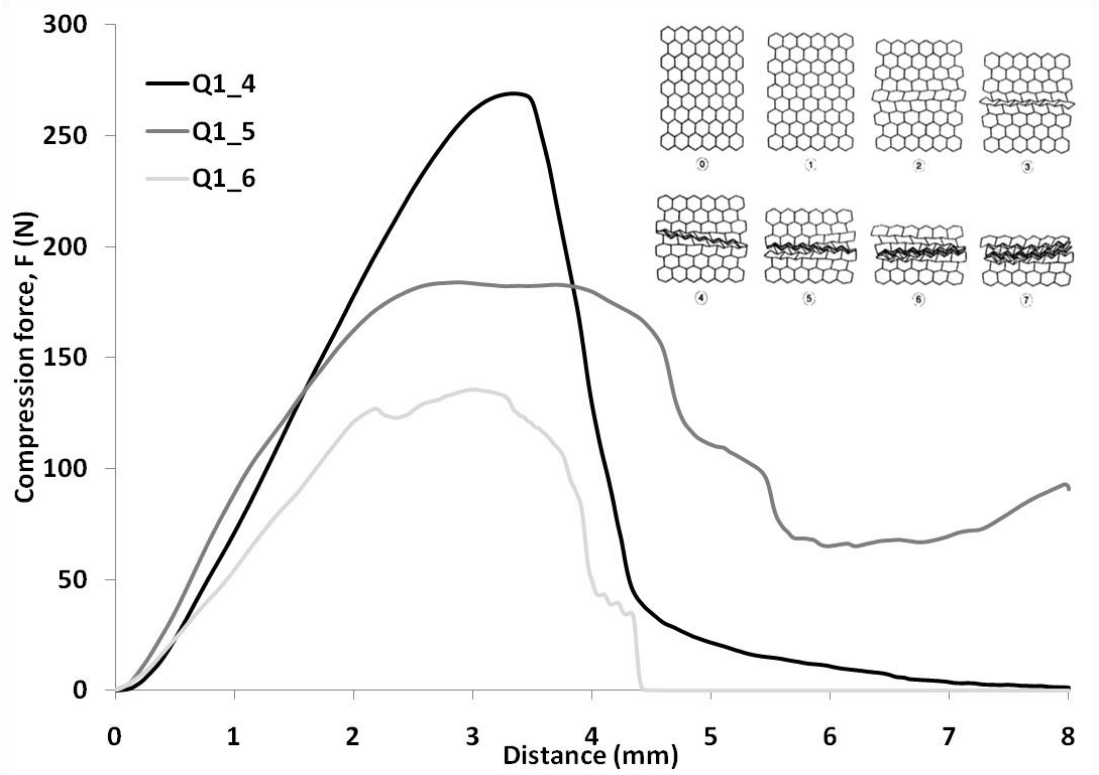

Fig. 8. Compressive stress-strain curve of some 3D printed snacks. Inner figure report a schematic representation of the crushing sequence of a honeycomb structure (from Gibson and Ashby, 1997).

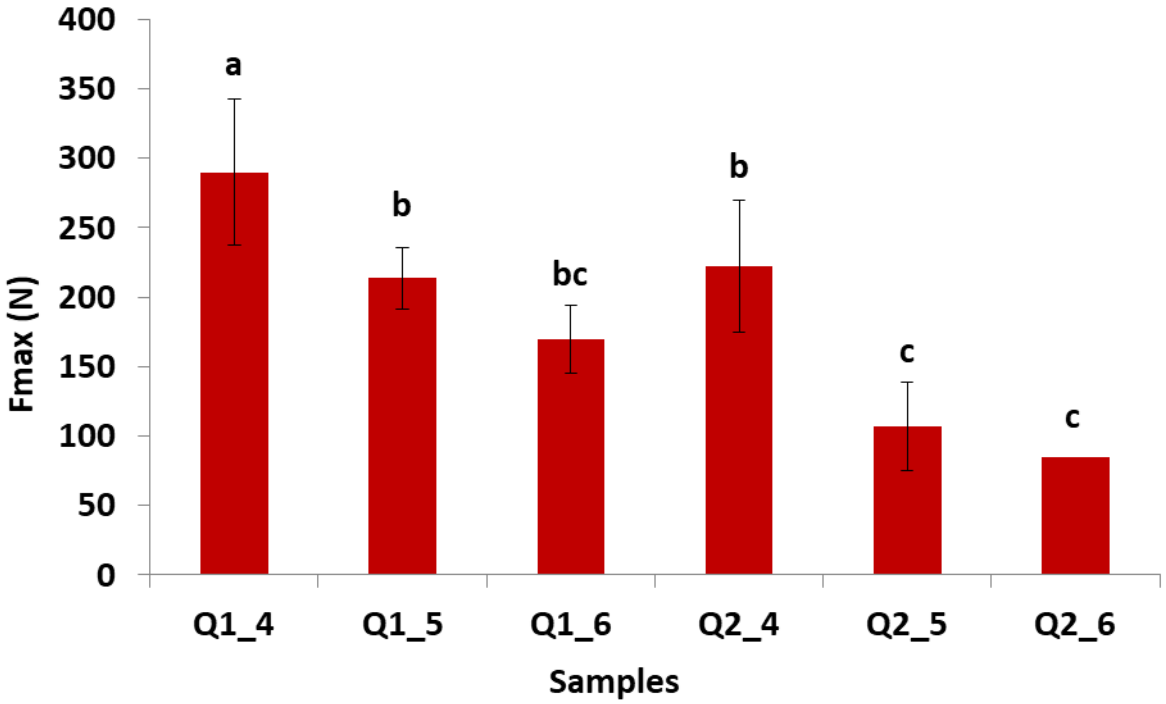

Fig. 9. Hardness of the 3D printed snack.

Finally, the dependence of the maximum force to break the 3D printed snacks to their relative density is reported in Fig. 10 where both the experimental data and the fit obtained by the analytical model of Eq. (2) are reported. As reported from Gibson and Ashby (1982b), in the case of 3D cellular materials (i.e. foam), n value is of 2 and 3 respectively for open cell and for closed cell. However, due to the complexity and the variability of the morphological properties of voids of food, and according to other authors (Scanlon and Zghal, 2001; Zghal et al., 2002), we fitted the experimental data by a more general modality leaving n value free to vary. The hardness of the 3D printed samples well agrees with the theoretical principle of the cellular materials properties as explained by Gibson et al. (1982a) and Gibson and Ashby (1982b, 1997). Indeed, apart some minor variability the value of Fmax significantly increased as a function of relative density of printed samples. The result of fitting showed the best correlation coefficient of 0.89 with n = 2.67 and C = 1211.12 ($p < 0.001$). Correlation coefficients overall ranged between 0.54 and 0.95 were found when Young's modulus or fracture/tensile stress were fitted as a function of relative density of wheat products or starch foams (Lourdin et al., 1995; Shogren et al., 1998; Scanlon and Zghal, 2001; Zghal et al., 2001, 2002) showing that our results are in accordance with other experiments. Also, Vancauwenberghe et al. (2018), who studied the effect of some morphological diversity of 3D printed edible gels, showed a good relationship between the porosity fractions of the gels and the Young's modulus. For what regards the value of C, recalling that it contains the maximum

compression force for the material solid, the estimated value intends that the cell wall of the printed structure could exhibit a maximum force of 1211.12 N. Although it is very hard to find literature data for a robust comparison we want to quote the paper of Scanlon and Zghal (2001) reporting data of critical stress parallel to long axis (compression) in bread samples with values in the range of 760–1350 N/m2 that are in the range of our findings.

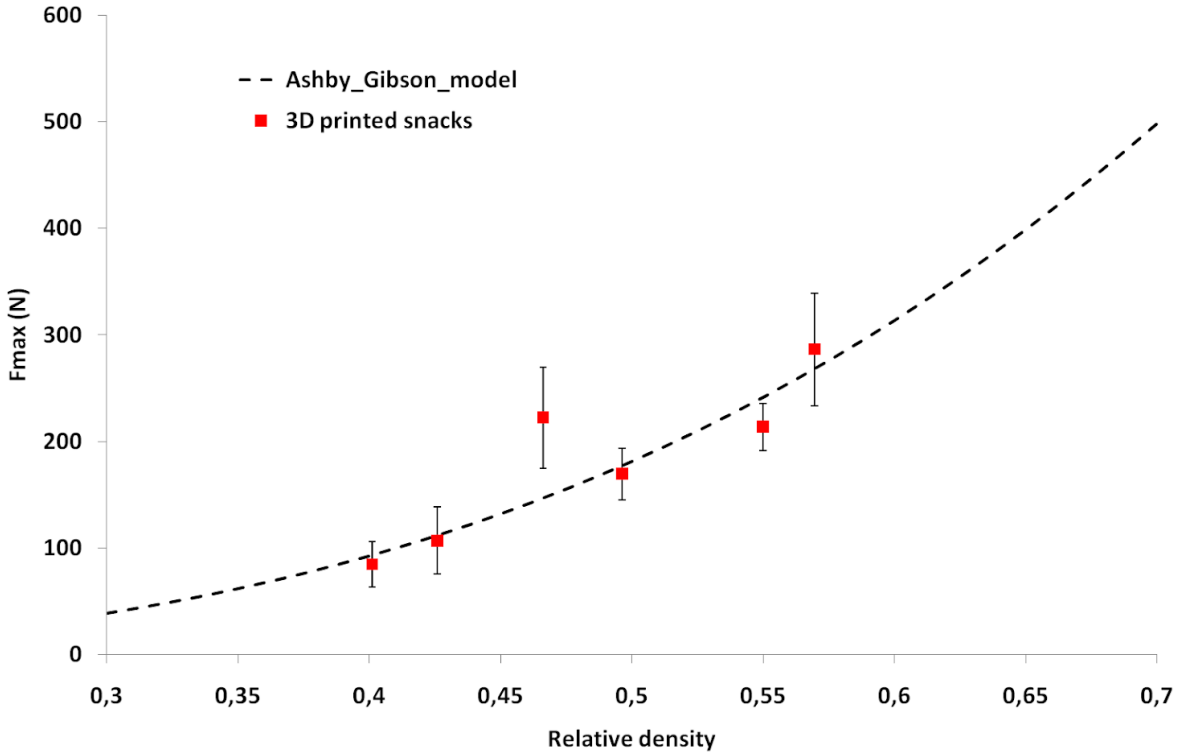

Fig. 10. Relationship between the maximum force to break the 3D printed samples and their relative density.

In addition, the expected results for open-cell foams is that mechanical properties are function of relative density with a power between 1 and 2 (Gibson and Ashby, 1997; Zghal et al., 2001, 2002); instead we found a higher value of 2.67. Cereal snacks contain many structural imperfections and inhomogeneities particularly after baking (as observed from microCT images) and such structures are not well represented by theoretical unit cell models of Gibson and Ashby (Silva & Gibson, 1997). All these defects would reduce the hardness of the samples and therefore the power of Eq. (2), n, for the curve of hardness, Fmax, versus relative density of the 3D printed snacks also would increase (Silva and Gibson, 1997; Zghal et al., 2002) more than the expected value of 2. However, the power n is greatly affected by several microstructure properties (Keetels et al., 1996) and some authors reported values lower than 2 for bread samples (Scanlon and Zghal, 2001; Zghal et al., 2001, 2002).

For instance, Zghal et al. (2002) suggested that the gas cells of bread crumb become stiffer with increasing proof time and decreasing relative density leading to an increase of Young's modulus and failure stress.

However, our results suggest that the hardness of the 3D printed snacks was mainly affected by the size and position of the pores designed in the 3D virtual model. This opens for the possibility of creating cereal-snacks with desired mechanical properties meeting specific consumer's requirements, as in the case of elderly people, or with the aim to get innovative texture perception. However, further experiments will have to confirm these data by using more complex structures and introducing the effect of baking on the morphological properties of internal voids and on mechanical properties of the end products.

4. Conclusion

This paper proved that 3D food printing may be used to generate controlled pores in cereal-based snacks with the aim to create novel food with different structural properties. Also, by modulating the number and the position of cubical-shaped pores it was possible to create 3D printed snacks with different hardness. The 3D CAD model was replicated with high fidelity showing 3D printed snacks without any macroscopic collapse or shape deformation also after baking process. However, the overall size of the printed snacks showed a reduction of 8% indicating that the printed samples were smaller than the virtual as results of dehydration during baking. Considering the designed pores, a fractional decrease of their length was observed from −13.56% and −26.92% that resulted by the crushing of the dough filament during printing and the partial collapse during baking. Contrarily, the overall porosity fraction of the 3D printed snacks significantly increases of 20–30% due to the creation of additional pores during dough deposition and baking.

The compression tests showed the reduction of the hardness of the 3D printed snacks as a function of their relative density proving that the printed snacks follow the theoretical principles of the cellular materials. Particularly, the hardness of the printed samples reduced from 289 N to 84 N for relative densities of 0.569 and 0.401, respectively.

Finally, by using the analytical model of Gibson and Ashby, it was possible to satisfactory fit experimental data of hardness ($r = 0.90$) but we revealed that the estimated constant n (the power of the Gibson and Ashby's model) was higher ($n = 2.62$) than the expected values of foams with open cell ($n = 2$). The heterogeneity of the microstructure of baked snacks is not well represented by the foam models of

Gibson and Ashby. Furthermore the creation of the new pores during dough deposition and baking reduced the hardness and therefore increases the power, n, of the model. Further research should address the modelling of the texture of printed food with more complex 3D structure modulating the number, shape and position of internal void. Moreover, the design should regard the creation of texture thought for specific requirements such as for elderly people that have mastication or swallowing problems as well as its relationship with masticatory muscle, jaw motion and satiety.

References

Aguilera, J.M. (2005). Why food microstructure?. *Journal of Food Engineering*, 67, 3-11. 10.1016/j.jfoodeng.2004.05.050

Cakir, E., Vinyard, J.C., Essick, G., Daubert, C.R., Drake, M., Foegeding, E.A. (2012). Interrelations among physical characteristics, sensory perception and oral processing of protein-based soft-solid structure. *Food Hydrocolloids*, *29*, 234-245. 10.1016/j.foodhyd.2012.02.006

Chen, L., & Opara, U.L. (2013). Approaches to analysis and modelling texture in fresh and processed foods – A review. *Journal of Food Engineering*, 119, 497-507. http://dx.doi.org/10.1016/j.jfoodeng.2013.06.028

Cohen, D.L., Lipton, J.I., Cutler, M., Coulter, D., Vesco, A., & Lipson, H. (2009). Hydrocolloid printing: a novel platform for customized food production. In: *Proceedings of the 21st Solid Freeform Fabrication Symposium*, Austin, USA.

Day, L., & Golding, M. (2016). Food structure, rheology and texture. In: L. Melton, F. Shahidi, P. Varelis (Eds.), *Encyclopedia of Food Chemistry* (pp.125-129). Academic Press, United States. http://dx.doi.org/10.1016/B978-0-08-100596-5.03412-0

Derossi A., Caporizzi, R., Azzollini, D., & Severini, C. (2018). Application of 3D printing for customized food. A case on the development of a fruit-based snack for children. *Journal of Food Engineering*, 220, 65-75. https://doi.org/10.1016/j.jfoodeng.2017.05.015

Derossi, A., Gerke, K.M., Karsanina, M.V., Nicolai, B., Verboven, P., & Severini, C. (2019a). Mimicking 3D food microstructure using limited statistical information from 2D cross-sectional image. *Journal of food engineering.* 241, 116-126. https://doi.org/10.1016/j.jfoodeng.2018.08.012

Derossi, A., Caporizzi, R., Ricci, I., & Severini, C., (2019b). Chapter 3 - Critical variables in 3D food printing. In: Godoi, F.C., Bhandari, B.R., Zhang, M. (Eds.), Fundamentals of 3D Printing and Applications, vol. 3. Elsevier Inc., ISBN 9780128145647, pp. 41–91. https://doi.org/10.1016/B978-0-12-814564-7.00003-1

Derossi, A., Paolillo, M., Caporizzi, R., Verboven, P., Vancauwenbergher, V., Nicolai, B., & Severini, C. (2019c). From plant tissue microstructure to new foods with novel sensory perception. An example of biomimetics of food mediated by 3D printing. In *8th International Symposium on 'Delivery of Functionality in Complex Food Systems'*. 7-10 July, Sheraton Porto hotel Conference Centre, Porto, Portugal.

Derossi, A., Paolillo, M., Caporizzi, R., & Severini, C. (2020). Extending the 3D food printing tests at high speed. Material deposition and effect of non-printing movements on the final quality of printed structures. *Journal of Food Engineering, 275*, 109865. https://doi.org/10.1016/j.jfoodeng.2019.109865

Devezeaux de Lavergne, M., van Delft, M., van de Velde, F., van Boekel, M.A.J.S., & Stieger, M. (2015). Dynamic texture perception and oral processing of semi-solid food gels: Part 1: Comparison between QDA, progressive profiling and TDS. *Food Hydrocolloids*, 43, 207-217. https://doi.org/10.1016/j.foodhyd.2014.05.020.

Dupont, D., Le Feunteun, S., Marze, S., & Souchon, I. (2018). Texture profile and correlation between sensory and instrumental analysis on extruded snacks. *Journal of Food Engineering*, 121, 9-14. http://dx.doi.org/10.1016/j.jfoodeng.2013.08.007

Endo, H., Ino, S., & Fujisaki, W. (2017). Texture-dependent effects of pseudo-chewing sound on perceived food texture and evoked feelings in response to nursing care foods. *Appetite*, 116, 493-501. https://doi.org/10.1016/j.appet.2017.05.051.

Feng, C., Zhang, M., Bhandari, B., & Ye, Y. (2020). Use of potato processing by-product: effects on the 3D printing characteristics of the yam and the texture of air-fried yam snacks. *LWT – Food Science and Technology, 125*, 109265. https://doi.org/10.1016/j.lwt.2020.109265

Foegeding, E.A., Stieger, M., & van de Velde, F. (2017). Moving from molecules, to structure, to texture perception. *Food Hydrocolloids*, 68, 31-42. http://dx.doi.org/10.1016/j.foodhyd.2016.11.009

Gao, J., Ong, J.J., Henry, J., & Zhou, W. (2017). Physical breakdown of bread and its impact on texture perception: A dynamic perspective. *Food Quality and Preference, 60*, 96-104. https://doi.org/10.1016/j.foodqual.2017.03.014

Gibson L.J., Ashby, F.R.S., Schajer, G.S., & Robertson, C.I. (1982a). The mechanics of two-dimensional cellular materials. *Proceedings of the Royal Society A, 382, 25-42*

Gibson, L.J., Ashby, M, F. (1982b). The mechanics of three-dimensional cellular materials. *Proceedings of the Royal Society A, 382, 45-59* https://doi.org/10.1098/rspa.1982.0088

Gibson, L.J., & Ashby, M.F. (1997). Cellular Solids: Structure and Properties. Cambridge University Press. https://doi.org/10.1017/CBO9781139878326

Godoi, F. C., Bhandari, B. R., Prakash, S., & Zhang, M. (2019). *Fundamentals of 3D Food Printing and Applications. (*1st ed.) Academic Press, USA

Godoi, F. C., Prakash, S., & Bhandari, B. R. (2016). 3D printing technologies applied for food design: Status and prospects. *Journal of Food Engineering, 179*, 44-54. 10.1016/j.jfoodeng.2016.01.025

Grood, J. P. W., & Grood, P. J. (2011). Method and device for dispensing a liquid. In: Google patents.

Hertafeld, E., Zhang, C., Jin, Z., Jakub, A., Russell, K., Lakehal, Y., Andreyeva, K., Bangalore, S.N., Mezquita, J., Blutinger, J., & Lipson, H. (2018). Multi-material three-dimensional food printing with simultaneous infrared cooking. *3D Printing and Additive Manufacturing*, 6(1), 68-74. https://doi.org/10.1089/3dp.2018.0042

Huang, M., Zang, M., Bhandari, B.. (2019). Assessing the 3D printing precision and texture properties of brown rice induced by infill levels and printing variables. *Food and Bioprocess Technology*, 12, 1185–1196. https://doi.org/10.1007/s11947-019-02287-x

Hutchings, J.B., & Lillford, P.J. (1988). The perception of food texture – the philosophy of the breakdown path. *Journal of Texture Studies*, 19, 103-115

Izdebska, J., & Tryznowska, Z. Z. (2016). 3D food printing e facts and future. *Agro FOOD Industry Hi Tech*, 27, 33-36.

Keetels, C. J. A. M., van Vliet, T., Walstra, P. (1996). Relationship between the sponge structure of starch bread and its mechanical properties. *Journal of Cereal Science*, *24*, 17-31 https://doi.org/10.1006/jcrs.1996.0034.

Kim, H. W., Bae, H., & Park, H. J. (2018). Reprint of: Classification of the printability of selected food for 3D printing: Development of an assessment method

using hydrocolloids as reference material. *Journal of Food Engineering*, *220*, 28-37. https://doi.org/10.1016/j.jfoodeng.2017.10.023

Kim, H. W., Lee, I. J., Park, S. M., Lee, J. H., Nguyen, M., & Park, H. J. (2019). Effect of hydrocolloid addition on dimensional stability in post-processing of 3D printable cookie dough. *LWT, 101,* 69-75. https://doi.org/10.1016/j.lwt.2018.11.019

Kohyama, K. (2015). Oral sensing of food properties. *Journal of Texture Studies*, *46*, 138-151. https://doi.org/10.1111/jtxs.12099

Lara, E., Cortes, P., Briones, C., & Perez, M. (2012). Structural and physical modifications of corn biscuits during baking process. *LWT - Food Science and Technology*, 44, 622-630

Laureati, M., Sandvik, P., Almli, V. L., Sandell, M., Zeinstra, G.G., Methven, L., Wallner, M., Jilan, H., Alfaro, B., & Proserpio C. (2020). Individual differences in texture preferences among European children: Development and validation of the Child Food Texture Preference Questionnaire (CFTPQ). *Food Quality and Preference, 80,* 103828. doi: https://doi.org/10.1016/j.foodqual.2019.103828

Le Tohic, C., O'Sullivan, J. J., Drapala, K. P., Chartrin, V., Chan, T., Morrison, A. P., Kerry, J.P., & Kelly, A. L. (2018). Effect of 3D printing on the structure and textural properties of processed cheese. *Journal of Food Engineering*, 220, 56-64. https://doi.org/10.1016/j.jfoodeng.2017.02.003

Le-Bail, A., Boumali, K., Jury, V., Ben-Aissa, F., & Zuniga, R. (2009). Impact of the baking kinetics on staling rate and mechanical properties of bread crumb and degassed bread crumb. *Journal of Cereal Science*, 50 (2), 235–240. https://doi.org/10.1016/j.jcs.2009.05.008

Lille M., Nurmela, A., Nordlund, E., Metsa-Kortelain S., & Sozer, N. (2018). Applicability of protein and fiber-rich food materials in extrusion-based 3D printing. *Journal of Food Engineering*, 220, 20-27. http://dx.doi.10.1016/j.jfoodeng.2017.04.034.

Lipton, J. I., Cutler, M., Nigl, F., Cohen, D., & Lipson, H. (2015). Additive manufacturing for the food industry. *Trends in Food Science and Technology*, 43(1), 114-123. 10.1016/j.tifs.2015.02.004

Liu, Z., Bhandari, B., Prakash, S., & Zhang, M. (2018a). Creation of internal structure of mashed potato construct by 3D printing and its textural properties. *Food Research International*, 111, 534-543. https://doi.org/10.1016/j.foodres.2018.05.075

Liu, Z., Zhang, M., Bhandari, B., & Yang, C. (2018b). Impact of rheological properties of mashed potatoes on 3D printing. *Journal of Food Engineering,* 220, 76-82. https://doi.org/10.1016/j.jfoodeng.2017.04.017.

Liu, Z., & Scanlon, M.G. (2003). Predicting mechanical properties of bread crumb *Transactions of Institute of Chemical Engineering*, 81C, 224-238

Lourdin, D., Della Valle, G. & Colonna, P. (1995). Influence of amylose content on starch films and foams. *Carbohydrate Polymers*, 27, 261-270 https://doi.org/10.1016/0144-8617(95)00071-2.

Mantihal, S., Prakash, S., Godoi, F., & Bhandari, B. (2017). Optimization of chocolate 3D printing by correlating thermal and flow properties with 3D structure modelling. *Innovative Food Science and Emerging Technologies*, *44*, 21-29. 10.1016/j.ifset.2017.09.012.

McClements, D.J., & Xiao, H. (2017). Designing food structure and composition to enhance nutraceutical bioactivity to support cancer inhibition. *Seminar in Cancer Biology*, 46, 215-226. 10.1016/j.semcancer.2017.06.003

Park, S.M., Kim, H.W., & Park, H.J. (2020). Callus-based 3D printing for food exemplification with carrot tissues and its potential for innovative food production. *Journal of Food Engineering,271,* 109781. https://doi.org/10.1016/j.jfoodeng.2019.109781.

Pascua, Y., Koc, H., Foegeding, E.A. (2013). Food Structure: roles of mechanical properties and oral processing in determining sensory texture of soft materials. *Current opinion in colloid & interface science, 18*(4), 324-333. 10.1016/j.cocis.2013.03.009.

Pasqualone, A; Laddomada, B; Spina, A., Todaro, A., Guzmàne, C.; Summo, C; Mita, G. & Giannone, V. (2018). Almond by-products: Extraction and characterization of phenolic compounds and evaluation of their potential use in composite dough with wheat flour. *LWT - Food Science and Technology*, 89, 299-306. http://dx.doi.org/10.1016/j.lwt.2017.10.066.

Paula, A.M., & Conti-Silva, A.C. (2014). Texture profile and correlation between sensory and instrumental analysis on extruded snacks. *Journal of Food Engineering*, 121, 9-14. http://dx.doi.org/10.1016/j.jfoodeng.2013.08.007

PERFORMANCE Project. Personalized Food using Rapind Manufacturing for the Nutrition of elderly consumers. www.performance-fp7.eu. Accessed: 17 December 2019.

Pulatsu, E.T., Su, J.W., Lin, J., & Lin, M. (2020). Factors affecting 3D printing and post-processing capacity of cookie dough. *Innovative Food Science & Emerging Technologies, 61,* 102316. 10.1016/j.ifset.2020.102316

Robin, F., Engmann, J., Pineau, N., Chanvrier, H., Bovet, N., & Della Valle, G. (2010). Extrusion, structure and mechanical properties of complex starchy foams. *Journal of Food Engineering,* 98(1), 19-27. https://doi.org/10.1016/j.jfoodeng.2009.11.016.

Santagiuliana, M., Christaki, M., Piqueras-Fiszman, B., Scholten, E. & Stieger, M. (2018). Effect of mechanical contrast on sensory perception of heterogeneous liquid and semi-solid foods. *Food Hydrocolloids*, 83, 202-212. https://doi.org/10.1016/j.foodhyd.2018.04.046.

Scanlon, M.G. & Zghal, M. C. (2001). Bread properties and crumb structure. *Food Research International*, 34, 841-864 https://doi.org/10.1016/S0963-9969(01)00109-0.

Severini, C., Derossi, A., & Azzollini, D. (2016). Variables affecting the printability of foods: Preliminary tests on cereal-based products. *Innovative Food Science & Emerging Technologies, 38,* 281-291. https://doi.org/10.1016/j.ifset.2016.10.001

Severini, C., Azzollini, D., Albenzio, M., & Derossi, A. (2018). On printability, quality and nutritional properties of 3D printed cereal based snacks enriched with edible insects. *Food research international, 106,* 666-676. 10.1016/j.foodres.2018.01.034.

Severini, C., Caporizzi, R., Fiore, A.G., Ricci, I., Oral, O.M., & Derossi, A. (2020). Reuse of spent espresso coffee as sustainable source of fibre and antioxidants. A map on functional, microstructure and sensory effects of novel enriched muffins, *LWT - Food Science and Technology, 119,* 108877. 10.1016/j.lwt.2019.108877

Shogren, R. L., Laeton, J. W., Doane, W. M. & Tiefenbacher, K. F. (1998). Structure and morphology of baked starch foams. *Polymer,* 39, 6649-6655 https://doi.org/10.1016/S0032-3861(97)10303-2.

Silva, L. J. & Gibson, L. J. (1997). The effect of non-periodic microstructure and defects on the compressive strength of two-dimensional cellular solids. *International*

Journal of Mechanical Sciences, 39, 5, 549-563 https://doi.org/10.1016/S0020-7403(96)00065-3.

Singh, A.P., & and Bhattacharya, M. (2005). Development of dynamic modulus and cell opening of dough during baking. *Journal of Texture Studies,* 36, 44–67.

Sudha, M.L.; Srivastava, A.K.; Vetrimani, R & Leelavathi, K. (2007). Fat replacement in soft dough biscuits: Its implications on dough rheology and biscuit quality. *Journal of Food Engineering*, 80 (3), 922-930. https://doi.org/10.1016/j.jfoodeng.2006.08.006.

Sun, J., Zhou, W., Yn, L., Huang, D. & Lin, L. (2018). Extrusion-based food printing for digitalized food design and nutrition control. *Journal of Food Engineering,* 220, 1-11. https://doi.org/10.1016/j.jfoodeng.2017.02.028.

Szczesniak, A. S. (2002). Texture is a sensory property. *Food Quality and Preference, 13,* 215–225. https://doi.org/10.1016/S0950-3293(01)00039-8

Torquato, S. (2002). Random Heterogeneous materials: Microstructure and Macroscopic properties. Springer-Verlang publishing

Tyagi, S.K., Manikantan, M.R., Oberoi, H.S., & Kaur, G. (2007). Effect of mustard flour incorporation on nutritional, textural and organoleptic characteristics of biscuits. *Journal of Food Engineering, 80,* 1043–1050. 10.1016/j.jfoodeng.2006.08.016

Vancauwenberghe, V., Delele, M.A., Vanbiervliet, J., Aregawi, W., Verboven, P., Lammertyn, J., & Nicolai, B. (2018). Model-based design and validation of food texture of 3D printed pectin-based food simulants. *Journal of Food Engineering*, 231, 72-82. https://doi.org. 10.1016/j.foodeng.2018.03.010

Vancauwenberghe, V., Mbong, V.B.M, Vanstreels, E., Verboven, P., Lammertyn, J., & Nicolai, B. (2019). 3D printing of plant tissue for innovative food manufacturing: Encapsulation of alive plant cells into pectin based bio-ink. *Journal of Food Engineering, 263,* 454-464. https://doi.org/10.1016/j.jfoodeng.2017.12.003

Van Hecke, E., Allaf, K. & Bouvier, J. M. (1995). Texture and structure of crispy-puffed food products I: mechanical properties in bending. Journal of Texture Studies, 26, 11-25 https://doi.org/10.1111/j.1745-4603.1995.tb00781.x.

Xu, Y., Tao, Y. & Shivkumar, S. (2016). Effect of freeze-thaw soft and firm tofu. Journal of Food Engineering, 190, 116-122 https://doi.org/10.1016/j.jfoodeng.2016.06.022 .

Yang, F., Zhang, M., Bhandari, B., & Liu, Y. (2018a). Investigation on lemon juice gel as food material for 3D printing and optimization of printing parameters. *LWT-Food Science and Technology*, 87, 67-76. https://doi.org/10.1016/j.lwt.2017.08.054

Yang, F., Zhang, M., Prakash, S., & Liu, Y. (2018b). Physical properties of 3D printed baking dough as affected by different compositions. *Innovative Food Science & Emerging Technologies*, 49, 202-210. https://doi.org/10.1016/j.ifset.2018.01.001

Yang, F., Zhang, M., Fang, Z., & Liu, Y. (2018c). Impact of processing parameters and post-treatment on the shape accuracy of 3D-printed baking dough. *International Journal of Food Science and Technology*, 54, 68-74. doi: 10.1111/ijfs.13904

Yolacaner, E.T., Sumnu, G., & Sahin, S. (2017). Microwave-assistedbaking. In: M. Regier, K. Knoerzer, H. Schubert (Eds.), *The Microwave Processing of Foods*. (pp. 117–141). Woodheadnpublishing. http://dx.doi.org/10.1016/B978-0-08-100528-6.00006-1

Wang, L., Zhang, M., Bhandari, B., & Yang, C. (2018). Investigation on fish surimi gel as promising food material for 3D printing. *Journal of Food Engineering*, 220, 101-108. https://doi.org/10.1016/j.jfoodeng.2017.02.029.

Zghal, M. C., Scanlon, M. G., & Sapirstein, H. D. (2001). Effects of flour strength. Baking absorption and processing conditions on the structure and mechanical properties of bread crumb. *Cereal Chemistry*, 78, 1-7 https://doi.org/10.1094/CCHEM.2001.78.1.1.

Zghal, M. C., Scanlon, M. G. & Sapirstein, H. D. (2002). Cellular structure of bread crumb and its influence on mechanical properties. Journal of Cereal Science, 36, 167-176 https://doi.org/10.1006/jcrs.2001.0445.

CHAPTER 6 Extending 3D food printing application: apple tissue microstructure as a digital model to create innovative cereal-based snacks

Antonio Derossi, Maddalena Paolillo, Pieter Verboven, Bart Nicolai, Carla Severini

Journal of Food Engineering

Journal of Food Engineering, 2022, 316: 110845

Abstract

Printing food consists of translating any idea of shape, dimension and internal architecture into a digital model, which may be replicated to get tangible food products. An intriguing and novel approach to use 3D printing – already used in the medical fields – is the mimicking of morphological properties of biological tissues aiming to replicate their unique functionalities. For the first time, we explored this approach and by utilizing the main morphological information of apple tissue contained in the microtomographic images we have generated innovative 3D printed snacks inspired by the plant tissues. While the morphologies of the printed sample satisfactorily matched the virtual model, the porosity fraction significantly changes from ~15% of the apple tissue to 14.4%-18.2% for printed dough and to 41.93%-45.90% for the baked snacks. Hardness increased from 0.69 N to 11.25 as a function of the number of layers while the Young's modulus did not change significantly from 20.73 to 31.84 MPa for 2 to 6 layers. Our results proved the capability of 3D printing to reproduce the salient features of apple tissue microstructure; also, after defining the main mechanical properties of the reference materials, we modelled the texture properties of 3D printed samples with sufficient agreement with the estimated and experimental data.

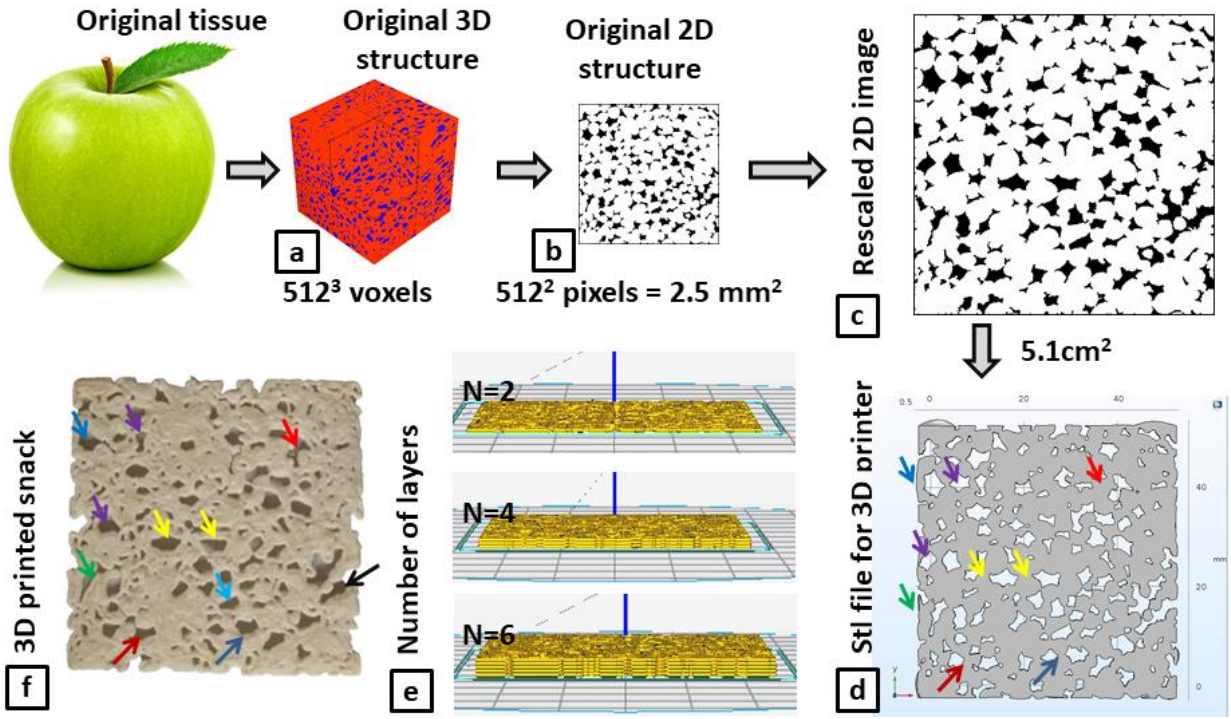

Figure 1 – Workflow employed for the printing of innovative cereal-snacks inspired by apple tissue structure. a) Original 3D structure is the X-ray CT reconstruction of apple tissue; b) Original 2D structure represents a single slice of the 3D reconstruction; c) rescaled 2D image; d) STL file is obtained by uploading the rescaled image on COMSOL; e) the STL file was stacked for 2, 4 and 6 times to get the model to be printed; f) example of 3D printed snack.

1.Introduction

Printing food consists of translating any idea of shape, dimension and internal architecture into a digital model, which may be replicated to get tangible food products. An intriguing and novel approach to use 3D printing – already used in the medical fields – is the mimicking of morphological properties of biological tissues aiming to replicate their unique functionalities. For the first time, we explored this approach and by utilizing the main morphological information of apple tissue contained in the microtomographic images we have generated innovative 3D printed snacks inspired by the plant tissues. While the morphologies of the printed sample satisfactorily matched the virtual model, the porosity fraction significantly changes from ~15% of the apple tissue to 14.4%-18.2% for printed dough and to 41.93%-45.90% for the baked snacks. Hardness increased from 0.69 N to 11.25 as a function of the number of layers while the Young's modulus did not change significantly from 20.73 to 31.84 MPa for 2 to 6 layers. Our results proved the capability of 3D printing to reproduce the salient features of apple tissue microstructure; also, after defining the

main mechanical properties of the reference materials, we modelled the texture properties of 3D printed samples with sufficient agreement with the estimated and experimental data. Our results proved the capability of 3D printing to reproduce the salient features of apple tissue microstructure; also, after defining the main mechanical properties of the reference materials, we modelled the texture properties of 3D printed samples with sufficient agreement with the estimated and experimental data.

2. Material and method

2.1 Dough preparation

Wheat flour (Granoro, Italy) (29.5 g/100g w.b), rice flour (Selezione Casillo, Italy) (29.5g/100g w.b.), olive oil (Desantis, Italy) (6g/100g w.b.), sodium chloride (1g/100g w.b.) and water (Lilia, Italy) (34g/100g w.b.) were purchased locally. The ingredients with 30g/100g of water were mixed for 150 s in a planetary kneader (model Cooking Chef, Kenwood Ltd. UK) at speed level of 1 (22 rpm), then, the other 4g/100g of water were added and mixed for 30 s. After this, the dough rested at room temperature for 30 min before printing experiments. The food formula was chosen on the basis of some previous preliminary experiments with some modifications performed to optimize its printability such as flowability, stability and adhesivity between different layers (Severini et al., 2018; Derossi et al., 2020).

2.2 Image acquisition and structure

X-ray microtomographic images of the parenchyma tissues of fleshy part of apple (cultivar Braeburn) were obtained as reported by Herremans et al. (2015) with cross sectional slices taken perpendicular to the fruit radius with an image pixel resolution of 4.9 μm.

Then, the X-ray images were cropped by using a squared region of interest of 512 pixels representing a surface fraction higher than 70% of total apple slice. A single 2D image was saved as Standard Tessellation Language file format (.STL) file and used as reference CAD model for printing experiments (Severini et al., 2018).

2.3 3D CAD model, slicing and printing experiments.

The .STL file was loaded into software CURA ver. 3.3.1 (Ultimaker) to generate the CAD models. Specifically, the .STL file was first rescaled at 5.1 cm in X and Y plane to allow the printing process to replicate with accuracy the main morphological feature of the apple tissues. Indeed, the current limits of the 3DFP technology do not allow to deposit food materials using a very thin nozzle size. Rather the main aim

here is to show that complex irregular deposition patterns, rather than simple regular ones, can be generated with 3DFP. The rescaled image was replicated for 2, 4 and 6-times in Z plane to get digital models of two (2A), four (4A) and six layers (6A). The following printing variables were defined: nozzle size = 0.64 mm; layer height = 0.60 mm, infill = 100%; infill pattern: concentric; print speed = 10 mm/s; flow = 95%. The 3D printing process has been performed by a Delta Wasp 3D printer mod. 2040 (Wasp, Italy). Then, the samples were baked individually in an ordinary oven (GFerrari, mod. G10075) at 100°C and for different times - 6, 8 and 11 minutes respectively for 2A, 4A and 6A samples - with the aim to obtain the same moisture content, xw, of 8.2 ± 1.1 g H2O/g w.b. Also, a low temperature of 100°C – rather than the 150-180°C - avoided the collapse and other structural problems during baking. Figure 1 shows a schematic representation of the workflow used during the experiments.

2.4 Physical and morphological analyses

Moisture content was determined in triplicate according to the gravimetric method as described in AOAC–925.10 (AOAC, 2005). The length, width and the height of 3D printed samples were measured in triplicate by using a manual calliper. Also, the photographic images of the samples were acquired by using a camera Canon, EOS 1200D. After the images were binarized, the most important morphological metrics and the porosity fraction were computed by using Image J (ver 1.53e).

2.6 Analysis of textural properties

The maximum peak of force of the samples was obtained according to the method of 3 points bend test according by Mudgil et al. (2017) with some modifications: pre-test of 1.5 mm/s, test speed of 2.0 mm/s, post-test of 10.0 mm/s, distance between the supports of 5.0 mm, trigger force of 5g. A TA-XT plus texture analyser (Stable Microsystems, Surrey, UK) equipped with a 50 N load cell was used for analysis. Young modulus E (N/m2), fracture stress σ (N/m2) and fracture strain ε were calculated according to Baltsavias et al. (1997).

2.7 Microstructural analysis

To acquire microstructural information, each sample was divided into 4 squared sub-samples by cutting in half on the x and y plane. Then two sub-samples were scanned by SkyScan 1174 micro-CT scanner (Brüker, Kontich, Belgium). Cross-sectional microtomographic images of 517(x) x 517(y) pixels with a resolution of 28.5 μm were obtained by an ROI of 1600 x 1600 pixels.

2.8 Finite element model

The CAD model was introduced in Comsol Multiphysics ver 5.3a (USA) in order to simulate the three points bend test previously reported; the surface of the sample was set as displacement boundary while the two fixed points where the sample located for the test were taken as fixed boundary. Also, the model consisted of three cylinders of which one was located at the middle of the surface where it was displaced downward at a speed of 2 mm/s; the other two are those on which the sample was located and they were set as fixed boundaries. A Young's modulus of 311 Mpa and a Poisson ratio of 0.50 were used as properties of the reference materials; specifically, the Young's modulus was computed by performing specific experiments later discussed in detail. The model was discretized on a total of more than 150,000 elements. A time dependent study was conducted for a total of 3 s with a step of 0.1s. The total displacement (m) and the principal stress (N/m2) were simulated. Then Young's Modulus was computed analytically as described above.

3. Results and discussion

The overall appearance of the baked samples shows that 3D printing satisfactorily captured the main morphological characteristics of the apple tissue structures, particularly for what regards the location, the dimension and the shape of the main pores, as indicated by the coloured rows in Figure 1. While the length, L, of the raw samples satisfactory matched the virtual model and the baked snacks showed minor modifications due to the dehydration effect, the height of the raw snacks was significantly higher, especially for the raw printed snacks (Table 1). This was expected due to the mechanical behaviour of the dough (mainly elastic properties) during the material deposition and, in addition, by the shape changes during the baking. Enlargements and shrinkage of the cereal-based 3D printed filaments are widely reported in many scientific papers (Severini et al., 2016; Arepally et al., 2020). Contrarily, the height of the baked samples reduced due to the shrinkage during dehydration in the oven (Derossi et al., 2020). The porosity fractions of the 3D printed samples exhibited high variations from the digital model, especially after baking, when the average values increased in the range 41.93% - 45.90% while the virtual models and the raw printed samples exhibited value of 15.1% and between 14.4% and 18.2%, respectively, which are in good agreement with the overall porosity of apple tissue (Herremans et al. 2014; Herremans et al., 2015; Nugraha et al. 2019). Similarly, a high difference between designed porosity and real porosity was observed also by Piovesan et al. (2020) who explored the capability to tune mechanical properties of biscuit by controlling the infill of 3D printed structure.

These first results support the idea of using 3D printing to create innovative food with unparalleled structures inspired by biological tissues. The reason why we observed a slight increase of porosity fraction for the raw 3D printed, is the very complex printing pathway consisting of both printing and non-printing movements (see supplementary material, M1) that may contribute to the creation of additional pores during deposition of the dough (Derossi et al., 2020). In addition, the increase of the pore sizes during baking was the main reason for the strong increase of porosity for the baked samples.

Regarding the texture of the baked samples, we observed the increase in the hardness from 0.69 N to 11.25 N ($p<0.05$) indicating highly brittle snacks. On the other hand, Young's modulus did not change significantly with values of 20.73±7.3 MPa, 18.95±9.6 MPa and 31.84±10.8 MPa ($p>0.05$) for 2A, 4A and 6A, respectively. This is also consistent with the data of the porosity fraction of baked samples as computed from X-ray microtomographic images, which ranged between 41.93±8.97 and 45.90±3.57 without any significant differences ($p>0.05$). This agrees with the well-known relationship between porosity fraction and the relative Young's modulus of food products (Derossi et al., 2021; Vancauwenberghere et al., 2018; Gibson et al., 1982). In order to model the texture properties of the 3D printed snacks, the characterization of the mechanical properties of the solid phase of baked samples has been essential; to do this, several slabs of the dough at approximately zero porosity (the material reference) were baked for different time and the corresponding Young's modulus as a function of moisture content are reported in Figure 2a. The obtained linear trend shows a correlation coefficient of 0.877 by which a value of 311 Mpa was estimated at 8 g H_2O/100g w.b. corresponding to the average moisture content of the 3D printed snacks after baking. This is of great importance due to the impact of the moisture content on the mechanical properties of food materials (Saleem, 2005; Piovesan et al., 2020).

	Digital model			3D printed snack			Baked snacks		
Model	**H (cm)**	**L (cm)**	**P (%)**	**H (cm)**	**L (cm)**	**P (%)**	**H (cm)**	**L (cm)**	**P (%)**
2A	0.18	5.12	15.1	0.29 ±0.02[a]	5.1 ±0.02[a]	18.2 ±2.7[a]	0.22 ±0.02[a]	4.85 ±0.06[a]	41.93 ±8.97[a]
4A	0.32	5.12	15.1	0.41 ±0.02[b]	5.1 ±0.01[a]	15.2 ±2.2[a]	0.31 ±0.02[b]	4.86 ±0.05[a]	45.90 ±3.57[a]
6A	0.41	5.12	15.1	0.58 ±0.04[c]	5.1 ±0.02[a]	14.4 ±1.0[a]	0.40 ±0.00[c]	4.86 ±0.05[a]	42.28 ±5.03[a]

Table 1 – Main morphological properties of the digital model and 3D printed samples (H, height, L, length, P, porosity fraction)

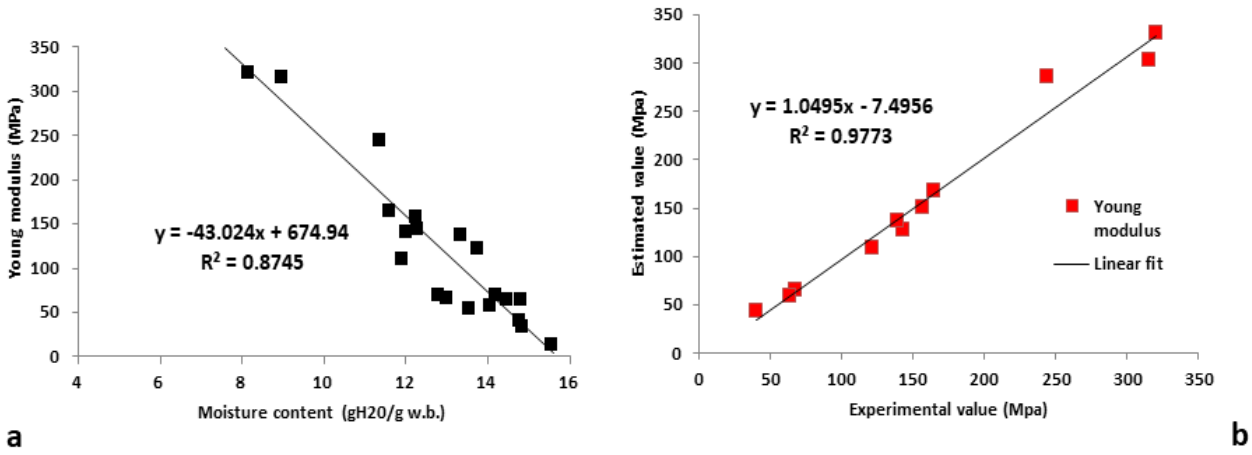

Figure 2 – Mechanical properties of the reference material at different moisture contents (a) and validation of the finite element model for the three points bend test (b).

Furthermore, the Finite Element Method (FEM) model of the three points bend test was tested and validated performing some preliminary time dependent studies by varying the material properties and the compression time and then by computing the stress-strain curve by which the Young's modulus was obtained (Figure 2b). The results proved the validity of the FEM model obtaining a correlation coefficient of 0.977.

Once the FEM was tested, we employed such model to estimate the Young's modulus of some CAD models having the same shape and dimensions of the printed snacks and with increased porosity fractions (Figure 3). By increasing the porosity fraction of such models, the Young's modulus decreased from 311 MPa of the reference material to 140.23 MPa, 71.23 MPa, 48.34 MPa and 27.82 MPa respectively with porosity fractions of 13%, 26%, 32% and 50%. In addition, when we introduced the experimental data of the 3D printed samples (Young's modulus of 20.73±7.3 MPa, 18.95±9.6 MPa and 31.84±10.8 MPa for the samples 2A, 4A, 6A) with porosity fraction of 41.93%, 42.28% and 45.9%, we observed a sufficient agreement with the FEM model. The observed discrepancies between experimental and estimated values are certainly caused by the 3D architecture of the FEM that we deliberately developed by introducing rectangular pores with predefined and ordered locations. Instead, in the printed samples the pores show a high diversity in shape and for their locations as results of the original apples tissue structure and other affecting factors such as the printing path, the presence of micropores inside the batter (Derossi et al. 2020) as well as the size increase during baking. Further improvement could be obtained by incorporating the 3D X-ray images of the printed snacks into the FEM model and to estimate the essential mechanical properties for different porosity fractions or voids located in different places of the whole structure. Once this is done, also from other biological tissues, multilayers 3D printed food with innovative and unparalleled properties could be obtained.

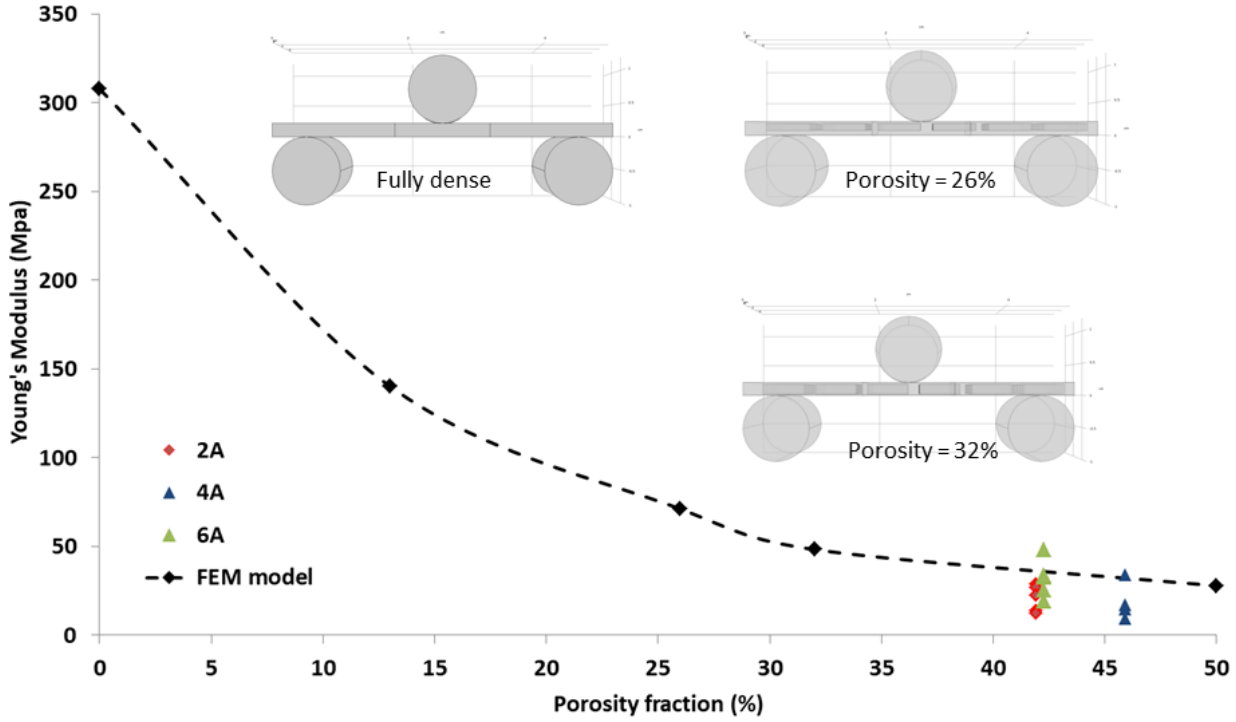

Figure 3 – Comparison of the FEM model and Young's modulus of innovative 3D printed snacks inspired by apple tissues. Black points indicate the estimated Young's Modulus by FEM for models with increased porosity fractions. Colour points indicates the experimental data.

4. Conclusion

The intriguing idea of mimicking the plant tissue structure by 3D printing technology to open to novel fascinating food, and innovative texture properties have been explored. The experiments utilized the 2D microtomographic images of apple tissues which first were rescaled from micro-to macroscale and then used as CAD models to print cereal snacks of different layers. The results demonstrated the overall feasibility of this approach satisfactorily resembling the salient morphological features of the apple structure. While the lengths of the samples well matched the CAD model, the height and the porosity fraction were significantly greater due to the formation of pores during the baking. Indeed, baked samples showed a porosity ranged between 41.93 and 45.90% versus the 15.1% of the apple tissues. The hardness of the 3D printed samples increased with the number of layers, from 2 to 6 while Young's modulus did not change significantly according to the similar porosity of the baked samples. To better understand and utilize these innovative structures inspired by apple tissue, the finite element method was used to predict Young's modulus of the printed structure. Overall, the model matched the experimental design, though, minor

discrepancies were reasonably caused by the simplified FEM model designed, for instance, with rectangular pores placed in ordered locations. However, further experiments, dedicated to the use of different vegetable microstructure and more reliable FEM models, are needed to open for 3D multi-layered snacks with unparalleled sensory and mechanical properties, marked innovation, and personalized food for specific consumers groups as, for instance, elderly or vulnerable people that need protein but suffer from mastication and swallowing problems.

5. References

AOAC (2005). Official method. 925.10. Solids (total) and moisture in flour in: Official methods of analysis (18th ed.), AOAC International, Gaithersburg (2005)

Arepally, D., Sudharshan, R., Tridib, R., Goswami, K., Datta, A. K. 2020. Biscuit baking: A review *LWT,* 131, 109726 *DOI:* 10.1016/j.lwt.2020.109726.

Baltsavias, A., Jurgens, A. and van Vliet, T. 1997. Factors affecting fracture properties of short-dough biscuits. *Journal of Texture studies,* 28 205-2019.

Campbell, C. L., Wagoner, T. B., Foegeding, E. A. 2017. Designing foods for satiety: The roles of food structure and oral processing in satiation and satiety. *Food Structure*, 13, 1-12

Chen, F., Zhang, M., Liu, Z., Bhandari, B. 2020. 4D deformation based on double-layer structure of the pumpkin/paper. *Food Structure* 27, 00168. https://doi.org/10.1016/j.foostr.2020.100168

Chen, C., Zhang, M., Guo, C., Chen, H. 2021. 4D printing of lotus root powder gel: Color change induced by microwave, *Innovative Food Science & Emerging Technologies*, 68, 102605. https://doi.org/10.1016/j.ifset.2021.102605.

Comber, R., Ganglbauer, E., Choi, J. H., Hoonhout, J., Rogers, Y., Ohara, K. et al. 2012. Food and interaction design: Designing for food in everyday life. *Human Factors in Computing Systems* 2767-2770, https://doi.org/10.1145/2212776.2212716

Derossi, A., Paolillo, M., Caporizzi, R. and Severini, C. 2020. Extending the 3D food printing tests at high speed. Material deposition and effect of non-printing movements on the final quality of printed structures. *Journal of Food Engineering* 275:109865. doi: 10.1016/j.jfoodeng.2019.109865

Derossi, A., Caporizzi, R., Paolillo, M., Severini, C. 2020. Programmable texture properties of cereal-based snack mediated by 3D printing technology. *Journal of Food Engineering*, 289, 110160 https://doi.org/10.1016/j.jfoodeng.2020.110160

Derossi, A., Caporizzi, R., Paolillo, M., Oral, M. O., Severini, C. 2021. Drawing the scientific landscape of 3D Food Printing. Maps and interpretation of the global information in the first 13 years of detailed experiments, from 2007 to 2020. *Innovative Food Science & Emerging Technologies*, 70, 102689. https://doi.org/10.1016/j.ifset.2021.102689

Dick, A., Bhandari, B. and Prakash, S. 2019. Post-processing feasibility of composite-layer 3D printed beef. *Meat Science* 153:9–18. doi: 10.1016/j.meatsci.2019.02.024

Dong, X., Pan, Y., Zhao, W., Huang, Y., Qu, W., Pan, J., Qi, H., and Prakash, S. 2020. Impact of microbial transglutaminase on 3D printing quality of Scomberomorus niphonius surimi. L*WT - Food Science and Technology* 124:109123. doi: 10.1016/j.lwt.2020.109123

Ghazal, A. F., Zhang, M., Liu, Z. 2019. Spontaneous color change of 3D printed healthy food product over time after printing as a novel application for 4D food printing. *Food and Bioprocess Technology*, 12, 1627-1645, https://doi.org 10.1007/s11947-019-02327-6

Gibson, L. J., Ashby, F. R. S., Schajer, G.S., Robertson, C. I. 1982. The mechanics of two-dimensional cellular materials. *Proceedings of the Royal Society A*, 382, 25-42 https://doi.org/10.1098/rspa.1982.0088

Guo, C., Zhang, M., Devahastin, S. 2021. Color/aroma changes of 3D-Printed buckwheat dough with yellow flesh peach as triggered by microwave heating of gelatin-gum Arabic complex coacervates. *Food Hydrocolloids*, 112, 106358. https://doi.org/10.1016/j.foodhyd.2020.106358

Haleem, A., Javaid, M., Khan, H., Suman, R. 2020. 3D printing applications in bone tissue engineering, *Journal of Clinical Orthopaedics and Trauma*, 11, S118-S124, https://doi.org/10.1016/j.jcot.2019.12.002.

He, C., Zhang, M., Guo, C. 2020. 4D printing of mashed potato/purple sweet potato puree with spontaneous color change. *Innovative Food Science & Emerging Technologies*, 59. 102250, https://doi.org/10.1016/j.ifset.2019.102250

Herremans, E., Melado-Herreros, a., Defraeye, T. Verlinden, B., Hertog, M., Verboven, P., Vald, J., Fernández-Valle, M. E., Bongaers, E., Estrade, P., Wevers, M., Barreiro, P., Nicolaï, B. M. 2014 Comparison of X-ray CT and MRI of watercore disorder of different apple cultivars. *Postharvest Biology and Technology*, 87, 42-50 https://doi.org/10.1016/j.postharvbio.2013.08.008

Herremans, E., Verboven, P., Verlinden, B. E., Cantre, D., Abera, M., Wevers, M., Nicolaï, B. M. 2015. Automatic analysis of the 3-D microstructure of fruit parenchyma tissue using X-ray micro-CT explains differences in aeration. *BMC Plant Biology*, 15, 264.

Jung Ko, H. J., Wen, Y., Choi, J. H., Park, B. R., Kim, H. W., Park, H. J. 2021. Meat analog production through artificial muscle fiber insertion using coaxial nozzle-assisted three-dimensional food printing. *Food Science and Technology* 52, 5, 1269-1275 doi.org/10.1111/ijfs.13394

Le Tohic, C., J. J. O'Sullivan, K. P. Drapala, V. Chartrin, T. Chan, A. P. Morrison, J. P. Kerry, and A. L. Kelly. 2018. Effect of 3D printing on the structure and textural properties of processed cheese. *Journal of Food Engineering* 220:56–64. doi: 10.1016/j.jfoodeng.2017.02.003

Liu, C., Ho, C., and Wang, J. 2018. The development of 3D food printer for printing fibrous meat materials. Paper presented at the 2017 *2nd International Conference on Innovative Engineering Materials (ICIEM 2017),* Philadelphia, October, 21-26, 2017. doi: 10.1088/1757-899X/284/1/012019

Liu, Z., He, C., Guo, C., Chen, F., Bhandari, B., Zhangac, M. 2021. Dehydration-triggered shape transformation of 4D printed edible gel structure affected by material property and heating mechanism. *Food Hydrocolloids*, 115, 106608. https://doi.org/10.1016/j.foodhyd.2021.106608

Majzoobi, M., Talebanfar, S., Eskandari, M. H., Farahnaky, A. 2017. Improving the quality of meat-free sausages using κ-carrageenan, konjac mannan and xanthan gum. *International Journal of Food Science & Technology, 52, (5),* DOI:10.1111/ijfs.13394 .

Mudgil, D., Barak, S., Khatkar, B.S. 2017. Cookie texture, spread ratio and sensory acceptability of cookies as a function of soluble dietary fiber, baking time and different water levels. *LWT*, 80, 537-542. https://doi.org/10.1016/j.lwt.2017.03.009

Nugraha, B., Verboven, P., Janssen, P., Wang, Z., Nicolai, B. 2019. Non-destructive porosity mapping of fruit and vegetables using X-ray CT, *Postharvest Biology and Technology* 150, 80-88, https://doi.org/10.1016/j.postharvbio.2018.12.016

Pant, A., Lee, A. Y., Karyappa, R., Lee, C. P., An, J., Hashimoto, M., Tan, U., Wong, G., Chua, C., K. and Zhang, Y. 2021. 3D food printing of fresh vegetables using food hydrocolloids for dysphagic patients. *Food Hydrocolloids* 114:106546. doi: 10.1016/j.foodhyd.2020.106546

Paolillo, M., Derossi, A., van Bommel, K., Noort, M., Severini, C. 2021. Rheological properties, dispensing force and printing fidelity of starchy-gels modulated by concentration, temperature and resting time. *Food Hydrocolloids*, 117, 106703. https://doi.org/10.1016/j.foodhyd.2021.106703

Park, S. M., Kim, H., Park, H. J. 2020. Callus-based 3D printing for food exemplified with carrot tissues and its potential for innovative food production. *Journal of Food Engineering*, 271, 109781, https://doi.org/10.1016/j.jfoodeng.2019.109781.

Piovesan, A., Vancauwenberghe, V., Aregawi, W., Delele, M. A., Bongaers, E., de Schipper, M., van Bommel, K., Noort, M., Verboven, P., Nicolai, B. 2020. Designing Mechanical Properties of 3D Printed Cookies through Computer Aided Engineering. Foods. 4;9 (12):1804. doi: 10.3390/foods9121804.

Pulatsu, E., Lin, M. 2021. A review on customizing edible food materials into 3D printable inks: Approaches and strategies. *Trends in Food Science and Technology*, 229418232. doi:10.1016/j.tifs.2020.11.023

Phuhongsung, P., Zhang, M., Bhandari, B. 2020. 4D printing of products based on soy protein isolate via microwave heating for flavor development. *Food Research International*, 137, 109605 https://doi.org/10.1016/j.foodres.2020.109605

Saleem, Q. 2005. Original article mechanical and fracture properties for predicting cracking in semi-sweet biscuits. *International Journal of Food Science Technology*, 40, 361-367. https://doi.org/10.1111/j.1365-2621.2004.00920.x

Severini, C., Derossi, A., Azzollini, D. 2016. Variables affecting the printability of foods: Preliminary tests on cereal-based products. *Innovative Food Science & Emerging Technologies*, 38, 281-291. https://doi.org/10.1016/j.ifset.2016.10.001

Severini C., Derossi A., Ricci I., Caporizzi R., Fiore A. 2018. Printing a blend of fruit and vegetables. New advances on critical variables and shelf life of 3D edible objects. *Journal of Food Engineering*, 220, 89 – 100. https://doi.org/10.1016/j.jfoodeng.2017.08.025

Teng, X., Zhang, M., Mujumdar, A. S. 2021. 4D printing: Recent advances and proposals in the food sector. *Trends in Food Science & Technology* 110, 349-363 https://doi.org/10.1016/j.tifs.2021.01.076

Tomasevic, I., Putnik, P., Valjak, F., Pavlic, B., Sojic, B., Markovinovic, A.B., Kovacevic, D.B. (2021). 3D printing as novel tool for fruit-based functional food production. Current Opinion in Food Science, 41, 138-145. https://doi.org/10.1016/j.cofs.2021.03.015

Unal, A., Arora, N. 2021. Chapter 15 - 3D printing in regenerative medicine. *Regenerated Organs*. Future Perspectives, 305-330. https://doi.org/10.1016/B978-0-12-821085-7.00015-4

Vancauwenberghe, V., Delele, M. A., Vanbiervliet, J., Aregawi, W., Verboven, P., Lammertyn, L. 2018. Model-based design and validation of food texture of 3D printed pectin-based food simulants *Journal of Food Engineering*, 231, 72-82. https://doi.org/10.1016/j.jfoodeng.2018.03.010

Vancauwenberghe, V., Baiye Mfortaw Mbong, V., Vanstreels, E., Verboven, P., Lammertyn, J., Nicolai, B. 2019. 3D printing of plant tissue for innovative food manufacturing: Encapsulation of alive plant cells into pectin based bio-ink. *Journal of Food Engineering*, 263. https://doi.org/10.1016/j.jfoodeng.2017.12.003

Wang, W., Yao, L., Zhang, T., Cheng, C., Levine, D. S., Ishii, H. 2017. Transformative appetite: Shape-Changing food transforms from 2D to 3D by water interaction through cooking. *Human Factors in Computing Systems*. 6123-6132, doi:10.1145/3025453.3026019

Wang, L., M. Zhang, B. Bhandari, and C. Yang. 2018. Investigation on fish surimi gel as promising food material for 3D printing. *Journal of Food Engineering* 220:101–8. doi: 10.1016/j.jfoodeng.2017.02.029

Wang, S., Zhou, G., Guan, J., Ma, Y., Liu, Z., Ren, B., Zhao, H., Watson, A., Jung. W. 2021. Inferring food types through sensing and characterizing mastication dynamics. *Smart Health*, 20, 100191. https://doi.org/10.1016/j.smhl.2021.100191

Zhou, X., Tenaglio, S., Esworthy, Hann, S., Cui, H., Webster, T., Fenniri, H., Zhang, L. 2020. Three-dimensional printing biologically inspired DNA-based gradient scaffolds for cartilage tissue regeneration *ACS Appl. Mater. Interfaces*, 12 (29), 33219-33228. https://doi.org/10.1016/j.biomaterials.2020.120287

Zhu S., Stieger M.A., van der Goot A.J., and Schutyser M.A.I. 2019. Extrusion-based 3D printing of food pastes: Correlating rheological properties with printing behaviour. *Innovative Food Science & Emerging Technologies*, 58, 102214, https://doi.org/10.1016/j.ifset.2019.102214.

CHAPTER 7 Extending the 3D food printing tests at high speed. Material deposition and effect of non-printing movements on the final quality of printed structures

Derossi Antonio, Maddalena Paolillo, Rossella Caporizzi, Carla Severini

Journal of Food Engineering

Volume 275, June 2020, 109865

Abstract

3D Food Printing has unprecedented ambitions but for its practical use the increase of the speed of material deposition is a challenge to tackle. We have extended the information on this aspect by using a workflow that analyzes the screw-based deposition, at medium-high speed and the effect of some undervalued variables on the quality of 3D printed cereal-based structure. The most familiar approach utilized to compute the right extrusion rate for a good replica of the 3D virtual model completely fails at high print speed. Improvements would be possible only by using a flow of 300% or by changing, as input data, the diameter of filament at 1.0 mm. However, additional irregularities are caused by undervalued variables such as retraction distance being the most important for the printing quality while the travel speed and retraction speed are crucial to reduce printing time. Finally, desirability approach was able to define the conditions capable to get a maximum desirability of 0.85 at speed of 200 mm/s.

1. Introduction

3D Printing (3DP) is an emerging technology capable to convert a virtual 3D model in a physical tangible structure through a layer by layer deposition process of different materials. 3DP belongs in Additive Manufacturing (AM) that is constantly extending its usage in many fields of applications such as biomedical engineering, aerospace, fast prototyping, jewellery, dental prosthesis and food (Lipton, 2017; Dankar et al., 2018; Liu et al., 2019). AM consists of several techniques such as Selective Sintering technology, Fused Deposition Modelling, Binder jetting, Inkjet printing, etc. which have significantly differences in theoretical principles and practical applications (Sun et al., 2015; Dankar et al., 2018; Sun et al., 2018; Liu et al., 2019). Fused Deposition Modelling (FDM) is the most used and studied 3D printing technique. It consists of depositing a fused filament of material while the printing-movements follow the pattern designed by the 3D CAD model (Pérez et al., 2019; Goyanes et al., 2014). First, FDM was utilized for thermoplastic materials such

as PLA and BSA, but later it was used in many other fields of applications (Bégin-Drolet et al., 2017; Asharaf et al., 2018; Godoi et al., 2018; Geng et al., 2019). For food, the majority of the edible materials – pastes, cereal-based food formulas, etc. – are commonly deposited by using three main mechanisms: syringe-based extrusion, air-pressure driven extrusion and screw-based extrusion (Sun et al., 2018; Pérez et al., 2019). 3D printing technology has visions of customization, decentralization and rapid fabrication and with regard to food sector, the creation of personalized/tailored food products, both in term of nutritional content and sensory properties, is one of the most interesting aims (Fay and German, 2008; Sher and Tutò, 2015; Bashiardes et al., 2018; Derossi et al., 2019a). Last five years have shown a sudden increase of the number of scientific experiments dedicated to 3D food printing. First, the attention has been posed on the diversity of food formulas employable as food-ink and on the effect of their rheological properties on printing quality (Cohen et al., 2009; Gong et al., 2014; Kim et al., 2017; Caporizzi et al., 2019). Later, many publications have elucidated the main effects of printing variables such as nozzle size, layer height (Severini et al., 2016, 2018; Liu et al., 2018; Yang et al., 2018a; Derossi et al., 2019), print speed (Kim et al., 2017; Yang et al., 2017; Vancauwenberghe et al., 2017a, 2017b; Severini et al., 2018) extrusion rate (Vancauwenberghe et al., 2017a; Hamilton et al., 2017; Lanaro et al., 2017; Le Tohic et al., 2018; Derossi et al., 2018a, Derossi et al., 2019), infill level (Lille et al., 2018; Manthial et al., 2018; Schutyser et al., 2018; Derossi et al., 2019) and the effect of the different material deposition techniques (Portanguen et al., 2019). In addition some pioneering publications have been focused on the theme of personalized food manufacturing. For instance, in our previous studies a 3D food structure able to meet the nutritional requirements of children of 3–10 years old (Derossi et al., 2018a) was created. Also, the capability to create 3D structures by using a blend of fruit and vegetables (Severini et al., 2018; Ricci et al., 2019) and the use of insect powder (Caporizzi et al., 2019) for 3D food printing application was studied. Furthermore, studies of Vancauwenberghe et al. (2017b) showed the possibility to create some printed structures enriched with encapsulated alive cells aiming to improve the overall nutritional properties. More recently, we have showed the results of experimental tests aiming to get cereal-based snacks having personalized textural properties (Derossi et al., 2018c). Also, as first example of biomimicking plant tissue microstructure, we have created soft multi-layered cereal-snacks for elderly people based on the 3D microstructure of apple tissue (Derossi et al., 2019c). However, some technological limits – particularly the speed of printing and the fidelity of the printed structure in comparison to the virtual model - dismiss the real application of 3D Food Printing (3DFP) for a mass customization.

With regard to the first challenge, the relevant literature reports experiments tested at low speeds. Generally, the lowest values are from 2 to 21 mm/s (Lille et al., 2018; Lanaro et al., 2017; Severini et al., 2018; Lee et al., 2019) while other authors printed at low-medium speeds between 15 and 40 mm/s (Severini et al., 2016; Kim et al., 2017, 2019; Wang et al., 2018; Yang et al., 2018b; Liu et al., 2018) and rarely, peoples utilized speed greater than 60–70 mm/s (Derossi et al., 2018b; Mantihal et al., 2018; Dianez et al., 2019). But, these values may be considered completely negligible when compared with what is possible to do when printing non-food materials (Hosny et al., 2018; Birbara et al., 2017; Lee et al., 2017; Diggs-McGee et al., 2019). For instance, study from Diggs-McGee et al. (2019) employed a print speed of 400–600 inches/min when studying the application of 3D printing to fabricate concrete building. Moreover, considering the most recent commercial printers for plastic materials, it is possible to work at 500 mm/s by using the Delta WASP 20 × 40 Turbo 2 (Wasp Project, Italy) or the Dynamo 3D One-Pro (D3D Dynamo3D, Italy). Furthermore, very recently the engineers from the Massachusetts Institute of Technology (MIT) opened for new opportunities by creating a FDM system 10 times faster than the commercial printers (MIT, 2019).

Unfortunately, we know little on application of 3DFP at high speed rate. When the movement of the printers in X, Y, Z significantly increased, there is the need to optimize many variables which play an important role on printing fidelity. Some of these are the travel movements (i.e. the non-printing movements), path planning, and the retraction of the material during non-printing movements, which (Kulkarami and Dutta, 1999; Jin et al., 2013; Gilberti et al., 2017) have been completely neglected in 3D food printing experiments.

Herein, we have addressed this issue by analyzing whether, by increasing the print speed of a commercial 3D printer more than the common limits used up to now, it is possible to replicate, with high fidelity, a designed 3D virtual model. With this regard we have explored the technical options to keep a good equilibrium between printing movements, in X, Y, Z axes, and the extrusion rate when using a screw-based deposition system. We also analyzed some non-printing variables on the quality of 3D printed cereal-based snack.

2. Materials and methods

2.1. Schematic representation of the workflow

With the aim to better clarify the main structure of this study, Fig. 1 shows the workflow for the 3D printing experiments.

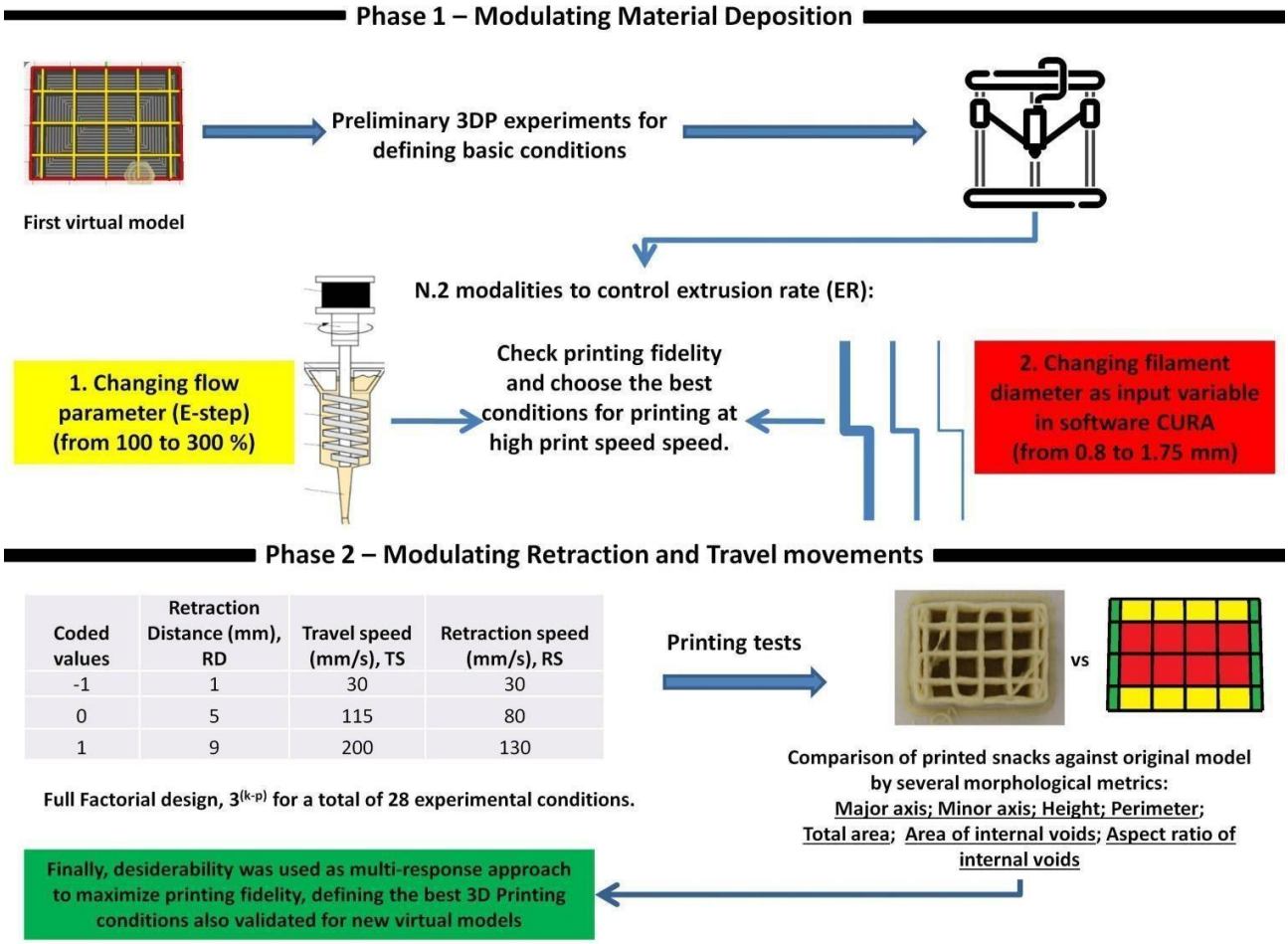

Fig. 1. Schematic representation of the workflow used during the experiments.

Briefly, a first series of experiments (phase 1) were focused on the effects of flow and the diameter of filament as options for modulating the amount of material deposited for unit of time when printing with speeds ranged between 15 and 200 mm/s. After collecting the data and defining the best options to print at high speed, we have analyzed the effects of some undervalued printing variables such as retraction distance (mm), travel speed (mm/s) and travel distance (mm) on the quality/fidelity of the printed objects against virtual model at medium-high speed of printing (phase 2). This was performed by employing a factorial design modulating the above variables at three levels and collecting the responses of several morphological metrics of the samples. Furthermore, all responses were utilized to get a desirability profile to define the best printing conditions able to maximize the quality of the objects with the lower printing time. Finally, the defined conditions were used in a validation step where 2 additional virtual models were printed and their quality was evaluated. Detailed information of the experimental conditions are reported below.

2.2. Raw materials and preparation of dough

Food formula utilized for printing experiments consists of dough prepared with wheat flour type 00 (according to the Italian Food Regulation, 2001) (62%), water (Lilia, Italy) (31%), extra virgin olive oil (Desantis, Italy) (6%) and sodium chloride (1%). All ingredients were purchased locally and stored at room temperature till the experiments. The choice of the ingredients was based considering some ordinary recipes for salty cereal-based snacks while their mass fractions were defined on the basis of preliminary experiments aimed to obtain a good printability. Dough preparation has required the kneading of all ingredients in a planetary kneader (model cooking chef, Kenwood Ltd. UK) for 3 min at speed level of 1 (22 rpm). Then, the dough was rest for 30 min before the 3D printing experiments.

2.3. Farinograph characteristics of the food formula

The rheological properties of the dough were measured by using a farinograph mod. AT (Brabender, Germany) according to the method Brabender/ICC/BIPEA. The analyses exhibithed an average mixing time of 7.34 BU (Brabender Units), a consistency of 1004 BU, and elasticity of 363.66 BU.

2.4. 3D virtual model and printing conditions

Our system (Delta 2040 equipped with a clay extruder kit 2.0 – Wasp Project, Italy) utilizes air pressure to push food material from the piston chamber to the screw-based extruder (Derossi et al., 2018a; Severini et al., 2016). According to physical material properties, pressure might be modulated to accommodate the amount of material deposited per unit of time. Additionally, the speed of the screw may be tuned by modifying the parameter flow that controls the speed of the E-axis. Based on preliminary experiments, the dough was loaded in a piston chamber by applying a pressure of 2 bar. The virtual model representing a block with a base of 40 × 30 mm and height of 15 mm was designed by using the software Tinkercad (Autodesk Inc.). Then the slicing step was performed by using CURA ver. 3.3.1. For the phase 1 some basic variables were in common for all the experiments: nozzle size of 0.84 mm, shell thickness 0.84 mm, layer height 0.7 mm, travel speed 30 mm/s and infill density 20%. For the phase 2, a full factorial design 3^(k-p) where k is the number of the independent variables (with k = 3 and p = 0) for a total of 28 experiments, was used to study the effects of the retraction distance RD (mm) , travel speed TS (mm/s), and retraction speed RS (mm/s). The retraction is a counter-clockwise movement that avoid oozing during non-printing movements. Retraction is defined by two values: the length of retraction and the speed of rectraction, respectively named retraction

distance and the retraction speed. Also, travel speed defines the rate of non-printing movements while print speed indicates how fast the printer moves during material deposition.

More specifically, RD was modulated at 1 mm, 3 mm, 5 mm, TS was set at 30 mm/s, 115 mm/s and 200 mm/s while RS was modulated at 30 mm/s, 80 mm/s and 130 mm/s. Table 1 reports the 28 printing conditions used for the experiments . After the printing tests, the objects were carefully weighed on analytical balance (Gibertini, EU-C 7500) and cooked in oven at 180 °C for 18 min.

Experiments	***Codes***			***Variables***		
	(x_1)	*(x_2)*	*(x_3)*	*Retraction Distance (mm)*	*Travel speed (mm/s)*	*Retraction Speed (mm/s)*
1	-1	1	0	1	200	80
2	0	1	0	5	200	80
3	1	0	0	9	115	80
4	-1	-1	0	1	30	80
5	0	1	-1	5	200	30
6	-1	0	0	1	115	80
7	0	0	0	5	115	80
8	1	0	-1	9	115	30
9	1	-1	1	9	30	130
10	1	-1	0	9	30	80
11	0	0	1	5	115	130
12	0	0	0	5	115	80
13	1	1	0	9	200	80
14	1	-1	-1	9	30	30
15	0	0	-1	5	115	30
16	1	1	-1	9	200	30

17	0	-1	1	5	30	130
18	0	-1	-1	5	30	30
19	-1	-1	1	1	30	130
20	-1	1	-1	1	200	30
21	0	1	1	5	200	130
22	-1	1	1	1	200	130
23	-1	0	-1	1	115	30
24	1	1	1	9	200	130
25	-1	0	1	1	115	130
26	-1	-1	-1	1	30	30
27	0	-1	0	5	30	80
28	1	0	1	9	115	130

Table 1 - Experimental design of 3D printing conditions.

2.5. Image analysis of 3D printed samples

Pictures of each sample were acquired by using a photo-camera Canon, EOS 1200D. After calibration the images were analyzed for their main morphological metrics by using the software ImageJ ver 1.52a. For each sample the following morphological properties were analyzed: major axis (mm), minor axis (mm), height (mm), perimeter (mm), total area (mm2). For the first three measures, at least 3 replicates were performed in different positions of a couple of samples for a total of 6 measures. Furthermore, additional measures were performed to analyze the properties of internal voids created by the infill pathway during printing. Since we had chosen a 'grid-type' path, the structure was divided in different parts of rectangular shape being different for their dimensions. For clarity we defined three classes of voids named as central, lateral and upper/lower voids, respectively highlighted in red, green and yellow in Fig. 2. For each class of voids the following metrics were analyzed: total area of the voids (mm2), aspect ratio (AR) defined as major axis/minor axis, and the average area for each type of voids. The relative deviation of such metrics between the virtual model and the printed samples was computed.

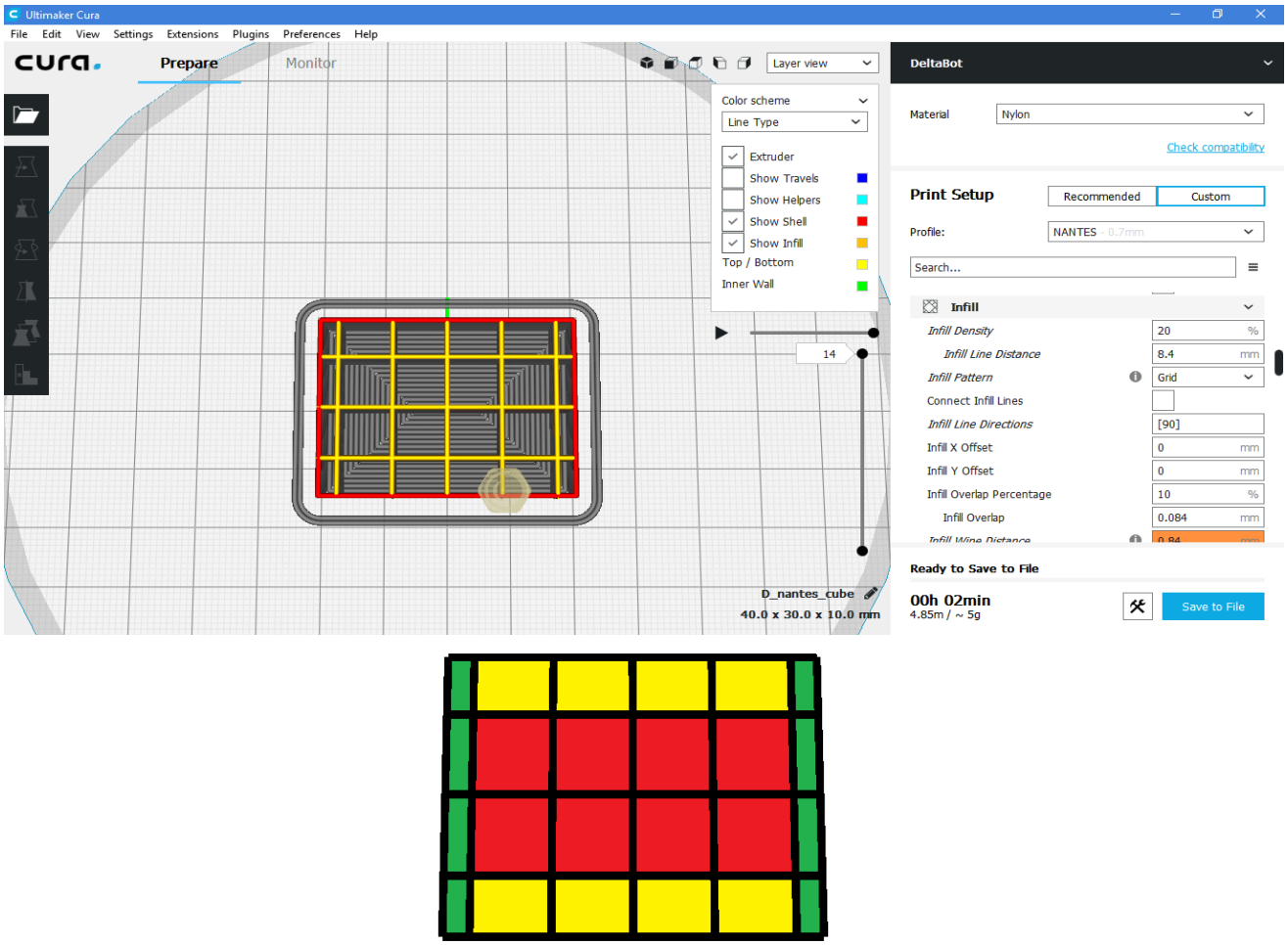

Fig. 2. Virtual model designed (left) and different internal voids designed by the infill pathway (right).

3. Results and discussion

3.1. Relationship between speed printing and extrusion rate. Preliminary data on their important equilibrium

For the majority of 3D printing applications a simple mathematical equation is commonly used to relate print speed and extrusion rate (Khalil and Sun, 2007):

$$ER\ (mm^3/s) = Dn\ (mm) * h\ (mm) * V_n\ (mm/s) \qquad (1)$$

Where the ER is the volume of the extruded/deposited material for unit of time (mm3/s), Dn is the nozzle diameter (mm), h is layer height and Vn is the desired print speed (mm/s).

Eq. (1) means that the volume of the material needed to build a physical structure faithful to the 3D virtual model is the result of nozzle diameter, layer height and the print speed (Wang and Shaw, 2005; Yang et al., 2018a). In many sectors, also in food

manufacturing, several authors utilized this formula to compute the critical value of layer height, hc, a useful values to get, for any print speed, the best printing fidelity. Some examples might be found for lemon gels (Yang et al., 2018a), surimi gels (Yang et al., 2018b), and for non-food material as well (Khalil and Sun, 2007). Furthermore, other authors used a modified version of Eq. (1) based on the assumption that the shape of deposited filaments has a cylindrical shape rather than of rectangular (Wang and Shaw, 2005; Yang et al., 2018a). The last aspect is able to greatly affect the quality of printing but being out of the main aim of our paper for more specific details we suggest the following reading (Derossi et al., 2019; Slic3R, 2017; Chilson, 2011; Baines, 2017). However, it is important to note that, despite the large usage of Eq. (1), it does not consider the rate of the screw that controls the amount of deposited material. The rotation of screw is controlled by a stepper motor that moves on the E-axis and its default rate is defined by the parameter E-step, literally the number of steps performed by the stepper motor to feed 1 mm of filament (Derossi et al., 2019a). For a given default value of E-step, when we increase the print speed, the rate of the screw also increase with the aim to keep a good equilibrium between printing movements and extrusion rate. So, when printing plastic materials any users usually don't care of the E-axis because the system is optimized for those material properties. But, when food materials are used we are in a completely different scenario and the behaviour of such edible materials could not satisfy Eq. (1) due to the effect of material properties (density, viscosity, adhesion to the screw, etc.). Indeed, as reported by Guo et al. (2019) the flow mechanism involved in the screw-based system may be very complicated and, depending on the viscosity of mashed potato, several issues such as the adhesion of the materials to the screw and the wall of extrusion tube, shear thinning around the screw resulting in idle spinning may occur posing significant obstacles to the material deposition during printing movements.

We have analyzed whether the increase of print speed leads to the rise of screw speed allowing depositing enough materials to obtain a high printing quality. Fig. 3 shows the results of some preliminary experiments in which the relations between print speed and the extrusion rate, ER, as computed from Eq. (1) is reported ; furthermore, two representative images of 3D food objects printed at low (15 mm/s) and high (200 mm/s) print speed, are shown. Note that the objects were obtained by keeping the flow at its default values of 100% with the aim to avoid any effect on the quality of the samples. The amount of the material deposited, for both the print speeds, is definitely not sufficient to replicate the virtual model with high accuracy or, in other words, there is a complete mismatching between extrusion rate and the movements of

the printer. Particularly, when using the higher print speed the food filaments were subjected to dragging and many ruptures occurred creating the worst structure. This proves that in disagreement with the overall application in 3D printing, Eq. (1) cannot be considered completely adequate for computing the extrusion rate needed to build, which accuracy, a 3D printed cereal-based snack when a screw-extrusion system is used. Yang et al. (2018a) performed similar experiments with a lemon gel with a good agreement between experimental and estimated values in a range of print speeds between 15 mm/s and 30 mm/s; while for further increases up to 35 mm/s they showed some defects due to dragging effects. To better understand the behaviour of dough deposition during printing, we compared the experimental data of ER against the computed values obtained by Eq. (1) (Fig. 4a). The figure strengthens the lack of trust on Eq. (1) that cannot precisely predict the amount of materials deposited. The only conditions in which estimated and experimental values well match is when a flow of 200% was used and for a print speed up to 15 mm/s. This means that to deposit the amount of food material as estimated by Eq. (1), would be necessary a rotation speed of the screw double than the default value of 100%.

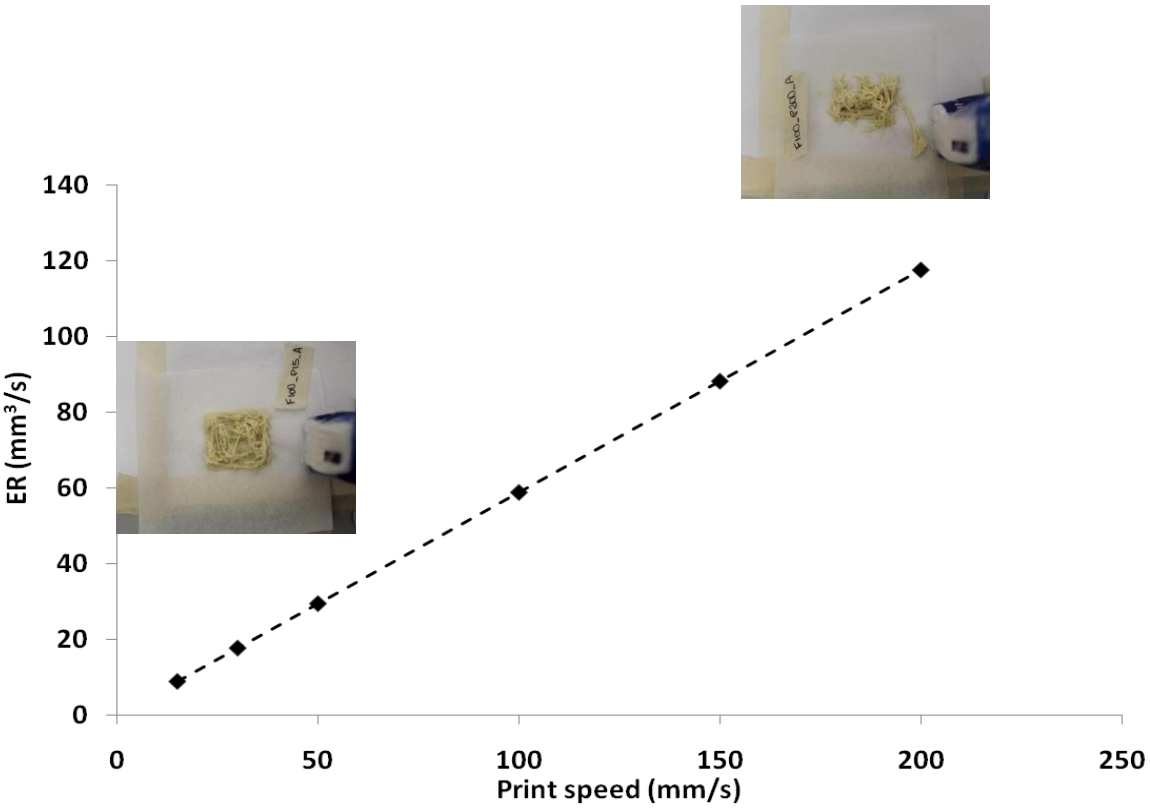

Fig. 3. Theoretical relations between extrusion rate, ER, and print speed. Representative images of the 3D samples dough printed at 15 mm/s and 200 mm/s are also reported.

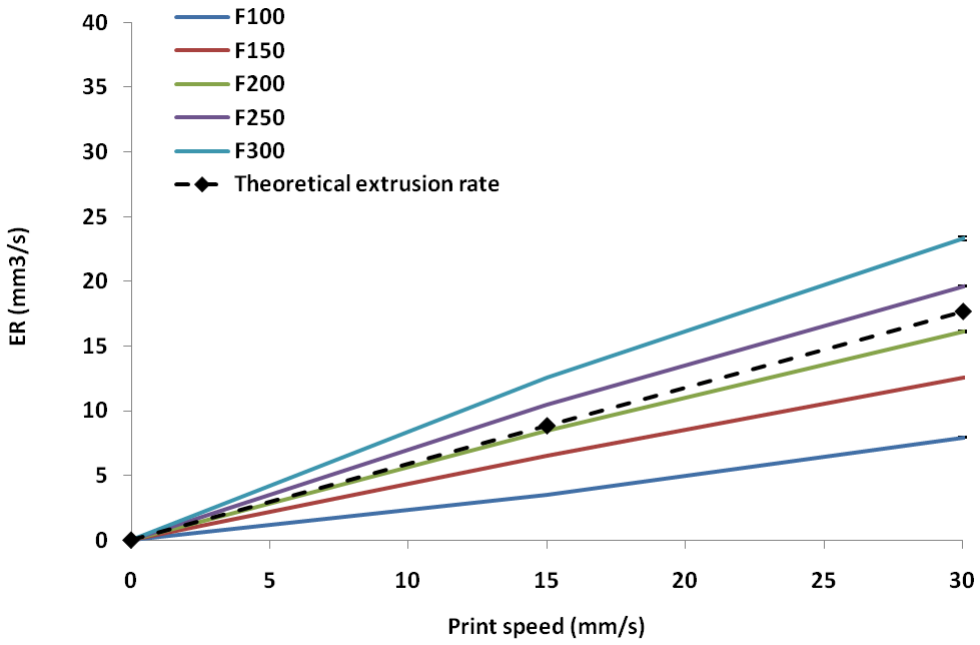

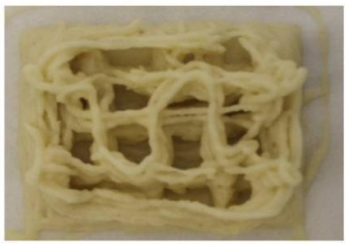

Flow 200 – Print speed 15 mm/s

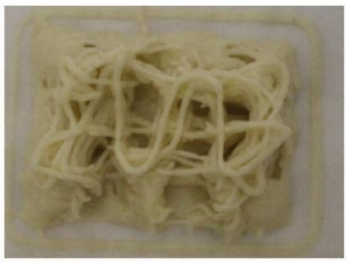

Flow 200 – Print speed 200 mm/s

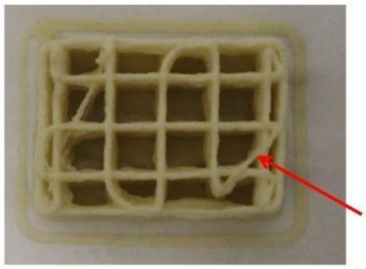

Flow 300 – Print speed 15 mm/s

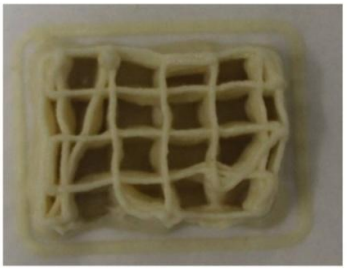

Flow 300 – Print speed 200 mm/s

Fig. 4. a) Comparison between experimental and estimated extrusion rate, ER, as a function of print speed and flow parameter between 100% and 300%. b) Representative images of different samples obtained in different conditions.

For any other case, the experimental values were significantly different than those computed from Eq. (1). Particularly, for flow values between 100% and 200%, Eq. (1) overestimated the extrusion rate, while by using flow values of 250 and 300 the equation underestimated the amount of food formula deposited. This may be observed in Fig. 4b reporting some representative images of the printed objects obtained in different experimental conditions. A formless structure was observed for flow value of 200% independently if we used the lowest or the highest print speed. This is because not enough material was deposited during printing movements. Inversely, when a flow of 300% was used, the samples showed a better fidelity of printing, particularly at low speed of 15 mm/s. However, all these samples still show some defects; firstly, the thick of each printed line was greater than the nozzle size indicating that an excess of deposited material (data not shown). Secondly, we can observe some lines of the printed samples that do not appear in the 3D model (highlighted with red raw). These irregularities are popularly called ‘oozing problems’ or ‘stringing’, and they represent the undesired deposition of materials during the non-printing movements.

These data open for relevant considerations: despite the general use of 3D printing for thermoplastic materials that allow to keep a good equilibrium between extrusion rate and printing movements at any print speed, for food materials deposited by a screw-based system the process is greatly affected by properties such as viscosity, wettability, density, etc. In addition, any change of the utilized ingredients could require some adjustments of the printing conditions due to the effects on the aforementioned rheological properties.

Furthermore to better understand the need of optimization of 3D Food printing we want to note that the G-code contains two commands for controlling the movements of the screw on E-axis: a) the E-position that means the length of the filament to feed into the extruder between the start and end point of each single printing movement and b) F-value indicating the feed-rate of that length of filament (Marlin, 2019). But, in food sector these parameters have not sense because we never have a food filament that feed the extruder. This open for future need of innovative systems and optimized G-codes for specific properties of food formulas and also more precise screw-based systems able to deposit food materials according to Eq. (1) or, additionally, for new mathematical approach able to explain the flow inside the such screw-based system. The deposition of food material obtained by a screw-based system is much more complicated than the syringe and the material properties of food formulation play an important role on the deposition behaviour, as proved by the study of Guo et al. (2019).

A second series of experiments has been focused on the capability to modulate the amount of deposited food formula by changing as input value the diameter of filament in the slicing software. Indeed, the reduction of this value permits to accelerate the rotation of the screw. The obtained structures indicate that the better input value was of 1.0 mm, against 1.75 mm that is the default value used during 3D printing (Fig. 5). Indeed in the latter case, the rotation of the screw was too slow making insufficient the amount of deposited dough for any print speed utilized. On the other hand, when using an input value of 0.8 mm an over deposition was observed creating a too large thickness of the dough along the pathway of the infill. The best printing condition was defined as follow: an input value of 1 mm for food filament and a print speed of 200 mm/s. This condition allowed obtaining the best agreement between virtual model and printed structure. More specifically, by analyzing the thickness of the main deposited lines we observed an average value of 0.95 mm against 0.84 mm of the virtual model, while an average value of 1.3 mm was measured when a value of 0.8 mm was used. On these bases, we decided to use the first condition for the next series of the experiments. However, it is worth to note that again some 'oozing effects' were still visible proving the need of a better control of the non-printing movements.

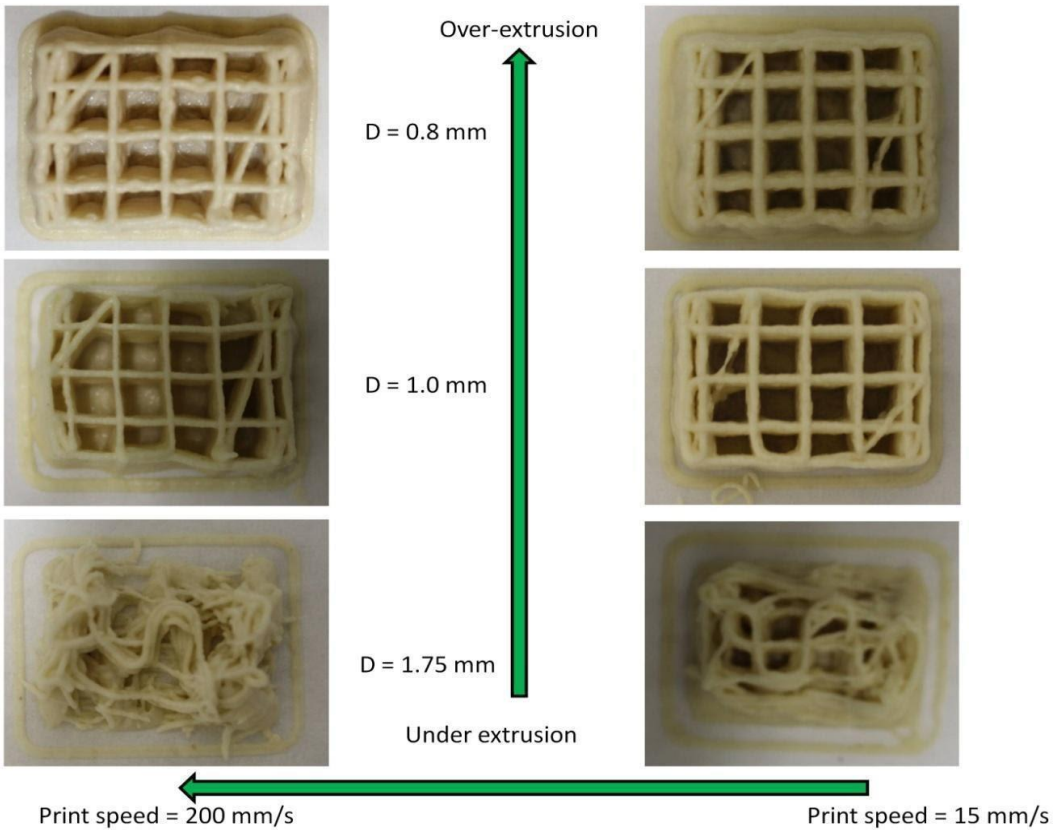

Fig. 5. Representative images of 3D printed dough obtained by modulating the filament diameter (D) and the print speed.

3.2. Effect of print speed and flow on printing time

We want to analyze the actual printing times of the samples as a function of the print speeds and flow values (Fig. 6a). Note that printing times were computed for the entire process including printing- and non-printing movements. First, the replicates of the experiments always exhibited a negligible variability overall less than 2 s. For this reason, the error bars were not included in the figure.

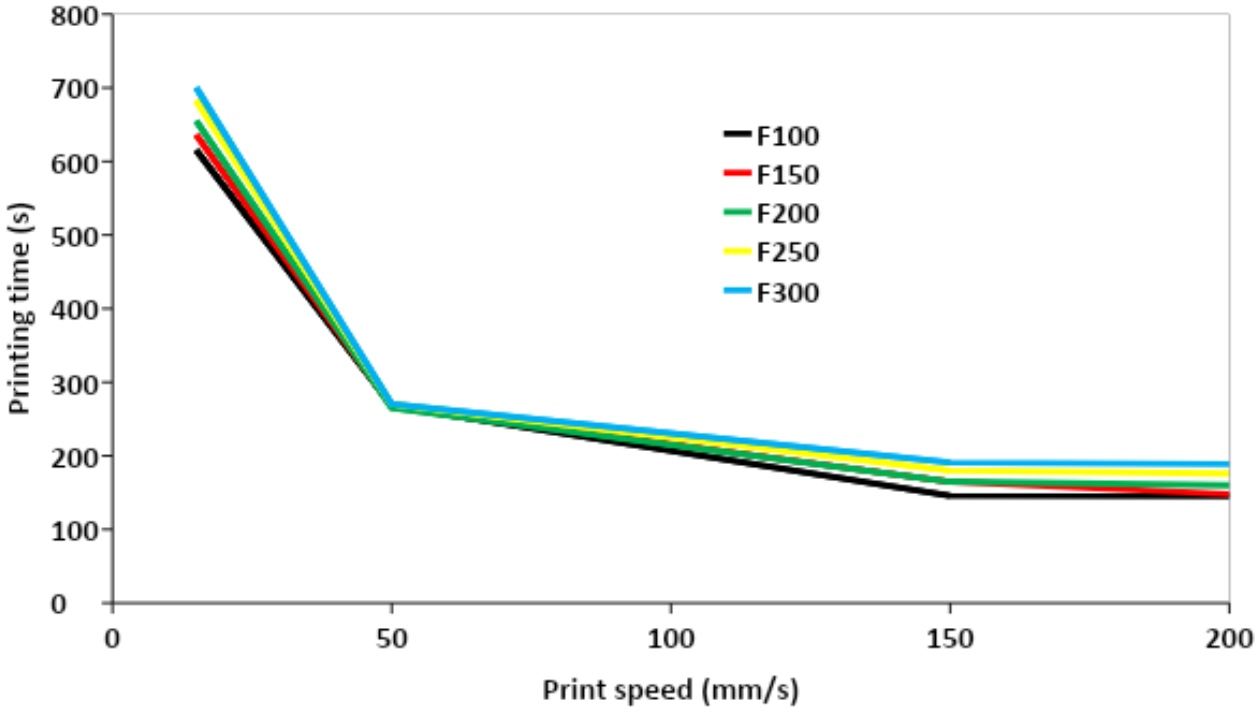

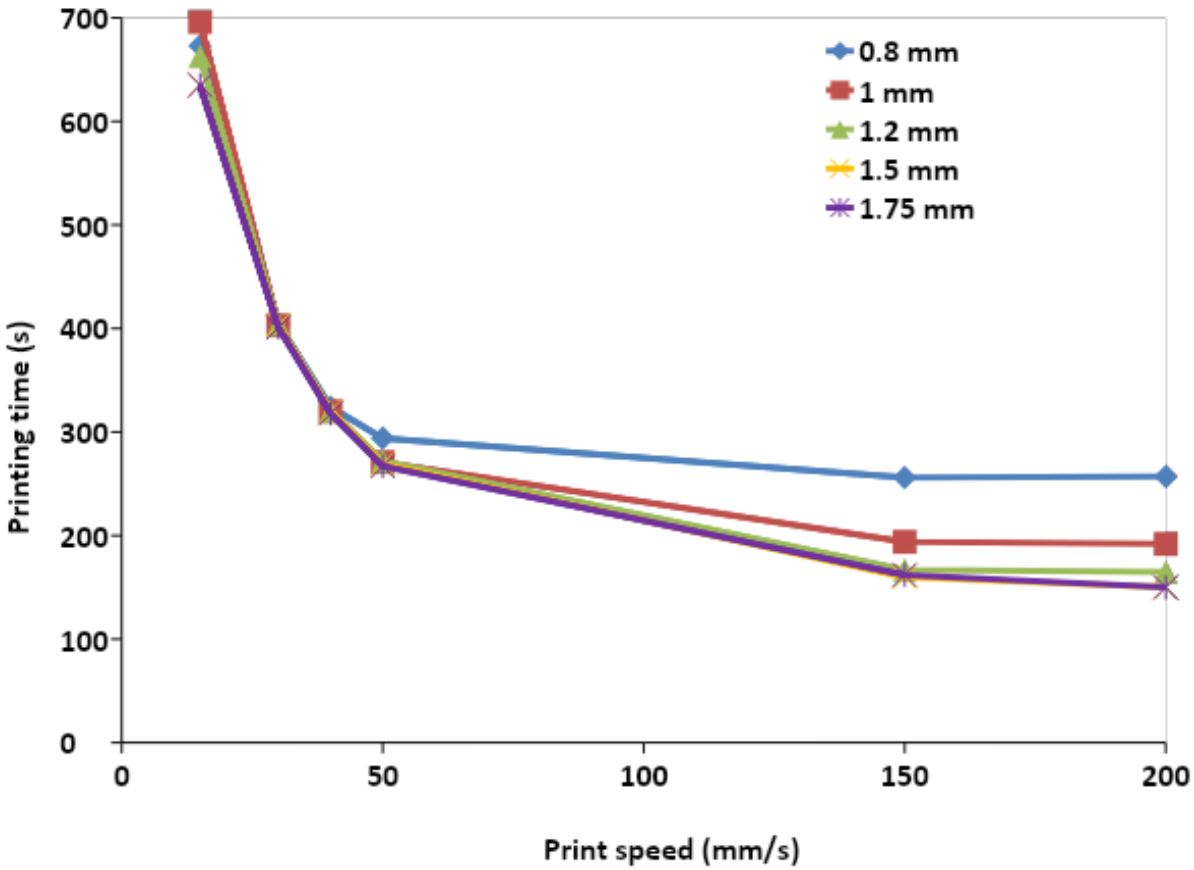

Fig. 6. Actual printing times during 3D food printing experiments. A) Data measured as a function of print speed and flow (F); B) Data measured as a function of filament diameter (D)

The data exhibit a clear exponential trend having a sudden reduction from 700 s to 270 s by increasing the print speed from 15 mm/s to 50 mm/s while a further increase of the speed did not reduce significantly the printing time, apart a slight reduction till 200 s for print speed of 150 mm/s. This data prove that there is a limit of the speed of printing movements that occurs for values over than 100–150 mm/s. Two main reasons may be discussed: 1. the effect of acceleration/deceleration of the printer; 2. the maximum rate of E-axis. The first point accounts for the limits of acceleration/deceleration of the printer which needs time to reach the desired value of print speed. Table 2 explains this behaviour. As example, considering a print speed of 200 mm/s, a length of ≈6.6 mm is necessary to accelerate from zero to the desired speed as well as to decelerate to zero before the printer stops and changes direction. For our samples considering the major length of 40 mm, the printer moves at 200 mm/s for a length only of 26.66 mm or, inversely, the average print speed (along the distance of 40 mm) was significantly lower than the desired value. Indeed, on the basis of our experiments, the average print speed was of 100–120 mm/s rather than 200 mm/s. The second effect means that if the maximum speed of E-axis is reached –

on the basis of the limit defined in the Marlin firmware - the printer slows down the movements along the other axes (X, Y and Z) aiming to keep a good equilibrium between the material deposition and the printing movements. However, from the data of Fig. 6a any significant variation has not been observed when improving the flow values ($p < 0.05$). Similar results were observed by analyzing the overall printing times as a function of the diameter of filament from 1.75 mm to 0.8 mm as input value of the slicing software (Fig. 6b). Indeed, apart the usage of value of 0.8 mm which produced the higher printing time, a significant reduction of the printing time from 700 s to 200 s was observed by increasing print speed from 15 mm/s to 100–150 mm/s for input value between 1 and 1.75 mm. Also, any further increase of print speed more than 150 mm/s did not produce a significant reduction of printing time ($p > 0.05$). On the basis of these preliminary tests we defined the following printing conditions: print speed of 200 mm/s; diameter of filament as input value of 1.0 mm. These conditions were used in the last series of experiments described in the next section of the paper.

Print speed (mm/s)	**Time to accelerate (s)**	**Minimum distance to accelerate (mm)**	**Minimum distance to decelerate (mm)**	**Distance at defined speed rate (mm) along major axis**	**Distance at defined speed rate (mm) along minor axis**
15	0.005	0.037	0.037	39.92	29.92
50	0.016	0.416	0.416	39.16	29.16
150	0.050	3.750	3.750	32.50	22.50
200	0.066	6.666	6.666	26.66	16.66
250	0.083	10.416	10.416	19.16	9.166

Table 2 - Actual conditions of acceleration/deceleration movements at different print speed.

3.3. Effects of the retraction and travel speed on printing time and the fidelity of printing

The previous data showed that although the modulation of the flow and of the diameter of filament, as input data, may help to increase the faithfulness of the printing, some discrepancies of the printed objects still remains.

Moreover, it is well known that these errors increase in number as much more is the number and/or the length of the non-printing movements. Indeed the ability to control the printing pathway is a very active field of research in 3D printing of plastic materials (Jin et al., 2017). To help remedy these inaccuracies, we studied the effect of the understudied variables retraction distance (mm), RD, retraction speed (mm/s), RS, and the travel speed, TS, on the main morphological properties of the samples. In addition, we analyzed how much these variables may affect the overall printing time that is the main question addressed in our paper. These effects and their statistical weights may be observed in Fig. 7, Fig. 8, Fig. 9. When considering the relative deviation of the perimeter of the samples (Fig. 7a) from the virtual model, only the retraction speed and retraction distance exhibited a significant effect ($p < 0.05$). Particularly, estimated effects of −2.88 and 4.33 were computed for retraction speed and retraction distance, respectively. The statistical analysis also shows the deviation of the perimeter of samples as a function of the retraction speed and retraction distance (Fig. 7b and c). Retraction distance negatively affects the quality of the replica while the speed of retraction had a positive effect. The retraction literally is a reverse movement that bring back the material aiming to reduce the pressure at the tip of the nozzle avoiding oozing during non-printing movements. Similarly, before starting to print an opposite movement is performed to renew the pressure at the tip of the extrusion system. In our case, retraction movements produced an excess of material deposition which enlarged the sample and, in turn, its perimeter. On the other hand, the increase of retraction speed reduced these defects because less material is deposited at the starting and end points of any printing movement. Intuitively, this is because there is less time for oozing and also because due to the low adhesives between of the dough and the screw, less material is deposited. So, if the increase of retraction distance hinders the printing quality, the increase of retraction speed may help to mitigate these morphological defects.

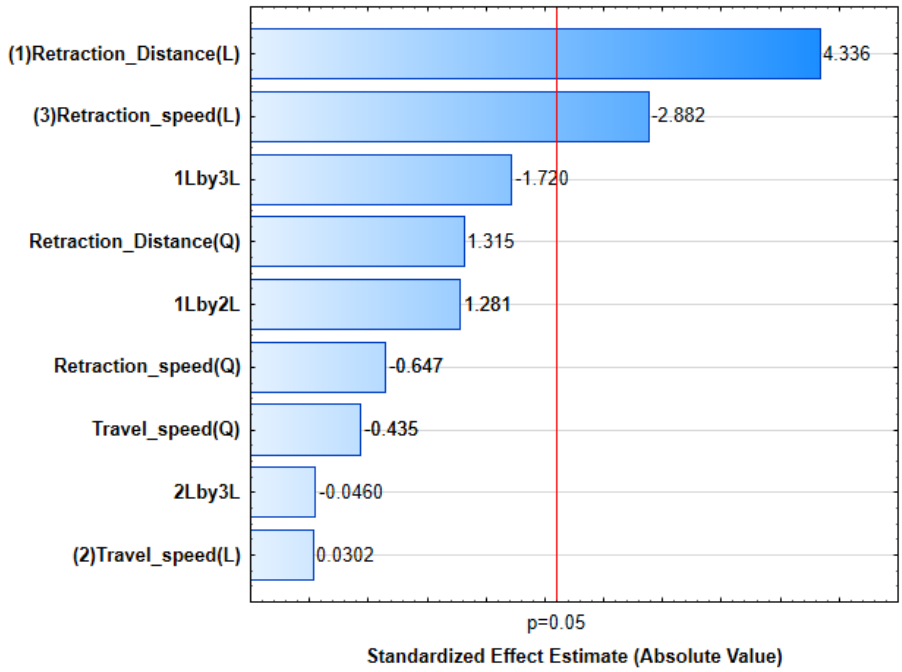

Fig. 7. Effects of retraction distance, retraction speed and travel speed on the relative deviation of the perimeter of printed object from 3D virtual model.

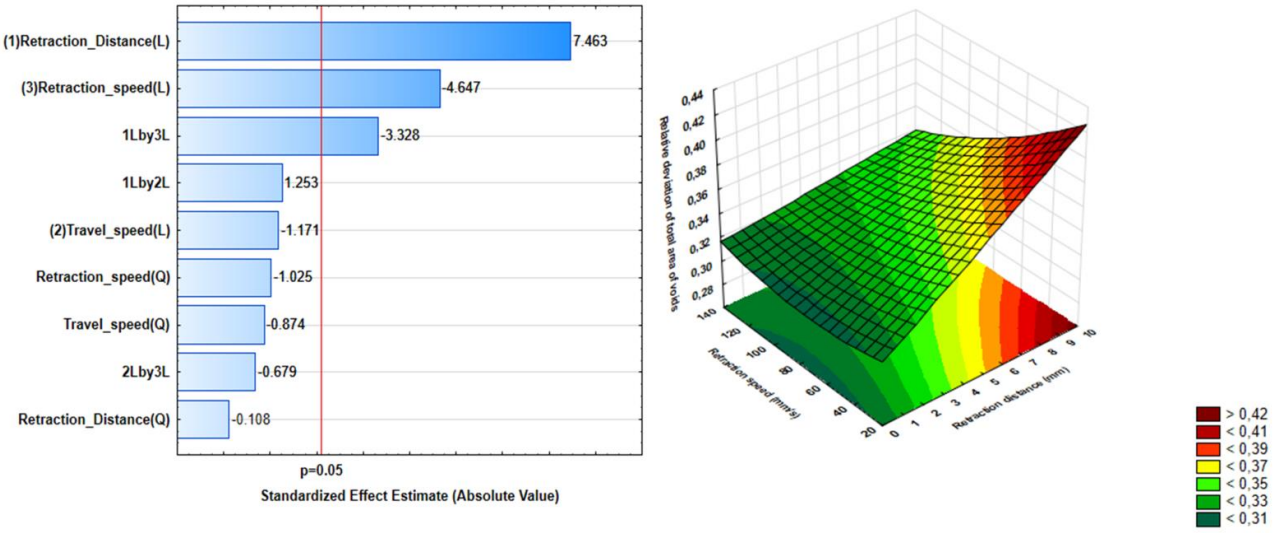

Fig. 8. Effects of retraction distance, retraction speed and travel speed on the relative deviation of the total area of voids.

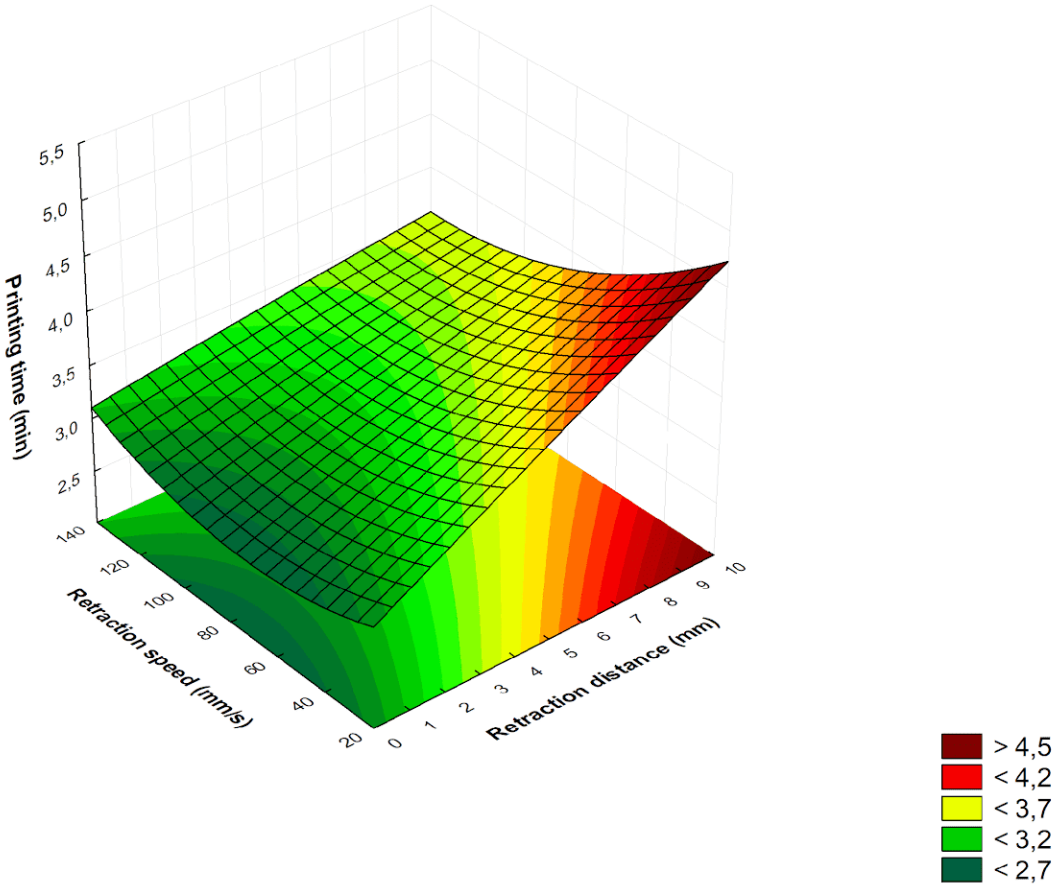

Fig. 9. 3D plot reporting the effect of independent variables on the overall printing time.

The effect of the studied variables on the total area of the voids phase of the samples is reported in Fig. 8.

Similarly, the retraction distance had a great and negative effect on the quality of the printed objects. When a high retraction distance was employed, the excess of deposited material increased the thick of either the internal lines of the objects as well as the thick of the external shell reducing, in large part, the void fraction of the sample. Indeed, a maximum deviation of 40% was obtained for the highest value of distance and speed retractions. Significantly better results were obtained with a small retraction distance of 1 mm which creates only minor discrepancies from the virtual model.

In addition we want to show and discuss the effect of the independent variables on the total printing time. As expected all three variables (retraction distance, travel speed and retraction speed) had an important effect with a major attention on the travel distance which exhibited an estimated effect of 12.65 indicating that its increase is very time consuming for 3D printing. Inversely, the increase of the travel speed and retractions speed allow reducing the time for the printing process with standardized effects respectively of −10.14 and −5.79 (data not show). Fig. 9 summarises these results, mainly analyzing the effect of retraction speed and retraction distance on the overall printing time. What is important to note is that the analyzed variables have a great impact on the printing time that showed values between 4.5 and 2.7 min.

All above interpretation are strengthen by the statistical analysis performed for the other physical and morphological parameters (Table 3). The majority of the morphological defects were observed on the lateral voids and they were significantly influenced by a linear effect of the retraction distance while, according to the previous discussion, their correspondence to the virtual model improved when increasing the retraction speed; indeed, standardized effects of 5.79 and −2.16 were observed indicating a direct and inverse relationships with the distance and the speed of retraction, respectively. According to the previous observation is also the effect on the total weight of the samples that increased from 13.2 g to 14.4 g employing retraction distance of 1 and 9 mm, respectively.

Total weight of sample	
Variable	**Standardized effect estimate (Effect/Err. Std)**
Retraction distance	3.46
Retraction speed	-2.13
Travel speed	-2.54
Relative deviation of the overall area of the centre voids	
Travel speed (L)	-7.18
Travel speed (Q)	-2.36
Relative deviations of the overall area of the lateral void	
Retraction distance	5.79
Retraction speed	-2.16
Relative deviations of the overall area of upper and lower voids	
Retraction distance	-
Retraction speed	-

Table 3 – Significant effects of the non-printing movements variables on some quality parameters characterizing the fidelity of printing.

3.4. Optimization of the printing process and validating tests

Finally, to address the reduction of the defects on the 3D printed objects and to minimize the printing time as much as possible, we employed a desirability approach. This method allows to put, in a single analysis, all the responses of the samples and to receive a single best condition capable to maximize the efficacy and the efficiency of the printing. Specifically, in our case the goal was to minimize the relative deviation of all morphological properties from the virtual model and to cut down the printing time, as well. As example, we first analyze the desirability profile of the perimeter of the samples (Fig. 10). The data were transformed by considering desirability values of 0 and 1 respectively when the relative deviation from the virtual model is at maximum or minimum value that means respectively the lower and the higher faithfulness of printing. The profile shows as the maximum desirability of 0.833 could be obtained by using a retraction distance of 1 mm, a travel speed of 200 mm/s and a retraction speed of 105 mm/s. This is in accordance with the previous data, for which by reducing the retraction distance and increasing the speed of both retraction and travel movements would be possible to minimize the oozing problems during the dough deposition. Then we analyzed the desirability profile of the 3D printed samples by including all the quality parameters (Fig. 11). The best achievable result was a desirability of 0.86 obtained in the following conditions: retraction distance of 1 mm, travel speed of 200 mm/s and retraction speed ranged between 90 and 130 mm/s. Summarising, we have defined the best values for travel speed and retraction capable to minimize the structural defects of our samples when printing at high speed of 200 mm/s. Finally, we have validated these conditions by printing others 3D virtual models of different size, infill level and infill pattern aiming to check if the fidelity of printing may remain good as in the previous cases (Fig. 12). Mainly we have edited the overall dimension of the virtual model till a rectangular shape of 100 mm × 90 mm, and the infill pathway. In both the cases, the overall aspect of the objects show a good capability to reproduce the virtual model with high fidelity even at print speed significantly higher than the common values used in the field of food sector.

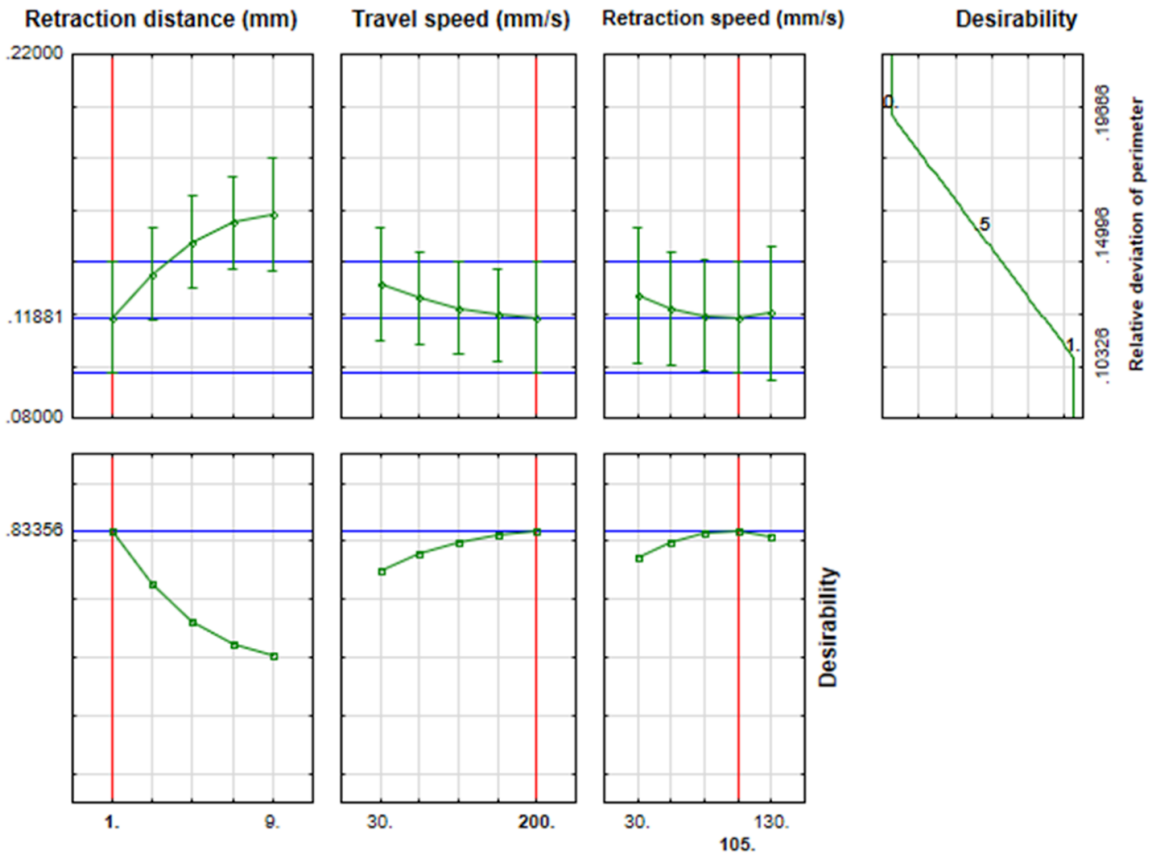

Fig. 10. Desirability profile for relative deviation of the perimeter of 3D printed samples as a function travel speed, retraction distance and retraction speed.

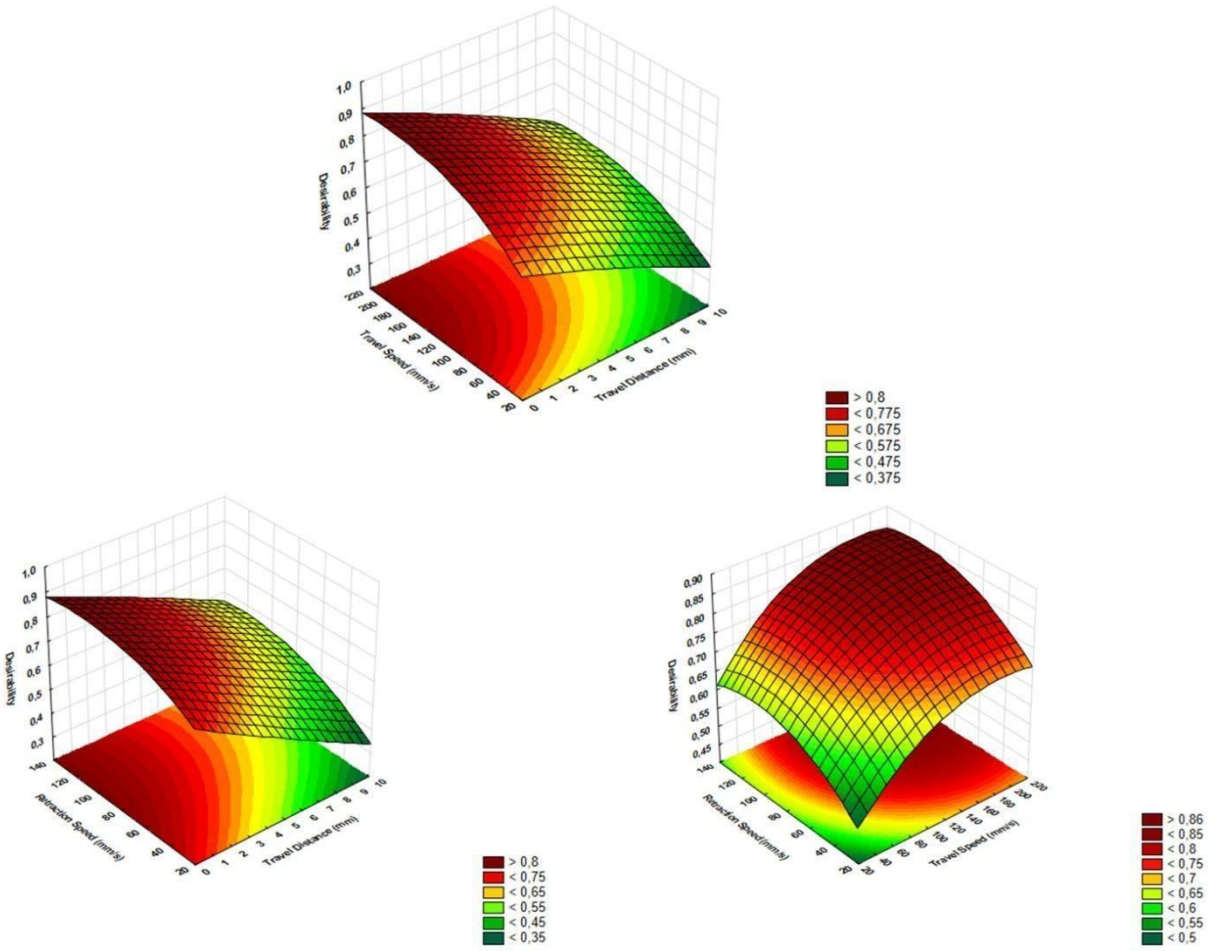

Fig. 11. Overall desirability, for all quality metrics, of 3D printed edible objects as a function of travel speed, retraction speed and retraction distance.

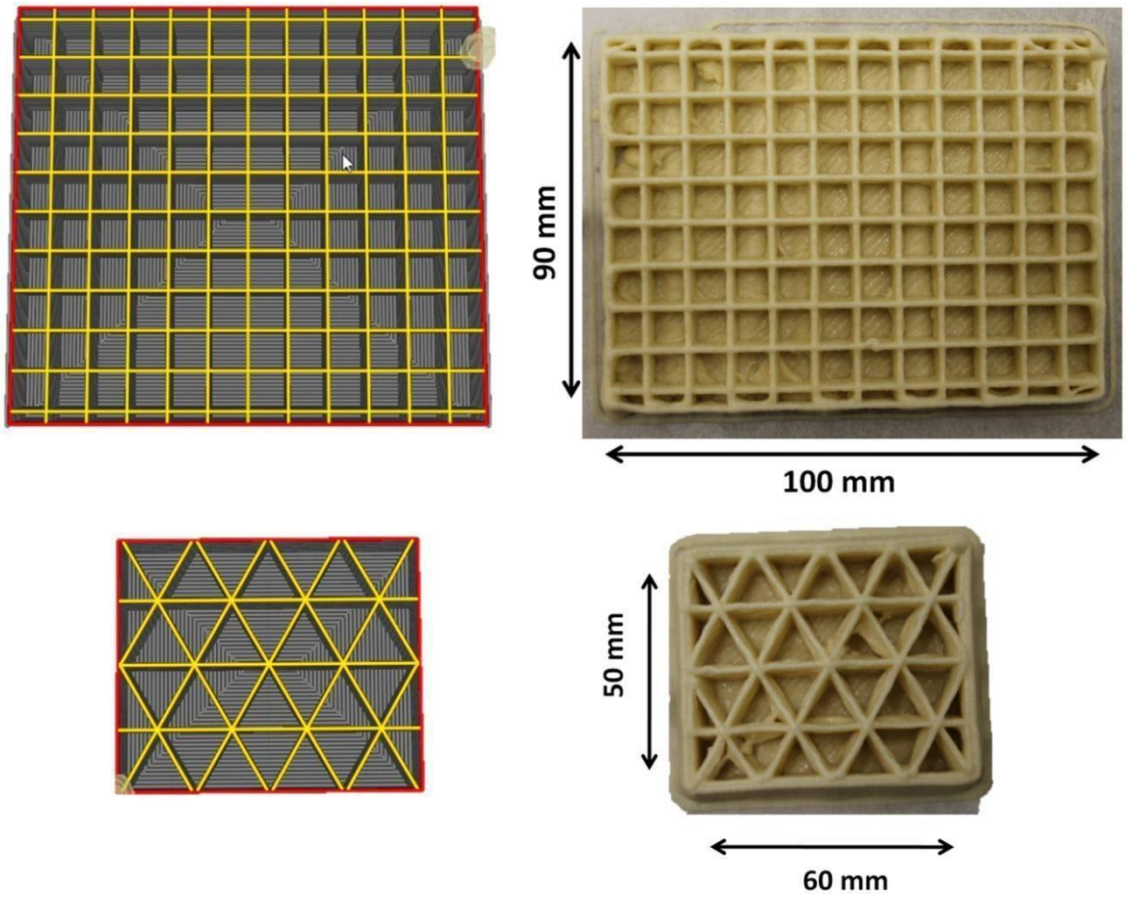

Fig. 12. Virtual and edible objects created by printing process at 200 mm/s.

4. Conclusion

We have performed a series of experiments with the aim to extend our knowledge on the 3D Food Printing beyond the common print speed limit of 70 mm/s. When printing a cereal-based dough at speed higher than 100 mm/s, the quality of printed objects was very low, with several defects. This is because the corresponding increases of the rotation of the screw on E-axis, was completely inadequate for depositing enough material during the fast printing movements. Two different options could be utilized to reduce this problem: to increase the flow parameter 3 times greater than the default value; to set, as input value of the slicing software, the diameter of the filament at 1.0 mm – against the common value of 1.75 mm –. However, some minor defects (oozing and stringing) remained as a results of the effects of some undervalued non-printing variables such as travel speed, retraction distance and retraction speed. After analyzing the weight of such non-printing variables on the quality of printed samples, we were able to get a good printing fidelity at speed of 200 mm/s in the following conditions: filament diameter 1.0 mm,

flow parameter of 100%. Finally, these conditions were validated for 2 additional virtual models with very good results.

References

Asharaf, M., Gibson, I., & Rashed, M.G., (2018). Challenges and prospects of 3D printing in structural engineering. In 13th International Conference on Steel, Space and Composite Structures. 31 January - 2 February 2018, Perth, Australia.

Baines, J. (2017). 3D Printing – Layer Height Under the Microscope. https://3dprinterchat.com (accessed 9 May 2017).

Bashiardes, S., Godneva, A., Elinav, E., & Segal, E. (2018). Towards utilization of the human genome and microbiome for personalized nutrition. Current Opinion in Biotechnology. Volume 51, 2018, 57-63. https://doi.org/10.1016/j.copbio.2017.11.013.

Bégin-Drolet, A, Dussault, M.A., Fernandez, S.A., Larose-Dutil, J., Leask, R.L., Hoesli, C.A., & Ruel, J. (2017). Design of a 3D printer head for additive manufacturing of sugar glass for tissue engineering applications. Additive Manufacturing, 15, 29-39. https://doi.org/10.1016/j.addma.2017.03.006.

Birbara, N.S., Otton, J.M., & Pather, N. (2017). 3D Modelling and printing technology to produce patient-specific 3D models. Heart, Lung and Circulation, 1-12. https://doi.org/10.1016/j.hlc.2017.10.017.

Caporizzi, R., Derossi, A., & Severini, C. (2019). Cereal-based and insect-enriched printable food: from formulation to postprocessing treatments. Status and perspectives. In Godoi, F.C., Bhandari, B.R., Zhang, M. (Eds.), Fundamentals of 3D Printing and Applications (4, pp. 93-116). Elsevier Inc., ISBN 978-0-12-814564-7. https://doi.org/10.1016/B978-0-12-814564-7.00004-3.

Chilson, L., (2011). Filament Tolerances and Printing Quality. http://www.protoparadigm.com/newsupdates/filamenttolerancesandprintquality/ (Accessed, 14 May 2017).

Cohen, D.L., Lipton, J.I., Cutler, M., Coulter, D., Vesco, A., & Lipson, H. (2009). Hydrocolloid printing: a novel platform for customized food production. In Solid Freeform Fabrication Symposium, 807-818. Austin, TX.

Dankar, I., Haddarah, A., Omar, F.E.L., Sepulcre, F., & Pujola, M. (2018). 3D printing technology: The new era for food customization and elaboration. Trends in Food Science & Technology, 75, 231-242. https://doi.org/10.1016/j.tifs.2018.03.018.

Derossi A., Caporizzi, R., Azzollini, D., & Severini, C. (2018a). Application of 3D printing for customized food. A case on the development of a fruit-based snack for children. Journal of Food Engineering, 220, 65-75. https://doi.org/10.1016/j.jfoodeng.2017.05.015.

Derossi, A., Caporizzi, R., Paolillo, M., Ricci, I., Fiore, A.G., & Severini, C. (2018b). New advances in 3D food printing. Fast printing and combined cooking-printing. In 32nd EFFOST – International Conference, 6-8 November, Nantes.

Derossi, A., Caporizzi, R., Paolillo, M., & Severini, C. (2018c). 3D Printing for products with personalized textural properties: a case study on the food structure of multilayered wheat-based snack. In 3th Food Structure Design Congress, Sept. 20-22th, Debrecen University Congress, Debrecen.

Derossi, A., Husain, A., Caporizzi, R., & Severini, C. (2019a). Manufacturing personalized food for people uniqueness. An overview from traditional to emerging technologies. Critical Review in Food Science Nutrition, 22, 1-19. http://doi.org.10.1080/10408398.2018.1559796.

Derossi, A., Caporizzi, R., Ricci, I., & Severini, C. (2019b). Critical Variables in 3D Food Printing. In Godoi, F.C., Bhandari, B.R., Zhang, M. (Eds.), Fundamentals of 3D Printing and Applications, (3, pp. 41-91). Elsevier Inc., ISBN 978-0-12-814564-7. https://doi.org/10.1016/B978-0-12-814564-7.00003-1.

Derossi, A., Paolillo, M., Caporizzi, R., Verboven, P., Vancauwenbergher, V., Nicolai, B., & Severini, C. (2019c). From plant tissue microstructure to new foods with novel sensory perception. An example of biomimetics of food mediated by 3D printing. In 8th International Symposium on ‘Delivery of Functionality in Complex Food Systems’. 7-10 July, Sheraton Porto hotel Conference Centre, Porto, Portugal.

Dianez, I., Gallegos, C., Brito-de la Fuente, E., Martinez, I., Valencia, C., Sanchez, M.C., Diaz, M.J., & Franco, J.M. (2019). 3D Printing in situ gelification of k-carrageenan solutions: Effect of printing variables on the rheological response. Food Hydrocolloids, 87, 321-330. https://doi.org/10.1016/j.foodhyd.2018.08.010.

Diggs-McGee, B.N., Kreiger, E.L., Kreiger, M.A., & Case, M.P. (2019). Print time vs elapsed time: a temporal analysis of a continuous printing operation for additive constructed concrete. Additive Manufacturing, 28, 205-214. https://doi.org/10.1016/j.addma.2019.04.008.

Fay, B.L., & German, J.B. (2008). Personalizing foods: is genotype necessary? Current Opinion in Biotechnology, 19, 121-128. https://doi.org/10.1016/j.copbio.2008.02.010.

Geng, P., Zhao, J., Wu, W., Ye, W., Wang, Y., Wang, S., & Chang, S. (2019). Effect of extrusion speed and printing speed on the 3D printing stability of extruded PEEK filament. Journal of Manufacturing Processes, 37, 266-273. https://doi.org/10.1016/j.jmapro.2018.11.023.

Gilberti, H., Sbaglia, L., & Urgo, M. (2017). A path planning algorithm for industrial processes under velocity constraints with an application to additive manufacturing. Journal of Manufacturing Systems, 43, 160-167. https://doi.org/10.1016/j.jmsy.2017.03.003.

Godoi, F.C., Bhandari, B.R. & Prakash, S. (2018). An introduction to the principles of 3D food printing. In Godoi, F.C., Bhandari, B.R., Zhang, M. (Eds.), Fundamentals of 3D Printing and Applications, (1, pp. 1-16). Elsevier Inc., ISBN 978-0-12-814564-7 https://doi.org/10.1016/B978-0-12-814564-7.00001-8.

Gong, J., Shitara, M., Seizawa, R., Makino, M., Kabir, M.H., & Furukawa, H. (2014). 3D printing of meso-decorated gels and foods. Material Science Forum Trans Tech Publ., 1250-1254. https://doi.org.10.4028/www.scientific.net/MSF.783-786.1250.

Goyanes, A., Buanz, A., Basit, A. W., & Gaisford, S. (2014). Fused-filament 3D printing (3DP) for fabrication of tablets. International Journal of Pharmaceutics, 476, 88-92. https://doi.org/10.1016/j.ijpharm.2014.09.044.

Guo, C.F., Zhang, M., & Bhandari, B. (2019). A comparative study between syringe-based and screw-based 3D food printers by computation simulation. Computers and Electronics in Agriculture, 162, 397-404. https://doi.org/10.1016/j.compag.2019.04.032.

Hamilton, C.A., Alici, G., & in het Panhuis, M. (2017). 3D printing Vegemite and Marmite: Redefining 'breadboards'. Journal of Food Engineering, 220, 83-88. https://doi.org/10.1016/j.jfoodeng.2017.01.008.

Hosny, A., Keating, S.J., Dilley, J.D., Ripley, B., Kelil, T., Pieper, S., Kolb, D., Bader, C., Pobloth, A.M., Griffin, M., Nezafat, R., Duda, G., Chiocca, E.A., Stone, J.R., Michaelson, J.S., Dean, M.N., Oxman, N., & Weaver, J.C. (2018). From improved diagnostics to presurgical planning: High-resolution functionally, graded multimaterial 3D printing of biomedical tomographic data sets. 3D Printing and Additive Manufacturing, 5 (2), 103-113. http://dx.doi.10.1089/3dp.2017.0140.

Jin, G., Li, W., & G\ao, L. (2013). An adaptive process planning approach of rapid prototyping and manufacturing. Robotics and Computer-Integrated Manufacturing, 29, 23-58. https://doi.org/10.1016/j.rcim.2012.07.001.

Jin, Y., He, Y., Fu, G., Zhang, A., & Du, J. (2017). A non-retraction path planning approach for extrusion-based additive manufacturing. Robotics and Computers – Integrated Manufacturing. 48, 132-144. http://dx.doi.org/10.1016/j.rcim.2017.03.008.

Khalil, S., & Sun, W. (2007). Biopolymer deposition of freeform fabrication of hydrogel tissue constructs. Materials Science and Engineering, C 27, 409-478. https://doi.org/10.1016/j.msec.2006.05.023.

Kim, H.W., bae, H., & Park, H.J. (2017). Classification of the printability of selected food for 3D printing: Development of an assessment method using hydrocolloids as reference material. Journal of Food Engineering, 215, 23-32. https://doi.org/10.1016/j.jfoodeng.2017.07.017.

Kim, H.W., Lee, J.H., Park, S.M., Lee, J.H., Nguyen, M.H., & Park, H.J. (2019). Effect of hydrocolloid addition on dimensional stability in post-processing of 3D printable cookie dough. LWT, 101, 69-75. https://doi.org/10.1016/j.lwt.2018.11.019.

Kulkarami, P., & Dutta, D. (1999). Deposition strategies and resulting part stiffnesses in fused deposition modeling. Journal Manufacturing Science Engineering, 12 (1), 93-103. doi:10.1115/1.2830582.

Lanaro, M., Forrestal, D.P., Scheurer, S., Slinger, D.J., Liao, S., Powell, S.K., & Woodruff, M.A. (2017). 3D printing complex chocolate objects: Platform design, optimization and evaluation. Journal of Food Engineering, 215, December 2017, 13-22. https://doi.org/10.1016/j.jfoodeng.2017.06.029.

Le Tohic, C., O'Sullivan, J.J., Drapala, K.P., Chartrin V., Chan, T., Morrison, A.P., Kerry, J.P., & Kelly, A.L. (2018). Effect of 3D printing on the structure and textural properties of processed cheese. Journal of Food Engineering, 220, 56-64. https://doi.org/10.1016/j.jfoodeng.2017.02.003.

Lee, H.L., Won, D.J., Kim, H.W., & Park, H.J. (2019). Effect of particle size on 3D printing performance of the food-ink system with cellular food materials. Journal of Food Engineering, 256, 1-8. http://doi.org/10.1016/j.jfoodeng.2019.03.014.

Lee, J.Y., An, J., & Chua, C.K. (2017). Fundamentals and applications of 3D printing for novel materials. Applied Materials Today, 7, 120-133. http://dx.doi.org/10.1016/j.apmt.2017.02.004.

Lille M., Nurmela, A., Nordlund, E., Metsa-Kortelain S., & Sozer, N. (2017). Applicability of protein and fiber-rich food materials in extrusion-based 3D printing. Journal of Food Engineering, 220, 20-27. http://dx.doi.10.1016/j.jfoodeng.2017.04.034.

Lipton, I.J. (2017). Printable food: the technology and its application in human health. Current Opinion in Biotechnology, 44, 198-201. http://dx.doi.10.1016/j.copbio.2016.11.015.

Liu, J., Sun, L., Xu, W., Wang, Q., Yu, S. & Sun, J. (2019). Current advances and future perspectives of 3D printing natural-derived biopolymers. Carbohydrates Polymers, 207, 297-316. https://doi.org/10.1016/j.carbpol.2018.11.077.

Liu, Z., Bhesh Bhandari, B., & Prakash, S., M. (2018). Creation of internal structure of mashed potato construct by 3D printing and its textural properties. Food Research International, 111, 534-543. https://doi.org/10.1016/j.foodres.2018.05.075.

Manthial, S., Prakash, S., Condi Godoi, F., & Bhandari, B. (2018). Optimization of chocolate 3D printing by correlating thermal and flow properties with 3D structure modeling. Innovative Food Science and Emerging Technologies, 44, 21-29. https://doi.org/ 10.1016/j.ifset.2017.09.012.

Marlin (2019). Marlin firmware documentation. Downloaded in date (8/04/2019). http://marlinfw.org/meta/download.

MIT (2019). New 3-D printer is 10 times faster than commercial counterparts. New design may open new opportunities for 3-D printing technology (http://news.mit.edu/2017/new-3-d-printer-10-times-faster-commercial-counterparts-1129, Accessed 11 Nov 2019).

Pérez, B., Nykvist, H., Brøgger, A.F., Larsen, M.B., & Falkeborg, M.F. (2019). Impact of macronutrients printability and 3D-printer parameters on 3D-food printing: A review. Food Chemistry, 287, 249-257. https://doi.org/10.1016/j.foodchem.2019.02.090.

Portanguen, S., Tournayre, P., Sicard, J., Astruc, T., & Mirade, P., S. (2019). Toward the design of functional foods and biobased products by 3D printing: A review. Trends in Food Science & Technology, 86, 188-198. https://doi.org/10.1016/j.tifs.2019.02.023.

Ricci, I., Derossi, A., & Severini, C. (2019). 3D Printed Food from fruits and Vegetables. In Godoi, F.C., Bhandari, B.R., Zhang, M. (Eds.), Fundamentals of 3D Printing and Applications, (5, pp. 117-149). Elsevier Inc., ISBN 978-0-12-814564-7. https://doi.org/10.1016/B978-0-12-814564-7.00005-5.

Schutyser M.A.I., Houlder, S., de Wit, M., Buijsse, C.A.P., & Alting, A.C. (2018). Fused deposition modeling of sodium caseinate dispersions. Journal of Food Engineering, 220, 49-55. https://doi.org/10.1016/j.jfoodeng.2017.02.004.

Severini, C., Derossi, A., & Azzollini D. (2016). Variables affecting the printability of foods: Preliminary tests on cereal-based products. Innovative Food Science & Emerging Technologies, 38, 281-291. https://doi.org/10.1016/j.ifset.2016.10.001.

Severini, C., Derossi, A., Ricci, I., Caporizzi, R., & Fiore, A. (2018). Printing a blend of fruit and vegetables. New advances on critical variables and shelf life of 3D edible objects. Journal of Food Engineering, 220, 89-100. https://doi.org/10.1016/j.jfoodeng.2017.08.025.

Sher, D., & Tutò, X. (2015). Review of 3D Food Printing. Temes de Disseny, 31, 105-117.

Slic3R (2017). Flow math. Understanding extrusion width. www.Slic3R (accessed 12 May 2017).

Sun, J., Peng, Z., Zhou, W., Fuh, J.Y.H., Hong, G.S. & Chiu, A. (2015). A review on 3D printing for customized food fabrication. Procedia Manufacturing, 1, 308-319. https://doi.org/10.1016/j.promfg.2015.09.057.

Sun, J., Zhou, W., Yn, L., Huang, D. & Lin, L. (2018). Extrusion-based food printing for digitalized food design and nutrition control. Journal of Food Engineering, 220, 1-11. https://doi.org/10.1016/j.jfoodeng.2017.02.028.

Vancauwenberghe, V., Katalagarianakis, L., Wang, Z., Meerts, M., Hertog, M., Verboven, P., Moldenaers, P, Hendrickx, M.E., Lammertyn, J., & Nicolai, B. (2017a). Pectin based food-ink formulations for 3-D printing of customizable porous food stimulants. Innovative Food Science and Emerging Technologies, 42, 138-150. https://doi.org/10.1016/j.ifset.2017.06.011.

Vancauwenberghe, V., Mbong, V.B.M., Vanstreels, E., Verboven, P., Lammertyn, J., & Nicolai, B. (2017b). 3D printing of plant tissue for innovative food manufacturing: encapsulation of alive cells into pectin based bio-ink. Journal of Food Engineering, 1-11. https://doi.org. 10.1016/j.foodeng.2017.12.003.

Wang, J., & Shaw, L.L. (2005). Rheological and extrusion behavior of dental porcelain slurries for rapid prototyping applications. Materials Science and engineering A, 397, 314-321. https://doi.org/10.1016/j.msea.2005.02.045.

Wang, L., Zhang, M., Bhandari, B., & Yang, C. (2018). Investigating on fish surimi gel as promising material for 3D printing. Journal of Food Engineering, 220, 301-308. https://doi.org/10.1016/j.jfoodeng.2017.02.029.

Yang, F., Zhang, M., & Bhandari, B. (2017). Recent development in 3D Food Printing. Critical Reviews in Food Science and Nutrition, 57 (14), 3145-3153. https://doi.org. 10.1080/10408398.2015.1094732.

Yang, F., Zhang, M., Bhandari, B., & Liu, Y. (2018a). Investigation on lemon juice gel as food material for 3D printing and optimization of printing parameters. LWT-Food Science and Technology, 87, 67-76. https://doi.org/10.1016/j.lwt.2017.08.054.

Yang, F., Zhang, M., Bhandari, B., & Yang, C. (2018b). Investigation of fish surimi gel as promising material for 3D printing. Journal of Food Engineering, 220, 101-108. https://doi.org/10.1016/j.jfoodeng.2017.02.029.

CHAPTER 8 Conclusions and future applications

8.1 The future of the research

In 2019 Prakash et al. described 3DFP as the layer-by-layer 3D printing technique owns the ability to change the internal structure of printed objects by varying infill patterns and infill percentages in order to control the density of the raw materials to fabricate freeform geometries with variable textural properties. Our research pushed up this aspect investigating the hypothesis of programming the texture, a food quality strictly linked to sensory perception of food. Our study showed how it is possible, starting from the same formulation, to create food with different mechanical properties, modulating the geometry and the level of porosity and finally making food through 3D printing. With this objective, a focal point will be the research of new structure, new dimension and in definitive a new aspect of food. This thesis has opened a window of opportunity on researching for the first-time new idea for food structure and design, leaving the patterns of geometric shapes but taking inspiration from nature, from intricate and complex structure of plant tissues demonstrating that with 3D printing it is possible to create food with enormous degrees of freedom.

Another aspect that is closely related to the 3D printing of food is the study of food formulas. As we described, not all the food is able to be printed or in some cases, they need the ad of some gelatin or structuring, in other cases they need to be subjected to some technological processes such as heating or dehydration. The rheological properties of food ink affect printing variables, choosing the most suitable printing technology and the design features. This thesis also investigated the possible changes of food formula during the time elapsed from the moment of preparation to the time of printing. This leads to the conclusion that even the rest times before printing can cause changes on the printing variables to achieve a good level of print fidelity.

Despite the fact that numerous steps forward have been made in about 10 years in the research field, there still seem to be many fields of study unexplored or to be deepened. Some of these are the correlation between mechanical and texture characteristics (gumminess, fracturing, crunchiness, etc.) and the design of foods regardless of the formulation; the printing of multi-material food combining different formulations with the aim of obtaining a complete customized meal also from the nutritional point of view; special cooking technologies to retention of the shape and structure and post processing; printing in 4 dimensions and much more.

8.2 The social impact and reduction of waste

The advantages obtainable from the use of 3DP in the food production exceed the design innovation and the customization. In fact, 3D printing allows the use of lower quantities of raw materials and lower energy consumption (Kietzmann et al., 2015) thus reducing the amount of waste generated. This concept can be transferred to food production with the potential to reduce food waste because 3D printing allows us to produce food only in the desired quantities and when this food – even personalized – is desired by the consumer (Dankar et al., 2018). In fact, the introduction of this technology at home will allow us to print meals with desired quantity, avoiding the opening of packaged products often oversized compared to the real individual consumption and subsequent large production of food waste. Moreover, at industrial scale, 3DFP could open the way to a total transition of the agro-industrial system towards on-demand production with benefits also from reduction of food waste.
Finally the 3D printing could show a positive impact on the possibility of stimulating social ties between individuals (Huang et al., 2017). In fact, this innovative technology adds greater ease of communication of messages improving mood and emotions, to the already stated power of aggregation that food can create, as well as an atmosphere of conviviality and is recognized by the entire international community (Dankar et al., 2018).

8.3 Prospective for the scaling up in industrial sector

The purpose of innovation in food service technology is to upgrade traditional methods of producing food products in terms of quality, quantity, time preparation, ingredient accuracy, nutritional content, texture, packaging, appearance and shelf-life and to increase the functionality of food. The prospective application of 3DFP can be considered in the three levels of the food production industry: consumer produced food, small scale food production and industrial scale food production (Lipton et al., 2015). The application of 3DFP would be a great prospect for food entrepreneurs in niche markets because it allows food makers to explore the customization of their otherwise mass produced and, in many cases, commoditized products (Manthial et al., 2020). Looking at the appearance of the industrial application of 3D printing technology or otherwise the commercial introduction, you may experience some difficulties. Some of these are the same described in the last paragraph but surmountable by the optimization of the process. In some cases it is a limit of technology such as the production time. It is why industrial-level application still seems a long way off. The adoption of 3DP at an industrial scale could be

challenging as the machine should be able to cope with a larger capacity (mass production) in a short time (with economies of scale). Therefore, further study is needed not only in developing an industrial scale 3D food printer but also in food product quality which includes the food material properties suitable for such large-scale printing.

More real instead it seems the application of 3DFP for the individual user consumer as a friendly printer enables individuals to use equipment easily. Some companies, in fact, have been designing for several years already simple and uncomplicated 3D printers for printing biscuits, chocolate and some decorations (Malone and Lipson, 2007; Sun et al., 2015; Molitch-Hou, 2014). Very interesting and feasible especially appears the application of 3DFP in small scale food production (restaurants, cafés, bakeries) creating a gourmet style in the presentation of food. 3D printing technology would be beneficial in the customization of unique products and value adding to artistry in foodstuffs (Manthial et al., 2020).

In conclusion, the time for application of 3d printing in food fields seems not so long. In some isolated cases, it is a reality, in others the strong influence of tradition and food culture is delaying the inclusion of this emerging technology. Besides, the technology needs an awareness-raising operation for consumers that would enhance consumers' or users' understanding and acceptance of the technology.

8.4 References

Additive Manufacturing. Materials, Processes, Quantifications and Applications, Pages 1-38. https://doi.org/10.1016/B978-0-12-812155-9.00001-3

Dankar, I., Haddarah, A., Omar, F.E.L., Sepulcre, F., Pujolà, M. (2018). 3D printing technology: The new era for food customization and elaboration. Trends in Food Science & Technology, Volume 75, Pages 231-242. https://doi.org/10.1016/j.tifs.2018.03.018

Huang, T., Tu, Z. C., Wang, H., Shangguan, X., Zhang, L., Niu, P., & Sha, X. M. (2017). Promotion of foam properties of egg white protein by subcritical water pre-treatment and fish scales gelatin. Colloids and Surfaces A Physicochemical and Engineering Aspects, 512, 171– 177.

Kietzmann, J., Pitta, L., Berthon, P. (2015). Disruptions, decisions, and destinations: Enter the age of 3-D printing and additive manufacturing. Business Horizons, 58, Issue 2, Pages 209-215. https://doi.org/10.1016/j.bushor.2014.11.005

Lipton, J.I., Cutler, M., Nigl, F., Cohen, D., Lipson, H. (2015). Additive manufacturing for the food industry. Trends in Food Science & Technology. 43, Pages 114-123. https://doi.org/10.1016/j.tifs.2015.02.004

Malone, E., Lipson, H. (2007). Fab@ Home: the personal desktop fabricator kit. Rapid Prototyping Journal, 2007.

Mantihal, S., Kobun, R., Lee, B. (2020). 3D food printing of as the new way of preparing food: A review. International Journal of Gastronomy and Food Science, 100260. https://doi.org/10.1016/j.ijgfs.2020.100260

Molitch-Hou, M. (2018). Overview of additive manufacturing process. In

Prakash, S., Bhandari, B. R., Godoi, F. C., Zhang, M. (2019). Future Outlook of 3D Food Printing. Fundamentals of 3D Food Printing and Applications, Chapter 13, Pages 373-381

Sun, J., Zhou, W., Huang, D., Fuh, J.Y.H., Hong, G., 2015. An overview of 3D printing technologies for food fabrication. Food Bioprocess Technol. 8 (8), 1605e1615